CELLULAR AND MOLECULAR ANALYSIS OF REGENERATIVE NEUROGENESIS IN THE ZEBRAFISH (*DANIO RERIO*) OLFACTORY EPITHELIUM

by

Yiğit Kocagöz

M.Sc., Molecular Biology and Genetics, Boğaziçi University, 2021

Submitted to the Institute for Graduate Studies in
Science and Engineering in partial fulfillment of
the requirements for the degree of
Doctor of Philosophy

Graduate Program in Molecular Biology and Genetics
Boğaziçi University
2021

CELLULAR AND MOLECULAR ANALYSIS OF REGENERATIVE NEUROGENESIS IN THE ZEBRAFISH (*DANIO RERIO*) OLFACTORY EPITHELIUM

DATE OF APPROVAL: 03.08.2021

ACKNOWLEDGEMENTS

A famous philosopher (Confucius) once said, "The hardest thing of all is to find a black cat in a dark room, especially if there is no cat." For a long time, I was so afraid of the darkness in my academic room that I forgot that a cat may even exist. Beginning my Ph.D. studies at Fishlab allowed me to remember what I was supposed to be searching for in the room. Eventually, I came upon a few hints about the cat, maybe its scent, so to speak. Besides the cat, I found many other things; friendship, love, disappointment, resentment... Altogether, my studies gently showed me that the life of a scientist is not confined to test tubes, but paves the way for us to taste all the humane feelings, one way or another. I can not express my gratitudes enough to my supervisor Stefan, not only for his continued support and encouragement, but also for his wisdom and honesty–which may sometimes hurt, but always helped me improve. Throughout my studies, I have seen a lot of people and had a lot of remarkable moments at the lab. I would like to thank all the old (SELİF, Uğurcan, Metin, Kardelen, Katerya, Ezgi, Arda, Sinem and Enes) and new (AYSU, Zeynep and Sinay) crew members for writing at least one whole page in my academic/personal journal. I am particularly grateful to Mehmet Can, who was always a perfect companion, for his friendship and all the cigarettes provided. I also would like to thank Şiran, who deserves special mention for many reasons, but mostly for her unique stubbornness and brutal honesty. Last but not least, I acknowledge with great thanks the support, love and patience from my family, who never understood my work but always appreciated the effort.

Throughout my project, I sought for the black cat and I am today proud to say that the cat exits and is somewhere in the room. Now is the time for others to find it.

I acknowledge support through TÜBITAK-BIDEB-2211-A Genel Yurt İçi Doktora Burs Programı. Work on the studies presented in this thesis has been supported by The Scientific and Technological Research Council of Turkey (TÜBITAK) through research grants 113T038 and 119Z081 to SHF.

ABSTRACT

CELLULAR AND MOLECULAR ANALYSIS OF REGENERATIVE NEUROGENESIS IN THE ZEBRAFISH (*DANIO RERIO*) OLFACTORY EPITHELIUM

The olfactory epithelium (OE) has a high regenerative capacity that ensures the lifelong replacement of olfactory sensory neurons (OSNs). Different modes of neurogenesis originate from the selective activity of two distinct stem cell populations in the OE. In mammals, maintenance and regenerative neurogenesis are attributed to the selective activity of globose basal (GBC) and horizontal basal cells (HBC), respectively. However, the identity and function of similar progenitor cells in the OE of non-mammalian vertebrates remain elusive. This study demonstrates that a dual progenitor cell system also exists in the zebrafish OE but with distinctive features when compared to mammalian models. HBC-like cells reside within the basal layer along the sensory OE, while GBC-like cells are confined to two isolated regions flanking the sensory OE. The positional and functional differences between these progenitor populations establish a balance between constitutive and regenerative modes of neurogenesis in the OE. Here, OE regeneration in response to global and OSN-specific injuries is examined in detail. The OE launches a rapid regenerative response upon chemical lesion, which results in HBC-like cell activation and OSN regeneration within the sensory OE. However, in response to selective OSN ablation, accelerated OSN regeneration is characteristically seen around the OE margins similar to the neurogenic activity in the intact OE. This crucial finding suggests that different injury conditions may affect HBC- and GBC-like cells selectively. RNA-sequencing analysis of the regenerating OE suggests that the diffusible signaling factor HB-EGF may have a critical role at the onset of regenerative neurogenesis. Exogenous HB-EGF administration induces OSN regeneration, while pharmacological inhibition of HB-EGF activity suppresses the regenerative response.

ÖZET

ZEBRABALIĞI (*DANIO RERIO*) OLFAKTÖR EPİTELİNİN REJENERATİF NÖROJENEZİNİN HÜCRESEL VE MOLEKÜLER ANALİZİ

Olfaktör epitelinin (OE), koku duyu nöronlarının (OSN) ömür boyu yenilenmesini sağlayan yüksek bir rejeneratif kapasitesi vardır. Farklı nörojenez şekilleri, OE'deki farklı iki kök hücre popülasyonunun seçici aktivitesinden kaynaklanır. Sürekli ve rejeneratif nörojenez, memelilerde sırasıyla küresel bazal (HBC) ve yatay bazal hücrelerin (GBC) seçici aktivitesine bağlanmıştır. Bununla birlikte, memeli olmayan omurgalıların OE'indeki benzer progenitör hücrelerin kimlik ve işlevleri belirsizliğini korumaktadır. Bu çalışma, zebrabalığı OE'nde memeli modellerdekinden farklı özelliklere sahip ikili bir progenitör hücre sisteminin bulunduğunu gösterir. HBC-benzeri hücreler, OE'in duyusal bölgesi boyunca bazal tabakada bulunurken, GBC-benzeri hücreler duyusal OE'i çevreleyen iki izole bölgede sınırlıdır. Progenitör hücre popülasyonları arasındaki bu konumsal ve işlevsel farklar, zebrabalığı OE'inde sürekli ve rejeneratif nörogenez şekilleri arasında bir denge kurar. Burada, genel ve OSN-spesifik hasara yanıt olan OE rejenerasyonu ayrıntılı olarak incelenmiştir. OE, kimyasal hasar sonucu, duyusal bölgede HBC-benzeri hücrelerin aktivasyonu ve OSN rejenerasyonu ile sonuçlanan hızlı bir rejeneratif yanıt başlatır. Öte yandan, seçici OSN hasarına karşılık hızlandırılmış OSN rejenerasyonu, karakteristik olarak OE sınırları çevresinde, hasarsız OE'ndeki nörojenik aktiviteye benzer bir şekilde görülür. Bu önemli bulgu, farklı hasar koşullarının HBC- ve GBC-benzeri hücreleri seçilimli etkileyebileceğini gösterir. Yenilenen OE'nin RNA dizileme analizi, yayılabilir sinyal faktörü HB-EGF'nin rejeneratif nörojenezin başlangıcında kritik bir rolü olabileceğini önermektedir. Eksojen HB-EGF uygulaması OSN rejenerasyonunu tetiklerken, HB-EGF aktivitesinin farmakolojik inhibisyonu kimyasal hasara karşı rejeneratif yanıtı baskılamaktadır.

TABLE OF CONTENTS

ACKNOWLEDGEMENTS iii
ABSTRACT iv
ÖZET v
LIST OF FIGURES x
LIST OF TABLES xiv
LIST OF SYMBOLS xv
LIST OF ACRONYMS/ABBREVIATIONS xvi
1. INTRODUCTION 1
1.1. Adult neurogenesis 1
1.2. Olfactory system 5
1.3. The olfactory epithelium 7
1.4. The OE regeneration and different injury approaches 9
1.5. Cellular and molecular components of the OE regeneration 10
1.6. Zebrafish as a model for regenerative studies 12
1.7. The zebrafish OE: anatomical structure, cellular components and regenerative characteristics 14
1.8. Importance of extracellular environment in the regenerative response . 22
1.9. Molecular interactions and functional significance of HB-EGF 23
2. PURPOSE 28
3. MATERIALS AND METHODS 30
3.1. Materials 30
3.1.1. Animals 30
3.1.2. Equipments and supplies 30
3.1.3. Buffers and solutions 30
3.2. Methods 31
3.2.1. Adult animal husbandry 31
3.2.2. Breeding and embryo handling 31
3.2.3. Chemical lesions on the OE 32
3.2.4. Olfactory nerve axotomy 32

3.2.5. HB-EGF administration to the OE 33
3.2.6. Drug administration 33
3.2.7. Tissue collection 33
3.2.8. Cryosectioning of tissue samples 34
3.2.9. Immunohistochemistry assays on tissue sections 34
3.2.10. Rabbit serum preparation 36
3.2.11. Immunohistochemistry with primary antibodies from the same host species 36
3.2.12. *In vivo* thymidine analogue incorporation 37
3.2.13. Confocal microscopy 38
3.2.14. Cell quantification and statistics 38
3.2.15. Total RNA extraction and cDNA synthesis 38
3.2.16. Cloning and antisense riboprobe synthesis for *hbegfa* and *ascl1a* 38
3.2.17. Riboprobe synthesis 40
3.2.18. Genomic DNA extraction 41
3.2.19. *Tg(krt5:EGFP)* transgenic line generation 41
4. RESULTS 43
4.1. Dynamics of tissue restoration in the damaged zebrafish OE 43
4.1.1. Degeneration of the zebrafish OE following Triton X-100 injury 44
4.1.2. Proliferative activity in the Triton X-100-lesioned zebrafish OE . 49
4.1.3. Analysis of the radial distribution of mitotic activity in the intact OE 54
4.1.4. Quantitative analysis of the radial distribution of mitotic activity in the damaged OE over time 55
4.1.5. Analysis of the proliferation rate in the regenerating OE over time 57
4.1.6. Analysis of the cell proliferation in the post-regenerative OE . . 60
4.1.7. Consecutive labeling of dividing cells before and after chemical injury 64
4.1.8. Selective ablation of OSNs by axotomy 70
4.1.9. Analysis of apoptosis induction after chemical injury and axotomy 71
4.1.10. Cellular proliferation after axotomy 74

4.1.11. Triton X-100-injured OE initiates regenerative neurogenesis . . 76
4.1.12. Spatiotemporal analysis of new-born OSNs following Triton X-100 exposure 82
4.2. Characterization of cell types that contribute to OE regeneration . . . 87
4.2.1. The zebrafish OE contains HBC-like cells 87
4.2.2. HBC-like cells exit dormancy and divide frequently upon chemical injury 89
4.2.3. Temporal activation of HBC-like cells is correlated with the phases of the regenerative response 91
4.2.4. HBC-like cells undergo self-renewal 93
4.2.5. The Zebrafish OE can induce regenerative responses after milder chemical stress 96
4.2.6. HBC-like cell activation is elevated under mild injury-conditions 98
4.2.7. HBC-like cell activation occurs after axotomy 100
4.2.8. Generation of *Tg(krt5:EGFP)* reporter line 104
4.3. Investigation of the role of HB-EGF signaling on cell proliferation and OSN neurogenesis in zebrafish OE 105
4.3.1. *hbegfa* is upregulated in the regenerating OE 106
4.3.2. Recombinant HB-EGF treatment stimulates proliferation in the OE 107
4.3.3. HB-EGF stimulates neurogenesis in the OE 111
4.3.4. Pharmacological inhibition of HB-EGF activity during OE regeneration 112
4.3.5. Inhibitory effects of GM6001 114
4.3.6. Inhibitory effects of Marimastat 118
5. DISCUSSION 122
5.1. The unique pattern of proliferation in the zebrafish OE 122
5.2. Two progenitor cell pools in the zebrafish OE 123
5.3. The functional significance of a dual progenitor system 125
5.4. HBC activation in different tissue conditions in relation with OSN neurogenesis 130

5.5. Characterization of the OE degeneration and regeneration upon injury 134
5.6. Sustentacular cells as a third non-neuronal basal population 136
5.7. Molecular cues that play stimulatory role in HBC activation 138
5.8. HB-EGF: a key component in regenerative response? 141
REFERENCES 146
APPENDIX A: Chemicals and reagents 186
APPENDIX B: Disposable and non-disposable Equipments 189

LIST OF FIGURES

Figure 1.1. Schematic overview of the zebrafish OE. 16

Figure 1.2. Cellular organization of the sensory OE. 17

Figure 1.3. Schematic diagram of HB-EGF signaling and downstream pathways. 25

Figure 4.1. Neuronal loss and regeneration upon Triton X-100 (Tr-X) treatment in the OE 45

Figure 4.2. Temporal profiling of HuC/D immunoreactivity upon Triton X-100 injury 47

Figure 4.3. Difference in the spatial distribution of BrdU-positive newborn cells in the intact and injured OE 50

Figure 4.4. Cellular proliferation within a week in intact and injured OE . . . 53

Figure 4.5. Positional profiling of newborn cells in the intact OE after 2 hr BrdU exposure 56

Figure 4.6. Positional profiling of BrdU-positive cells during OE regeneration. 58

Figure 4.7. Temporal profiling of BrdU/pH3 double-positive cells after chemical injury. 61

Figure 4.8. Radial positioning of newborn cells along the sensory region of intact OE and regenerated OE over time. 62

Figure 4.9. Sequential labeling of newborn cells before and after Triton X-100 treatment. 66

Figure 4.10. Positional analysis of sequentially labeled newborn cells of intact and regenerating OEs at 1 dpi. 67

Figure 4.11. Sequential labeling of newborn cells before and after Triton X-100 treatment. 69

Figure 4.12. Positional analysis of IdU- (red) and CldU- (green) positive newborn cells along the radial axis in regenerating OE at 3 dpi. 70

Figure 4.13. Active Caspase-3 immunolabeling under different tissue conditions 73

Figure 4.14. Mitotic activity after axotomy. 77

Figure 4.15. Representative image of an axotomized lamella. 78

Figure 4.16. *In situ* hybridization of *ascl1a* and anti-Sox2 immunohistochemistry on intact and regenerating OE at 2 dpi. 79

Figure 4.17. Identification of BrdU/Ascl1-double positive cells cells by immunohisochemistry in intact and regenerating OE. 81

Figure 4.18. Analysis of Ascl1 labeling at 2 dpi. 83

Figure 4.19. Pulse-chase approach to analyze OSN regeneration upon Triton X-100 injury. 84

Figure 4.20. Quantitative analysis of OSN regeneration upon Triton X-100 injury. 86

Figure 4.21. Identification of HBC-like cells in the intact zebrafish OE. 90

Figure 4.22. Krt5/BrdU double-positive HBC-like cell respond to Triton X-100 treatment. 92

Figure 4.23. Quantitative analysis of active HBC-like cells. 94

Figure 4.24. Analysis of BrdU-labeled HBC-like cells in intact and restored OE. 97

Figure 4.25. Diluted Triton X-100 solutions affect the OE. 99

Figure 4.26. HBC-like cells respond to mild chemical injury. 101

Figure 4.27. Quantitative analysis of mild injury response. 102

Figure 4.28. Positional profiling and core-sensory-specific comparison of intact and axotomized OE at 3 dpi. 104

Figure 4.29. Generation of the *Tg(krt5:EGFP)* reporter line. 105

Figure 4.30. *hbegfa* is expressed in the regenerating OE. 108

Figure 4.31. HB-EGF enhances cell proliferation in the OE. 110

Figure 4.32. HB-EGF enhances neurogenesis. 113

Figure 4.33. GM6001 impairs regenerative proliferation. 116

Figure 4.34. Analysis of GM6001-mediated suppression at 1 dpi. 117

Figure 4.35. Marimastat impairs regenerative proliferation. 119

Figure 4.36. Analysis of Marimastat-mediated suppression at 1 dpi. 121

LIST OF TABLES

Table 3.1. List of primary antibodies used in this study. 35

Table 3.2. List of secondary antibodies used in this study. 36

Table A.1. List of chemicals and reagents 186

Table B.1. List of disposable and non-disposable equipments 189

LIST OF SYMBOLS

bp	Base pair
dpf	Days post fertilization
dpi	Days post injury
dpp	Days post pulse
G	Gauge
hpi	Hours post injury
kb	Kilobase
L	Liter
M	Molar
ml	Mililiter
mM	Milimolar
mg	Miligram
ng	Nanogram
pM	Picomolar
μg	Microgram
μl	Microliter
μm	Micrometer
°C	Celcius

LIST OF ACRONYMS/ABBREVIATIONS

Ascl1	Achaete-Scute Family BHLH Transcription Factor 1
AOB	Accessory Olfactory Bulb
Axt	Axotomized
BrdU	5-Bromo-2'-deoxyuridine
BSA	Bovine Serum Albumin
cDNA	Complementary DNA
CldU	5-Chloro-2'-deoxyuridine
DIG	Digoxigenin
DNA	Deoxyribonucleic Acid
dNTP	Deoxyribonucleic Acid
EDTA	Ethylenediaminetetraacetic acid
EGF	Epidermal Growth Factor
GBC	Globose Basal Cell
HBC	Horizontal Basal Cell
HB-EGF	Heparin-Binding EGF-like Growth Factor
HuC/D	Hu Protein C/D
IdU	5-Iodo-2'-deoxyuridine
IHC	Immunohistochemistry
ILC	Interlamellar Curve
Krt5	Keratin 5
MMP	Matrix Metalloprotease
mRNA	Messenger RNA
MS222	Ethyl 3-aminobenzoate methanesulfonate salt
OB	Olfactory Bulb
OE	Olfactory Epithelium
OMP	Olfactory Marker Protein
OR	Olfactory Receptor
OSN	Olfactory Sensory Neuron

PBS	Phosphate Buffered Saline
PBST	Phosphate Buffered Saline with Tween-20
PCR	Polymerase Chain Reaction
PFA	Paraformaldehyde
p63	transformation-related Protein 63
pH	Potential/Power of Hydrogen
pH3	Phosphohistone H3
RNA	Ribonucleic Acid
RT	Room Temperature
OCT	Optimal Cutting Temperature
SEM	Standard Error of the Mean
SDS	Sodium Dodecyl Sulfate
SNS	Sensory / Non-sensory border
Sox2	SRY-Box Transcription Factor 2
Tr-X	Exposed to Triton X-100 treatment
Tris	Trisaminomethane
TBST	Tris-Buffered Saline and Tween-20
UV	Ultraviolet
VNO	Vomeronasal Organ

1. INTRODUCTION

1.1. Adult neurogenesis

Neurogenesis refers to the generation of functional neurons that are assembled into new or successfully integrated into existing neuronal network. During embryonic development, the majority of the neuron generation arises from progenitor cell pools that are located in the neural tube. Most neurogenesis in higher vertebrates is completed embryonically, however, various animal models demonstrate that neurogenesis does not necessarily turn off after postnatal development but may persists in specific neurogenic regions throughout life. Thus, production of multiple neuron types with divergent functions is maintained by neuronal progenitor cell pools in the neurogenic niches of central and peripheral nervous systems. Adult-born neurons go through distinct morphological maturation stages to become functional and eventually establish synaptic contacts within the already-existing neural circuit.

Although first observations date back to the first half of the 20th century, the existence of adult neurogenesis had been largely neglected by the scientific community until the late 1980s [1]. The early studies reported mitotic activities in the adult brain but it remained uncertain whether the mitotic activity gave rise to neuronal or glial lineages. Major findings were flourished in the 1960s with the introduction of thymidine-labeling methods [2]. As a milestone, Joseph Altman demonstrated the presence of newborn glia- and neuron-like populations in regenerating tissue of the lesioned rat brain [3]. The study was not entirely conclusive with respect to the identity of the generated cells, however, articles from later years confirmed the neuronal identity of the adult-born cells in different neural tissues, such as the olfactory bulb and dentate gyrus of the hippocampus [4,5]. Evidence for adult-born neurons was further supported by findings from different models such as songbirds, teleosts, and humans [6–8]. These studies show that adult neurogenesis is evolutionary-conserved among vertebrates, although its rate and competent brain regions vary among species [9].

In the last few decades, improved fate mapping, birth timing, and lineage tracing studies, such as alternatives to radioactive thymidine labeling [10] and genetic labeling using Cre/Lox recombination [11] significantly expanded our understanding of adult neurogenesis.

Adult neurogenesis is usually used as a broad term that covers all postembryonic neurogenic activities under a variety of tissue conditions. In principle, two main modes of adult neurogenesis can be distinguished: constitutive and regenerative neurogenesis in the intact and lesioned nervous tissue, respectively. Both modes share certain essential molecular pathways and mechanisms but may also show profound differences in characteristic properties, such as differences in intracellular proliferation signals, progenitor cell identity, and upstream signals that are required for the induction and maintenance of neurogenesis.

Constitutive neurogenesis can be defined as a persistent mode of continuous generation of nerve cells throughout adulthood. The lifelong persistence distinguishes this mode from other types of post-natal neurogenic events, such as delayed developmental processes [1]. Nevertheless, young neurons generated by active progenitor cells cover only a small fraction of the total neuronal population in some regions of the nervous system. For instance, Kaplan reported that only 0.011% and 0.025% of neurons were labeled with radioactive-thymidine in the rat visual cortex (30 days post impulse) and hippocampus (20 days post impulse), respectively [12, 13]. However, other neuronal structures, such as the peripheral olfactory system may show considerably higher neurogenic activity.

Constitutive neurogenesis in the adult mammalian brain occurs only in a few and spatially restricted regions. Persistent generation of neurons is only seen in specific areas that are tightly regulated by the surrounding stem cell niche. The most predominant neurogenic regions of the mouse brain are found in the ventricular-subventricular zone (V-SVZ), dentate gyrus (DG), and olfactory bulb (OB) (at which neurons arrive by migration) [14, 15].

Because neurogenic regions are restricted in space, neuronal migration is a fundamental process during the maintenance of neural tissues. In the brain, a subset of newborn neuroblasts (undifferentiated neuron precursors) migrate from the V-SVZ to their target in the OB for maturation and circuit integration, whereas neurogenesis in the DG occurs in a narrow layer called the subgranular zone and newborn neurons only show a limited migratory behavior to more apical layers within the DG [16].

Regenerative neurogenesis, which is the second common mode of adult neurogenesis, describes a set of restorative processes that occur due to non-physiological conditions. Unlike the constitutive mode, regenerative neurogenesis is not a persistent but a responsive event and is induced by a substantial change in homeostasis and/or tissue integrity. Thus, it is tightly controlled and actively repressed by molecular components in the absence of a traumatic stimulus. In the intact tissue, the quiescent state of reserve progenitor cells is essential to maintain mitotic balance. Injury and structural damage then activate quiescent progenitor cells and initiate rapid and transient cell proliferation. Regenerative neurogenesis largely depends on the presence of distinct progenitor pools, although persistently dividing progenitor cells may also participate in the regenerative response. A rapid immune response often accompanies the recruitment of dormant progenitors during regenerative neurogenesis. Acute inflammation during the time of injury is necessary for the establishment of a regenerative niche and the initiation of the proliferative response [17]. However, many of the extrinsic factors that regulate regenerative neurogenesis are not well understood. Both modes of adult neurogenesis are conserved across all vertebrates [18]. However, the extent of neurogenic activities shows a systematic decrease over evolution and higher vertebrates contain fewer neurogenic zones in their brains than lower vertebrates [9]. As introduced above, adult neurogenesis in the mammalian brain is restricted to two zones in mammals (V-SVZ, DG) once embryonic development is completed. A third region, the OB, mainly serves as a terminal organ for young interneurons migrating from V-SVZ, rather than being a separate proliferation zone itself. On the other hand, non-neuronal proliferation is more commonly seen in the brain. For instance, gliogenesis occurs frequently in fewer restrictions in the mammalian brain [19].

Neurogenesis in humans appears to share common principles with other mammalian species, however, important differences also exist. Neuronal migration from the V-SVZ to the OB appears to cease already during infancy [20]. A separate study demonstrates that the contribution of neuronal migration from V-SVZ to the neuronal pool in the OB is very low in a cohort of psychiatric patients [21]. These findings suggest that the OB is likely to generate a limited number of newborn cells locally in humans, instead of hosting only migrating neuroblasts [22]. In addition to phylogenetical differences with other mammals, the level of neurogenic activities in humans remains controversial, due to the few numbers of reported cases. A recent study reports that adult neurogenesis persists in human DG in a slow but age-independent manner [23]. In contrast, another recent study was not able to detect any newborn neurons in the same area and concludes that the neuronal generation reduces drastically after puberty, thereby opposing the idea of persistent neurogenesis in the human brain [24].

In contrast to mammals, however, adult neurogenesis is more widespread in non-mammalian vertebrates. In birds, neuronal generation occurs frequently in the lateral walls of the lateral ventricles and neuronal precursors are found throughout wide regions of the telencephalon [25, 26]. Newborn neurons migrate along radial fibers and reach various locations in the brain [27, 28]. Reptilian species also show multiple neurogenic regions, including a neuronal migratory behavior destined to the OB. As in the avian samples, a substantial amount of neural production occurs in the walls of the lateral ventricle in the reptilian telencephalon [29]. Limited studies on the adult frog brain similarly point to a greater number of proliferation compartments than reptiles, including telencephalon and other brain areas [30, 31]. The size and number of neurogenic areas are even higher in fish species. Studies on different teleost species reveal multiple proliferative areas along the entire brain axis. These areas are constitutively active and presumably serve a slow but persistent growth in brain size [9,32,33]. These studies on multiple species indicate that certain characteristics of adult neurogenesis is conserved in all vertebrates, while others may be more species- or taxon-specific.

In a life-long functional nervous system, a persistent and endogenous capacity for cell renewal is essential to compensate for any gradual neuronal loss that may occur. Although adult neurogenesis seems to occur at a low rate in humans, impairment of the process is often associated with a number of neurodegenerative disorders [34]. Understanding the mechanisms that regulate the neuron renewal under different tissue conditions and through different modes of adult neurogenesis touches on important questions related to nervous system plasticity and offers important insights into the molecular aspects of neurological disorders with a prospect for the development of therapeutic remedies.

1.2. Olfactory system

Although most of the literature on adult neurogenesis focuses on the components of the central nervous system, especially the brain, the phenomenon can also be observed in other neural systems, including peripheral sensory organs. Among these, the olfactory system is particularly interesting for its high capacity to undergo both constitutive and regenerative neurogenesis efficiently throughout life [35]. The olfactory stimuli is first recognized by the binding of the odorant to the receptors located on sensory neuron membrane. The receptor-ligand interaction activates a cascade of signaling events, resulting in the opening of cation channels and depolarization of the sensory neuron [36, 37]. The action potential that is generated by the dendrites of the sensory neuron moves down the axon terminal and is propagated into the OB and then into the higher-order centers where perception of the odorant is developed. Different odorants are recognized by a small number of receptors from a large repertoire with selective responsiveness and each odorant information is conveyed to the brain on a different neural circuit. Maintaining these circuits in the long run and rewiring them upon an intervention, such as an injury condition, require tightly controlled mechanisms. The olfactory system possesses these mechanisms in advance and conserves them evolutionarily across species.

The process of odorant detection occurs in the olfactory organs and two distinct primary organs can be recognized with the main olfactory epithelium (OE) and the vomeronasal organ (VNO). The OE is found in the dorsal nasal cavity and projects axon bundles of sensory neurons to the glomerular layer of the main OB. Glomeruli are spherical processing modules in which axon terminals form synaptic contacts with dendrites of mitral and tufted cells that project to the various olfactory cortices. The second organ, the VNO, is located in the ventral side of the nasal cavity and sends its axons to the accessory olfactory bulb (AOB), where they synapse within glomeruli. While the OE is specialized for the detection of the majority of common odorant molecules, the VNO is believed to be largely specific for the detection of pheromones [38].

The circuits between OE-OB and VNO-AOB constitute two separate and parallel pathways within the olfactory system with their own sets of sensory neurons, receptor gene families, and histochemical properties, although partial functional overlapping may occur [39]. The wiring of the olfactory conduction follows the same organization in OE-OB and VNO-AOB. In both systems, sensory neurons expressing the same receptor (therefore receiving the same chemical stimuli) converge on the same one or few glomeruli [40, 41]. An olfactory sensory neuron (OSN) expresses only one allele of a singular receptor gene from a repertoire of 1100 genes and innervate the target glomeruli from an array of 1800-2400 glomeruli [42, 43]. The numbers are smaller in teleosts; adult zebrafish has a receptor repertoire of approx. 300 genes and 80-140 individual glomeruli per OB [44–46]. In both mammalian and teleost models, hundreds to thousands of OSNs are connected to their corresponding glomerulus to transmit sensory information. The glomerular activation pattern represents a code for the identity of an odor molecule transmission of the signals to the pyriform cortex may result in smell perception.

While the main olfactory system is evolutionarily conserved among vertebrates, not all species are equipped with the accessory VNO system. Birds and fish do not have a separate VNO or AOB and rely largely on the main OE-OB circuit for odor recognition [47]. In humans, a VNO is not readily detectable after birth and its functional relevance are subject of debate [47, 48]. The main system in VNO-lacking teleosts is expected to serve for the detection of both OE- and VNO-specific odorants, as both chemosensory receptors (ORs and TAARs) and vomeronasal receptors (V1R and V2R) are expressed in the same OE [49]. Two additional chemosensory structures have been described in mammals for olfaction: The septal organ of Masera and the Grueneberg Ganglion. The septal organ is a small cluster of sensory neurons in the air path and responds to a subset of odors that are also recognized by the OE. Molecularly, OSNs in the septal organ resembles OSNs in the OE, they express receptor genes belonging to OE-specific receptor families and send their axonal projections to the main OE [50]. Finally, Grueneberg Ganglion is another cellular cluster at the tip of the nose, that is specialized for pheromonal communication [51]. Both septal organ and Gueneberg Ganglion are unique to several mammalian species and their functional importance has not been fully clarified.

1.3. The olfactory epithelium

In all vertebrates that are investigated so far, the main OE appears to be the most conserved organ for odor detection. Its presence is essential for a functional olfactory system, whereas VNO is absent and its functions are acquired by the OE in several species. The OE is a sheet of multi-layered tissue that is made up of three primary cell types: OSNs, basal cells, and supporting sustentacular glial cells.Odorant detection is sustained by receptors found on the dendritic surface of bipolar OSNs whose axons synapse in the OB. As mentioned before, mature OSNs express only a single receptor gene (out of hundreds or thousands of candidate genes) and converge to specific glomeruli, depending on their gene of choice. In rodents, OSNs residing in OE express receptors from OR/TAAR families, whereas OSNs in the VNO express receptors from V1R/V2R families [52–54].

Regardless of their receptor choice, all OSN bodies occupy the apical layer of their corresponding organ. Immature neurons and transit-amplifying neurally committed cells are found in the mid-layers and migrate vertically to apical layers as they mature and differentiate. In addition to the well-defined OSNs, the apical OE also hosts a sporadic, heterogeneous population called microvillous cells. Some of these cells express receptors related to chemosensation, although their functional significance and participation in the sense of smell remain elusive [55].

Basal layers, on the other hand, are populated by non-neuronal progenitor populations, which are categorized in two distinct cell types: globose basal cells (GBCs) and horizontal basal cells (HBCs). Seemingly unique to the OE [56], GBCs comprise heterogeneous progenitor cell subsets whose persistent activity is critical for constitutive OSN neurogenesis in the intact OE. GBCs proliferate frequently and are capable of giving rise to all neuronal and non-neuronal populations in the OE [57–59]. Some subsets maintain their stemness by expressing Sox2 and Pax6 [60], whereas others follow a neuronal fate by expressing basic helix-loop-helix (bHLH) proneural factors such as Ascl1, NeuroD1, and Neurog1 [61–63]. Most of GBC subsets are mitotic and neurogenic activity in the intact OE is often attributed to GBC proliferation [62, 64], although slow-cycling, label-retaining GBC subsets also exist [65].

HBCs, which constitute the second most common basal population, are found in the basalmost layer of the OE. HBCs are flat in shape and arranged distantly to each other in a single-cell layer, unlike the cluster-forming GBCs. This population characteristically expresses molecular markers such as Keratin 5 and Keratin 14, which are required for the cellular attachment to the basal lamina [66, 67]. HBCs are capable of undergoing mitosis, however, they remain mostly in a quiescent state in the intact tissue [66]. HBCs rarely contribute to OSN neurogenesis in the intact tissue but become activated upon extensive structural damage of the OE. Injury-induced HBCs undergo symmetric division to self-renew and later differentiate into active GBCs, which contribute to OSN neurogenesis to compensate for the loss after severe chemical injury [68].

A third non-neuronal population is constituted by sustentacular cells. Providing physical and metabolic support for the OE, sustentacular cellss function analogously to the neural glial cells in the nervous system [69]. Some of the OSN dendrites are enwrapped by sustentacular cells, thereby acquiring possible molecular and functional differences from naked OSNs [70]. Cell bodies of sustentacular cells are characteristically interspersed among the OSN dendrites in the apical layer and can therefore easily diffuse metabolic solutes to neighboring neurons in proximity [71]. Unlike what is observed in rodents and *Xenopus*, sustentacular cells of the zebrafish OE reside in basal layers, together with GBCs and HBCs [71–73]. This unique positioning suggests that sustentacular cells may have other functional roles in teleost OE homeostasis, that are not conserved in higher vertebrates.

1.4. The OE regeneration and different injury approaches

The OE is a unique neural organ with remarkable regenerative capacity and has been used as a neuroregenerative model for a long time. Early reports on systematic injury studies date back to the second half of the 19th century when the transection of the nerve bundle connecting the OE with the OB was used as the primary injury technique [74]. In 1940, a study from Japan extensively analyzed the retrograde degeneration caused by nerve transection in mouse OE and described an induced enhancement in mitotic activity for the first time [75]. Researchers started focusing on the neuroregenerative aspects of the OE in the late 1970s. Studies on multiple animal models demonstrated that the OE can recover from nerve transection by neurogenesis [76–78]. The epithelial recovery is followed by the reinnervation of the OB, and functional OSNs from the recovered OE can respond to odor stimulation in a short time [78]. However, the spatial organization between the transected OE and the OB after recovery appeared to be altered; some axons target different areas in the OB and some areas remain devoid of axonal projection [79]. Animals subjected to nerve transection also show alterations in odor perception [80].

Transection experiments were slowly replaced or coupled with the use of chemical agents after the 1950s, as easy accessibility of the OE surface allowed researchers to apply neurotoxic agents to the tissue directly. Early studies demonstrated that direct contact of 1% Zinc Sulfate with the OE results in rapid degeneration followed by a rapid recovery in various animals such as monkeys, frogs, and rabbits [81–83]. The nonionic detergent Triton X-100 was also shown to be an effective agent to cause a direct and reversible lesion in OE [84–86]. In the 1990s, methyl bromide at low concentration was frequently used in rodent studies, as the long-term inhalation of the gas causes the death of most OSNs and sustentacular cells in the OE, leaving only a fraction of basal cells behind. Restoration afterward is completed within eight weeks in rats [87].

The type of injury that is applied to the OE affects the subsequent regenerative response substantially. Chemical lesion provides a direct degeneration model that resembles environmental injuries that occur in the natural habitat but at the expense of cellular-specificity. On the other hand, techniques that rely on retrograde degeneration, such as nerve transection and removal of the OB (bulbectomy), affect only OSNs, thereby providing a selective injury on the tissue secondary to the axonal damage. Studies based on the use of these two fundamentally different approaches demonstrated the substantial capacity of the OE to reconstitute its integrity under different tissue conditions. It should be emphasized that different types of injuries drive different cellular and molecular components into the regenerative response. Understanding the degenerative conditions is therefore crucial to analyze the selective contribution of progenitor cells to the OE regeneration more accurately.

1.5. Cellular and molecular components of the OE regeneration

Functional OSNs are generated by basal cell populations in both intact and regenerating OE. As mentioned above, basal populations of the OE are mostly composed of heterogenous GBC subsets and homogeneous HBCs. Uniquely, sustentacular cells are also positioned in basal layers of the OE in zebrafish and are presumed to have regulatory roles in basal cell proliferation.

Progenitor cells derived from basal cell pools express developmental transcription and stem cell factors such as Sox2 and Pax6, which control the balance between self-renewal and neurogenesis in undifferentiated cells and prevent premature differentiation [60, 88]. The regulatory roles of these two transcription factors appear to be counteractive; Pax6 promotes neuronal differentiation, whereas Sox2 maintains the stemness state and expands the multipotent progenitor pool [89]. Basic helix-loop-helix (BHLH) transcription factors play important roles in the distinct differentiation steps of the neuronal lineage. As progenitor cells commit to a neuronal fate, they first start expressing proneural BHLH factor Ascl1 [90,91]. Ascl1 expression is necessary for the induction of Neurogenin-1, which is another BHLH transcription factor that acts as a regulator for differentiation in immediate neuronal precursors [91]. Neurogenin-1 expression precedes the upregulation of a third BHLH transcription factor, NeuroD1 that is required for irreversible neuronal diferentiation. Most OSNs are generated from NeuroD1-expressing progenitor cells. Genetic perturbation of NeuroD1 greatly depletes OSN regeneration but neurogenesis is not completely shut down in the OE, suggesting that alternative mechanisms may overcome the gene loss and contribute to differentiation [63]. Precursors that differentiate into immature neurons start expressing GAP-43 which is implicated in axonal growth and regeneration [92]. As the axonal projections reach their target glomeruli, OSNs characteristically express Olfactory-Marker-Protein, OMP, which has critical roles in chemosensory transduction and functional maturation of OSNs [93]. The heterogeneous GBC pools include active cells from all intermediate stages before GAP-43 expression, which is indicative of neuronal differentiation but only the early Sox2 and Ascl1-expressing cells may constitute true stem cells. On the other hand, the quiescent progenitor population is largely composed of HBCs, whose activation state is strictly controlled by the characteristic expression of p63, a member of the p53 tumor-suppressor family known for its regulatory role in epithelial quiescence [94]. Both GBCs and HBCs are capable of giving rise to all cell types [67,95], and their distinct proliferation properties result in two different modes of OE neurogenesis. Constitutive neurogenesis is maintained by persistent GBC proliferation, whereas regenerative neurogenesis relies on the injury-induced activation of HBC pools.

Slow-dividing, quiescent GBC subsets have also been implicated in the regenerative process [65], however, major reconstitutive properties of the OE are largely attributed to the transient downregulation of endogenous p63 and subsequent HBC activation, as lineage tracing experiments reveal [67, 68].

Under physiological conditions, HBCs are held in a quiescent reserve state. The quiescent state of HBCs is tightly controlled by the niche, since an unnecessary activity may result in early stem cell exhaustion and depletion, as well as overproduction of sensory neurons. HBCs are responsive to injury, however, the degree and time course of activation may depend on the type of injury. Direct disruption of the OE by chemical agents stimulates HBCs to divide, whereas selective OSN elimination by removal of the OB or nerve transection usually does not [68]. During chemically-induced OE regeneration, active HBCs are found in multiple layers in the tissue at earlier phases, as opposed to inactive HBCs that reside only in a single basal layer [96]. The occupancy of supra-basal layers by active HBCs is temporary, active HBCs differentiate into transit-amplifying heterogeneous GBC subsets and give rise to multiple lineages throughout regeneration. Meanwhile, several active HBCs of the basal layer self-renew to maintain the reserve stem cell pool. At later phases, HBCs upregulate p63 expression and become quiescent again. Regulation by p63 expression is critical for tissue renewal; genetic knock-out of p63 leads to impaired HBC development, while viral p63 overexpression suppresses HBC activation in the injured tissue [94, 96]. Thus, p63 appears to serve as an important molecular switch that regulates the transition between quiescent and active HBC states.

1.6. Zebrafish as a model for regenerative studies

Modeling neuroregeneration in vertebrates is informative yet challenging since not all organisms are equally ideal for research on tissue renewal as the extent of regenerative capacities is often inversely correlated with the phylogenetic position of a species. Regeneration in mammals, for instance, is often characterized by limited cellular proliferation and intense scar formation due to collagen production [97].

Scar-free regeneration is also present in mammals, however most of this highly restorative activity disappears postnatally [98]. On the other hand, teleosts and several amphibians possess seemingly limitless and life-long regenerative abilities, these animals can heal even severe tissue lesions and regrow amputated appendages and neuronal structures in a relatively short time. Among the lower vertebrate species, the zebrafish (*Danio rerio*) has been emerging as a versatile model for regeneration studies in multiple tissue types.

Originally imported from Southeast Asia in the 1800s, zebrafish gained global attention among scientific communities as a model organism to study vertebrate development, after George Streisinger and his colleagues established pioneering methods for cloning experiments and mutagenesis screens on embryos in the 1980s [99, 100]. Starting from the early 2000s, zebrafish were intensively used for regenerative studies of various organs, including neural tissues. While injury applied to mammalian neural tissue often results in scar formation, increased gliogenesis, and limited neuroplasticity [9,101], zebrafish can substantially compensate for the neuronal loss by rapid proliferative response both in central and peripheral nervous systems [102–104]. Using a surgical stabbing method on the zebrafish telencephalon, it has been demonstrated that radial glial-like cells at the ventricle of the lesioned hemisphere generate newborn neurons that occupy the wound area and restore the tissue architecture completely within a year [105]. A similarly high regenerative capacity on neuroplasticity is observed in the injured spinal cord, in which new motor neurons and interneurons are generated by progenitor ependymo-radial glial cells during recovery [106]. In addition to the increased neurogenesis, a remarkable feature of regeneration in the zebrafish central nervous system is its permissive nature to axonal regrowth, which is highly restricted by the inhibitory glial and extracellular environment in the mammals [107,108]. Zebrafish can undergo robust axonal regrowth upon nerve transection, resulting in morphological and functional recovery in a short time [109]. Fish subjected to severe spinal cord injury regain their swimming abilities within 8 weeks, due to the highly plastic and restorative potential of the spinal cord [110].

Regenerative neurogenesis is also well-reported in sensory organs such as the lateral line and retina [104, 111]. In the retina model, regenerative neurogenesis is sustained by dedifferentiation and subsequent proliferation of Müller glial cells upon light and stab injury [112, 113]. Certain genes encoding growth factors and cytokines are highly upregulated in the injury niche, that act as paracrine signals and stimulate the dedifferentiation and proliferation of tissue-resident Müller glial pools [104].

All the observations above demonstrate that the neuronal niche in zebrafish provides a unique and high capacity for regenerative response in multiple tissue models. This high capacity makes zebrafish an exceptionally important and informative organism for the determination of regulatory mechanisms involved in the neuroregenerative response [9,114]. Zebrafish research offers a large number of injury models which allow to investigate regenerative events from divergent aspects, such as stem cell biology, behavioral analysis, and drug screening [115–117]. In particular, its small body size and aquatic life-cycle make zebrafish a suitable model organism for neuropharmacological investigations of various chemicals, particularly water-soluble compunds. Finally, the amenability of zebrafish to transgenicity allows researchers to utilize cell-type-specific genetic systems, such as Lox-Cre technology, for cellular fate mapping, and to generate knock-in and knock-out models for the functional analysis of candidate proteins [118–120]. With these characteristics, studies on zebrafish serve as a guide for the in-depth understanding of tissue renewal across species and for the discovery of novel regenerative strategies that may be employed for other vertebrates, including humans.

1.7. The zebrafish OE: anatomical structure, cellular components and regenerative characteristics

The olfactory system has essential roles in teleost behaviors, such as migration, predator and contaminant avoidance, kin recognition, detection of food and spawning sites [121]. Fish achieve a sense of smell by detecting a large variety of odorants, including amino acids, nucleotides, bile acids, gonadal steroids, and prostaglandins [122,123]. These nonvolatile compounds do not evoke a smell sensation in humans [124].

As in all other vertebrates, odorants are detected by OSNs in fish, however, the sensory system has distinct features in fish at anatomical and histological levels. Teleosts don't have an accessory olfactory system and utilize only the OE-MOB circuit for odor detection. In zebrafish, two OEs reside at the dorsal extremity of the snout and project to OBs that are located adjacent to the rostral telencephalon [125]. Water carrying odorant molecules flows through the anterior nasal cavity, contact the OE for a short time interval and exit from the posterior outlet. The short presence of dissolved odorants in the cavity is sufficient to trigger signal transduction in OSNs. The OE comprises multiple intricately folded epithelial sheets whose apical sides are exposed to water flow. Basal sides of adjacent epithelial sheets outside the central raphe are attached to the same lamina propria and form a lamella structure, whereas epithelial sheets facing the central raphe are detached from the lamina propria to form a curved fold. The epithelial folding allows for an increase in the surface area of the OE [126] and leads to a bilaterally symmetric lamellar organization of tissue. The numbers of lamellae of each OE in a pair are equal, although this number varies between individuals. The OE is usually formed by 12-21 lamellae that are arranged radially around the central raphe [125,126] (Figure 1.1). New lamellae are persistently added from the anterior side of OE, although occasional epithelial invaginations may occur between older lamellae [126].

Each OE lamella is divided into different regions along the radial axis. OSNs are not distributed uniformly along the axis but reside only in specific locations. Borders for the region populated by OSNs (named as "sensory region") starts from the curved epithelial sheets facing the raphe (named as "interlamellar curve" / ILC) and extends radially to 2/3th of the corresponding lamella (Figure 1.1). Borders of the sensory region can be specifically determined by OSN-specific markers such as OMP, pan-neuronal RNA-binding protein HuC/D, or transient receptor potential cation channel type C2 (TrpC2) [127–129]. The non-sensory region covers the remaining peripheral epithelium which contains goblet cells and ciliated non-sensory cells with apical epithelial projections [125].

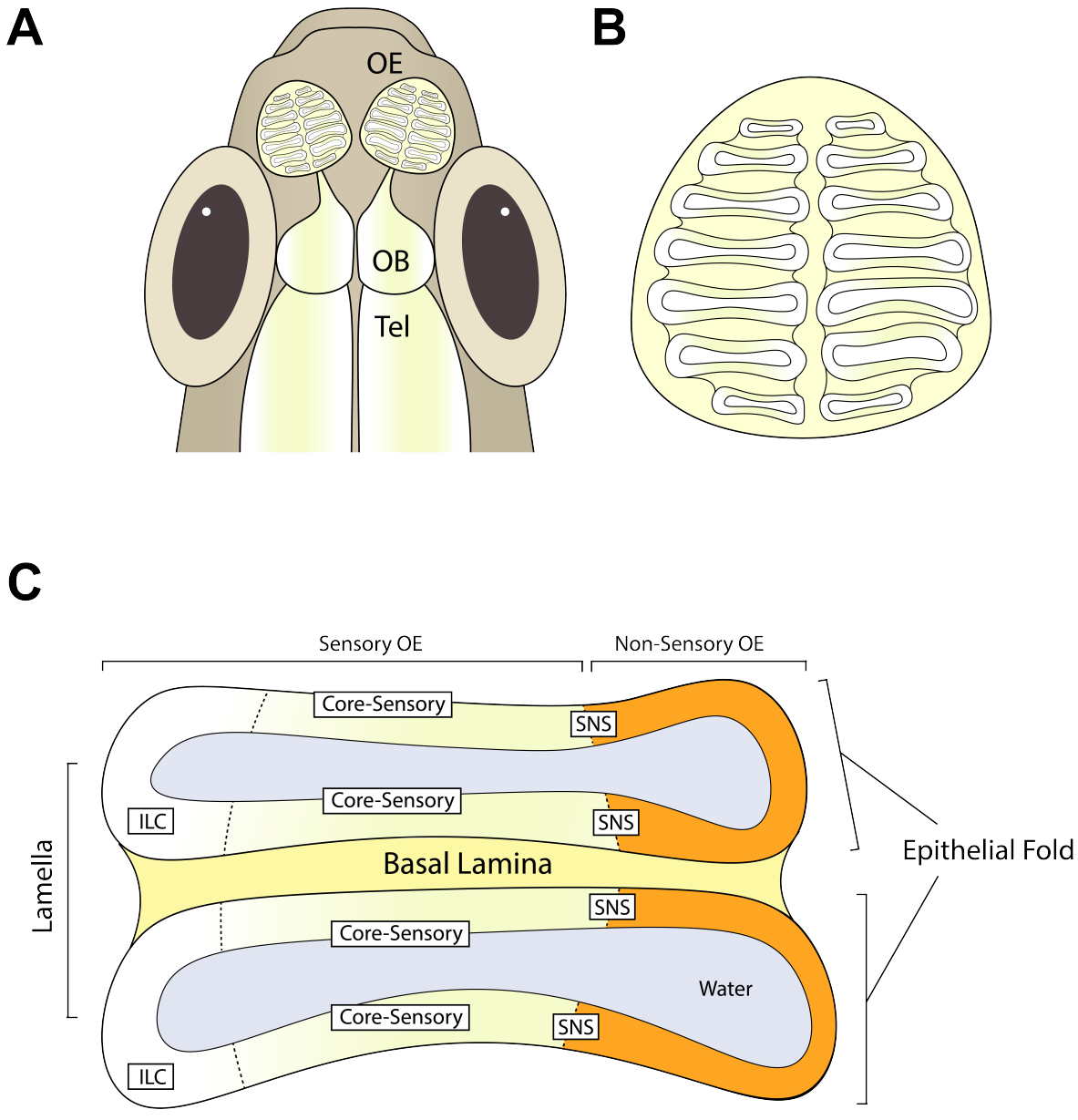

Figure 1.1. Schematic overview of the zebrafish OE. A. Localization of the OE in the body and its connectivity to the brain. Tel: Telencephalon. B. Representative horizontal view. C. Lamellar organization of the OE.

Sensory and non-sensory regions serve different functions in the tissue. The sensory region is responsible for chemosensation due to its occupancy by large OSN groups, whereas the non-sensory region supports tissue integrity by high keratin expression and houses goblet cells responsible for mucus production. The functional significance of mucus production in zebrafish is not completely understood, however, it may indirectly contribute to odor detection by protecting OSNs from hazardous materials and improving the conditions for chemosensation [130]. The distribution of different cell types in the zebrafish OE follows a baso-apical hierarchy. OSNs occupy the apical layers of the sensory region, while non-neuronal populations reside in basal layers. OSNs are comprised of five different cell types that are divergent in terms of morphology, molecular nature, and odor preference: ciliated, microvillus, crypt, kappe, and pear [125,131–134] (Figure 1.2).

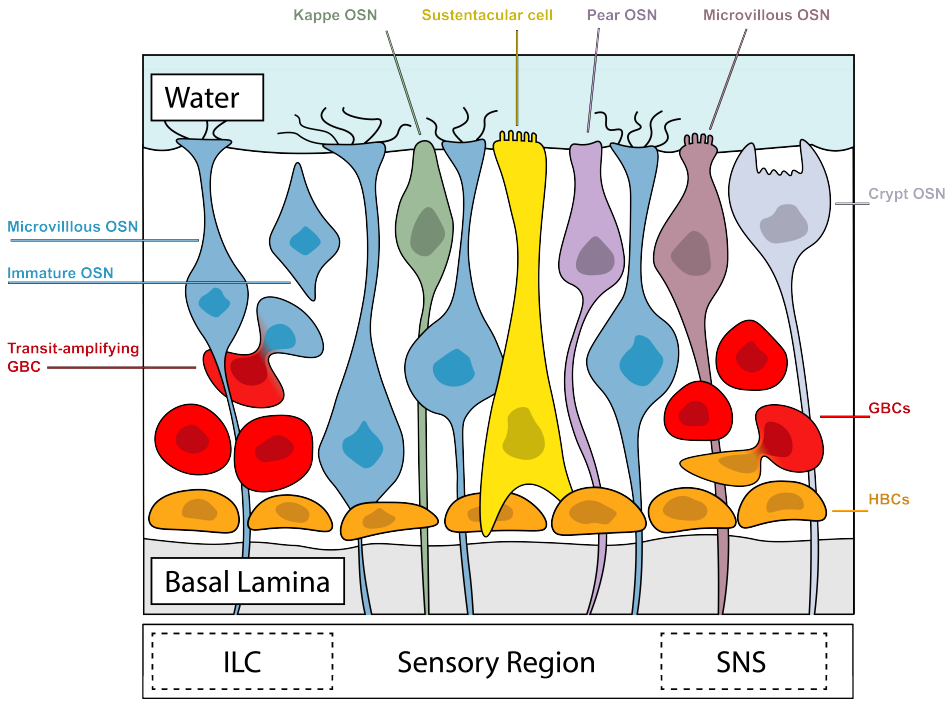

Figure 1.2. Cellular organization of the sensory OE.

Ciliated OSNs have long, apically elongated dendrites with cilia, and their cell bodies are usually found in mid-apical layers. Members of the ciliated population characteristically express a single receptor gene of OR or TAAR families [135,136].

Microvillus OSNs have thick dendrites populated by microvilli, and they are found in more apical layers that ciliated OSNs reside in. This population expresses genes from V1R and V2R families for receptor choice [137]. Ciliated and microvillus OSNs can be detected by established olfactory markers OMP and TrpC2, respectively [129]. The molecular content of microvillous OSNs appears to be different in zebrafish from the counterpart cell type in rodents, as rodent microvillus OSNs also exist but express OMP [136]. Both ciliated and microvillus OSNs are bipolar neurons specialized for signal transduction and conserved in all vertebrate models, although microvillous OSNs reside in VNO in higher vertebrates, instead of the OE [126]. On the other hand, the remaining three OSN types are low in number and appear to be unique to the fish OE.

Crypt cells, which constitute the largest population among the remaining three OSN types, have a large globular morphology and bear both cilia and microvilli in the apical portion of the cell body [125]. They are found in apical layers of the OE and can be detected by TrkA and S-100 immunoreactivity [138–140]. Details on the olfactory receptor choice of crypt neurons remain mostly unknown, although VR1-like receptor *ora4* is shown to be characteristically expressed in the majority of this cell type [141] (Oka et al., 2012). Kappe neurons with a lower occurrence in the OE show positional and morphological similarities with crypt neurons. These neurons have round shapes with microvilli on their apical somata. However, kappe neurons display a distinct G_{alpha}-olf immunoreactivity, which is not seen in crypt populations, thereby constituting a separate OSN subtype in the OE [132]. Finally, a pear-shaped OSN subtype can be distinguished from other minor OSN types by the characteristic expression of a recently identified adenosine receptor Ac2. Pear OSNs are morphologically different from ciliated OSNs, although both populations can be detected by OMP immunoreactivity. Unlike other OSN types, pear OSNs distinctively respond to adenosine by Ac2 activity and contribute to the detection of metabolites that are released from nearby organisms [134]. In addition to their molecular and functional differences, all these three OSN subtypes innervate different glomeruli in the OB [131, 132, 134], therefore cause possibly different sensations and behavioral outcomes.

Unlike OSN types, identification and characterization of different non-neuronal populations in the zebrafish OE remain largely elusive despite the large tissue area these cells occupy. Non-neuronal cell pools are positioned at basal layers of the OE and participate in metabolic and structural support to the OE integrity as well as tissue-renewal and neurogenesis. Progenitor pools in the zebrafish OE are not completely defined, however, studies on constitutive neurogenesis and injury response strongly suggest that a dual progenitor system is conserved in zebrafish, in which different multipotent cells contribute to different modes of cellular proliferation and neurogenesis under various tissue conditions [73, 86, 127]. A heterogeneous proliferating cell population is largely responsible for tissue-renewal under physiological conditions. Similar to GBCs in the rodent models, these proliferating cells express certain neuronal differentiation markers such as *dla*, *ascl1a*, and *neurod* and give rise to neuronal lineage [127]. However, the radial positions of the basally-located GBC-like cells in the OE is different from mammalian GBCs. GBC-like cell clusters are specifically localized to the radial margins of the sensory OE, unlike mammalian GBCs which are uniformly found in the basal sides of the entire OE [59]. In addition to GBC-like cells, zebrafish OE also possesses a label-retaining, slow-cycling basal cell population which are found at the basal layer of the OE as an evenly spaced, continuous cellular band. These cells show molecular similarities with HBCs of the mammalian OE and contribute to cellular proliferation upon tissue injury [73]. The radial positioning of GBC- and HBC-like cells provides the zebrafish OE with a unique and selective neurogenesis pattern that dynamically changes under different experimental conditions. Zebrafish OE also includes supportive sustenacular cells. However, unlike the apically-positioned sustenacular cells in other vertebrates [142], somata of zebrafish sustenacular cells reside in basal layers and mingle with other non-neuronal cells in the sensory OE. The somata elongate apically, providing contact with nearby OSNs. Zebrafish sustenacular cells can be distinguished by their unique cytoskeletal structures, which is easily marked by cytokeratin II immunoreactivity [73, 143]. The essential roles of sustenacular cells in zebrafish OE are not completely understood, although they may provide the OE with mechanical and metabolic support as well as contribute to the regulation of proliferative activities under different conditions.

Due to the unique positioning of GBC- and HBC-like cells in the radial axis, neurogenic activities in zebrafish OE follow a spatial pattern that is not seen in higher vertebrates. Constitutive neurogenesis occurs in either the basal side of the ILC that is facing the central raphe or of the sensory-nonsensory border where the OSN occupancy ceases ("SNS" border). Mitotic activity within the central regions of sensory OE occurs rarely. Specialization of the ILC and SNS as discontinuous neurogenic sites causes newborn cells to be concentrated in a ring-like distribution pattern on the transverse plane. This unique distribution profile show similarities with the concentric patterns of different OR-expressing OSN populations [144], therefore suggesting a zonal organization model for zebrafish OE at first glance. However, this model is misleading and doesn't fully explain the tissue dynamics in the zebrafish OE. In a zonally organized structure, the OE is divided into fixed domains and each domain is permissive to a certain set of OSNs with predefined receptor choices. In other words, different OR-expressing OSNs occupy different regions in the OE. However, sequential labeling with different thymidine analogs demonstrates that the newborn OSNs in the zebrafish OE are not confined to specific regions and are progressively shifted away from their birth zones to more central regions of the sensory OE throughout their lifespan, where they are needed to compensate for the daily cellular loss in the tissue [127]. This migratory behavior appears to be unique to teleost species as newborn OSNs of higher vertebrates don't migrate long distances in lateral directions [68,145]. The persistent lateral movement of OSNs shows that the zebrafish OE doesn't have a fixed and but a spatially dynamic organization in terms of OSN distribution. The content of the molecular cues that affect the lateral movement remains elusive, however, it appears that these cues stimulate fate-committed and differentiated cells to move to their destined positions while restricting the positions of undifferentiated progenitor cells and keeping them at the ILC and SNS. While the persistence of constitutive neurogenesis and the spatial patterning of newborn cells are sustained by position-specific GBC-like pools, the cellular response upon injury has different characteristics. Particularly, the contribution of quiescent HBC-like pools plays an important role in regenerative neurogenesis (this study).

Similar to HBCs of higher vertebrates, HBC-like cells of the zebrafish OE express characteristic epithelial markers, such as p63 and keratin 5, and are found in the basal layer in an evenly spaced order [66,67]. The proliferation properties of HBC-like cells have not been investigated in detail before, and their activation upon injury has been reported only recently [73]. Unlike mammalian HBCs, zebrafish HBC-like cells are responsive to both direct epithelial injury and selective OSN elimination by nerve transection, however, the timing and the extent of active HBC-like cell contribution to OSN regeneration appears to be dependent on the type of injury (this study). As in other animal models, the zebrafish OE shows a remarkable capacity of reconstituting itself upon injury. There are a number of injury methods that are widely used to study zebrafish OE regeneration. Nasal irrigation of neurotoxic agents is a feasible method adopted by many studies [73,86,146], although other approaches, such as mechanical stress by wax plug insertion into the nasal cavity, also exist [147]. Direct epithelial injury in the OE results in rapid and substantial loss of cells from the OSN population, followed by deafferentation of the OB which is associated with impaired olfactory function [133]. However, the tissue responds to the injury condition rapidly, and fish regain their olfactory-mediated behaviors in a short time. Nonionic surfactant Triton X-100 application into the nasal cavity leads to massive neuronal loss accompanied by a decrease in epithelial thickness within the first day. A regenerative response immediately follows the degenerative phase, reconstituting the entire tissue within a week [86] (this study). Similarly, zinc-sulfate exposure causes rapid degeneration and regeneration within two weeks [148]. Upon exposure to either of the chemical agents above, OSNs repopulate the sensory region immediately and reinnervate the OB. Regenerative neurogenesis in the injured tissue is achieved substantially by surviving progenitor populations, however, detailed identifications of these progenitor cells and molecular pathways involved in the process remain mostly elusive. Unlike constitutive neurogenesis, regenerative response in zebrafish OE is not restricted to predefined regions but occurs along the entire lamella. The observation that injury-induced proliferation follows a different spatial pattern from the persistent generation of neurons strongly suggests that a quiescent progenitor cell population with a different tissue distribution contributes to the regenerative response in the OE.

The injury-responsive nature of HBC-like cells strongly suggests that these cells may contribute to tissue renewal and be responsible for the robust increase as well as altered spatial distribution profile of proliferating cells during recovery. The induced alterations in proliferation activities are transient, as the HBC-like cell proliferation ceases and cells return to their quiescent state, once the tissue recovery is substantially over (this study).

1.8. Importance of extracellular environment in the regenerative response

Despite the advanced techniques that allow us to monitor the OE recovery precisely, very little is known about the immediate molecular changes in the injured tissue. Various fundamental pathways are believed to be either triggered or suppressed by the corrosive nature of the injury agent. Revealing the signaling pathways that are involved in the activation of quiescent progenitor cells is essential to comprehend the molecular mechanisms behind regenerative neurogenesis, which may help us gain insight into new potential therapies for critical neurodegenerative disorders.

The neurogenic niche is a complex environment that is regulated by the balance among various cellular and extracellular components (chemokines, cytokines, ions, etc.). Certain events, such as increased ROS concentrations and robust inflammatory responses in a persistent and recurring way are largely regarded as detrimental to the nervous system [149, 150]. On the other hand, there is growing evidence on the beneficial effects of these events during the onset of the regeneration [17, 151]. It was recently demonstrated that endogenous ROS release mediates the repositioning of the notochord cells, which are essential for the regenerative response, to the wound site after tail amputation in zebrafish [152]. Similarly, an acute release of inflammatory components is required for the initiation of regenerative neurogenesis in the brain [17]. These studies indicate that the molecular alterations in the niche at the onset of regeneration may provide favorable conditions for neurogenesis in the long run, despite their potentially detrimental effect on the surviving cells if inflammatory conditions persist for a long time.

Among the factors associated with the regenerative response, the EGF family member heparin-binding epidermal growth factor-like growth factor (HB-EGF) appears to play vital roles in tissue repair. HB-EGF is synthesized as a membrane-bound protein that can be found either in soluble or transmembrane form in the tissue under different conditions. Similar to ROS and cytokines, elevated levels of endogenous HB-EGF can have detrimental outcomes; its expression is widely seen in tumors and associated with the acquisition of tumor aggressivemess [153, 154]. On the other hand, it has been demonstrated in several models that the active form of HB-EGF is involved in tissue repair throughout the body [155–157]. Biological roles of HB-EGF have not been investigated in the context of the OE regeneration before, however, its transient and robust upregulation at mRNA level upon chemical injury suggests that HB-EGF may influence signal transduction under injury conditions (this study).

1.9. Molecular interactions and functional significance of HB-EGF

HB-EGF is a transmembrane glycoprotein with an EGF domain and a heparin-binding domain that provides a high affinity for heparin and heparan sulfate glycoglycans [158]. It acts as a ligand for receptor tyrosine-protein kinase receptor EGFR (ERBB1; Her1; EGFR) and ERBB1/ERBB4 heterodimers at high affinity [159, 160]. HB-EGF promotes signal transduction through different combinations of ERBB1 and ERBB4 receptor dimers [159] and initiates molecular events leading to cell growth, proliferation, and migration [161, 162]. ERBB1/4 signaling regulates various downstream pathways, such as MAPK/ERK, AKT-PI3K-mTOR, and JAK/STAT, that have critical roles in cell physiology [163, 164]. Figure 1.3 describes the ERBB1/4 dimerization and downstream signaling pathways. Besides being a ligand for ERBB1/4 signaling, the transmembrane form of HB-EGF also acts as a receptor for diphtheria toxin [165]. HB-EGF is initially synthesized as a membrane-bound protein known as proHB-EGF. This form, which can serve as a receptor for diphtheria toxin sensitivity, acts on cells in proximity through juxtacrine signaling. The transmembrane form of HB-EGF is believed to be growth-inhibitory and have cytoprotective roles on epithelial cells [166,167].

Proteolytic cleavage of the extracellular domain, on the other hand, allows the factor to become soluble, diffuse to distant locations, and act as a ligand. This particular type of cleavage is known as "ectodomain-shedding" and performed by a variety of metalloproteases (also called "sheddases" in this context), including matrix-metalloproteases (MMPs) and a disintegrin and metalloproteases (ADAMs) [168]. In the ADAM family, which is composed of 33 members, ADAM 10, 12, and 17 are believed to be the primary sheddases involved in HB-EGF ectodomain shedding [169]. Because excessive sheddase activity is often followed by a subsequent elevation in active/soluble HB-EGF levels in various cancer types, certain pharmacological strategies target at inhibiting the activity of aforementioned ADAMs in order to suppress the activation of HB-EGF-mediated cascades in tumor cells [170, 171].

Functional studies on the soluble form of HB-EGF date back to the early 2000s. Experiments in knock-out mice demonstrated the necessity of the growth factor in cardiac development [172] . The absence of HB-EGF during embryogenesis results in high mortality while surviving mice develop critical malformations such as abnormal valve formation and cardiac hypertrophy [172, 173]. Prolonged overexpression of HB-EGF during embryogenesis can also have adverse effects, such as fibrosis in the pancreas [174]. However, different tissues respond differently to the overexpressed conditions. For instance, infant mice, whose intestine overexpress HB-EGF locally, develop resistance to necrotizing enterocolitis [175].

Studies on HB-EGF's role in organ development are limited due to the high mortality rate of knock-out models, however, its involvement in regeneration is well-reported in multiple adult tissues. In the skin, elevated levels of active HB-EGF are found in the burn wound fluid. Immunohistochemical analysis detects HB-EGF abundance in regenerating epithelial cells. HB-EGF expression is uniformly distributed within the wound site. In contrast, the expression is sharply restricted to the basal epithelium in the intact tissue [176]. An increase in HB-EGF levels is also observed under other stress conditions, such as exposure of the tissue to oxidative agents or excisional wounds [177, 178].

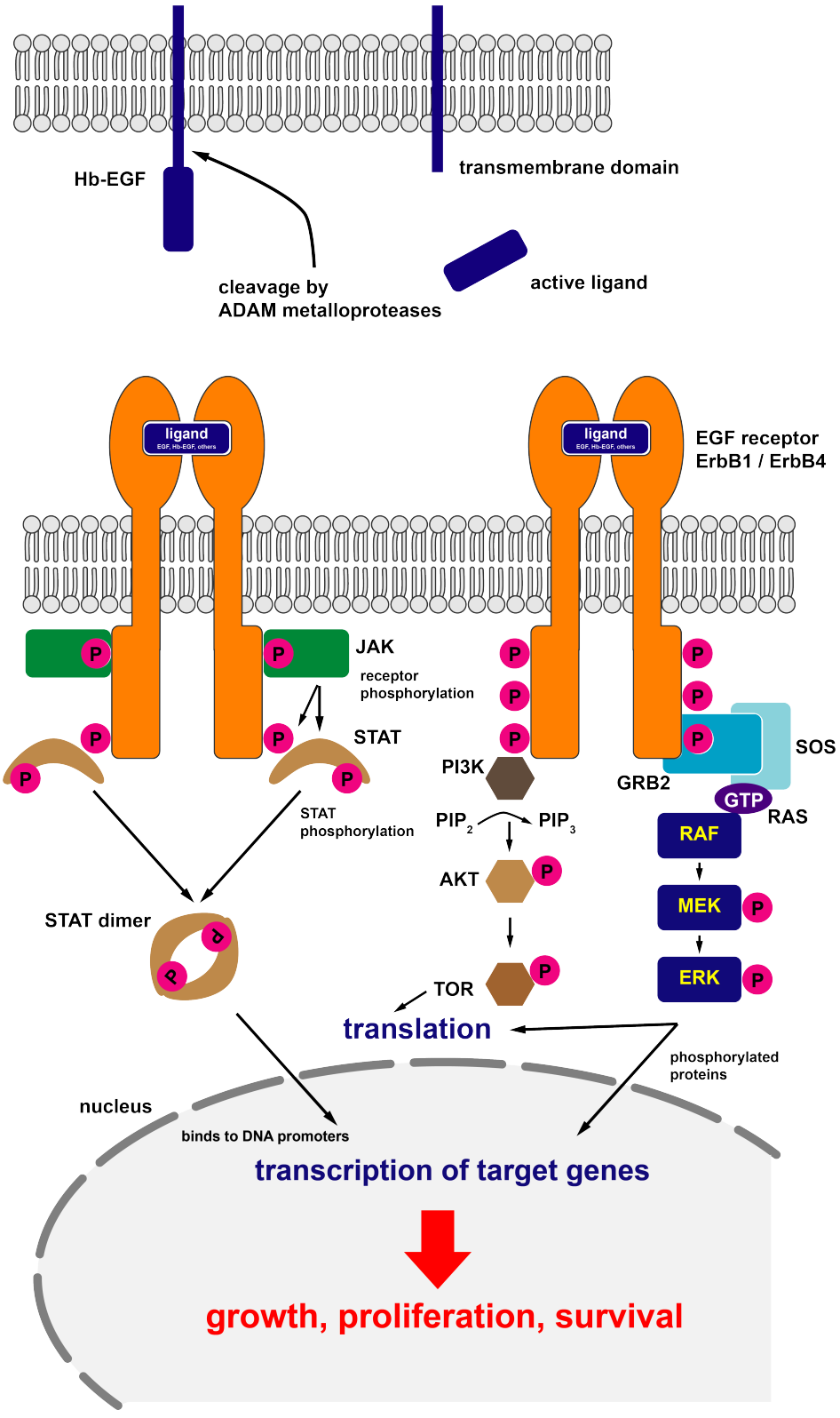

Figure 1.3. Schematic diagram of HB-EGF signaling and downstream pathways.

During skin restoration, HB-EGF promotes keratinocyte migration rather than proliferation, as it is shown that cell migration but not cell growth is impaired in HB-EGF deficient mice [179]. On the other hand, the release of the growth factor in the liver has a mitogenic influence on hepatocytes. HB-EGF drives hepatocytes through cell cycle in the partial hepatectomy model, leading to enhanced proliferation after injury [180]. HB-EGF deficiency also increases the risk of fibrosis, which is an outcome of the failed restoration, after chronic liver injury [181]. In the brain, endogenous protein levels of HB-EGF are higher than of other EGF ligands and HB-EGF contributes to neuronal survival as well as cellular proliferation [182]. Exogenous delivery of HB-EGF promotes neurogenesis; mice, in which neurogenesis declines by age, show enhanced proliferation in the DG and V-SVZ when HB-EGF is infused into the lateral ventricle [183]. Hypoxic and ischemic conditions also promote HB-EGF expression. The upregulation is mainly associated with the subsequent induction of neurogenesis upon injury [184]. The exogenous administration of HB-EGF is shown to enhance regenerative neurogenesis effectively after injury. Administration of recombinant HB-EGF intracerebroventricular administration enhances precursor proliferation after focal cerebral ischemia, although the number of newborn cells showing migratory behavior is reduced [185]. Adenoviral approach to recombinant HB-EGF delivery also leads to increased neurogenesis. Unlike in the case of intraventricular injection, enhanced regenerative neurogenesis is accompanied by increased numbers of migrating cells to the lesion site in the viral method [186]. Intranasal administration, as a third method for HB-EGF delivery, is also capable of promoting both subventricular proliferation and newborn cell migration to the demyelinated lesion when the corpus corpum is chemically damaged [187].

Finally, recent studies point out the involvement of HB-EGF in the regenerative processes of sensory organs. So far, the most comprehensive work has been done in the retina. HB-EGF's influence on the retina is seen in ischemic injury models, where breakage of the blood-retinal barrier causes edema [188]. Retinal edema has many cytotoxic outcomes, including the swelling of Müller glia cells, which constitute the essential progenitor population in the tissue [189].

HB-EGF has a neuroprotective role in Müller glia physiology, and its expression hinders cell swelling after ischemia [188]. In addition to its neuroprotective effects, HB-EGF is also necessary for retinal regeneration after direct physical injury [113]. Moreover, exogenous administration of active HB-EGF stimulates neurogenesis in the uninjured retina by inducing glial dedifferentiation and the following proliferation [113].

As mentioned above, the biological roles of HB-EGF in the OE have not been investigated before. However, a previous study demonstrates that HB-EGF's primary receptor EGFR is characteristically expressed in HBC populations, although its functional significance remains elusive [190]. This important evidence for EGFR-signaling and the injury-induced upregulation of the growth factor make HB-EGF an ideal candidate for analysis, which may have crucial involvement in the OE regeneration.

2. PURPOSE

The identification and characterization of progenitor cell populations in the zebrafish OE, that play role in different modes of neurogenesis are not investigated in detail. To maintain continuous OSN replacement, progenitor cells proliferate and differentiate into young OSNs throughout life in the zebrafish OE. Importantly, the molecular and positional balance between different progenitor cell pools regulates the selective induction of different neurogenesis modes under various tissue conditions. An in-depth understanding of the OE regeneration requires detailed temporal profiling of the actively proliferating cells as well as identification of signaling molecules that affect the activation of progenitor cell pools that remain dormant under physiological conditions. In this study, as my first aim, I investigated the regenerative capacity of the OE and characterized the tissue response under different tissue conditions by using extensive chemical and cell-type-specific physical injury models. To show the robust yet reversible change in tissue dynamics upon chemical injury, I quantified the sensory area occupied by OSNs throughout regeneration and analyzed the number and positions of proliferating cells by BrdU incorporation assay. In addition, to demonstrate the presence of a dormant progenitor cell pool in the OE, I labeled proliferating cells selectively with different thymidine analogs before and after chemical lesioning.

For further analysis of injury-responsive cells, I investigated the contribution of HBC-like cells to the tissue response, that proliferate characteristically upon chemical stress conditions. HBC-like activation and OSN regeneration were also spatially analyzed after OSN-specific ablation and compared with the tissue response upon extensive and nonspecific chemical insult. Finally, transcriptome analysis throughout the OE regeneration after chemical injury was performed to elucidate molecular components that may have critical roles in HBC-like cell activation. The analysis showed transient yet robust upregulation of *hbegfa*, the transcript of an EGF-related peptide which is known for its involvement in regenerative events in multiple tissue types.

To demonstrate the stimulatory role in the OE, I administered exogenous recombinant human HB-EGF to the OE and assessed the effects on cellular proliferation and OSN neurogenesis. These experiments were coupled with the inhibition of endogenous HB-EGF activity by using two broad-spectrum metalloprotease inhibitors on the lesioned OE *in vivo*. I analyzed cellular proliferation quantitatively and spatially to assess the suppression in the OE regeneration upon drug treatment.

3. MATERIALS AND METHODS

3.1. Materials

3.1.1. Animals

Adult zebrafish (*Danio rerio*, 6 months of age and older) used throughout this study were provided by a local pet shop and handled at the research animal facility of Boğaziçi University Center for Life Sciences and Technologies.

3.1.2. Equipments and supplies

A detailed list for the chemicals and reagents used in this study can be found in Appendix A. Disposable and non-disposable equipments are listed in Appendix B.

3.1.3. Buffers and solutions

Buffers and solutions used for zebrafish maintenance were prepared according to [191]. Other buffers used in molecular biology experiments were described in corresponding sections.

3.2. Methods

3.2.1. Adult animal husbandry

Animals were kept in 1L, 3L, or 10L freshwater tanks at a constant 28°C and under 14/10 hr light/dark cycle with a stocking density of 5 fish/L. Tanks were connected to an automated fish housing system that provides continuous filtration, aeration, and ultra-violet sterilization (Stand Alone System, Aquatic Habitats). The major ion balance of the artificial freshwater was supplied by dissolving 2 g sea salt, 0.84 g $CaSO_4$ and 7.5 g Na_2CO_3 in 100 L of reverse osmosis water. Fish were fed twice a day with dry flake, live brine shrimp larvae (*Artemia sp.*), and frozen food cubes made from brine shrimps, worms, and algae.

The use of experimental zebrafish for this study has been approved by the Institutional Ethics Board for Animal Experiments at Bogazici University (BÜHADYEK) under titles 2012-11-28 ("Olfactory neurogenesis during tissue maintenance and repair"), 07.09.2018 ("The role of heparin-binding epidermal growth factor (HB-EGF) signaling during regenerative neurogenesis in the zebrafish olfactory epithelium"), and amendment 2020-17. All experiments and procedures were performed in accordance with relevant guidelines and regulations, including the National Animal Protection Act (Turkish national law number 5199, "Hayvanları Koruma Kanunu", published 24.06.2004), the directive 2010/63/EU of the "European Parliament and the Council of 22. September 2010 on the Protection of Animals Used for Scientific Purposes" and the "Guide for the Care and Use of Laboratory Animals" (NRC2011) of the Association for Assessment and Accreditation of Laboratory Animal Care (AAALAC).

3.2.2. Breeding and embryo handling

In order to generate embryos for genetic material microinjection, female and male adult zebrafish were placed in a breeding tank with approximately 500 ml artificial freshwater during the evening.

Fish were kept in the breeding tank to acclimate to each other until the next morning and separated with a removable glass divider to control the timing of spawning. The spawns were collected via a Pasteur pipette 15-30 minutes after the divider was removed in the morning and transferred to petri dishes filled with E3 embryo medium. The medium was daily renewed and dead embryos were removed from the petri dish. Five days after fertilization, larvae were transferred into freshwater-containing chambers and fed with unicellular protozoan *Paramecium caudatum*. until they grow up to the size in which they can consume dry flake.

3.2.3. Chemical lesions on the OE

Adult fish were anesthetized with 0.03% MS222 solution (Sigma) until they become unresponsive to tail pinch but maintained opercular movement. Fish were then removed from the water and transferred into the groove of either a wet paper-tissue or a sponge surface under a stereomicroscope. As standard irrigation procedure, approximately 1 μl of solution of 1% Triton X-100 and 0.1% phenol red in 0.1 M PBS was applied to the right naris with a pulled-out glass capillary tube for 90 seconds. The detergent solution was then flushed away by rapid irrigation of freshwater and fish were placed back in their tanks.

3.2.4. Olfactory nerve axotomy

Adult fish were anesthetized with 0.03% MS222 solution and placed onto a wet paper-tissue surface under a stereomicroscope. Axotomy of the nerve bundle was carried out as described in [192]. An insulin needle (size: 30G) or a microblade was used to penetrate through the epidermis dorsally. The needle/blade was positioned 1 mm caudal of the OE and inserted 3 times at a slant angle of 45°. Immediately after the procedure, fish were put back to freshwater tanks for recovery.

3.2.5. HB-EGF administration to the OE

Adult fish weighing approximately 1 g were given 1 μg of human recombinant HB-EGF (RD Systems). Anesthetized fish were placed into the groove of a paper tissue under a stereomicroscope with heads protruding slightly. A 200 μl pipette tip was cut with a scissor to widen its opening and placed into the mouth. Pipette entrance of the tip was connected to 0.015% MS222 solution on a with a plastic hose. The tank containing anesthetic solution was put on a flat surface above the stereomicroscope and water flow was caused by the force of gravity. An attached plastic switch was used to adjust the flow rate. The administration was not performed before fish remained immobile except for the opercular movement. The OE of anesthetized fish was irrigated with approximately 5 μl of 200 ng/μl HB-EGF dissolved in 0.1% BSA/PBS solution.

3.2.6. Drug administration

Metalloprotease-inhibitory agent solutions used in this study were either given intraperitonally (Marimastat - Sigma M2699) or dissolved in freshwater (GM6001 - Tocris 2983). Before intraperitoneal injection, Adult fish were anesthetized with 0.03% MS222 and placed into the groove of a sponge surface. The fish were positioned with the abdomen up and gills in the trough. A 0.5 ml U100 insulin syringe (size: 30G) was used to penetrate into the midline between pelvic fins. The maximum volume of injected material did not exceed 50 μl.

3.2.7. Tissue collection

To dissect the peripheral olfactory organ, adult fish were euthanized by chilling in ice water, which results in instant hypothermic shock [193]. 10 minutes after the last opercular movement, each animal was decapitated for tissue dissection. Heads were then placed in a plastic dissection dish filled with ice-cold 1X PBS. The OEs were separated from cranial bones and skin tissues were peeled off by fine forceps. For *in situ* hybridization, the dissection was performed with DEPC-treated 1X PBS.

3.2.8. Cryosectioning of tissue samples

For immunohistochemistry, dissected OEs were immediately placed in rubber molds filled with optimal cutting temperature compound OCT (Sakura Technologies). Samples were stored either at -20°C or at -80°C for later use. Once they are completely frozen, samples were sectioned in the desired thickness of 12 μm at -20°C in the pre-cooled cryostat chamber (Leica). Tissue sections were placed onto positively charged glass slides. For immunohistochemistry experiments, tissue sections were dried in the oven at 60°C for 1 hr, then either immediately used for further processing or stored at -80°C for later use.

For the immunohistochemistry assays for Ascl1, a novel heat-induced antigen-retrieval method was employed [194]. Dissected OEs were incubated in 4% PFA/PBS solution at 4°C overnight. Then, samples were washed with 0.1% PBS-T three times and then transferred to a 1.5 ml tube filled with 150 mM Tris solution at pH 9. Samples were then incubated 5 minutes at RT, followed by the heat induction at 70°C for 15 minutes. The samples were re-washed with 0.1% PBS-T three times (5-7 minutes each) and embedded in the mold with OCT solution. Frozen samples were sectioned as described above.

3.2.9. Immunohistochemistry assays on tissue sections

Borders of the glass slides were marked with the water-repellant PAP pen to create a hydrophobic barrier. Sections were rehydrated and fixed with 4% cold PFA/PBS solution at pH = 7.4 for 10 minutes. Following the fixation, slides were placed in a glass Coplin jar and washed 3 times for 5-7 minutes with 0.1% (v/v) Tween20/PBS solution (PBS-T) at RT. During the washing step, the jar was stirred gently on an orbital shaker. For immunohistochemistry assays including antibodies for detection of cell type markers with 5-Bromo-2'-deoxyuridine (BrdU) labeling, slides were treated with 4 N HCl for 15 minutes at RT to denature DNA and expose BrdU epitope [195]. HCl-induced antigen retrieval was followed by successive 0.1% PBST washes.

To avoid the unspecific binding of the antibodies to endogenous immunoglobulins, the sections were blocked with 3% (w/v) bovine serum albumin (BSA)/PBS-T blocking solution for 1 hr at RT. After the blocking solution was poured away, sections were incubated in a fresh blocking solution containing primary antibodies in a plastic chamber at 4°C overnight. The dilutions of the primary antibodies used throughout this study are listed in Table 3.1:

Table 3.1. List of primary antibodies used in this study.

Antigen	**Host**	**Dilution**	**Manufacturer**	**Reference**
Ascl1	Rabbit	1:300	Sigma HPA029217	[196]
BrdU/IdU	Mouse	1:250	Beckon Dickinson 347580	[127, 197]
BrdU/CldU	Rat	1:250	Abcam ab6236	[73, 127, 197]
Caspase-3	Rabbit	1:250	BD Pharmingen 559565	[127]
HuC/D	Mouse	1:500	Life Technologies 1661237	[73]
Krt5	Rabbit	1:1000	BioLegend 905501	[73]
P63	Rabbit	1:1000	Genetex GTX124660	[198]
PH3	Rabbit	1:250	Millipore 04-817	[127]
Sox2	Rabbit	1:1000	Genetex GTX124477	[73]

For the immunohistochemistry assays for IdU/CldU sequential labeling, sections were first incubated with mouse anti-BrdU primary antibody for IdU detection at 4°C overnight. The excess antibody solution was removed the next day and the slides were rinsed in PBS solution for 5 minutes 3 times, then washed with TBST buffer (36mM Tris, 50mM NaCl, 0.5% tween-20; pH 8.0) for 30 minutes with agitation at 220 rpm at 37°C for 20 minutes as described in [197]. High-stringency TBST wash was followed by rat-BrdU primary antibody incubation for CldU at 4°C overnight. Following the overnight primary antibody incubation, the antibody solution on the slides was gently poured into a fresh 1.5 ml tube for later re-use and stored at -20°C. Sections were washed with 0.1% PBS-T three times and then incubated with fresh 3% BSA blocking solution containing secondary antibody for 2 hours at RT in dark.

The dilutions of the secondary antibodies used throughout this study are listed in Table 3.2:

Table 3.2. List of secondary antibodies used in this study.

Conjugated Dye	Antigen	Dilution	Manufacturer
Alexa-488	Mouse/rat/rabbit IgG	1:800	Thermo Fisher Scientific
Alexa-555	Mouse/rat/rabbit IgG	1:800	Thermo Fisher Scientific
Alexa-633/637	Mouse/rat/rabbit IgG	1:800	Thermo Fisher Scientific
Cy2	Mouse IgG	1:250	Jackson Immuno.
Cy5	Rabbit IgG	1:250	Jackson Immuno.

3.2.10. Rabbit serum preparation

Approximately 1.5 ml of blood was collected from an adult rabbit in a 2 ml plastic tube. The collection was incubated at RT for 30 minutes for coagulation, then centrifuged at 4°C at 2000 g for 15 minutes. Serum was collected in a sterile plastic tube and incubated at 56°C for 30 min for heat-inactivation. Inactivated serum was immediately put on ice and stored at -20°C for later use.

3.2.11. Immunohistochemistry with primary antibodies from the same host species

Important note: The sequence of primary antibody incubation is critical for the process described below. To avoid atypical signals, treatment of a control set with primary antibodies in reverse order is advised (i.e. first staining with anti-sox2/anti-Krt5, second staining with anti-p63).

Multiple labeling with antibodies raised in the same host species (anti-Krt5, anti-p63, anti-sox2, all in rabbit) was performed according to the protocol described in [199]) Tissue collection and cryosectioning were performed as described in 3.2.7 and 3.2.8.

For immunohistochemistry, sections were processed as described in 3.2.9 until the end of the blocking step with 3% BSA/PBS. Samples were incubated in the blocking solution with 1:1000 diluted anti-p63 primary antibody at 4°C overnight. The next day, the solution was recollected for re-use, and samples were washed with 0.1% PBS-T for 15 minutes at RT 4 times, followed by incubation with 1:800 diluted Alexa-647 anti-rabbit secondary antibody in 3% BSA/PBS for 2 hours at RT in dark. The samples were washed with 1XPBS for 10 min at RT 4 times, then incubated with 10% heat-inactivated rabbit serum in 0.1% PBS-T for 3.5 hrs at RT in dark. To saturate the open paratopes in the secondary antibody, the samples were washed 3 times with PBS and once with 0.1% PBS-T for 10 minutes. To cover the epitopes of anti-p63 antibody that can be recognized in the further steps, samples were incubated with 40 μg/ml of AffiniPure unconjugated Fab fragments against rabbit primary antibody (Jackson ImmunoResearch, Cambridge, UK) at 4°C overnight in dark. Samples were washed 3 times with PBS and once with 0.1% PBS-T for 10 minutes, then incubated in the blocking solution with 1:1000 diluted anti-Krt5 or anti-sox2 primary antibody at 4°C overnight in dark. Samples were then washed with 1XPBS 4 times for 10 minutes and incubated with 1:800 diluted Alexa 488 anti-rabbit secondary antibody in 3% BSA/PBS for 2 hours at RT in dark. As the final step, samples were washed with 1XPBS 2-3 times for 5 minutes at RT.

3.2.12. *In vivo* thymidine analogue incorporation

In all BrdU incorporation assays, adult fish were incubated in a freshly prepared BrdU/freshwater mixture (30 mg/L BrdU) between 2hr – 14d with a density of 5 fish/L. For incubations longer than 24hr, BrdU/freshwater mixture was changed daily. Fish were kept in dark during and after incubation due to the light sensitivity of BrdU. For IdU/CldU sequential labeling assays, fish were initially kept in IdU/freshwater mixture (30 mg/L IdU) for 24 hours. Fish were moved to a freshwater tank for 1 or 2 days to remove unincorporated IdU molecules from the circulatory system and the OEs were lesioned as described in 3.2.3. The OE lesioning was followed by the second incubation in CldU/freshwater mixture (30 mg/L CldU) for 24 hr immediately or two days after.

3.2.13. Confocal microscopy

Digital images of immunohistochemistry samples were taken with Leica Confocal SP5-AOB and SP8 microscopes (Leica Microsystems, Wetzlar, Germany). Images were acquired using either 20X or 40X objectives at 1024x1024 and 2048x2048 pixel resolution.

3.2.14. Cell quantification and statistics

Quantifications of labeled cells in the OE were performed using Fiji image analysis software. To visualize and analyze labeled cells in the OE segments, Cells were individually marked on lamella/epithelial fold images. Marked positions were saved as regions of interest and assembled in R software environment. LibreOffice Calc spreadsheet software was used for statistical computing. Graphs were drawn in LibreOffice Calc and redesigned in Adobe Illustrator vector-based design program.

3.2.15. Total RNA extraction and cDNA synthesis

Total RNA of the regenerating and intact OEs were purified using Trizol reagent (Sigma) for transcriptome analysis and cDNA synthesis. The purification was performed according to the manufacturer's instructions and later stored at -80°C. Transcriptor First Strand cDNA Synthesis Kit (Sigma) was used for cDNA synthesis. The reaction mix was prepared with 400 ng of purified RNA and carried out as instructed in the manufacturer's guideline. Synthesized cDNA was stored at -20°C for later use.

3.2.16. Cloning and antisense riboprobe synthesis for *hbegfa* and *ascl1a*

Template sequences for antisense riboprobe synthesis were amplified from the zebrafish OE cDNA by polymerase chain reaction (PCR). Oligonucleotide primer sets were designed in Vector NTI Advance 11 and SnapGene 1.1.3 software tools.

PCR amplifications with mixtures containing, per reaction, up to 100 ng of cDNA template, 2.5 μl of 10 pM forward primer, 2.5 μl of 10 pM forward primer, 1 μl of 100 mM dNTP mix, 10 μl of 5X OneTaq standard reaction buffer (NEB) and 0.5 μl of OneTaq DNA polymerase (NEB – M0480), were performed in a thermocycler machine with an initial denaturation step of 5 minutes at 95°C followed by 30 cycles of 30 seconds at 95°C, 30 seconds at 58°C, and 1 minute at 72°C. The final volume per reaction was adjusted to 50 μl with nuclease-free water.

5 μl aliquots of PCR amplifications were loaded into 1% agarose gel made with 1X TAE buffer and 0.5 μg/ml ethidium bromide. Fragments were resolved by electrophoresis at 80-120 V and visualized by Bio-Rad Geldoc XR System. Fragments at the desired size were cut out from the agarose gel and purified by PCR clean-up kit (Roche) according to the manufacturer's instructions. Purified fragments were quantified by NanoDrop UV spectrophotometer (ThermoFisher Scientific) and an aliquot from each was re-loaded into a freshly prepare 1% agarose gel for quality check.

Purified PCR products were inserted into pGEMT-Easy T-vector (Promega). The ligation mix was prepared in accordance with the manufacturer's instructions and the reaction occurred at 16°C overnight. The ligation products were then transformed intoDH5 strain of textitE. coli by exposing cells to heat shock. 50 μl of competent cells were incubated with 5-10 μl of ligation product on ice for 30 minutes, followed by the heat shock step at 42°C for 90 seconds. Shocked cells were kept on ice for 5 minutes and incubated in 700 μl of LB Broth medium at 37°C for 1 hr. Cells were then spread on ampicillin-containing LB agar plates and incubated at 37°C for 18 hours for colony formation. Colonies were transferred onto a fresh ampicillin-containing LB-agar plate, grown at 37°C for 18 hours, and selected by colony PCR with the reaction and cycle protocols described above. One insert-specific primer and one vector-specific primer (T7 or Sp6) were chosen per reaction and reactions were performed for both possible orientations of insert fragments (2 reactions per colony). Selected colonies were grown in 5 ml ampicillin-containing LB broth at 37°C for 18 hours and plasmids were isolated by Miniprep kit (Roche).

Purified plasmids were quantified by NanoDrop UV spectrophotometer and 1.5 μg of each purification was sent to Macrogen Europe B.V. for sequencing. Received sequence outcomes were analyzed in NCBI online Blast service and SnapGene 1.1.3 software tool.

Transcript IDs and primer pairs used for amplification are listed as follows: 423 bp fragment of ENSDART00000056005.5 between ascl1a-F: 5'-GTTCGCCTGTATCC-TCATACTC-3' and ascl1a-R: 5'-GTCTATCAGGGCAAACCTTCT-3', 823 bp fragment of ENSDARG00000075121.4 between hbegfa-F:5'-TGAGGAGGAGGATGAAG-AGTATTA-3' and hbegfa-R':5-CTACATTCCCAACCCTGAAGAG-3'.

3.2.17. Riboprobe synthesis

Riboprobe constructs were linearized with restriction enzymes according to insert orientation. Linearized constructs were purified by phenol/chloroform extraction and resuspended in DEPC-treated nuclease-free water. In vitro transcription was performed with DIG RNA labeling kit (Roche). The reaction mix includes the ingredients as follows: 1 μg of linearized construct, 2 μl of 10x transcription buffer, 2 μl of DIG RNA-labeling mix, 2 μl of RNA polymerase (T7 or SP6, depending on the orientation of the insert). The final volume was adjusted to 20 μl with nuclease-free water. The mix was incubated for 2 hours at 37°C and purified by LiCl precipitation. The precipitated pellet was resuspended with 50 μl of DEPC-treated nuclease-free water. 1 μl of RNAse inhibitor was added to prevent contamination. The resuspension was then aliquoted, quantified by NanoDrop UV spectrophotometer (OD_{260}), and stored at -80°C for later use. For quality check, 2 μl of aliquot was mixed with 4 μl of formamide and 2 μ of DEPC-treated water. The mix was denatured for 5 minutes at 100°C and immediately chilled on ice. The riboprobes were resolved by electrophoresis on a freshly prepared gel and visualized by Bio-Rad Geldoc XR System.

3.2.18. Genomic DNA extraction

An adult fish (1 g) was were euthanized by chilling in ice water for 15 minutes and then quick-frozen in liquid nitrogen. The whole body was pulverized in a ceramic mortar and collected in a 50 ml plastic tube. The tissue pulver was then incubated in 10 ml of preheated lysis buffer (10 Mm Tris at pH 8.5, 5 Mm EDTA, 0.2% SDS, 150 μg/ml Proteinase K) at 55°C overnight on a rotator. The next day, 5 ml of phenol/chloroform/isoamyl alcohol (25:24:1) was added into the tube and gently mixed. Once the emulsion occurred, the mix was centrifuged at 3000-4000 g at RT for 3 minutes. The supernatant was transferred into a new tube and extracted with 2 x volume of chloroform. The last supernatant was transferred into a new tube and 1 x volume of isopropanol was added. The tube was shaken gently until DNA is visible. DNA was then gently transferred into a 1.5 ml tube and washed with 70% ethanol. The tube was dried on the table at RT (overnight, if needed) and DNA pellet was resuspended with nuclease-free water. Concentration was measured with quantified by NanoDrop UV spectrophotometer (OD_{260}).

3.2.19. *Tg(krt5:EGFP)* transgenic line generation

3kb-promoter region of *krt5*, identified by [200] was amplified using krt5-F (5'-CCATGGCTTCTGTCGTCTACG-3') and krt5-R primers (5'-CTCGAGGCACAAC-TAACGCACTCTGC-3') by Q5-high fidelity polymerase (NEB). The PCR mix is as follows: 100 ng of zebrafish genomic DNA, 2.5 μl of 10 pM forward primer, 2.5 μl of 10 pM forward primer, 1 μl of 100 mM dNTP mix, 10 μl of 5X Q5 reaction buffer (NEB), 0.5 μl of Q5 DNA polymerase. The final volume was adjusted to 50 μl with nuclease-free water. PCR was performed in a thermocycler machine with an initial denaturation step of 5 minutes at 95°C, followed by 30 cycles of 30 seconds at 95°C, 30 seconds at 64°C, and 4 minutes at 72°C. Fragments were resolved by electrophoresis at 80-120 V and purified by PCR clean-up kit (Roche). 15 ng of purified PCR product was and subcloned into pJET 1.2 blunt vector (Thermo Scientific). Transformation, colony selection, and plasmid purification were performed as described 3.2.14.

Purified plasmids were sequenced and 4 μg of a single plasmid containing the promoter region in the desired orientation were digested with NcoI and XhoI restriction enzymes. The digested fragment was then cloned into pTAL vector (pT2AL200R150G) upstream of enhanced GFP (EGFP) reporter.

To generate *Tg(krt5:EGFP)* transgenic line, transposase mRNA was first synthesized *in vitro* using mMESSAGE mMACHINE™ sp6 Transcription Kit (Invitrogen). pCS-TP vector, which contains cDNA of the transposase gene was linearized with NotI and purified either by PCR clean-up kit (Roche) or by ethanol precipitation. 1 μg of the linearized template was later used for in vitro transcription. The reaction mix was prepared according to the manufacturer's instructions but incubated for 4-6 hours at 37°C, instead of 1 hr. The synthesized mRNA was purified by either phenol/chloroform extraction reagents provided by the kit or by ethanol precipitation. After dissolved in nuclease-free water, purified mRNA was quantified by NanoDrop UV spectrophotometer and diluted to 75 ng/μl with nuclease-free water. For quality-control, 2 μl of purified mRNA was mixed with 4 μl of formamide and 2 μl of nuclease-free water and denatured at 100 °C. The denatured mix was immediately chilled on ice and then resolved by electrophoresis. The remaining aliquots were stored at -80 °C until the microinjection date. On the morning of the microinjection procedure, laid eggs were immediately collected from the breeding tanks and placed on the injection platform made of 2% agarose gel. RNA/DNA mix was prepared and filled into glass capillaries. Content of the mix is as follows: 500 ng of *Tg(krt5:EGFP)* plasmid, 0.5 μl of 1 M KCl, 0.5 μl of 0.5% phenol red solution, 1.5 μl of 75 ng/μl transposase mRNA. The final volume was adjusted to 5 μl with nuclease-free water. Approximately 1 nl of the mix was injected either into the cytoplasm or the yolk syncytial layer of the egg at the 1-cell stage at 0-30 minutes post-fertilization. EGFP expression was observed the next day under a fluorescence microscope and embryos that show fluorescence signals on their body were selected for growth. 6 months later, adult fish were placed in breeding tanks and their eggs were collected. Fish whose eggs express EGFP were selected as the F0 founder group and crossed regularly to maintain the F1 transgenic line.

4. RESULTS

The regenerative capacity of the OE is highly remarkable and has been demonstrated in a variety of vertebrate studies, including primate, rodent, amphibian, and fish models [77, 87, 126, 201]. However, an in-depth analysis of OE regeneration at the cellular and molecular level in teleost species has not been performed. One of the main aims of this study is to analyze the cellular and molecular events that occur during zebrafish OE regeneration, in comparison to similar events in rodent models. The analysis will reveal if major principles of inter- and intracellular signaling during the OE regeneration are conserved across species or whether species-specific differences exist. An important advantage of the zebrafish OE is the observation that the transitions between two complementary modes of OSN neurogenesis, the steady and constitutive generation of new neurons in the intact OE [127] and the transient but abundant generation of neurons in damaged tissue, can easily be followed over a relatively short time course [73].

The findings of this study will be presented in three parts. First, a quantitative analysis describing the overall dynamics of OE restoration after injury will be presented. In the second part, the contribution of HBC-like cell activation to OE regeneration will be characterized in detail. Lastly, findings on the molecular components that play key roles during regenerative neurogenesis will be described.

4.1. Dynamics of tissue restoration in the damaged zebrafish OE

This section aims at the characterization of cell proliferation and tissue restoration during de- and regeneration of the zebrafish OE upon injury at tissue level. First, OE degeneration by Triton X-100 and the reappearance of OSNs will be described over a relevant time course of up to 168 h post injury. This description will be followed by the spatiotemporal analysis of regenerative proliferation in the OE.

The injury-induced change in the tissue distribution of proliferating cells will be compared with the pre-defined pattern of constitutive proliferation and progenitor groups contributing to either (or both) of the proliferative activities will be distinguished through the use of multiple thymidine analogs. The effects of tissue-wide and unspecific chemical injury of the OE will also be compared with targeted nerve transection experiments that selectively affect OSNs with respect to the occurrence of proliferating progenitors and apoptotic cells. Finally, the neurogenic characteristics of Triton X-100-induced regenerative response will be revealed by immunostaining for the neuronal progenitor cell marker Ascl1 and a spatiotemporal analysis of newborn OSNs in BrdU pulse-chase experiments.

4.1.1. Degeneration of the zebrafish OE following Triton X-100 injury

The choice of injury-method has critical effects on the cellular response, the time course, and the outcome of regenerative responses. The severity and cell-type selectivity of the applied injury may not only affect the decision which cell types respond to the damage but also the time course of initiation and maintenance of the regenerative response. Unlike other structures of the nervous system, OSNs residing in the OE are not protected from the outside environment and make direct contact with diverse chemical agents that include not only odorant molecules but also harmful compounds [202]. Therefore, the integrity of the OE can easily be affected by exposure to neurotoxic agents that are applied from outside. Administration of chemical agents by nasal irrigation is a feasible and routinely followed approach in chemosensory regeneration studies, both in teleost and rodent models [85–87, 203, 204]. In this study, the nonionic surfactant Triton X-100 was used to structurally damage the OE, to destroy OE cells, and to induce the unfolding of a regenerative response. Triton X-100 is a common and affordable laboratory detergent and its corrosive effects on the unprotected OE has been documented [86, 204]. In this study, the application of the Triton X-100 solution to the zebrafish OE was performed according to the methodological approach described by [86].

The intact adult zebrafish OE is organized into a limited number of bilateral olfactory lamellae that extend from the midline raphe and which structure the OE into adjacent epithelial folds [125]. The lamellar epithelial tissue exhibits a unique polarity, in which an outer region of non-neuronal cells surrounds an inner neuroepithelium that contains OSNs, sustentacular glial cells, and various neurogenic progenitor populations. The lamellar partitions covering the outer region and neuroepithelium are referred to as "non-sensory" and "sensory" regions, respectively, due to their selective occupancy by OSNs and other functional differences. Each lamella is composed of two fused neuroepithelial tissues with opposite basal-to-apical polarity. Adjacent epithelial sheets of the same lamella are attached to a common lamina propria, which is a thin layer largely composed of connective tissue. Neighboring lamellae are connected through the extension of a single epithelial sheet that forms a U-shaped fold at the ILC close to the midline raphe.

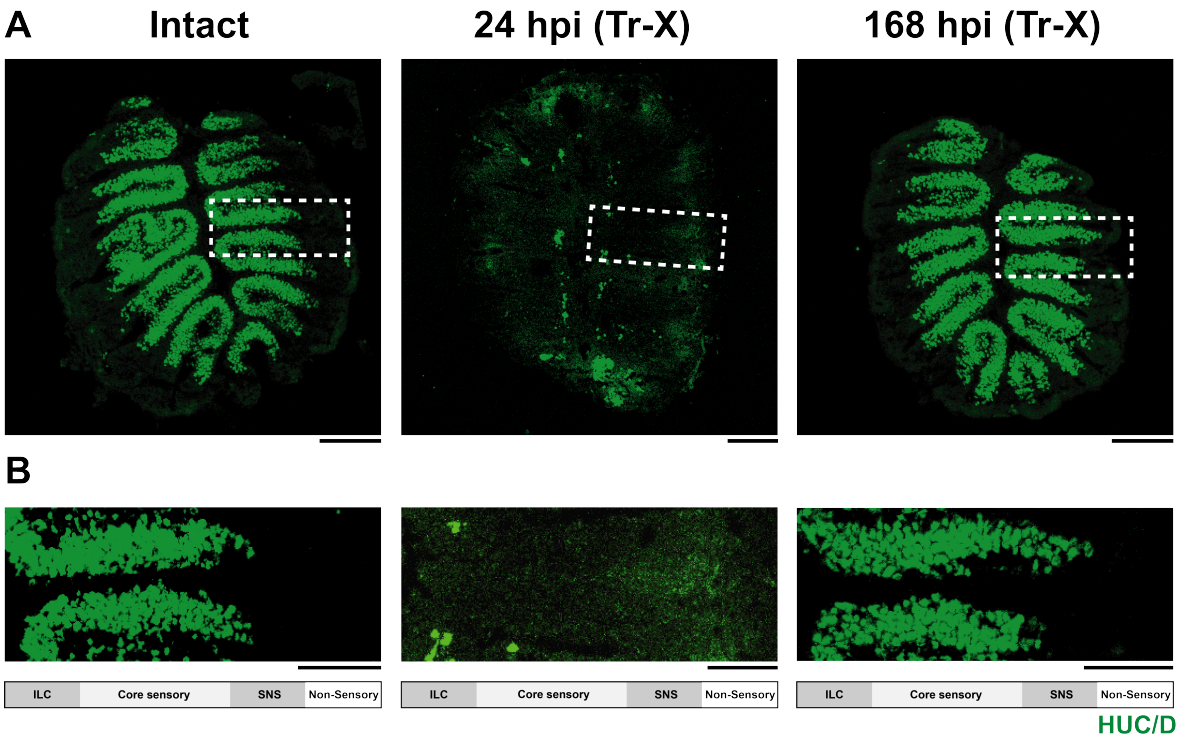

Figure 4.1. Neuronal loss and regeneration upon Triton X-100 (Tr-X) treatment in the OE. OSNs are labeled by anti-HuC/D antibody. A. Horizontal sections of dorsal OE. B. Representative high power images. Scale bars: 100 µm (A) and 50 µm (B).

The sensory and the non-sensory OE are sharply separated along the lamella and the transition can be easily determined by anti-HuC/D immunohistochemistry which selectively labels mature OSNs (Figure 4.1). Hu proteins are RNA-binding proteins that share homology with ELAV family in Drosophila [205]. Neuronal Hu proteins, HuB, HuC and HuD, are specifically found in neurons in vertebrates [206]. Occupancy of HuC/D-positive OSNs starts from the ILCs in the center of the OE and extends to the border between the sensory and the non-sensory regions (SNS) which encompasses about one-half to two/third of each lamella along the radial dimension. The sensory region covers roughly 30 to 35 percent of the entire tissue area on horizontal cross-sections through the OE (see below for a detailed analysis).

To analyze the temporal dynamics of OE degeneration and tissue restoration, the change in OSN occupancy was measured after chemical injury by the injection of 1% Triton X-100 solution (abbreviated as "Tr-X" in figures) into the nasal cavity of anesthetized adult zebrafish. The OE was exposed to the detergent solution for 90 seconds after which the solution was washed out with a jet of clean tank water. In all experiments reported here, Triton X-100 application was performed selectively on one OE and consistently to the right side, while the left OE was kept intact and served as internal control. Upon 1% Triton X-100 treatment, OSNs degenerated rapidly and most of the mature HuC/D-positive neurons were lost 24 hours post injury (hpi) (Figure 4.1). The loss of HuC/D-positive OSNs was usually accompanied by the thinning of the sensory epithelium ,as reported previously [86]. Both the thickness of the epithelial layers and OSN occupancy in the sensory region were largely restored within 168 hpi, as can be judged by the reappearance of the multilayered epithelial morphology of HuC/D-positive cells. In order to describe the time course and the magnitude of the de- and regenerative phases more accurately, The area occupied by HuC/D-positive cells was measured at different time points (4, 12, 24, 72, 120 and 168 hpi) for 3 animals per time point (Figure 4.2). The change in the HuC/D area was assessed by comparing the average values of Triton X-100-treated and intact OEs of the same fish to control for inter-individual differences in OE size.

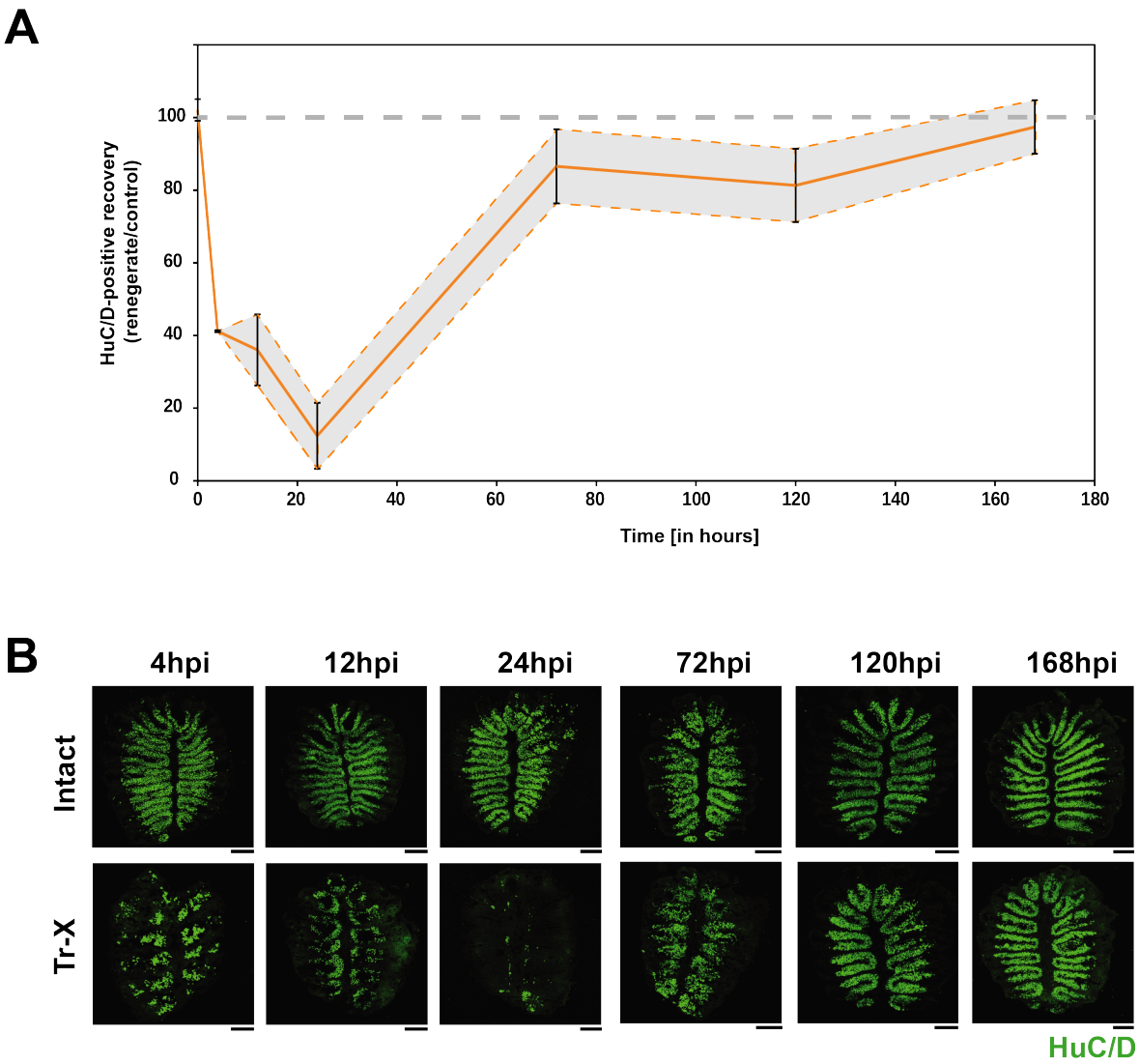

Figure 4.2. Temporal profiling of HuC/D immunoreactivity upon Triton X-100 injury. A. The recovery curve of HuC/D-positive area. Gray area represents the standard error. B. Representative sections from different time courses. Scale bars: 100 µm.

These values were normalized to the ratio of right OE values to left OE values of a separate control group (n = 3) that did not received Triton X-100 treatment. Upon injury, only 41.1 ± 0.3% (mean ± SEM) of the area remained HuC/D-immunoreactive at 4 hpi, when compared to control OEs. The loss of HuC/D-positive cells was statistically significant ($p_{(4hpi/control)}$ = 0.0004; unpaired Student's t-test, $t_{(4hpi/control)}$ = -4.3082) and most prominent around the central sections of the sensory region, where the epithelial thickness decreased most. The remaining HuC/D-positive cells no longer formed a uniform and coherent tissue and their distribution appeared fragmented, as regions with dense HuC/D-positive cell groups were interrupted by sections that were devoid of HuC/D-positive cells. Isolated clusters of HuC/D-positive cells were largely localized to the margins of the sensory regions and prominent in the curved sections of the ILC facing the inner raphe. Further OE degradation is a rapid and progressive process; and only 36.0 ± 9.7% ($p_{(12hpi/control)}$ = 3.6 x 10^{-13}; unpaired Student's t-test, $t_{(12hpi/control)}$ = -11.2601) and 12.4 ± 9.1% ($p_{(24hpi/control)}$ = 3.1 x 10^{-15}; unpaired Student's t-test, $pt_{(24hpi/control)}$l = -0.1131) of the area occupied by HuC/D-positive cells remained at 12 hpi and 24 hpi, respectively. Only small neuronal clusters could be detected at the ILC at 24 hpi, probably because the detergent could not reach efficiently into the tight space between lamellae as opposed to the more open central and peripheral regions of the sensory OE that have better access to water flow and the corrosive solution. Shortly after degeneration reached a maximum at 24 hpi, the OE transitioned to regeneration. The HuC/D-positive area increased rapidly to 86.5 ± 10.2% of the internal control at 72 hpi ($p_{(72hpi/control)}$ = 0.013; unpaired Student's t-test, $t_{(72hpi/control)}$ = -2.2464). Nevertheless, the organization of the cell groups still appeared fragmented and less dense in the injured OE than in the intact OE. The fragmented appearance of the neuronal organization vanished almost completely around 120 hpi, at which the area occupied by HuC/D-positive cells recovered to 81.3 ± 10.1% ($p_{(120hpi/control)}$ = 0.0138; unpaired Student's t-test, $t_{(120hpi/control)}$ = -2.6278). At 168 hpi, the appearance of the injured OE was virtually identical to the intact OE in terms of neuronal occupancy and tissue size and there was no statistical difference between the HuC/D-positive areas of the injured and intact OE (97.4 ± 7.4%, $p_{(168hpi/control)}$ = 0.5251; unpaired Student's t-test, $t_{(168hpi/control)}$ = -0.6435).

4.1.2. Proliferative activity in the Triton X-100-lesioned zebrafish OE

The initial loss and subsequent recovery of HuC/D immunoreactivity in the sensory region upon Triton X-100 exposure suggests the unfolding of a rapid regenerative response triggered in the OE, which most likely goes along with increased neurogenic cell proliferation. Thus, the changes in the proliferation pattern and the contribution of newly generated cells to the tissue restoration were investigated by the analysis of cell division and neuronal markers. Cells that divide within a defined time interval can be easily traced by 5-bromo-2'-deoxyuridine (BrdU) incorporation assays [207]. BrdU is a synthetic nucleoside that is incorporated into DNA during replication as a substitute for thymidine. The incorporated analog persists in newborn cells that underwent DNA replication during S-phase and is further inherited by daughter cells during subsequent cell division, allowing the fates of dividing cells to be traced over time.

Constitutively cycling cells in the intact zebrafish OE reveal a uniquely organized pattern. Abundant mitotic activities are observed consistently and exclusively around the central and peripheral margins of the sensory region at the ILC and SNS, respectively [127, 208, 209]. Although their activity rates may vary, both proliferation zones at the ILC and SNS are capable of generating the primary subtypes of OSNs in the OE, the ciliated and microvillous neurons, and do not bear a major functional difference [127]. cell division outside these two circumscribed regions can be observed; however, it occurs only sporadically and may give rise to non-neuronal basal cells in most cases.

To analyze the distribution of dividing cells in the injured OE, adult zebrafish were incubated in tank water containing 30 mg/mL BrdU for 24 hours immediately after Triton X-100 application to the OE. As in the previous experiments, only the right OE was exposed to the detergent, while the left OE was left intact to serve as internal control. At the end of the incubation period, OEs were dissected and analyzed for BrdU incorporation by immunohistochemistry.

As expected, large clusters of BrdU-positive cells could be observed at the ILC and SNS of the intact OE, preferentially on dorsal cross section. The sensory OE was largely devoid of BrdU-positive cells. However, a characteristically different distribution of BrdU-positive cells could be observed in the injured OE, that was less restricted than in the intact OE. In the injured OE, an increased prominence of BrdU-positive cells could be observed within the sensory region (Figure 4.3). Thus, tissue injury by Triton X-100 exposure induces a novel pattern for mitotic activity, that is different from the intact OE. This pattern of mitotic activity most likely includes the proliferation of additional progenitor cells that remain largely quiescent in the intact OE.

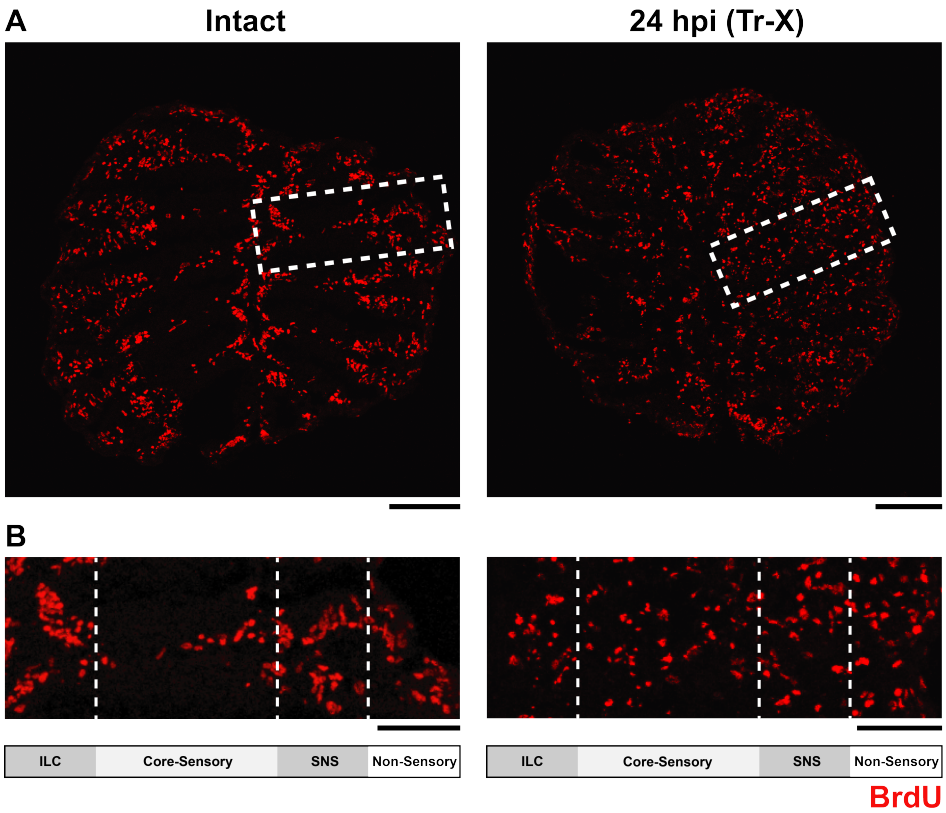

Figure 4.3. Difference in the spatial distribution of BrdU-positive cells in the intact and injured OE. A. Dorsal cross-sections of intact and injured OE samples at 24 hpi. B. High power images of individual lamellae. Scale bars: 100 µm (A) and 50 µm (B).

Triton X-100 exposure results in the rapid loss and subsequent recovery of HuC/D immunoreactivity (Figure 4.2), which was interpreted as the loss and recovery of OSNs. However, the alternative possibility that detergent treatment transiently shuts down HuC/D expression in mature neurons without causing any significant loss in neuronal population also exists. To discriminate between these possibilities and to better understand any potential link between the injury-induced proliferative activity in the sensory OE to OSN neurogenesis, injured OEs were analyzed after an extended period of BrdU incubation that covered the entire regeneration phase of 7 days. To do so, fish were kept in BrdU-containing water for one week after detergent treatment; a period which is sufficient for near-complete tissue recovery (Figure 4.2). To ensure the continuity of BrdU incorporation, the tank water was exchanged daily for freshly prepared BrdU water. Newborn cells were detected by anti-BrdU immunohistochemistry, while OSNs were detected by anti-HuC/D immunohistochemistry to visualize the relative positions of constitutive proliferation zones and newly generated OSNs (Figure 4.4).

In the intact OE, a dense population of newborn BrdU-positive cells was found close to the ILC and SNS due to continuous cycling of GBC progenitors in these positions. Different from the short-term exposure described in 4.1.2, however, most of the BrdU-positive cells at the ILC and SNS shifted towards the center of the sensory OE and were largely double-positive for HuC/D immunoreactivity, indicating that cells born in these positions are committed to a neuronal fate and had sufficient time to develop into mature OSNs (Figure 4A and 4A').

In addition, a small but obvious number of BrdU-positive cells could be detected, that were born within the sensory region. These cells were most likely generated from slow-cycling cells that became more evident after extended BrdU exposure. Interestingly, most of these cells were positioned in the basal layers of the lamella and did not show HuC/D immunoreactivity, indicating their non-neuronal identity and that few, if any OSNs were generated from the mitotic activity of these cells. These observations are consistent with previous finding showing that cell proliferation within the sensory OE contributes only to a small fraction of mature OSNs in the intact tissue [127].

In contrast, both the number and distribution of BrdU-positive cells were significantly different in the regenerated OE after one week of BrdU exposure. Almost the entire OE tissue was densely occupied by BrdU-positive cells, suggesting that most OE cells were generated in response to tissue injury and were not older than one week at the time of analysis (Figure 4.4B and B'). Unlike in the intact OE, BrdU-positive cells were not restricted to the ILC and SNS and were widely prominent in the sensory and the non-sensory regions. In addition to their increased overall occurrence, BrdU-positive cells within the sensory OE were not only found in the basal OE but in multiple layers, including the more apical layers in which amplifying progenitors and mature OSNs reside. Consistent with the near-complete OSN recovery at this point (Figure 4.2), nearly all HuC/D-positive cells were also double positive for BrdU immunoreactivity, suggesting that almost all OSNs were newly generated during regeneration. In addition, the sensory/nonsensory organization of the OE was reestablished as a sharp transition between central and peripheral OE regions could be observed in the HuC/D staining pattern.

These findings demonstrate that the spatial pattern of cell division in the injured OE is different from the pattern of mitotic activity in the intact OE. This change in proliferative dynamics is largely characterized by the induction of additional mitotically active regions within the sensory OE, that are dormant under intact physiological conditions. The spatial changes that occur in the proliferative activity disrupt the previously defined and restricted distribution of constitutively cycling cells and appears to be characteristic for the regenerative phase. More importantly, the additional proliferation sites within the sensory OE appear to be constructive and neurogenic, as a significant number of BrdU/HuC/D double-positive cells could be observed at the end of the first week of regeneration. The observation that most of the HuC/D-positive cells were also positive for the proliferation marker suggests that HuC/D expression is not transiently suppressed in OSNs after Triton X-100 exposure but that OSNs indeed undergo cell death upon the exposure and that most, except for a few surviving cells within the ILCs, are newly generated during regeneration.

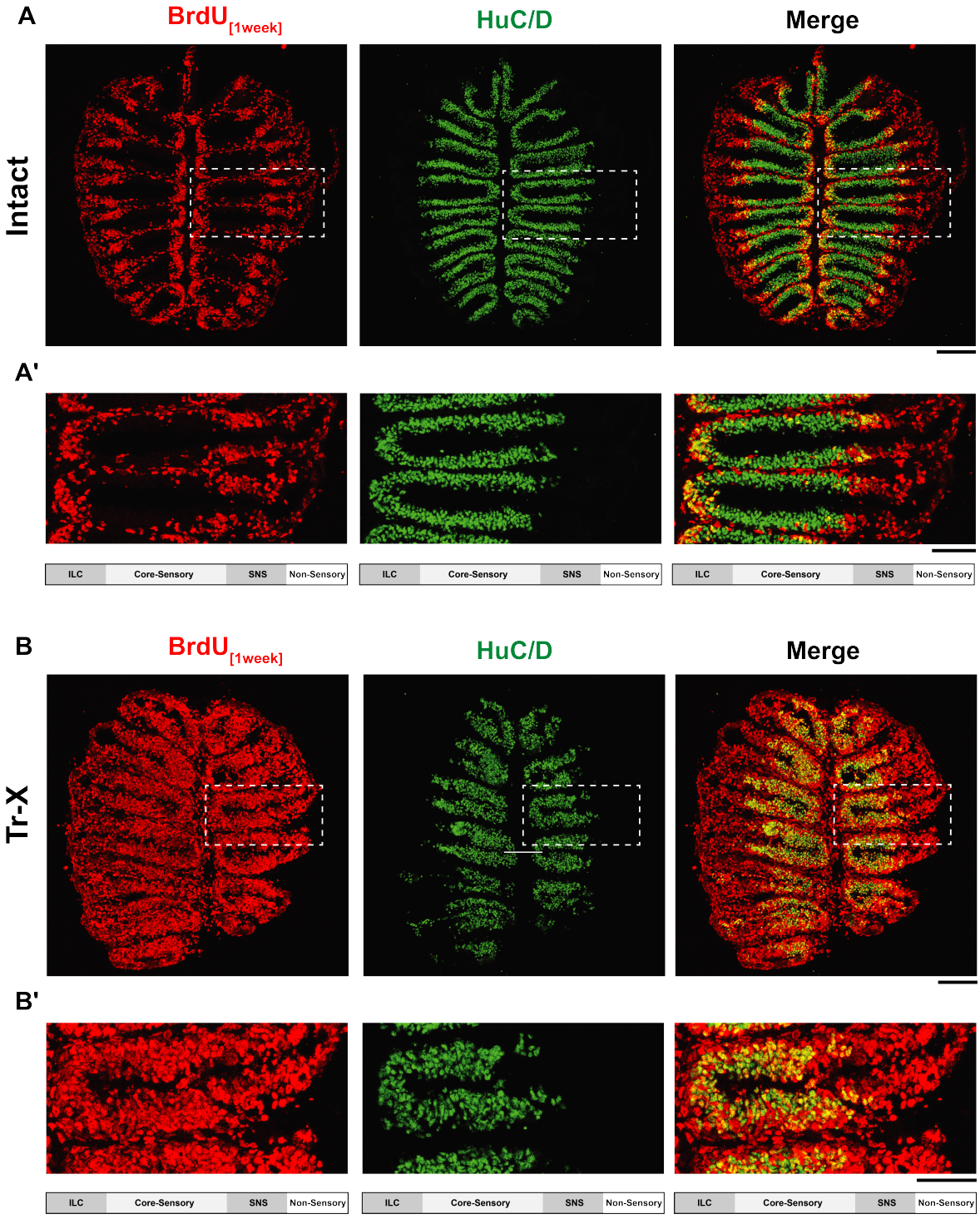

Figure 4.4. Cellular proliferation within a week in the intact and injured OE. A and A'. Whole section and high-power images of Intact OEs. B and B': Regenerated OEs. Scale bars:100 µm (A and B) and 50 µm (A' and B').

4.1.3. Analysis of the radial distribution of mitotic activity in the intact OE

In order to describe the proliferative behavior of the intact OE quantitatively, the radial distances of the positions of BrdU-positive cells to the ILC were measured relative to the total length of the lamella on which the positive cells were found. For this experiment, adult fish (n = 3) were kept in BrdU-containing water for 2 hours before the analysis, and OEs were analyzed for BrdU-immunoreactivity. To generate a unique positional index along the radial axis of the OE, the central and peripheral margins of the lamellae were defined as tissue borders and the epithelial area between these extremes was divided into 10 equidistant radial segments. Based on the in-depth analysis of the distribution profile of HuC/D-positive cells in previous work [127], two segments covering the central edge (segments: 0–0.2 in Figure 4.5A) were chosen to represent the ILC. The adjacent four segments covering the central sections of the lamella represent the rest of the sensory region (named as "Core-Sensory" in the figures), followed by another four segments that include the SNS and non-sensory OE. The SNS is composed of HuC/D-positive round cells that are neighboring to HuC/D-negative non-sensory cells with distinct elongated cell bodies extending from basal positions towards the apical surface [125]). These two distinct cell populations are densely located in close proximity to each other. Therefore, the two segments that cover the area of the transition in cell morphology (0.6-0.8) were chosen for the quantitative representation of SNS. The most peripheral segments (0.8-1) remained to describe the non-sensory region.

The positional information of each cell was normalized to the length of the lamella on which they locate to determine their scores in the radial index. Due to quantitative differences in the baseline proliferative activities between individual animals, the data are presented as frequency histograms in Figure 4.5A. Absolute cell numbers for each index score are displayed in Figure 4.5B on box plots. As expected, the majority of BrdU-positive cells that were born in the intact OE during the incubation period could be found at either of two defined proliferation zones, the ILC and SNS.

To simplify the visual presentation, the cell counts in segments belonging to the same epithelial regions were summed and represented as bar graphs in Figure 4.5C. The ILC and SNS covered 57.3 ± 1.1% (mean ± SEM) of overall BrdU-positive cells in the tissue (27.3 ± 0.5% and 30 ± 0.6%, respectively). On the other hand, only 10.5 ± 2.0% of BrdU positive cells could be found in the sensory region (excluding the ILC), despite the fact that this area corresponds to 40% of the entire tissue. The remaining BrdU-positive cells (32.1 ± 0.4%) were located in the non-sensory region. However, BrdU-positive cells in the non-sensory region are not evenly distributed and cells were found in the segment adjacent to SNS more frequently (0.8-0.9, 18.5 ± 0.1%) than in the outermost segment (0.9-1, 13.7 ± 0.2%). Thus, the positional profiling of BrdU-positive cells along the radial axis suggests a bimodal distribution of newborn cells along the lamella. One peak of this bimodal distribution is found at the ILC, while the other peak covers the SNS and the adjacent section of the non-sensory region.

4.1.4. Quantitative analysis of the radial distribution of mitotic activity in the damaged OE over time

To gain insight into the changes of the proliferation pattern after OE injury, BrdU incorporation assays were conducted on injured OEs for consecutive days of regeneration between 1 dpi and 5 dpi. The profile obtained from the intact OEs (Figure 4.5A and 4.5B) was used as control profile for comparison. Three fish per experimental time point were used for analysis. After Triton X-100 treatment, animals were transferred to freshwater tanks and the tank water was changed daily. To label newborn mitotic cells, animals were transferred to BrdU-containing tank water 2 hours prior to analysis. As can be seen in Figure 4.6, positional profiling of newborn cells revealed a uniform distribution early after injury, rather than the bimodal distribution encountered in control OE. At 1 dpi, approximately 11% of BrdU-positive newborn cells could be counted per segment across the entire sensory region (0-0.6) with only minor fluctuation in numbers. This percentage was considerable higher than the average percentage obtained from the sensory region excluding the ILC of the intact OE, which could be as low as 1%.

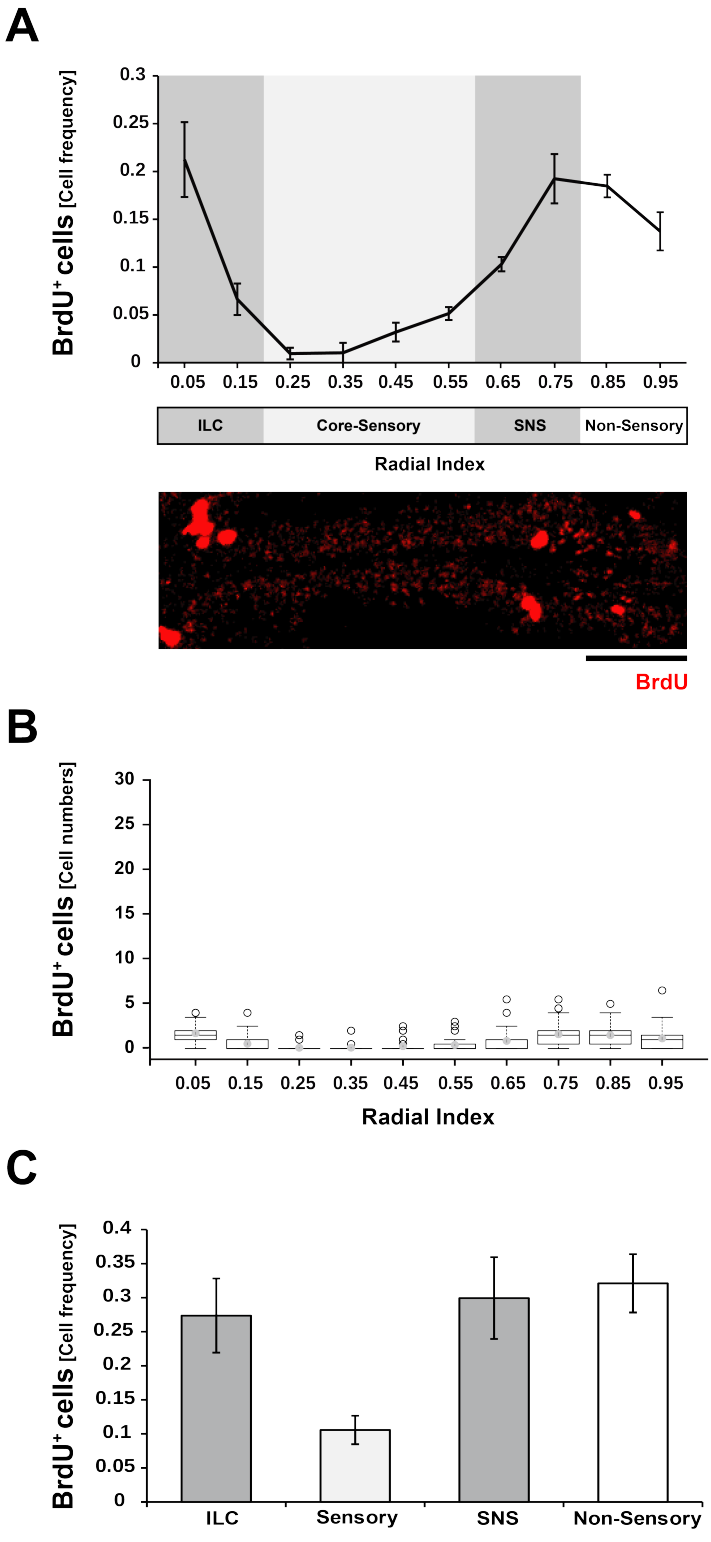

Figure 4.5. Positional profiling of newborn cells in the intact OE after 2 hr BrdU exposure. A. Frequency distribution. B. Box-plot representation. Y-axis is set to 30 for comparison with Figure 4.6B. C. Zonal distribution. Scale bar: 50 µm (A).

The increased occurrence of newborn cells within the sensory region persisted throughout the entire experimental timeline until 5 dpi. Starting at 4 dpi, a proliferation pattern with pronounced activity at the ILC and SNS could be observed again. This reversion to the two-peaked distribution pattern suggests that the regenerative response within the sensory region is transient and that the OE resumes the pre-injury activity at the ILC and SNS.

In addition to the changes in the distribution pattern that can be observed after injury (Figure 4.6A, orange curves), the absolute numbers of BrdU-positive cells per segment was also increased during regeneration, irrespective of the segment position. The box plots in Figure 4.6B show that the numbers of BrdU-positive cells in the regenerating segments increased 6.5 fold compared to the numbers in the intact OE (Figure 4.5B). A peak in the proliferative activity can be observed around 3 dpi and the increase in the overall number of BrdU-positive cells declined to 5.2 fold by 5 dpi.

4.1.5. Analysis of the proliferation rate in the regenerating OE over time

The BrdU incorporation assays described above revealed the spatio-temporal dynamics of the regeneration response in the injured OE over time. As the elevated cell numbers in Figure 4.6 clearly demonstrate, the change in the spatial pattern of the regenerating OE is accompanied by a progressive increase in the proliferation rates. However, rate estimation of fast-cycling populations only from BrdU assay can be misleading, since the analog persists in nucleus long after the end of cell division, including the nuclei of cells that divided after the end of the BrdU pulse. Therefore, BrdU labeling is a simple and efficient molecular tool to analyze cumulative long-term effects and fate-mapping. Alternatively, detection methods for mitosis-specific markers are more precisely coupled to cell divisons and allow for a better estimate for the time course of the number of cells undergoing active division. Among the complex molecular events that occur during cell division, phosphorylation of histone 3 (pH3) on serine 10 is an essential step required for proper chromosome condensation during mitosis and is widely used to reveal actively dividing cells by anti-pH3 immunoreactivity [210].

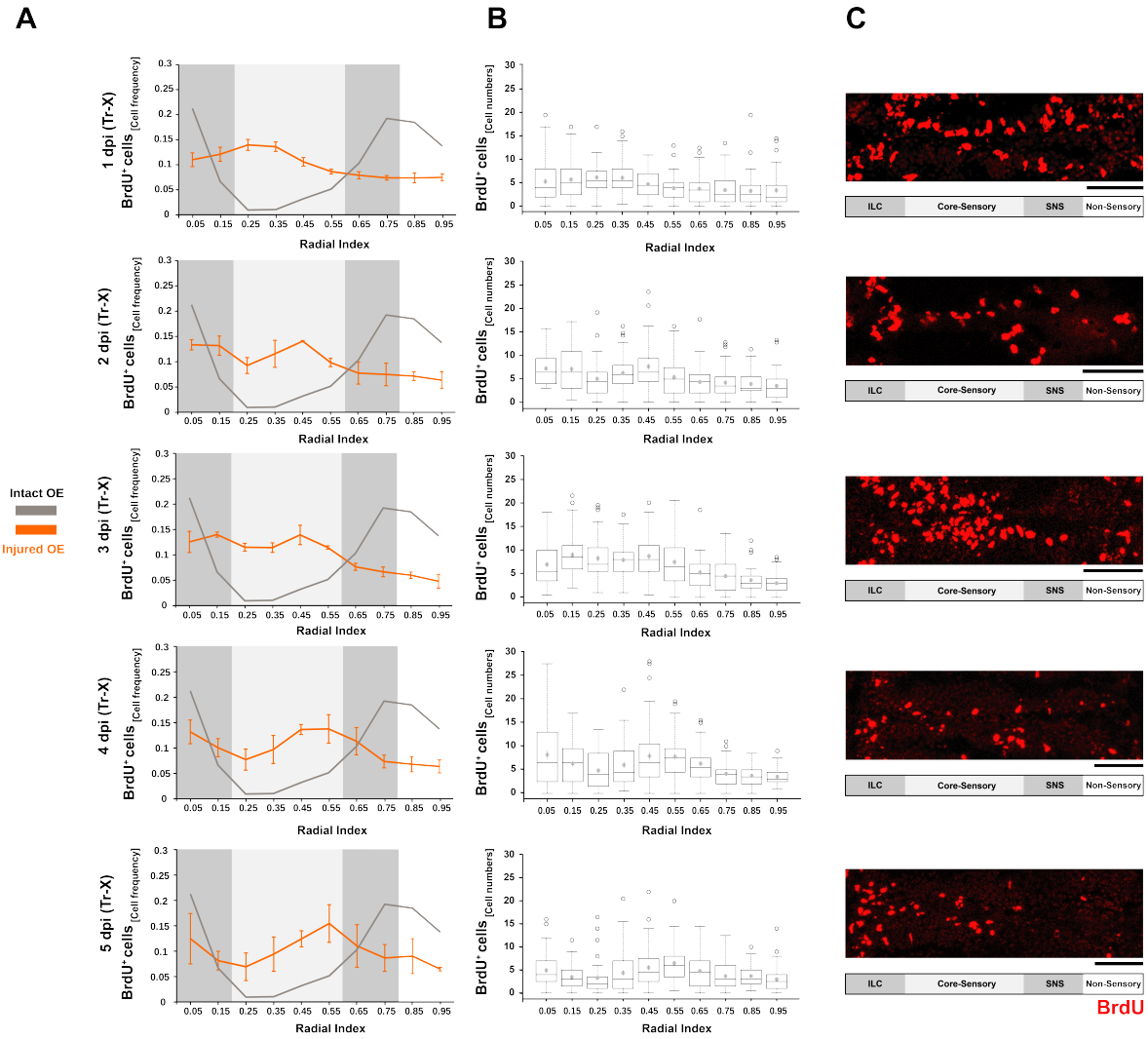

Figure 4.6. Positional profiling of BrdU-positive cells during OE regeneration. A. Frequency plots of the regenerating (orange) vs. intact OE from Figure 4.5A (gray). Box-plot analysis. C. Representative confocal images. Scale bar: 50 µm (C).

To label cells in the late G2 or M phase, OE samples from the previous analysis in sections 4.1.3 and 4.1.4 were colabeled by anti-pH3 immunohistochemistry (Figure 4.7). To exclude aberrant or premature mitotic events, only mitotic cells that passed through S phase were taken into count by scoring BrdU/pH3 double-positive cells.Representative double-positive cells are indicated with white arrowheads in Figure 4.7A', whereas an unscored pH3-positive cell that has no BrdU-immunoreactivity is indicated with a black arrowhead.

Horizontal sections (n = 210) of all intact OEs analyzed in sections 4.1.3 and 4.1.4 (n = 21) contained only a few cells under mitosis on average (4.3± 0.2 cells/section, mean ± SEM), which is consistent with previously reported calculation (6.6 ± 1.3 cells/section, [127]). Average numbers of BrdU/pH3-positive cells in the regenerating OEs, on the other hand, showed a progressive increase, starting from 24 hpi. Boxplots in Figure 4.7B display the varied, yet increased numbers in mitotic cells of the regenerating OEs over control groups (n = 30 sections per time point). The average value obtained from regenerates (13.6 ± 2.6 cells/section) was more than two times higher than in the internal control group at 24 hpi (5.4 ± 0.8 cells/section). The average value of the regenerates increased to 16.6 ± 1.3 cells/section at 48 hpi, and reached a maximum of 33.3 ± 3.0 cells/section at 72 hpi while the average value remained the same in the control group at both time points (4.2± 0.5 cells/section).After 72 hpi, the number of pH3/BrdU cells declined to 28.7± 1.9 cells/section at 96 hpi in comparison to 5.1 ± 0.5 cells/section in the control group. The decline in the regenerating OE was prominent at 120 hpi with an average of 12.1 ± 1.1 cells/section, yet this value was still higher than that of the control group (5.8 ± 0.7 cells/section).

To better describe the dynamic changes in mitotic activity over time, cell numbers obtained from regenerating OEs were normalized to that from the corresponding control groups. The internally normalized values were re-normalized with the mean of ratios between left and right OEs of intact control groups from 4.1.3. The double-normalization reveals the fold-changes in the regenerating OEs over time, which can be interpreted as the proliferation rate relative to the intact OE.

As shown in Figure 4.7C, regenerating OEs had 1.8 ± 0.8 (mean ± SEM) times more mitotic cells at 24 hpi than control OEs. The fold-change increased in the following days (3.6 ± 1.1 and 6.7 ±0.9 times at 48 hpi and 72 hpi, respectively). After 72 hpi, the mitotic activity in the regenerating OE started to decline to 5.2 ± 1.4 in 96 hpi and to 1.8 ± 0.9 at 120 hpi. The temporal profiling shows that the proliferation rate in the regenerating OE reaches its highest value around 72 hpi. The mitotic activities in the tissue largely, although not fully, return to pre-injury conditions quantitatively by 120 hpi.

4.1.6. Analysis of the cell proliferation in the post-regenerative OE

The dynamics of cell proliferation detailed above suggest that damage-induced mitotic activity increases to a maximum by 72 hpi. The observed increase in cell proliferation stems largely from the mitotic activity of cells within the sensory OE. This is in contrast to the spatially restricted distribution pattern of proliferating cells in the intact OE, which can be observed predominantly, yet not exclusively, at the ILC and SNS. There are only few sporadic cells along the sensory region, that are mitotically active in the intact OE. Unlike in the rodent OE, where newborn OSNs move from basal to apical layers along the sensory region as they mature, new OSNs in zebrafish are generated at the ILC and SNS and shift laterally from their birth zones to more central positions of the sensory region over time [73, 127]. The increase in the damage-induced mitotic activity is followed by a decline to pre-injury rates by 120 to 168 hpi. This raises the question whether the decline in the regenerative mitotic activity describes the return of pre-injury activity in the OE, that is defined by cell divisions at the ILC and SNS, and persistent cellular shift to the central regions or if the uniform mitotic activity across the entire OE is maintained at steady, yet lower levels in the restored OE. Thus, an analysis of the long-term effects of the chemical injury on cell proliferation may shed light upon these different scenarios. For this purpose, injured fish (n = 4) were subjected to BrdU incorporation continuously for one week to label all mitotically active cells and were analyzed at various late time-points up to 60 days post pulse (dpp).

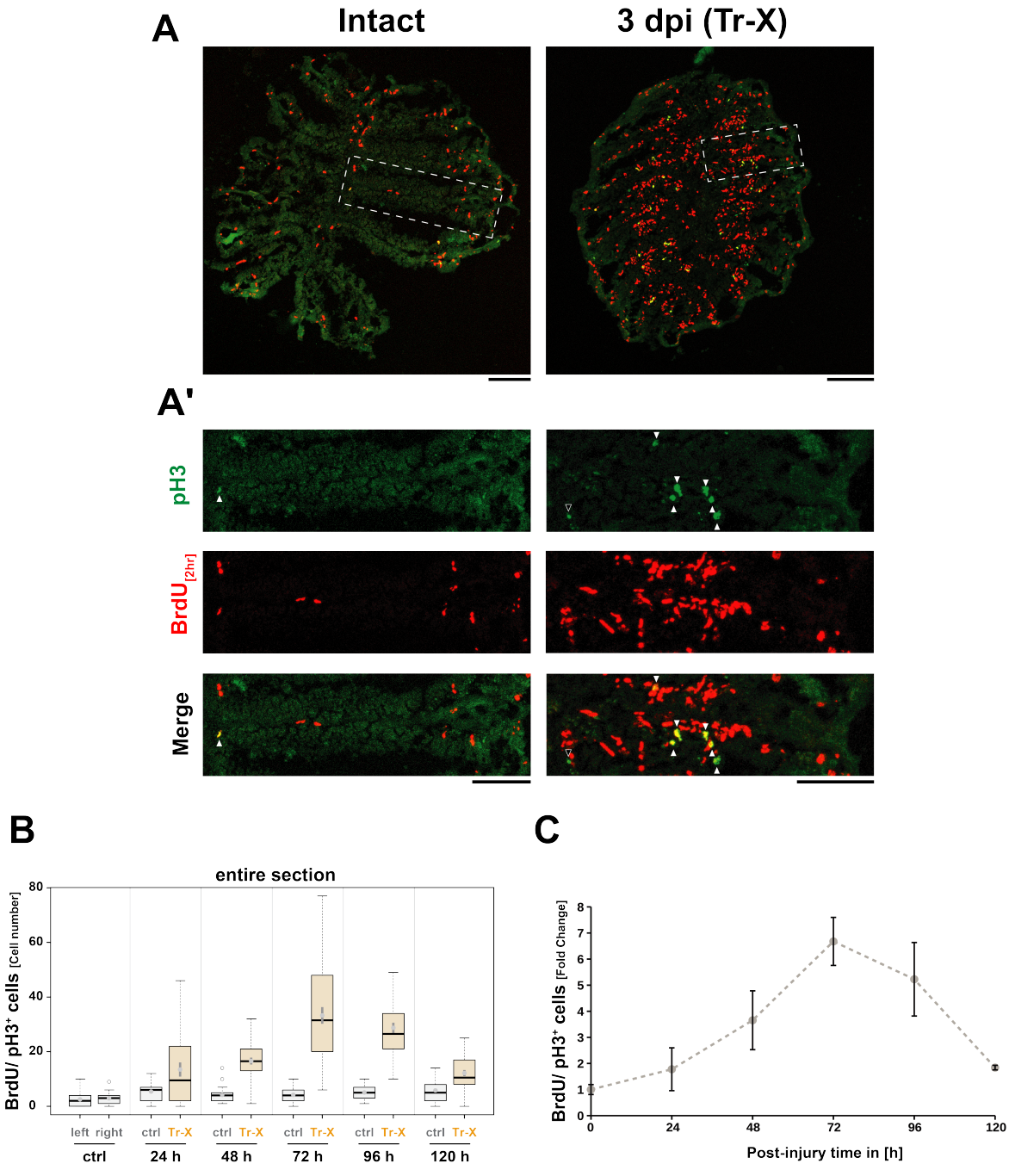

Figure 4.7. Temporal profiling of BrdU/pH3 double-positive cells after chemical injury. A. and A'. Representative OE sections at 3 dpi. B. Box-plot analysis. C. Fold changes in proliferation over the time course. Scale bars: 100 µm (A) and 50 µm (A').

As always, Triton X-100 application was only performed to the right OEs while left OEs were kept intact as internal control. Following tissue damage and BrdU labeling, animals were transferred to fresh water tanks for defined time intervals, except for one fish that was analyzed immediately after the BrdU pulse and another fish that was chosen for prolonged BrdU-incubation for 60 dpp analysis. Because the longest incubation period (60 dpp) exceeded the cellular lifespan of OSNs in the OE (30 days, according to [127]), the BrdU pulse was given for two weeks continuously instead of one week in this experimental setup to increase the number of BrdU-positive cells that survive the two-month analysis period. Radial position scores of BrdU-positive cells were determined at 0, 7, 30, and 60 dpp. Anti-HuC/D immunoreactivity was used to visualized OSNs and the dimensions of the sensory region. The scores of BrdU-positive cells obtained from each time-point were plotted in Figure 4.8 to visualize the progressive shift of labeled cells within the sensory region over time.

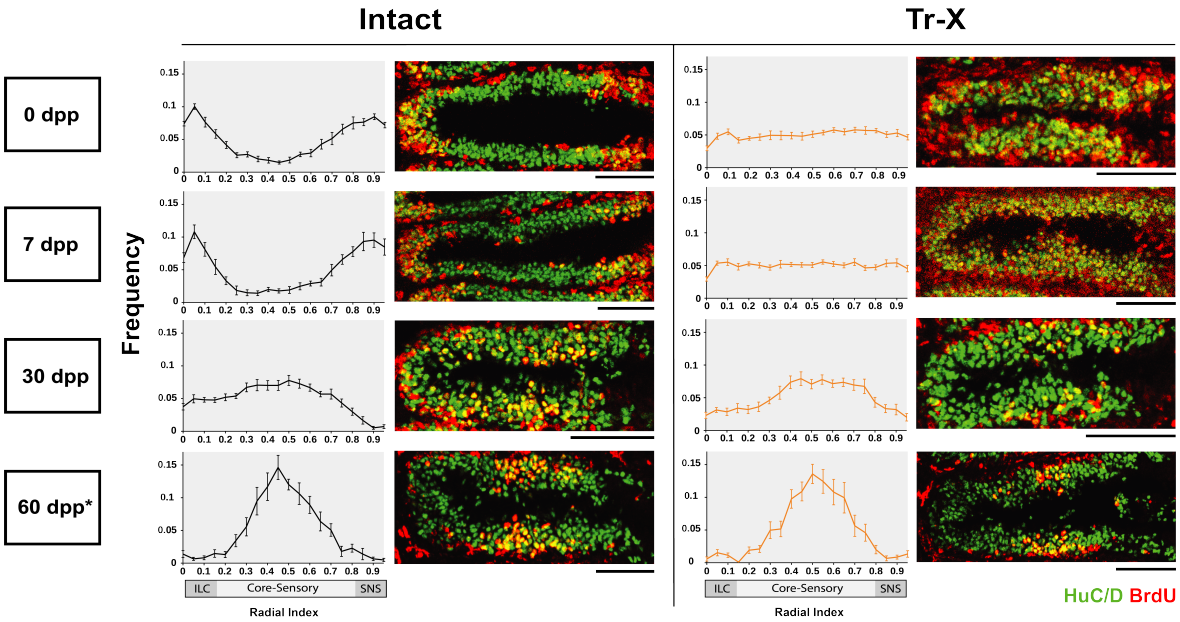

Figure 4.8. Radial positioning of newborn cells along the sensory region of intact OE and regenerated OE over time. dpp: Days post injury. *: Fish analyzed at 60 dpp was subjected to BrdU solution for 2 weeks after detergent treatment. Scale bars: 50 µm.

In the intact OE, BrdU-labeled cells were densely packed at the ILC and SNS in the tissues that were obtained immediately after one week BrdU pulse and at 7 dpp. The majority of BrdU-positive cells occupied basal and multiple supra-basal layers around the two proliferation zones, whereas sporadic BrdU-positive cells within the sensory region were typically found only in the basal layer.

The clusters of the labeled cells around the ILC and SNS became less dense at 30 dpp, as cells had largely shifted away from the proliferation zones and occupied multiple layers within the sensory region, resulting in a more or less homogenous distribution. However, 60 days after the BrdU pulse, the labeled cells accumulated in the middle of the sensory region where they occupied intermediate and apical layers. Thus, the analysis of the long-term fate of adult-born OSNs in the intact OE corroborates previous observations, which suggest that constitutive mitotic activity at the ILC and SNS progressively pushes older OSNs towards the center of the OE.

As expected from the analysis shown above (Figure 4.6), the early time points of the regenerated OE displayed a distribution profile that is distinct from the distribution of BrdU-positive cells in the intact OE. Immediately after the BrdU pulse and at 7 dpp, virtually all cells in the sensory region are positive for BrdU, irrespective of the radial and basal-to-apical position.

Already at 30 dpp, an accumulation of labeled cells in the center of the sensory region could be observed and the distribution profile closely resembled that of the intact tissue. The accumulation in the center of the sensory region became even more evident at 60 dpp and the distribution profiles of regenerated and intact OE were largely identical.The result indicates that adult newborn cells tend to converge in the middle of the lamella, irrespective of whether the OE is injured or intact. This observation strongly suggests that the change in the proliferative activities and migratory behaviors of OSNs that occur during recovery are not permanent and that the OE reverts to constitutive neurogenesis from the ILC and SNS once it is fully restored.

4.1.7. Consecutive labeling of dividing cells before and after chemical injury

The change in the pattern of BrdU-positive cells that is observed immediately after injury suggests that tissue damage triggers mitotic activity in a distinct progenitor population that is dormant in the intact OE and shows a different tissue distribution from constitutively active GBC-like cells at the ILC and SNS. However, the possibility exists that the loss of most OSNs within 24 hpi may enable redistribution of surviving cells, including mitotically active progenitor cells. Thus, fast-cycling cells from the ILC and SNS could be displaced to more central positions in the OE as a consequence of the disorganized tissue morphology after injury. To discriminate between these possibilities, cycling cells were sequentially labeled with different thymidine analogs, before and after Triton X-100-treatment. The procedure is similar to BrdU-incorporation, but the use of two different analogs allows to distinguish between separate rounds of cell divisions and therefore identify cell groups that showed proliferative activity before and/or after injury [197].

In order to trace the origins of newborn cells that proliferate during the regenerative response, animals were subjected to 5-iodo-2-deoxyuridine (IdU) and 5-chloro-2-deoxyuridine (CldU) before and after Triton X-100 exposure, respectively. Fish (n = 3) were initially incubated in IdU-containing freshwater (30 mg/L) for 24 hours in dark. At the end of the IdU incorporation period, fish were transferred to clean tank water devoid of thymidine analogs for 24 hours to wash out unincorporated analogs from tissues. The right nasal cavities of fish were treated with 1% Triton X-100 solution and left OEs were left intact as internal controls.

The injury application was followed by immediate CldU incubation (30 mg/L) for 24 hours, in which CldU was incorporated into newly synthesized DNA of injury-induced proliferating cells. After the second incubatory period, immunohistochemical detection of IdU and CldU incorporation was performed with IdU- and CldU-specific antibodies. A schematic description of the experiment is given in Figure 4.9A.

Incorporated thymidine analogs are stable and persist in DNA after cell division, and, thus, labels both the cells that actively divided during the labeling pulse and their daughter cells during subsequent divisions of labeled cells. Based on this principle, Figure 4.9A indicates the potential outcomes expected from sequential labeling. Cells labeled exclusively with IdU correspond to mitotic events that occurred just during the pre-injury phase. On the other hand, single CldU-positive cells constitute the progenitor subset that divided only after injury. Finally, IdU-CldU double-positive cells reflect multiple divisions of the same progenitor cells at different times before and after injury. As expected, IdU- and CldU-positive cells showed virtually identical distributions in the intact OE (Figure 4.9B). As seen for single BrdU incorporation experiments (Figure 4.3), IdU- and CldU-positive cells were largely clustered at the ILC and SNS with the earlier labeled IdU-positive cells shifted slightly further towards the mid-sensory OE. Interestingly, only rare CldU/IdU double-positive cells could be observed (19.5 ± 4.1 / horizontal OE section, mean $\pm$ SEM) and occurred predominantly at the ILC and SNS, suggesting that different cells divided during the two labeling periods.The tissue distribution of IdU-positive cells (pre-injury activity) in the injured OE largely resembled the distribution of the cells in the intact OE. However, the number of IdU-positive cells was lower in the injured OE than in intact control OE, suggesting that these cells, or their progeny, have also been affected by Triton X-100 treatment. Figure 4.9B displays representative images for comparison between injured and intact OE samples. The injury predominantly affected IdU-positive cells close to the SNS, while cells at the ILC were largely spared, probably because of the lower accessibility of the Triton X-100 solution.. Importantly, only sporadic IdU-positive cells could be found within the sensory region, suggesting that no major reshuffling of progenitors has occurred as a consequence of tissue damage. CldU-positive cells (post-injury activity), on the other hand, showed a more uniform distribution of labeled cells across the entire OE, including the sensory region. As in the intact OE, IdU/CldU double-positive cells were rare but showed a two-fold higher frequency in the regenerating OE (47.2 ± 10.1 / horizontal OE section). Importantly, double-positive cells in the regenerating OE were also mostly located at the ILC (Figure 4.10B) and seem to contribute to the induced patterning in the sensory region only minorly, despite their increased number.

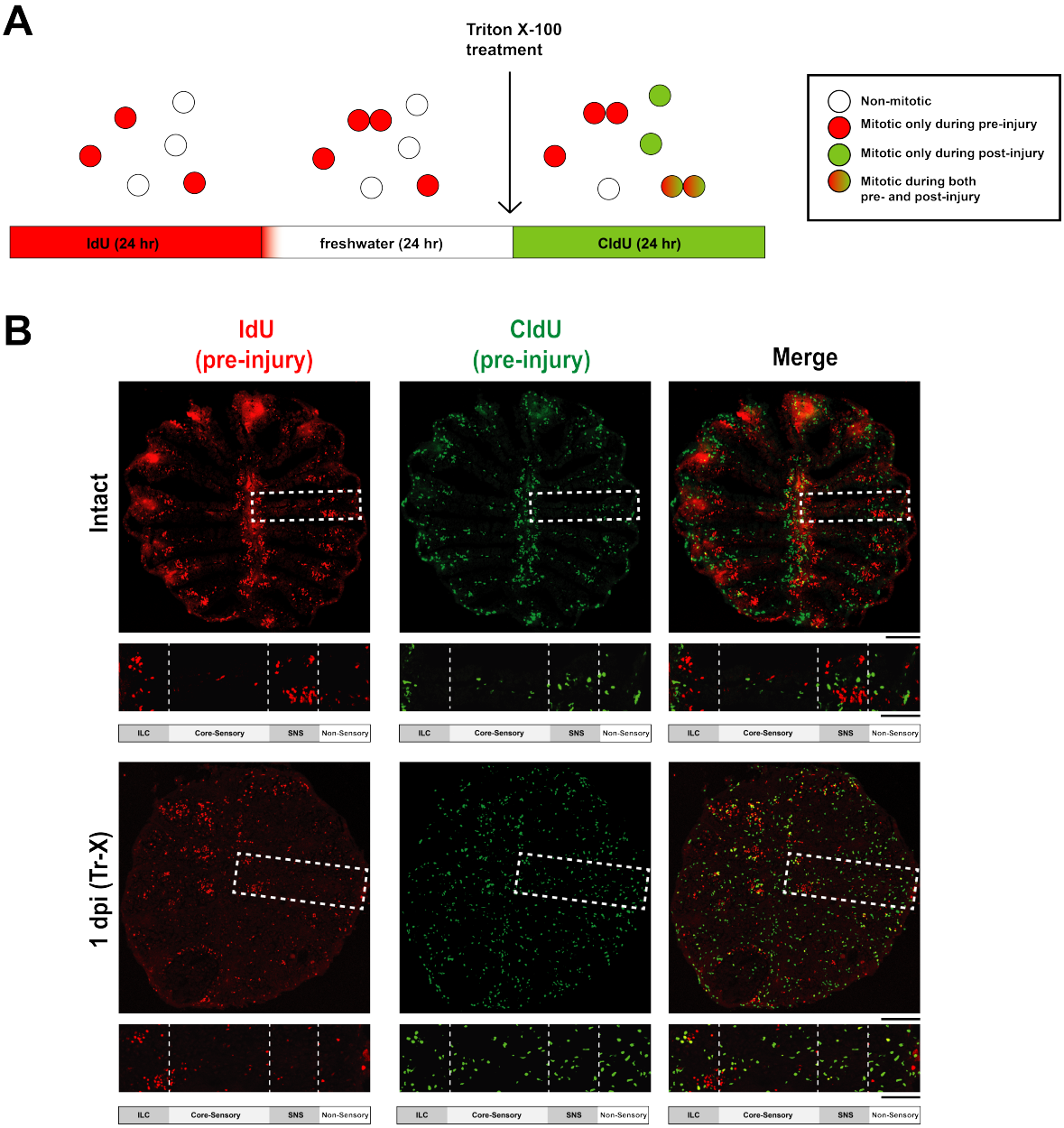

Figure 4.9. Sequential labeling of newborn cells before and after Triton X-100 treatment. A.Schematic description of the experimental design. B. Representative results of IdU and CldU labeling. Scale bars: 100 µm (section) and 50 µm (lamella).

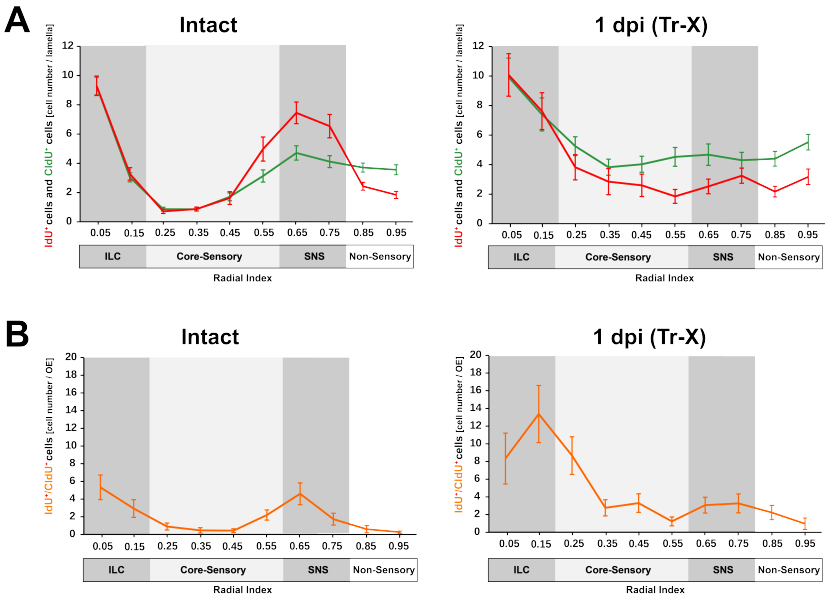

Figure 4.10. Positional analysis of sequentially labeled newborn cells of intact and regenerating OEs at 1 dpi. A. IdU- (red) and CldU- (green) positive newborn cells per lamella. B. IdU/CldU double-positive cells (orange) per OE section. .

The positional analysis of the distribution of labeled cells in individual lamellae pointed out that IdU- and CldU- positive newborn cells were distributed differently from each other after Triton X-100 injury, although low numbers of both newborn pools complicated accurate analysis (IdU-positive cells: 39.9 ± 4.4 / lamella, CldU-positive cells 53.9 ± 4.4 / lamella). Therefore, an alternative experimental setup was employed to label an additional number of cells (Figure 4.11). In this alternative paradigm, one fish was subjected to IdU-incorporation for 24 hours, then transferred to and kept in thymidine-free water for 48 hours. A longer pre-injury gap was chosen to let the pool of cells that was labeled by IdU to expand and to withstand the severity of Triton X-100 injury. The fish was then injured with Triton X-100 solution and transferred back to thymidine-free water for another 48 hours. At 48 the end of this period, the fish was transferred to CldU-containing water for 24 hours, which covers the period of highest cell proliferation during the regenerative phase according to the previous assessment in 4.1.5 (Figure 4.11A).

Changing the experimental conditions revealed a more pronounced difference in the patterns of IdU- and CldU-positive newborn cells. While the number of IdU-positive cells was even lower under this condition (21 ± 1.5 cells/lamella), CldU labeled cells were generated considerably more as a result of the regenerative response (93.9 ± 5.5 cells/lamella) (Figure 4.11 and Figure 4.12). Similar to the outcomes of the first setup, most of the remaining IdU-positive cells were found at the ILC in this alternative setup. Unlike the single-peaked and ILC-weighted distribution of IdU-positive cells, CldU-positive cells were largely localized along the entire sensory region. Importantly, double immunoreactivity against both analogs was again rarely seen, and only 7.0 ± 3.1 IdU/CldU-double positive cells could be detected per horizontal OE section. These double-positive cells did not show any obvious positional preference due to their rare occurence per lamella.

Both experimental setups described above are preliminary and require additional trials for conclusive analysis and sufficient statistical power. However, the obtained results are strong enough to rule out the possibility that cellular displacement as a consequence of disorganized tissue morphology causes an altered distribution pattern of GBC-like progenitors in the injured tissue. The abundance of CldU-positive cells and the rare occurrence of IdU/CldU-positive cells in both experiments strongly suggests that post- and pre-injury cycling cells belong to different progenitor pools that are active under different tissue conditions. In addition, the rare yet evident occurrence of IdU/CldU-positive cells at the ILC at 1 dpi suggests that region-specific GBC-like cells divide independently of the injury condition. The progenitor populations that are inactive in the intact OE, on the other hand, become activated by the injury and repopulate the sensory region, whereas the constitutively dividing cells have little contribution to tissue restoration after injury.

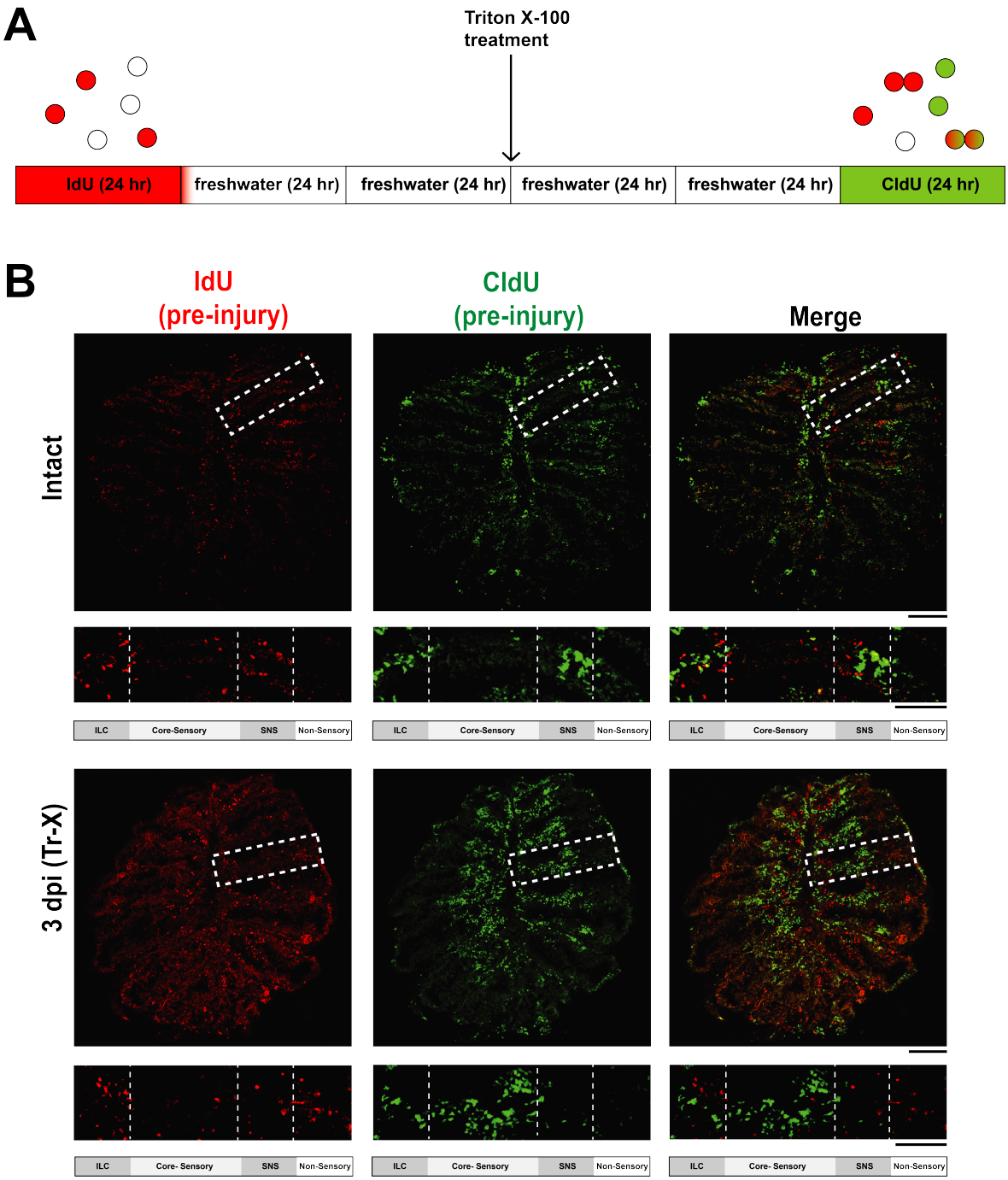

Figure 4.11. Sequential labeling of newborn cells before and after Triton X-100 treatment. A.Schematic description of the experiment. B. Representative results of IdU/CldU labeling at 3 dpi. Scale bars: 100 µm (section) and 50 µm (lamella).

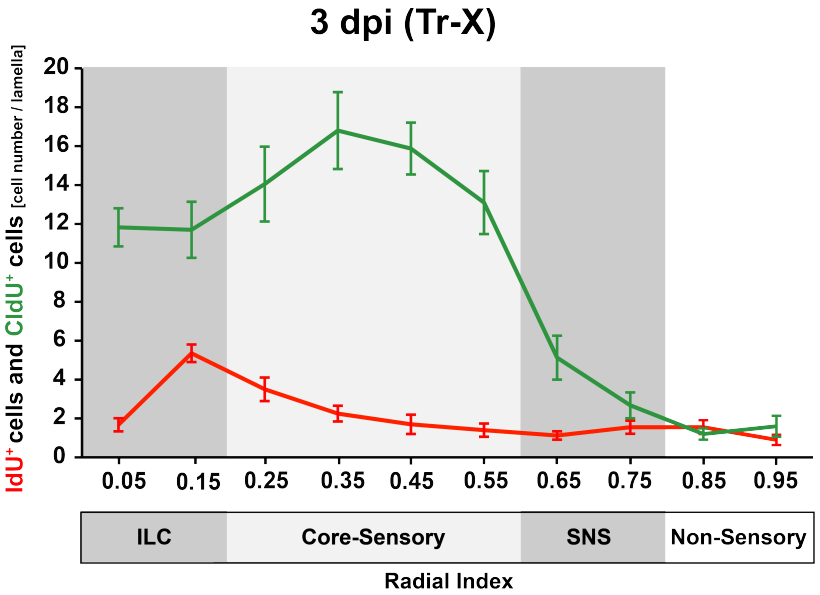

Figure 4.12. Positional analysis of IdU- (red) and CldU- (green) positive newborn cells along the radial axis in regenerating OE at 3 dpi.

4.1.8. Selective ablation of OSNs by axotomy

The chemical injury paradigm that was applied in the experiments detailed above simultaneously affects all cell types in the OE, including neuronal, glial, and other structural cells that contribute to tissue integrity and homeostasis. It has been shown in rodent models that structural damage to non-OSN cells, particularly to sustentacular cells, is required to activate the mitotic response in dormant HBC progenitors [211]. In contrast, selective ablation or damage to OSNs has little impact on HBCs but efficiently and selectively stimulates GBCs, which contribute to constitutive OSN neurogenesis in the intact OE [94]. A simple experimental paradigm to selectively ablate OSNs is transection of the olfactory nerve which results in retrograde degeneration of neurons [212]. The strong bias in the distribution of dividing cells in the intact and chemically-injured OE at the ILC/SNS and sensory OE, respectively, raised the question whether selective ablation of OSNs by axotomy would stimulate a mitotic pattern that is distinct from the pattern seen upon Triton X-100 lesion. In this approach, axon bundles emanating from the OE and projecting to the OB were physically transected by micro blades.

As in the chemical injury approach, only one axon bundle was severed while the bundle between the other OE and OB remained intact to serve as internal control. Unlike the Triton X-100 treatment in which all cell types are nonspecifically exposed to the chemical agent, axotomy predominantly, if not exclusively affects OSNs.

4.1.9. Analysis of apoptosis induction after chemical injury and axotomy

Apoptosis is a fundamental process during development, as well as constitutive, and regenerative neurogenesis in the mammalian OE [213–215], however, its role in the zebrafish olfactory organ remains largely unexplored.

In order to investigate apoptotic events in both intact and regenerating OE, tissue samples were analyzed for the immunoreactivity against active caspase-3 (Figure 4.13A). As in the previous experiments, HuC/D immunoreactivity was chosen to detect mature neurons and assess the severity of the resulting injury. In contrast to findings obtained in rodent models in which OSN turnover is apoptotic [214,216], no caspase-3-positive cell could be observed in the intact zebrafish OE. This result corroborates the previous report, which showed that apoptosis is rare in the intact zebrafish OE and that alternative, non-apoptotic cell death mechanisms contribute to the elimination of senescent OSNs [127]. Triton X-100 treatment at 8 hpi and 24 hpi, on the other hand, resulted in the sparse induction of caspase-3-positive cells with a seemingly random distribution across the OE. No caspase-3/HuC/D double-positive cells could be detected in the analyzed tissue sections of the injured OEs for unknown reasons.

While a mild difference in the occurrence of apoptotic cells seems to exist between intact and chemically-treated OE, only a sparse induction of caspase-3-positive cells occured after chemical lesion. Interestingly, the number of apoptotic cells was elevated in the axotomized OE (abbreviated as “Axt” in the figures) at 8 hpi and 24 hpi (Figure 4.13B and B’), suggesting that nerve transection in zebrafish indeed results in retrograde degeneration of OSNs by apoptosis.

The induction of caspase-3-positive cells by nerve transection appeared to be non-specific in terms of radial position and caspase-3/HuC/D double-positive apoptotic OSNs were present in the sensory region at the time of the analysis at both time points (Figure 13B', pointed with white arrowheads), however, the number of apoptotic OSNs was still lower than expected, probably because most OSNs were already eliminated from the damaged tissue. Moreover, there were also clusters of caspase-3 positive cells in the peripheral non-sensory OE which normally does not contain any OSN, suggesting that the dying OSNs may have released factors that induced non-autonomous apoptosis in the neighboring non-neuronal cells.

Overall, the caspase-3 analysis suggests that zebrafish OSNs follow alternative, caspase-independent cell death mechanisms, such as necrosis or necroptosis in the intact and chemically-injured zebrafish OE [217]. Compared to these tissue conditions, however, OSNs underwent detectable apoptosis in the axotomized OE.

While the number of apoptotic cells was increased after axotomy, caspase-3-positive OSNs were not overtly abundant at the time points analyzed. It is possible that OSN degeneration in nerve-transected animals is fast and that HuC/D staining pattern at the time of the analysis (8h and 24 h after axotomy) only revealed OSNs that were not, partially, or circumstantially affected by the axotomy. Thus, analysis at different earlier time points after nerve transection will be necessary to understand if apoptosis is a main contributing process to OSN degeneration after axotomy. The observations above show that cell death in the OE can be induced by different methods and outcomes, and that the pattern and density of caspase-3-positive cells are different in response to chemical agents and physical denervation. This further demonstrates that the cell death response of the OE is differentially affected by the type of injury applied, which may lead to different downstream events at tissue level during regeneration.

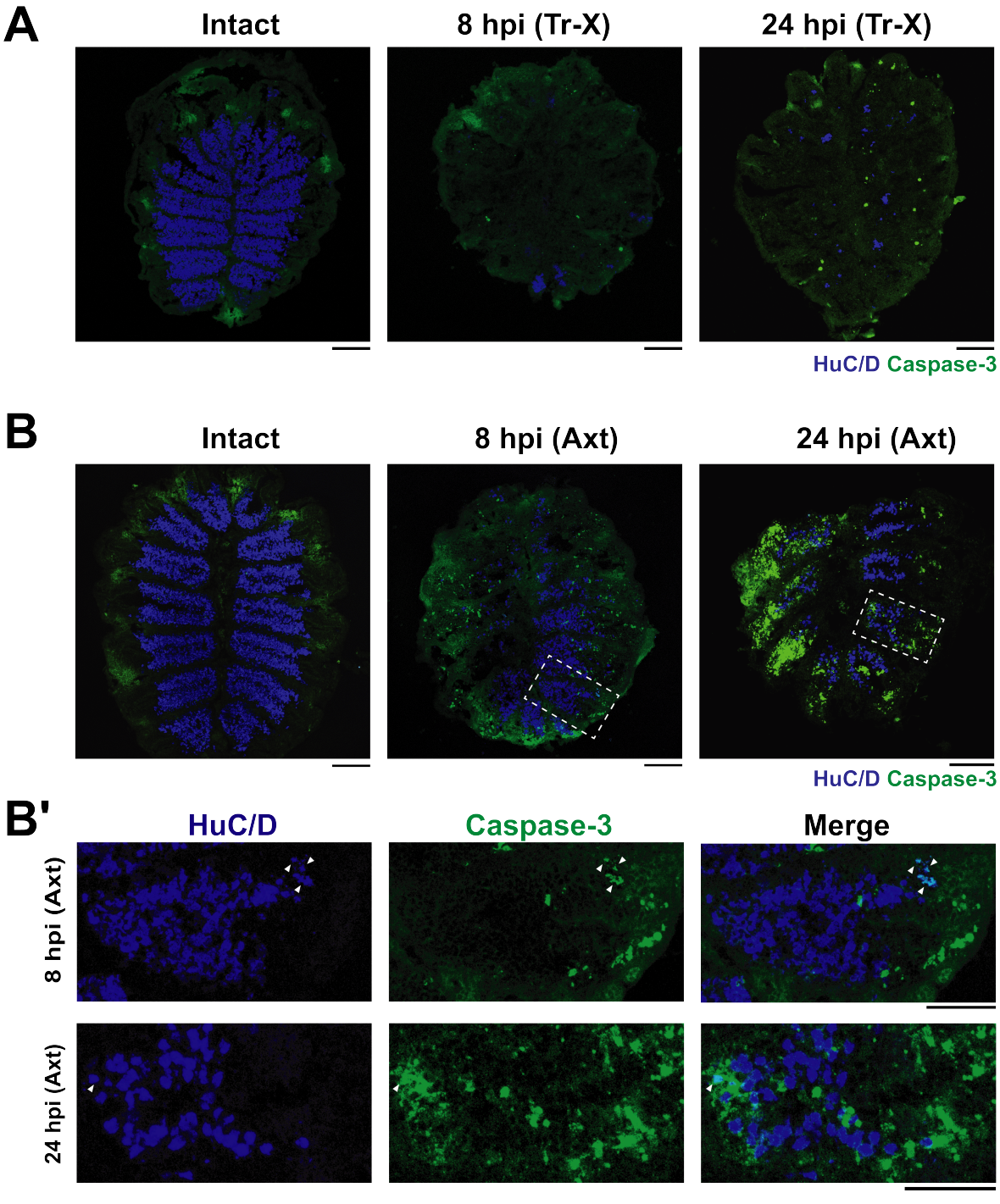

Figure 4.13. Active Caspase-3 immunolabeling under different tissue conditions. Triangles: Apoptotic neurons. Mature neurons are labeled by anti-HuC/D antibody. Axt: Axotomized OE. Scale bars: 100 µm (A and B) and 50 µm (B').

4.1.10. Cellular proliferation after axotomy

To understand the effects of nerve transection on the proliferation dynamics of the two pools of OE progenitor cells, the spatial distribution of BrdU-positive newborn cells was analyzed after incubating one axotomized fish in BrdU-containing water for 24 hours at 1 dpi. As in the Triton X-100 treatments, the left OE remained intact to serve as internal control, and only the axon bundle of the right OE was transected. HuC/D staining was used to visualize the unaffected and newborn neurons. The axotomized OE at 1dpi displayed a distribution pattern of BrdU-positive newborn cells that was different from the pattern in the intact OE (Figure 4.14A). The decrease in epithelial thickness of the area occupied by HuC/D-positive cells that did not retain BrdU indicated that many but not all OSNs degenerated within 24 hours after the procedure. BrdU-positive cells were sporadically and uniformly found along the entire axotomized OE but none of these cells showed HuC/D immunoreactivity, suggesting that OSN neurogenesis did not start at 1 dpi.

For the quantitative and spatial analysis of a later time point, fish (n =3) were axotomized and kept in fresh water for two days and then subjected to BrdU-exposure for 24 hours at 3 dpi. BrdU-positive cells were identified from 60 horizontal epithelial folds of 3 axotomized OEs (20 per OE) and from 60 folds of internal control OEs for comparison. The uniform distribution pattern of BrdU-positive cells was more pronounced at 3 dpi than at 1 dpi (Figure 4.14A and 4.14B).

The core sensory region between ILC and SNS of the axotomized OE had a total number of 21.0 ± 1.0 (mean ± SEM) cells/epithelial fold whereas the intact OE had only 7.5 ± 0.8 cells/epithelial fold in the same region. The difference in cell numbers between the intact and axotomized core sensory regions corresponded to a 2.8-fold increase in mitotic activity in the axotomized OE and was statistically significant ($p_{(axotomized/control)} = 1.8 \times 10^{-19}$; unpaired Student's t-test, $t_{(axotomized/control)} = -84.1136$).

Unlike Triton X-100-treated OE at 3 dpi (Figure 4.2), the sensory region, as indicated by HuC/D staining, showed poor signs of recovery in the axotomized OE at 3 dpi. Axotomy resulted in extensive loss of neurons in the OE and HuC/D-positive BrdU-negative OSNs were mostly found at the ILC. The relatively high occurrence of BrdU-negative OSNs at the ILC suggests that either the ILC has neuroprotective effects that retards the degradation of the transected neurons or that OSN neurogenesis started and was complete at the ILC before BrdU-labelling, probably because of ongoing constitutive OSN neurogenesis at the ILC. There were also BrdU/HuC/D double-positive OSNs at 3 dpi, most of which were again located at the ILC (Figure 4.14B'). Interestingly, the average number of BrdU/HuC/D-double positive cells in the axotomized OE (8.5 ± 0.9) was identical to the number in the intact OE (8.5 ± 0.8). This notwithstanding, the ILC regions showed significant difference in OSN generation between the intact and axotomized OE. The ILC of the intact OE contained 4.3 ± 0.6 BrdU-labeled HuC/D-positive OSNs, while there were 6.4 ± 0.8 BrdU-labeled HuC/D-positive OSNs at the ILC of the axotomized OE. The difference in newborn OSN numbers at the ILC corresponded to a 1.5-fold increase, which was statistically significant ($p_{(axotomized\ ILC/intact\ ILC)} = 0.0361$, unpaired Student's t-test, $t_{(axotomized\ ILC/intact\ ILC)} =$ -16.4234).

In addition, a few BrdU-positive OSNs could be found outside the ILC that were distributed along the sensory OE and around the SNS. A representative lamella is presented in Figure 4.15, on which OSN neurogenesis occurs in two discontinuous regions. This observation suggests that the limited generation of neurons in the axotomized OE was accomplished by either one of two proliferation zones at the ILC and SNS at the time of analysis. The generation of newborn OSNs in the axotomized OE, therefore, appears to be identical to processes in the intact OE, although the rate of OSN neurogenesis at the ILC was slightly elevated in the axotomized OE. The positional and quantitative profiles of newborn OSNs suggest that the induced OSN neurogenesis in the axotomized OE is sustained by the divisions of progenitors located at the ILC and SNS, possibly GBCs that contributed to constitutive OSN neurogenesis in these regions.

Abundant BrdU-positive HuC/D-negative cells in the core sensory region, on the other hand, either require more time to develop into mature OSNs after BrdU-incorporation or represent non-neurogenic mitotic events triggered by the loss of OSNs.

4.1.11. Triton X-100-injured OE initiates regenerative neurogenesis

The results described in the above sections indicate that the zebrafish OE induces a unique proliferation pattern upon chemical injury, which affects neuronal and non-neuronal cells. However, the contribution of the injury-induced proliferation to OSN neurogenesis was not directly assessed. The recovery of HuC/D-positive mature neurons after injury suggests that OSNs are generated but in itself is not sufficient to prove that the induction of mitotic activity within the sensory OE contributes to regenerative neurogenesis. Loss and regain of HuC/D immunoreacitivity after Triton X-100 exposure could also be the result from increased activity of ILC- and SNS-located GBC-like cells. Therefore, tissue expression of early neurogenesis markers during regeneration after injury was examined to directly demonstrate that neurogenesis occurs in the sensory OE as a part of the injury response. In order to detect and evaluate injury-induced neuronal commitment of progenitors, intact and regenerating OEs were analyzed for Achaete-scute familiy bHLH transcription factor 1 (Ascl1) immunoreactivity.

Ascl1 (also known as Mash1 in mammals) is a helix-loop-helix transcription factor widely known for its role in neuronal commitment [90,91]. Progenitors producing Ascl1 follow a neuronal fate and develop into mature OSN in the OE. Cells at the later stages of OSN lineage shut down *ascl1* expression and produce Hu proteins and other markers to promote terminal differentiation and exit from the cell cycle [218].

The zebrafish genome contains two paralogs of *ascl1*; *ascl1a* and *ascl1b*. Both paralogs have divergent expression patterns during development [219] and it has been previously shown that there is specific *ascl1a* localization to the proliferating cells at the ILC and SNS, in which constitutive OSN neurogenesis occurs [127]. In contrast, the intact sensory OE is completely devoid of *ascl1a* expression.

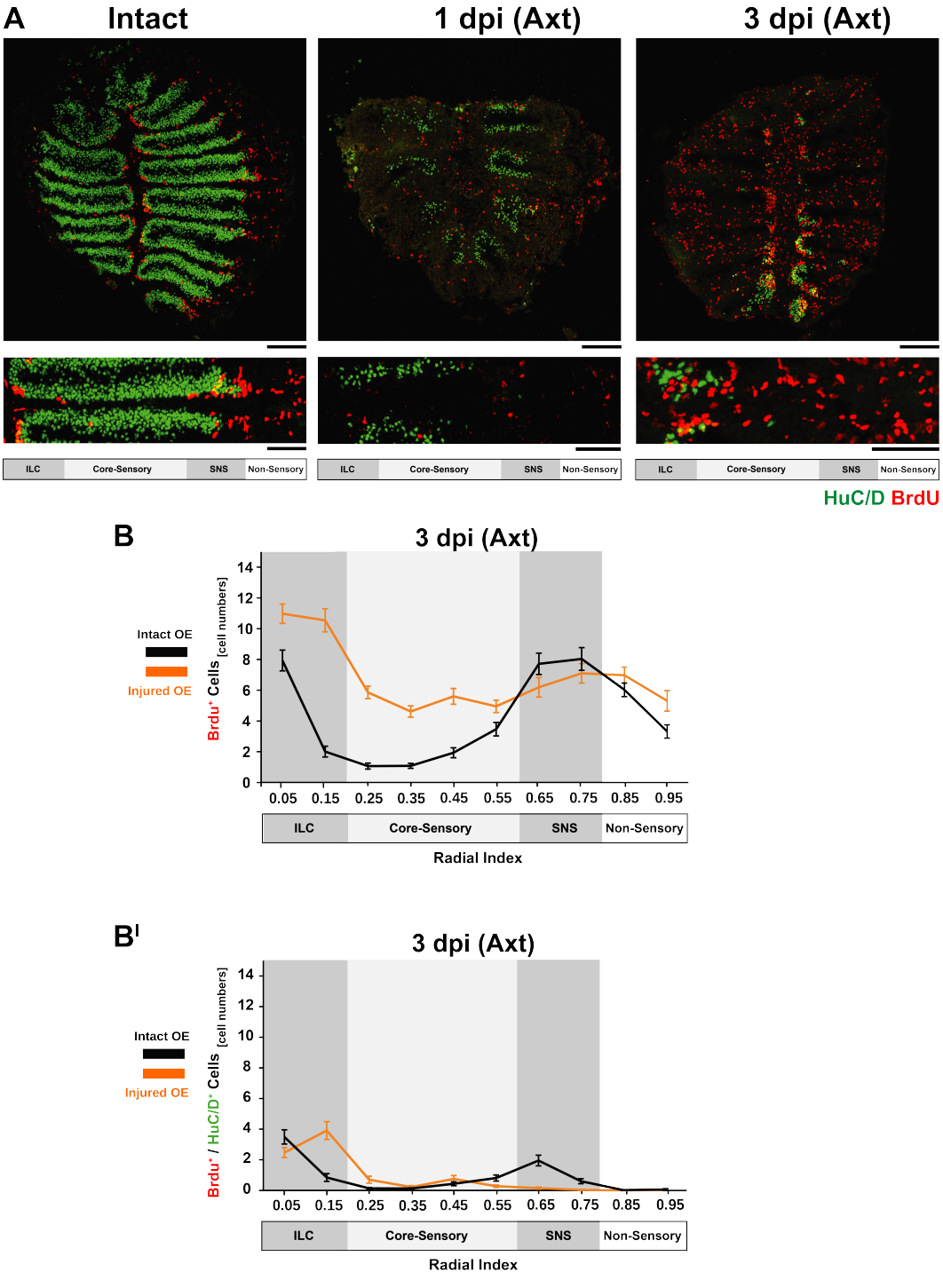

Figure 4.14. Mitotic activity after axotomy. A. BrdU and HuC/D labeling. B and B'. Distribution of BrdU-positive (B) and double-positive cells (B') of the intact (black) and axotomized (orange) OE. Scale bars: 100 µm (section) and 50 µm (lamella).

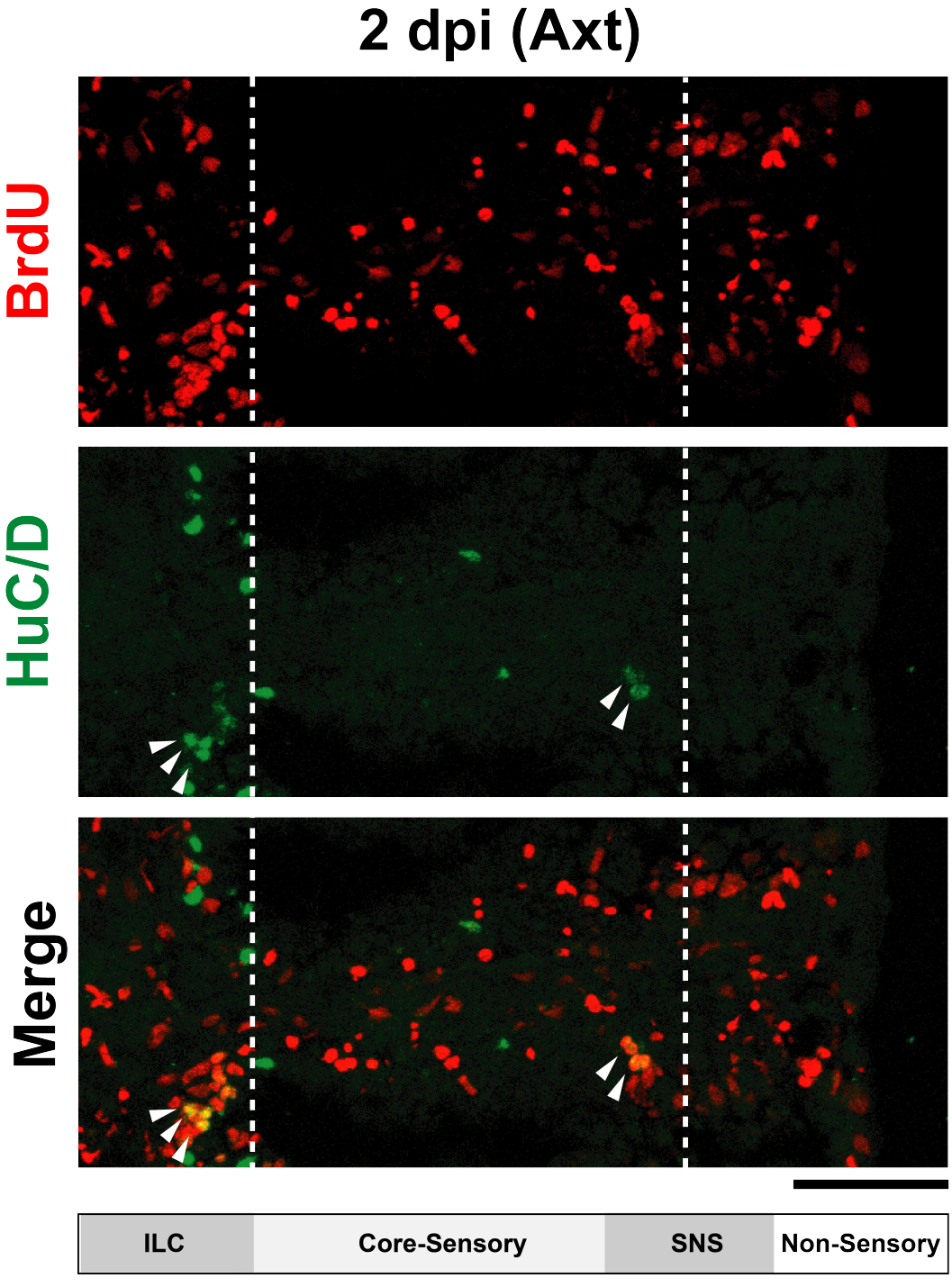

Figure 4.15. Representative image of an axotomized lamella that is labelled by anti-BrdU and anti-HuC/D antibodies. Arrowheads: Double-positive cells. Scale bar: 50 µm.

Cells committed to OSN lineage at the ILC express the universal undifferentiated cell marker Sox2 and *ascl1a* transcript simultaneously (Figure 4.16). At 2 dpi after Triton X-100 treatment, the occurrence of Sox2-positive cells with ascl1a expression increases along the OE, particularly in the sensory region which is not neurogenic in the absence of injury conditions.

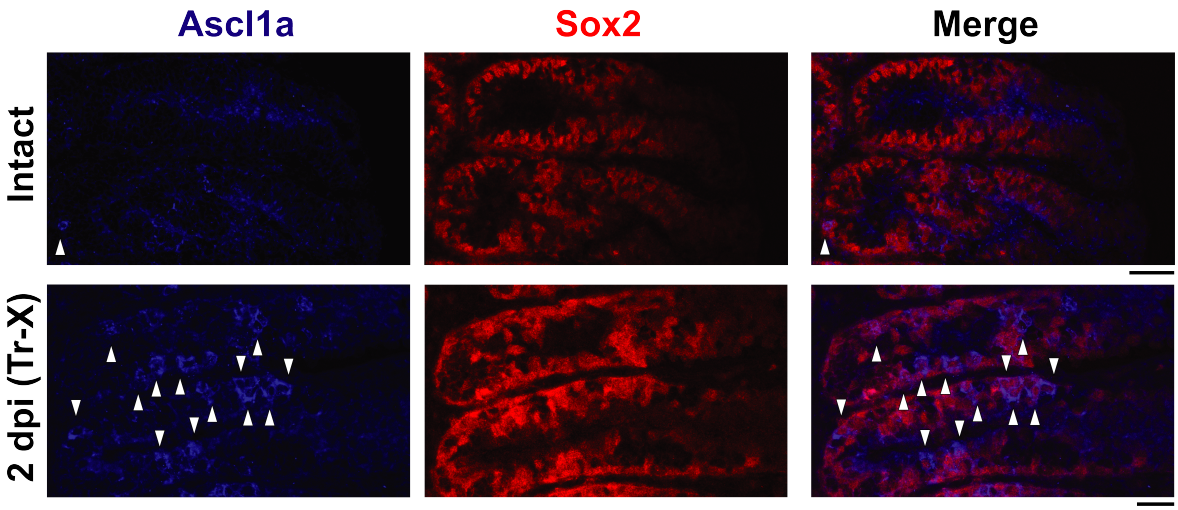

Figure 4.16. *In situ* hybridization of *ascl1a* and anti-Sox2 immunohistochemistry on intact and regenerating OE at 2 dpi (Triton X-100). Triangles: Committed neural progenitors. The images are provided by Kardelen Güler. Scale bars: 50 µm.

To quantify the number of cells committed to OSN lineage after injury, the number of Ascl1-positive cells was scored during the early phase of regeneration at 1 and 2 dpi on cross sections through the injured OE and their radial distances to the ILC was measured. OEs on the right side of the head were treated with Triton X-100 solution and OEs on the left side were left intact to serve as internal control. However, Ascl1-immunoreactivity could not be detected in tissue sections at 1 dpi. For the quantitative analysis of OEs at 2 dpi, Triton X-100-treated fish (n = 3) were subjected to BrdU incubation continuously from the onset of 2 dpi to the time of analysis. The tissue morphology partially recovered by 2 dpi and allowed for accurate measurements of cell distances to the ILC.

As previously shown [127], Ascl1-positive cells were few in number and found mainly at the ILC in the intact OE (Figure 4.17). These cells often showed BrdU-immunoreactivity, suggesting that most of Ascl1-positive cells were mitotically active. Ascl1-positive cells also never were double-positive for HuC/D, suggesting that ascl1 expression is shut down before OSNs reach maturity. Unlike in the intact OE, the regenerating OE showed a high abundance of BrdU/Ascl1-positive cells at 2 dpi. Interestingly, not only the number of BrdU/Ascl1-positive cell was elevated in the regenerating OE, but also the pattern of their distribution along the lamellae changed. Many BrdU/Ascl1-positive cells could be found along the entire sensory region of the damaged OE, instead of just at the ILC in the intact tissue.

To compare the quantitative change in the Ascl1-positive cells between the intact and Triton X-100 treated OE, 1094 Ascl1-positive cells from 166 lamellae of 24 cross sections from 3 injured OEs and 225 Ascl1-positive cells from 143 lamellae of 36 cross sections from 3 internal control OEs were analyzed for their occurrence and radial position in the OE.

Triton X-100 injury clearly induced an increase in the overall number of Ascl1-positive cells. While on average onlu 1.5 $\pm$ 0.1 (mean $\pm$ SEM) cells/lamella could be detected in the intact OE, a four-fold increase of 6.1 $\pm$ 0.9 cells/lamella could be seen in the injured OE at 2dpi (Figure 4.18A). The newly induced BrdU/Ascl1-double positive cells covered 91 $\pm$ 1% of the total Ascl1-positive cells in the injured OE (998 cells from 3 OEs), while BrdU/Ascl1-positive cells constituted 85 $\pm$ 2% of the total Ascl1-positive cells in the intact OE (185 cells from 3 OEs) (Figure 4.18B).

Interestingly, the percentage of fast-cycling cells was slightly yet significantly higher in the regenerating OE than in the intact tissue , suggesting that the injury-induced progenitor niche in the sensory OE has inductive effects on the cell cycle of Ascl1-positive pool and increase the percentage of fast cycling subset ($p_{treated/intact}$ =0.0084, unpaired Student's t-test, $t_{treated/intact} = 2.6505$).

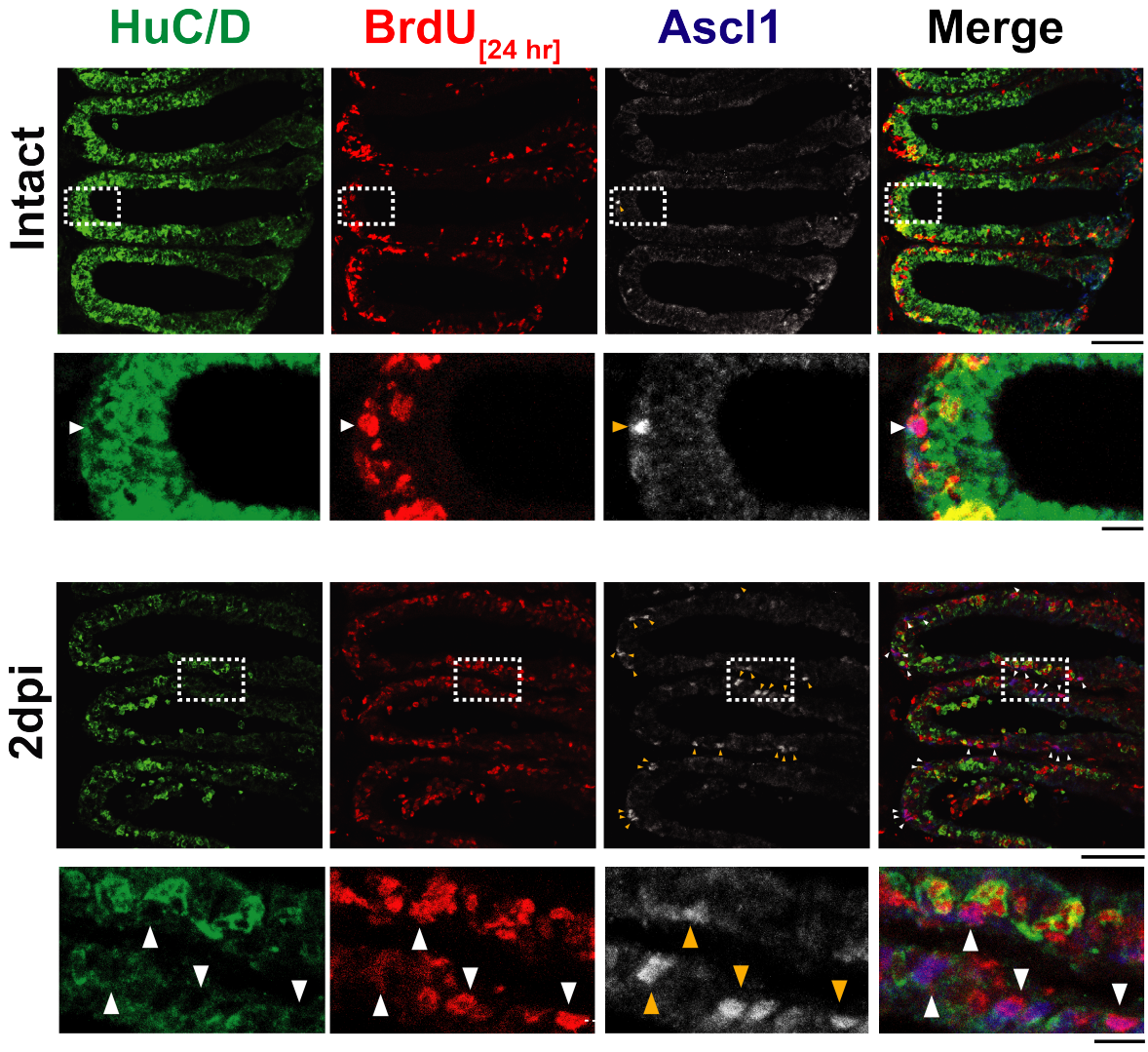

Figure 4.17. Identification of BrdU/Ascl1-double positive cells cells by immunohisochemistry in intact and regenerating OE. BrdU/Ascl1 double-positive and HuC/D-negative cells are shown by triangles. Scale bar: 50 µm and 10 µm (Close-up).

To describe the change in the distribution pattern of BrdU/Ascl1-positive cell, the distances of individual cells to the ILC were measured and scored relative to the full length of the lamella (Figure 4.18C). Only lamellae bearing at least one or more BrdU/Ascl1-positive cells were evaluated. In the intact OE, the number of BrdU/Ascl1 double-positive cells were 1.3±0.1 cells/lamella (n = 185 from 143 lamellae from 24 sections of 3 OE) and these cells were mostly localized at the ILC region (segment range: 0-0.2). the number and positioning of double-positive cells was significantly increased in the injured tissue (n = 998 from 166 lamellae from 36 sections of 3 OE). The overall number of BrdU/Ascl1-positive cells increased 4.3-fold in the injured OE, when compared with average number obtained from the intact OE (1.3 ± 0.1 cells /intact lamella vs. 5.6 ± 0.9 cells/ injured lamella). Plotting the radial positions of BrdU/Ascl1-positive cells according to their index score revealed a broad distribution across the sensory region (segment range: 0-0.6) with a peak at the ILC (Figure 4.18C).

This result shows that the rapid injury response of the dormant cells in the sensory OE after Triton X-100 exposure leads to the generation of committed progenitors of the neuronal lineage with a similar spatial distribution profile as activated HBC-like cells, which will be described in later sections, suggesting that Ascl1-positive cells that occur after damage are HBC-derived.

4.1.12. Spatiotemporal analysis of new-born OSNs following Triton X-100 exposure

Spatial analysis of Ascl1-positive cells at 2 dpi showed that the proliferative response to injury is neurogenic, however, the analysis does not reveal during which time-point after the injury most of the new-born neurons were generated. Since the differentiation and maturation of neurons is a complex and timed process, the temporal analysis of HuC/D immunoreactivity alone (Figure 4.2) can not accurately inform about the time-points at which neurons were born during regenerative neurogenesis.

Similarly, the temporal profiling of all new-born cells by BrdU incorporation assays by itself (Figure 4.7) can not directly reveal this aspect, since the relative proportions of progenitors, transit-amplifying cells, committed neuronal precursors and mature neurons among the overall proliferating cells can not be determined only by BrdU label and additional markers are required to reach meaningful conclusions. A plausible approach to this problem could be a BrdU pulse-chase experiments on label-retaining post-mitotic neurons. When present in the tank water, BrdU is taken up by all proliferating cells during the pulse and persists in the nucleus even after the cells differentiate terminally.

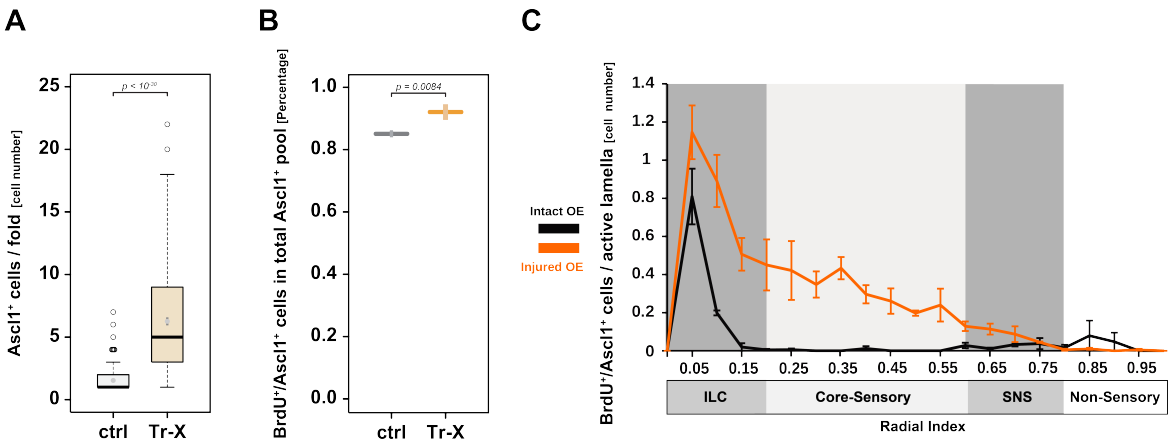

Figure 4.18. Analysis of Ascl1 labeling at 2 dpi. A. Number of Ascl1-positive cells per epithelial fold. B. Ratio of BrdU/Ascl1 double-positive cells. C. Distribution of double-positive cells along the intact (black) and regenerating OE (orange).

Quantification of BrdU-retaining neurons after progressive pulse-labelling intervals at different regeneration time points would allow to determine when most cells were born and during which period OSN neurogenesis contributed to the most to regeneration of the neuronal population.

For the pulse-chase contribution assay after injury, adult zebrafish (n = 3 per time point) were subjected to Triton X-100 injury and separated into three groups, which received a 24 h BrdU pulse during the first, third, or fifth day following the injury. Regardless of the time of pulse, all animals were analyzed at 7 dpi at which tissue regeneration is largely complete. The group labeled at 1 dpi was transferred to BrdU-containing tank water immediately, while the 3, and 5 dpi groups were kept in tank water until the onset of the pulse. OE samples were dissected and analyzed for the radial position and quantity of BrdU/HuC/D double-positive cells (Figure 4.19A).

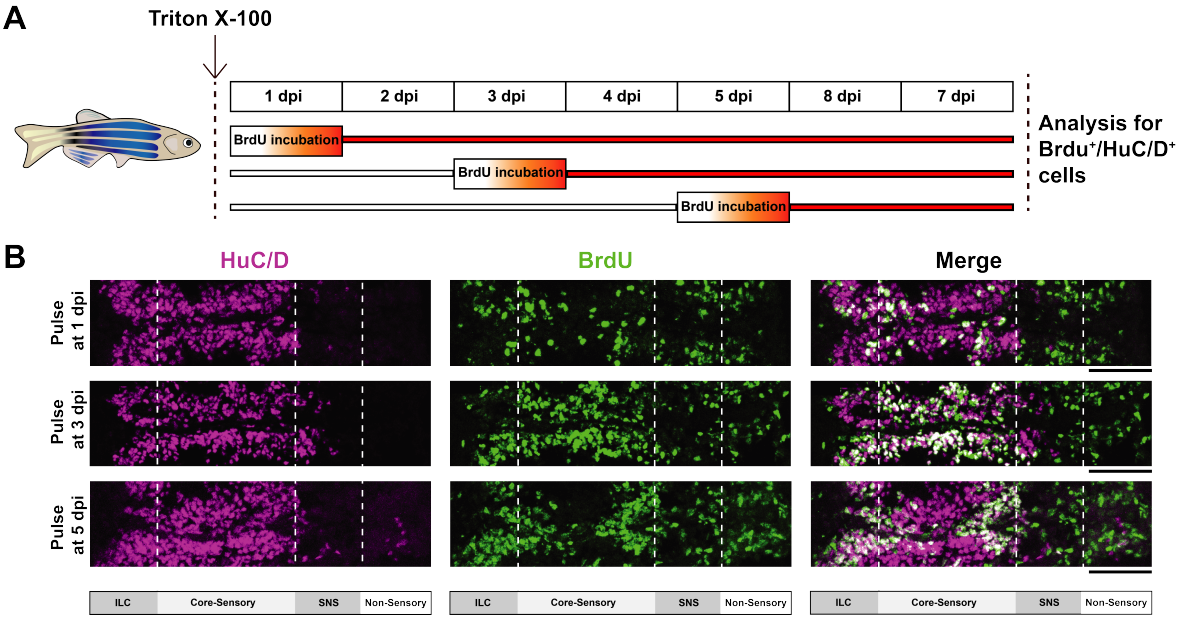

Figure 4.19. Pulse-chase approach to analyze OSN regeneration upon Triton X-100 injury. A. Experimental setup. B. Representative images of regenerated OEs that are BrdU-labeled at 1, 3 and 5 dpi. Scale bars: 50 µm.

OE regeneration was largely complete in all fish by 7 dpi, as revealed by anti-HuC/D staining and the presence of densely packed OSNs in the sensory regions (Figure 4.19B). The distribution of BrdU/HuC/D-positive OSNs that were labeled at different time points along the core sensory region showed quantitative and spatial differences in a progressive manner (Figure 4.20).

The restored OEs labeled at 1 dpi displayed a relatively uniform distribution of HuC/D/BrdU double positive cells, while a two-peaked distribution was observed in the intact OE, as expected. In order to assess the contribution of regenerative neurogenesis selectively, the ILC and SNS were excluded from the quantification and only double positive cells located within the core sensory region (segments: 0.2-0.6) were compared. The total cell number obtained from the restored OE that was labeled at 1 dpi was slightly, yet significantly higher than that obtained from intact internal controls 15.2 ± 0.9 neurons/core sensory OE in the intact tissue vs. 22.3 ± 1.2 neurons / core sensory OE in the restored tissue,$p_{restored/intact} = 4.7 \times 10^{-6}$, unpaired Student's t-test, $t_{restored/intact}$ = -4.8214) (Figure 4.20).

The distribution pattern of labeled cells changed characteristically in the restored OEs that were labeled at 3 dpi. BrdU/HuC/D double-positive OSNs were largely distributed across the sensory region of the restored OE, whereas labeled OSNs were localized at either of two proliferation zones in the intact OE. The core sensory region became highly mitotic in the restored OE and contained 73.8 ± 3.0 neurons on average. On the other hand, occurrence of the newborn neurons in the sensory region remained very low in the intact OE (5.1 ± 0.7 neurons/core sensory OE, $p_{restored/intact} = 5.0 \times 10^{-32}$, unpaired Student's t-test, $t_{restored/intact}$ = -22.2202). More importantly, the change in the distribution of OSN neurogenesis and increase in the total number of labeled OSNs were more prominent in this experimental set, indicating that the regenerative response and the activation of progenitor cells, that are initiated at 1 dpi are maintained and become more extensive at 3 dpi.

In the group that was labeled at 5 dpi, the average number of BrdU/HuC/D double-positive OSNs in the core sensory region was still significantly higher in the restored OE (37.0 ± 1.9 neurons/ core sensory OE) than in the intact control (10.4 ± 1.3 neurons/ core sensory OE, $p_{restored/intact} = 1.9 \times 10^{-19}$, $t_{restored/intact}$ = -87.7469). However, the difference between the restored and intact OEs was less pronounced at this time, suggesting that the OE reverts to pre-injury neurogenesis by 5 dpi.

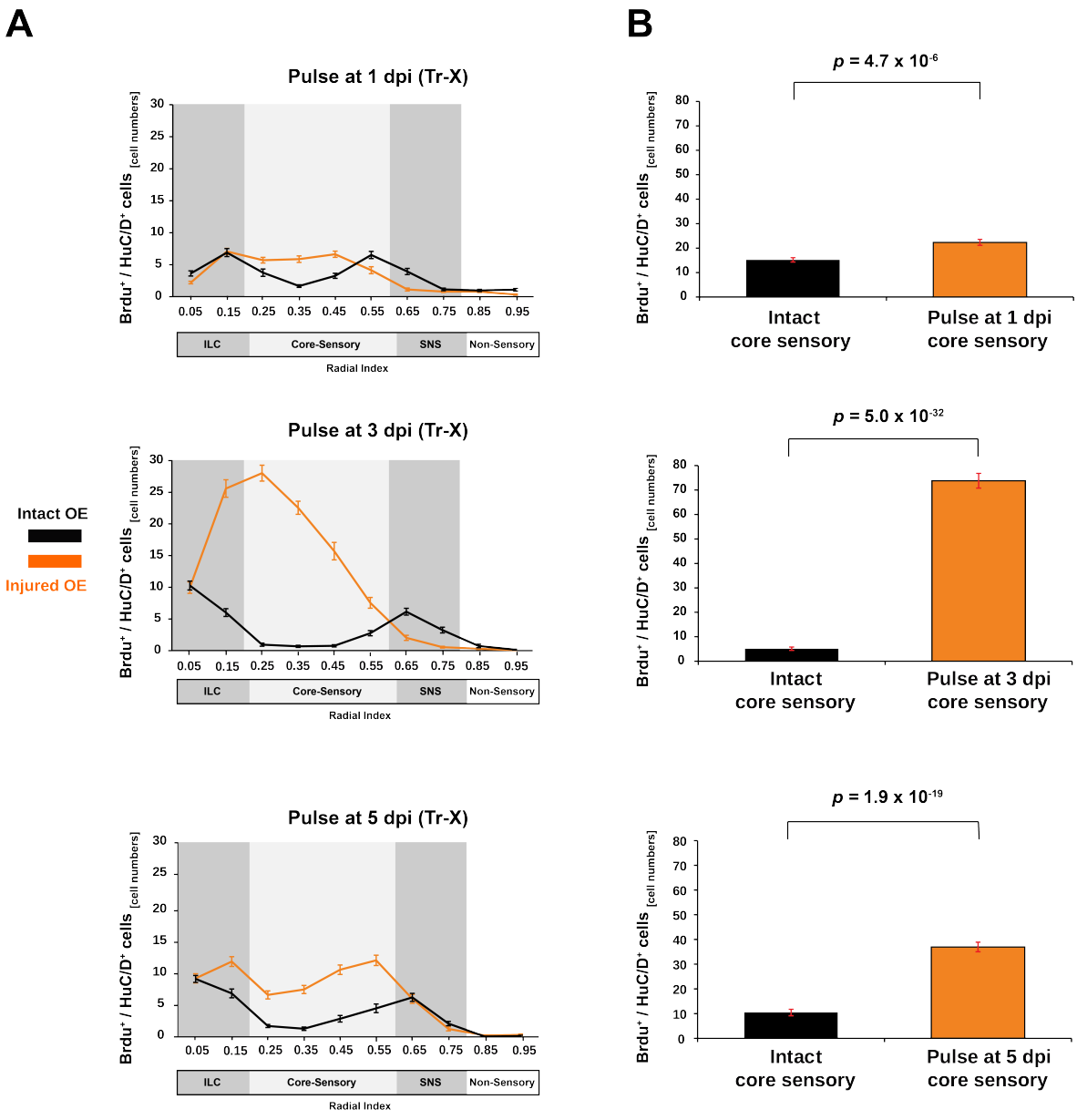

Figure 4.20. Quantitative analysis of OSN regeneration upon Triton X-100 injury. A. Positional profiling of BrdU/HuC/D double-postive cells in intact (black) and fully regenerated (orange) OE. B: Quantitative comparison of core sensory OEs.

The newborn OSNs labeled at 5 dpi formed an elevated bimodal distribution and there was an apparent decrease in the number of labeled cells, when compared to the restored OEs labeled at 3 dpi. The positions of the labeled OSN clusters at the ILC and around SNS resembled the distribution of the internal control, although the amplitudes of intact and restored OE distribution curves varied in the sense that a larger number of cells could be observed in the damaged tissue. The bimodal character of the distribution in the restored OE suggests that the OE resumed to constitute neurogenesis at the time of the labeling. This finding shows that regenerative neurogenesis follows progressive spatiotemporal patterns, in parallel with the general dynamics of the induced proliferation that were characterized in the previous sections. The generation of young neurons occurs abundantly at 3 dpi and the enhanced neuronal generation is followed by a reduced and regionally localized neurogenic activity at later phases.

4.2. Characterization of cell types that contribute to OE regeneration

This section focuses on the identification and characterization of HBC-like cells in the zebrafish OE and their potential involvement in regenerative neurogenesis. HBC-like cells will firstly be identified in the OE by immunohistochemistry with antibodies against relevant marker proteins and their organization in the OE will be described in the intact and chemically-injured samples. Then, their proliferative activity will be assessed under different tissue conditions.

4.2.1. The zebrafish OE contains HBC-like cells

As described in the previous section, efficient regenerative neurogenesis can be observed in the zebrafish OE, however, different from rodent models, cell types that function as progenitors and contribute to OSN neurogenesis in the damaged OE were not known at the beginning of this study. Generally, the vertebrate OE contains three fundamentally distinct non-neuronal cell populations that all play a role in OE regeneration: sustentacular cells, GBCs and HBCs. Among those, GBCs and HBCs have been shown to function as neuronal progenitor cells under different tissue conditions [68].

Studies demonstrated that dormant HBCs serve as reserve stem cells in the intact OE but become proliferative and generate all OE-specific cell types upon epithelial injury [67, 68]. GBC activity, on the other hand, is commonly associated with the maintenance of neuronal homeostasis in the intact tissue, although the contribution of slow-cycling GBC subsets to regeneration has also been suggested [65]. The identification of all GBCs at tissue level is challenging due to their molecular and functional heterogeneity. In the zebrafish OE, cells with GBC characteristics, based on the expression of Ascl1, have been localized to the ILC and SNS, in line with their predominant contribution to maintenance neurogenesis in the intact OE [127]). On the other hand, HBC populations appear to be more homogeneous with distinct morphological features and immunohistological characteristics.

HBCs are flat-shaped cells that are attached to the basal lamina. Under physiological conditions, HBCs are mitotically quiescent and rarely differentiate [68]. HBC dormancy is mostly attributed to the expression of truncated p63 (Np63) which is a transcription factor belonging to p53 tumor suppressor family [220]. At physiological levels, The p63 protein regulates cellular dormancy and represses differentiation of HBCs in the OE [94, 221]. Upon injury, p63 is downregulated, possibly by degradation through the ubiquitin-dependent proteasomal pathway [222]. This degradation anticipates HBC activation, leading to self-renewal and differentiation of HBCs into transient GBC-like cells and ultimately into OSNs and sustentacular cells [67].

To identify and characterize HBC-like cells in the zebrafish OE, immunohistochemical analysis of p63 and the cytoskeletal marker Keratin5 were performed, that are characteristically expressed in quiescent HBC pools of the rodent OE [221]. Both marker proteins were distinctively colocalized in a coherent but discontinuous single-cell layer in the basal sensory region (Figure 4.21A). Krt5/p63 double-positive cells along the sensory region had a flat morphology and were adherent to basal lamina. The peripheral non-sensory region also contained Krt5/p63 double-positive cells, however, these cells displayed a pyramidal morphology with distinct apical protrusions and were densely packed in multiple epithelial layers, instead of forming a single-cell layer.

To better discriminate between HBCs in the sensory OE and other non-neuronal cell types that express the same marker genes in the non-sensory OE, immunohistochemistry against Keratin5 and the undifferentiated cell marker Sox2 was performed on intact OE sections. Sox2-positive cells were abundantly found in basal and multiple intermediate layers in the sensory OE and a basal subset of Sox2-positive cells showed Keratin-5 immunoreactivity (Figure 4.21B). These Sox2/Krt5 double-positive cells residing in the basal sensory OE formed a single cell-layer which was visually identical to the position of Krt5/p63 double-positive cells. In the non-sensory OE, Sox2-positive cells were only sporadic and did not show Keratin-5 immunoreactivity, indicating that Krt5-positive cells residing in the basal sensory OE and in the non-sensory OE are not identical cell types at the molecular level.

These observations suggest that the zebrafish OE contains a distinct and homogenous basal cell type in the sensory region, that differs from non-sensory cells expressing the same markers in terms of organization and molecular content but shares similar morphological and immunohistochemical characteristics with HBCs in higher vertebrates.

4.2.2. HBC-like cells exit dormancy and divide frequently upon chemical injury

One characteristic feature of HBCs is their slow-mitotic cycling under physiological conditions [68, 94], which also appears to be conserved in the Krt5/p63 double-positive HBC-like cells in zebrafish as well. When subjected to BrdU incubation for 24 h, most of the HBC-like cells did not incorporate the BrdU label. On the other hand, the number of BrdU-positive cells within the HBC-like cell population became substantially elevated upon chemical injury (Figure 4.22). In addition, distinct morphological changes were coupled with the increase in mitotic activity. Unlike quiescent HBC-like cells that remain morphologically flat, active HBC-like cells in the sensory region extended protrusions and occupied supra-basal layers.

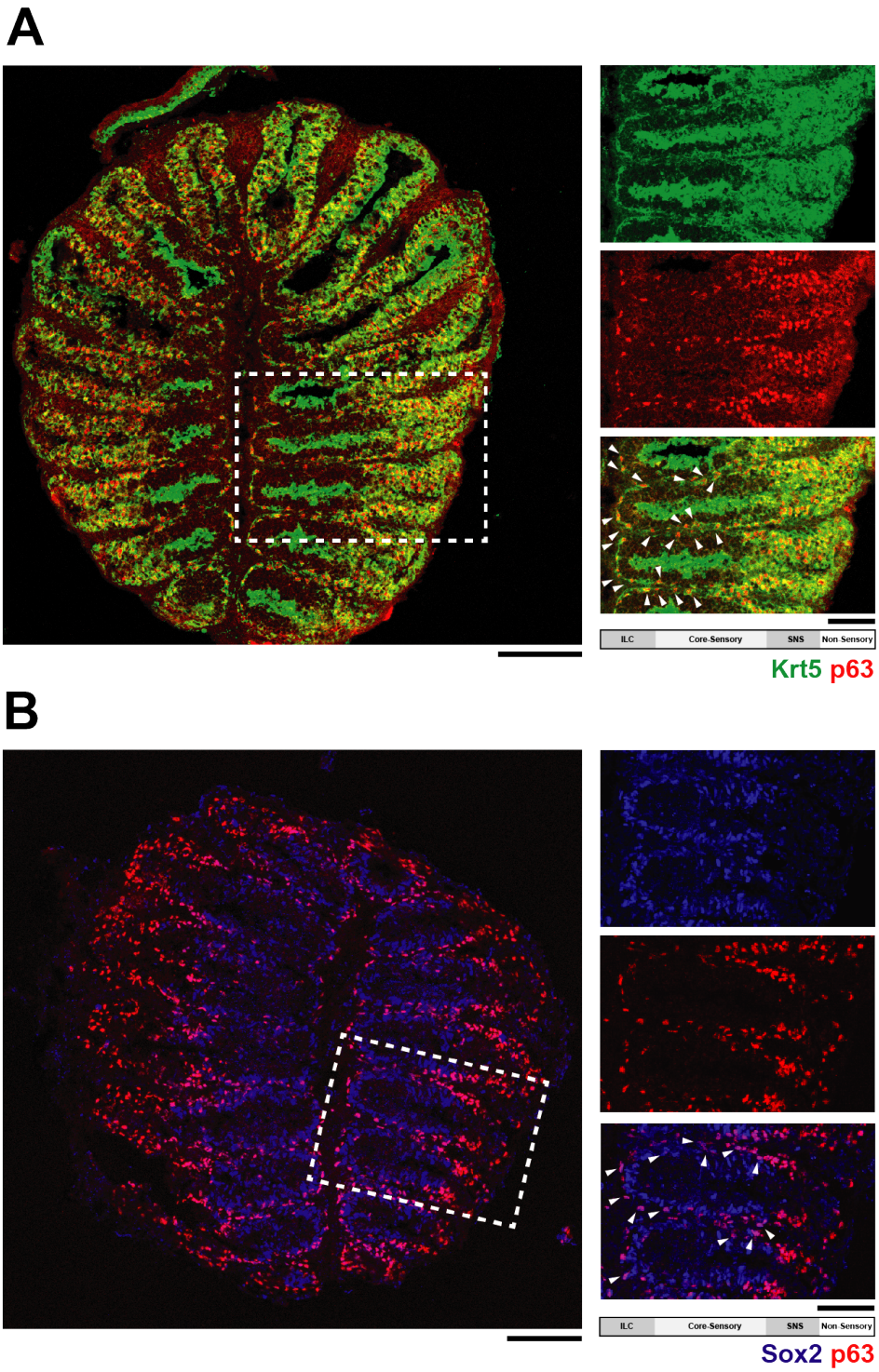

Figure 4.21. Identification of HBC-like cells in the intact zebrafish OE. A. Krt5 and p63 Labelling. B. Sox2 and p63 labelling. Arrowheads: double-positive cells in the sensory OE. Scale bars: 100 µm (section) and 50 µm (lamella).

The invasive behavior of HBC-like cells in the supra-basal layers is transient, as cells in the fully regenerated OE do not show the same signs of protrusive extensions or multilayer organization. Fully regenerated OEs only contain a single-cell-layer of HBC-like cells adherent to the basal lamina, which looks identical to the cellular organization in the undamaged OE.

4.2.3. Temporal activation of HBC-like cells is correlated with the phases of the regenerative response

In order to profile HBC-like cell activation during the regenerative response, cycling HBC-like cells, that were identified by Krt5 expression, were labeled with BrdU at progressive time points after damage (Figure 4.23). Animals were initially divided into three groups for the early (1 dpi), mid (3 dpi), and late (5 dpi) phases. After receiving the chemical injury to the right nose, fish were kept in freshwater until the onset of the desired 24 h-long BrdU incubation period. All OE samples were analyzed immediately at the end of BrdU incubation. As in the previous experiments, left OEs remained intact to serve as internal control. In the case of 1 dpi group, the freshwater step was skipped and animals were put into BrdU-containing water immediately after injury by Triton X-100 treatment. A cycling HBC-like was defined as a cell that reacts with BrdU and Krt5 antibodies along the sensory region between segments 0 and 0.6 according to the radial index scoring system.

The number of mitotically active HBC-like cells was noticeably increased in the injured OE at 1 and 3 dpi but was identical to control OEs at 5 dpi (Figure 4.23A and 4.23B). The core sensory region of the injured OE (segments: 0.2-0.6) contained 7.2 ± 0.5 (mean ± SEM) BrdU/Krt5 double-positive cells per lamella at 1 dpi, whereas the intact control had only 3.5 ± 0.3 cells on average ($p_{1dpi/control}$ = 1.1 x 10^{-19}, unpaired Student's t-test, $t_{1dpi/control}$ = 6.726). At 3 dpi, 11.3 ± 1.1 BrdU/Krt5 double-positive cells could be found in the core sensory region, whereas the intact control had 7.1 ± 0.7 on average ($p_{3dpi/control}$ = 0.0020, unpaired Student's t-test, $t_{3dpi/control}$ = -3.1772).

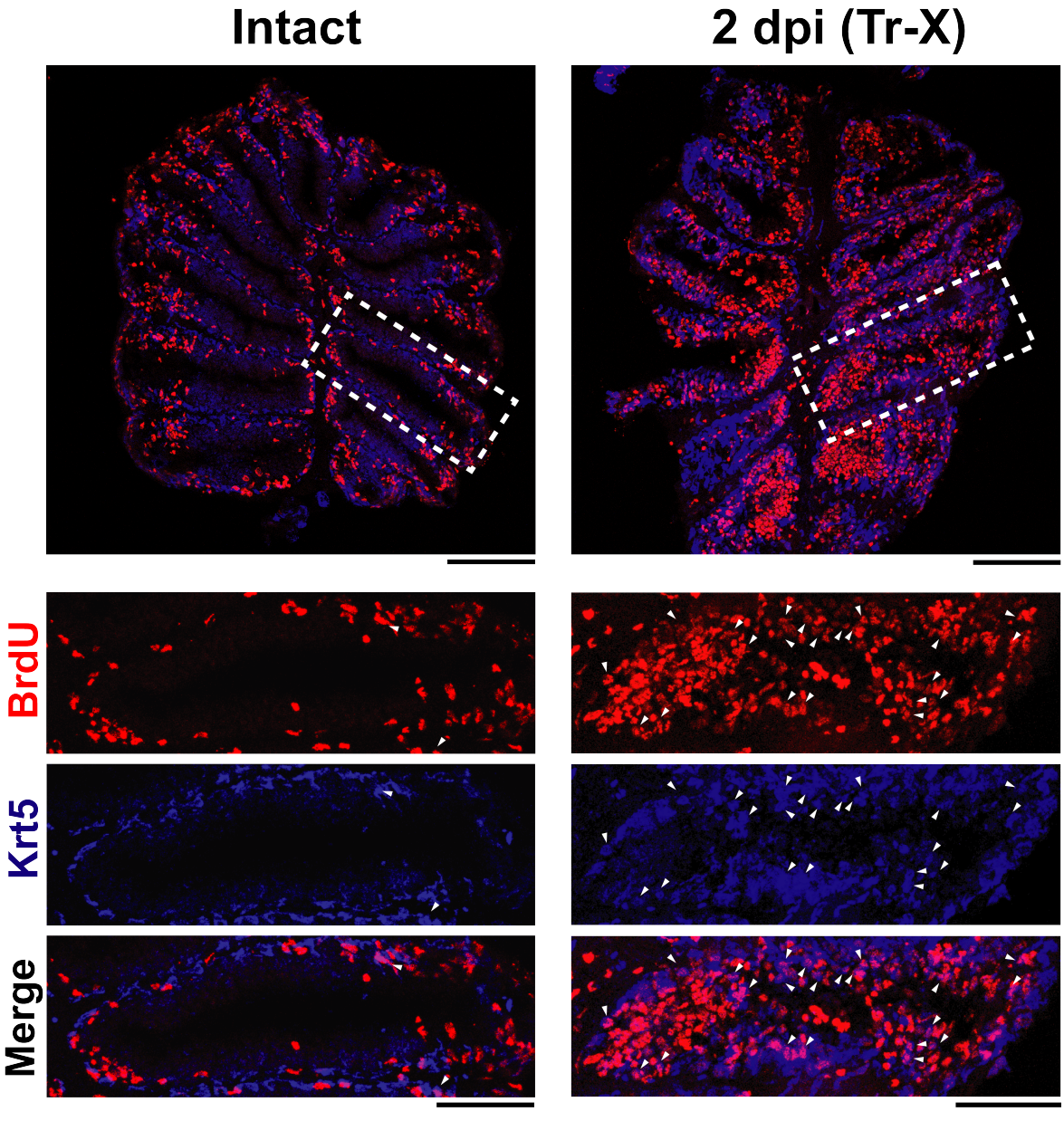

Figure 4.22. Krt5/BrdU double-positive HBC-like cell respond to Triton X-100 treatment. Scale bars: 100 µm (section) and 50 µm (epithelial fold).

Intact OEs had characteristically only one BrdU/Krt5 double-positive cell per radial segment across the sensory region while the non-sensory region had a slightly higher number of Krt5/BrdU double-positive cells but these cells are likely to have a role in the recovery of peripheral non-neuronal cells, rather than contributing to OSN neurogenesis. In contrast, the injured OE at 1 and 3 dpi showed a uniformly increased activity along the sensory region. The number of active cells declined at 5 dpi and the distribution of the injured OE appeared visually identical to the internal control. The distribution profiles and the quantitative result were alike at 5 dpi labeling (3.0 $\pm$ 0.3 in the injured OE vs. 2.4 $\pm$ 0.2 in the intact OE, $p_{5dpi/control} = 0.1614$, unpaired Student's t-test, $t_{5dpi/control} = 1.4096$), suggesting that HBC-like cells are activated only transiently during the early phase of regeneration and revert to dormancy at later phases.

These findings suggest that HBC-like cells exist in the basal OE and that these cells conserve the functional characteristics of HBCs, that can be observed in other species upon injury. HBC-like cell activation is a transient event and ends already before OE regeneration is complete. This is in agreement with the hypothesis that early activation of HBCs results in the generation of Ascl1-positive GBC-like progenitors that undergo multiple rounds of cell divisions before differentiating into neurons in rodents [94] and zebrafish (Figure 4.17 and 4.18).

4.2.4. HBC-like cells undergo self-renewal

Activated HBCs repopulate the OE by mitotic cycling and subsequent generation of fast cycling GBCs. However, not all activated HBCs can terminally differentiate into other post-mitotic cell types, since such an event would result in the irreversible depletion of the HBC pool. HBCs could either divide into two equivalent HBCs (self-renewal) or undergo asymmetric division, which generates a fast cycling GBC and a HBC. If newborn HBCs perpetuate the reserve pool, they will remain inactive and not cycle as frequently as other activated HBCs. Hence, detecting labeled newborn HBCs in the fully restored OE can give insight into the regenerative background of the tissue.

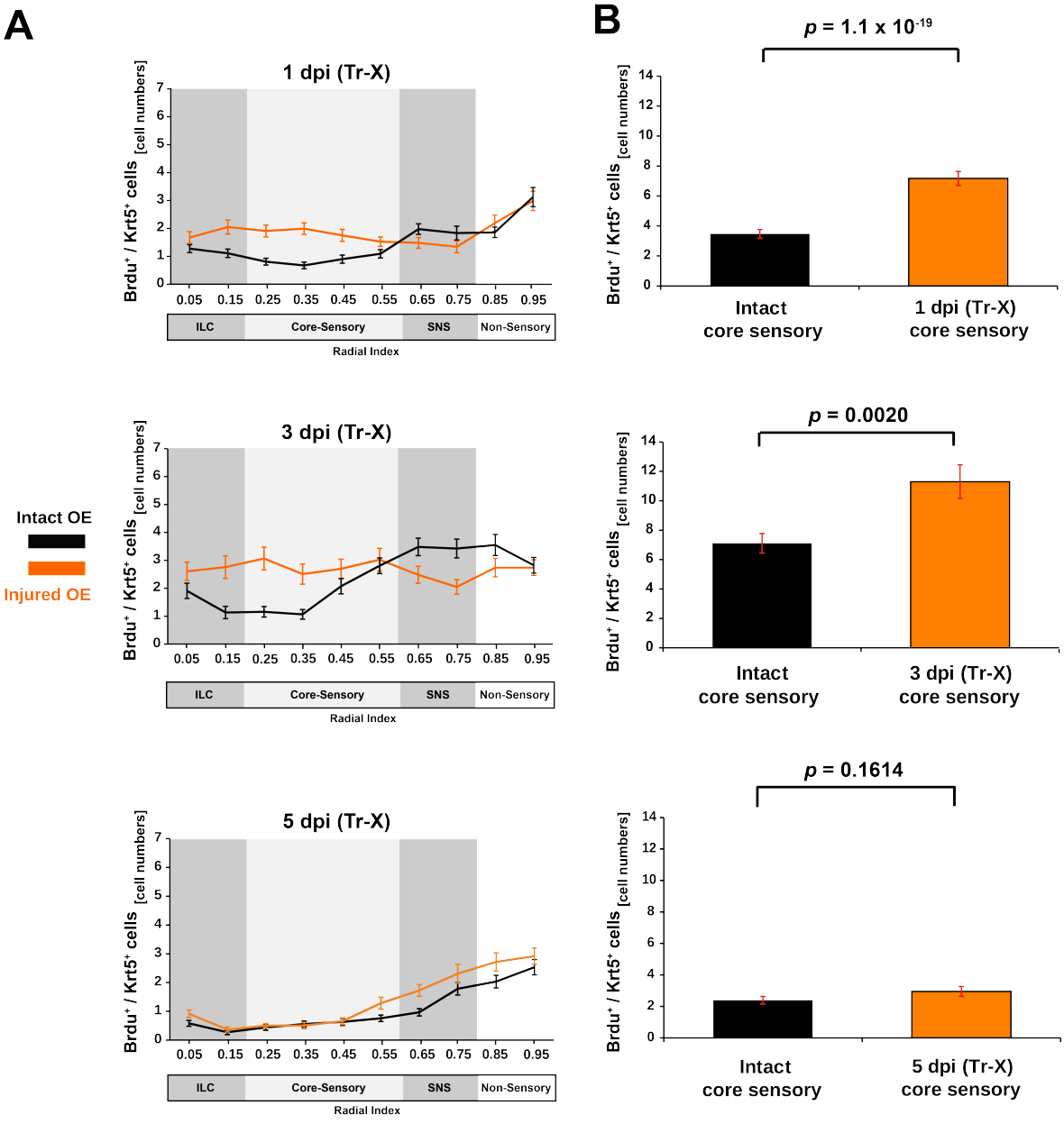

Figure 4.23. Quantitative analysis of active HBC-like cells. A. Positional profiling of BrdU-labeled HBC-like cells in intact (black) and regenerating (orange) OEs. B: Comparison of active HBC-like cell numbers in the core sensory region.

In order to analyze progression of the HBC-like cell pool, the experimental animals analyzed in 4.1.12 were further analyzed for Krt5 and BrdU immunoreactivity. In these experiments, the mitotically cycling cells were labeled at 1, 3, or 5 dpi and the OE samples were analyzed at 7 dpi, thus the end of regeneration. Therefore, the analysis could also reveal the presence of label-retaining adult born HBC-like cells that contribute to the maintenance of the reserve pool. Symmetrically dividing HBC-like cells that do not contribute to the reserve pool but exclusively to the tissue restoration and fast cycling HBC-like cells are expected to dilute the incorporated BrdU due to successive divisions and show no or low BrdU immunoreactivity.

Similar to the spatiotemporal profiling of the active HBC-like cells; label-retaining HBC-like cells showed a uniform distribution across the regenerated OE at 7 dpi, yet, the distribution pattern changed progressively. The number of adult-born HBC-like cells labeled at 1 dpi within the core sensory region of the restored OE was 4.6 ± 0.6 (mean ± SEM) per lamella, while the number was significantly lower in control tissue (2.6 ± 0.2, $p_{restored/intact} = 0.0049$, unpaired Student's t-test, $t_{restored/intact} = -2.9038$). In the test group labeled at 3 dpi, the difference between the number of labeled HBC-like cells the restored versus the intact core sensory OEs was even higher (1.4 ± 0.2 in the control OE vs. 5.1 ± 0.5 in the restored OE, $p_{restored/intact} = 6.5 \times 10^{-9}$, $t_{restored/intact} = -6.5556$).

The difference was relatively small yet still present between the intact and restored OEs labeled at 5 dpi, as the distribution curves approached each other in shape and position. (2.7 ± 0.2 in the control OE vs. 4.8 ± 0.3 in the restored OE, $p_{restored/intact} = 1.5 \times 10^{-7}$, $t_{restored/intact} = -5.5923$) The slightly higher amplitude in the restored sensory OE implies that some HBC-like cells still remained activated at the time of the labeling. Figure 4.24 displays the distribution patterns and the quantitative differences of the labeled newborn HBC-like cell population between the restored and intact OEs. These findings together suggest that HBC-like cell activation contributes to the generation of GBCs and self-renewal of HBC-like cells.

In the restored OE, the number of BrdU-labeled HBC-like cells are lower when cells were labeled at 1 dpi than when they were labeled at 3 dpi, possibly because active HBCs of the earlier phase (1 dpi) contribute to the generation of fast-cycling GBC progenitors that commit to the neuronal lineage, while active HBC-like cells of later phase (3 dpi) also contribute to the restoration of the HBC-like cell pool. The generation of label-retaining HBC-like cell population declines noticeably at 5 dpi and possibly remains at physiological levels after the tissue is fully restored.

4.2.5. The Zebrafish OE can induce regenerative responses after milder chemical stress

The acute regeneration response and activation of HBC-like cells described above were caused by the nonspecific and severe injury of the tissue, which affects most of the resident cell types. Direct contact of the OE with 1% solution of Triton X-100 usually results in morphological changes and reorganization of the tissue structure.

The reorganization is not always compatible with accurate measurements of cell numbers and positions. For instance, in addition to neurons and glial cells, Triton X-100 could affect progenitor cells directly, eventually destroy HBC-like cells resulting in slower or less efficient tissue responses. To establish alternative experimental models that are defined by better preservation of tissue integrity, a titration assay was performed for different concentrations of Triton X-100 ranging from 0.05–1 % (Figure 4.25A). The aim of the experiment was to investigate whether mild injury conditions, affecting largely superficial cells on the apical side are sufficient to trigger a regenerative response. Animals treated with different concentrations of Triton X-100 solution were subjected to BrdU incorporation for 24 hours at 2 dpi. To further attenuate the effect of Triton X-100, OEs were exposed to the detergent agent only for 60 sec in all treatments, expect for the standardized 1% application of 90 sec against which the results were compared. Different parameters were examined in the samples, such as proliferative acitivies (BrdU incorporation), loss of OSNs (anti-HuC/D immunoreactivity), and morphological integrity of HBC-like cells (anti-Krt5 staining).

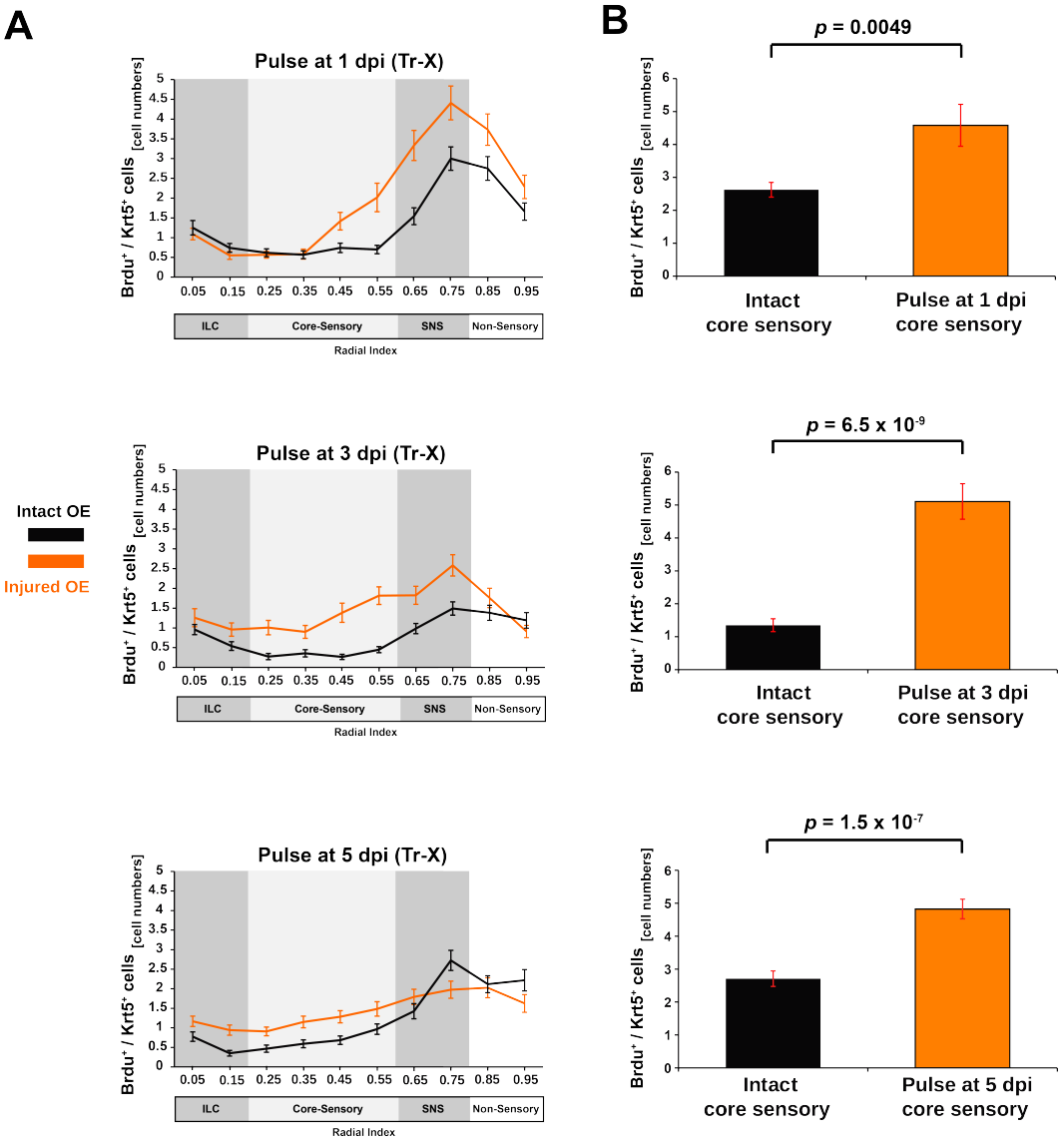

Figure 4.24. Analysis of BrdU-labeled HBC-like cells in intact (black) and restored (orange) OE. A. Positional profiling of label-retaining HBC-like cells at 7 dpi. B. Comparison of label-retaining HBC-like cell numbers in the core sensory region.

All Triton X-100 concentrations above 0.05% resulted in recognizable changes in tissue morphology and a decrease in epithelial thickness that appeared to be correlated with increasing Triton X-100 concentration. More importantly, increased proliferative activities in progenitor cells coupled with OSN neurogenesis along the sensory OE could also be observed in all samples at the time of analysis. Moreover, BrdU/Krt5 double-positive HBC-like cells were found abundantly in OEs exposed even to diluted detergent solution. The loss of OSNs appeared to occur gradually and was most significant in 1% treatment.

The 0.05% treatment, which was the lowest concentration tested, did not cause any visible loss in OSN density along the sensory region.Most interestingly, the formation of branched protrusions and multilayered occupancy of Krt5-positive HBC-like cells were largely absent for all treatments except the standard application of 1% Triton X-100. The increase in the number of flat-shaped Krt5/BrdU double-positive cells along the basal sensory region implies that activation and morphological changes of HBC-like cells are not necessarily mutual events but that the latter is a consequence of the composition of the OE in layers above the layer of HBC-like cells. Figure 4.25B displays representative images of mild and severe treatments.

The results obtained from the titration assay reveals that diluted Triton X-100 treatments as low as 0.1% can potentially trigger repair neurogenesis in the HBC-like cell niche and provoke a regenerative response in the OE even in the absence of major disturbances in tissue integrity.

4.2.6. HBC-like cell activation is elevated under mild injury-conditions

In order to understand whether HBC-like cells are activated after milder injury conditions, fish (n = 3) were treated with 0.1% Triton X-100 solution for 60 sec, followed by an extended BrdU incubation period of 48 h. This concentration and duration of chemical exposure appear to be the threshold for the induction of regeneration, according to the titration assay shown in 4.25.

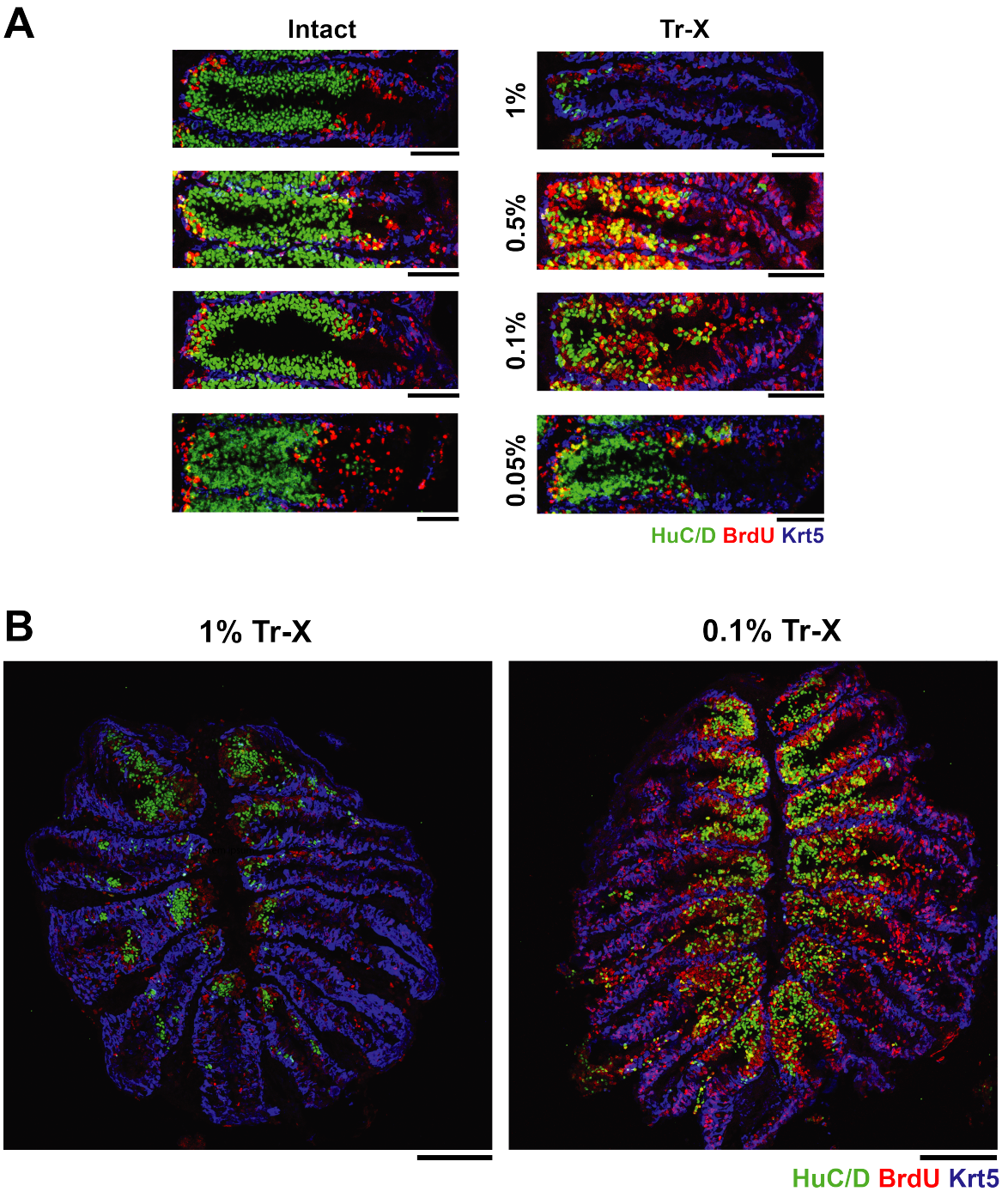

Figure 4.25. Diluted Triton X-100 solutions also affect the OE. A. Epithelial folds that are exposed to Triton X-100 at low concentrations at 2 dpi. B. OE sections upon 1% and 0.1 % after Triton X-100 treatment. Scale bars: 50 µm (A) and 100 µm (B).

Since the milder conditions with diluted chemical agent could result in a slightly different regenerative response with unique features, such as a weaker proliferative activity or a temporal change in degenerative-to-regenerative shift, the BrdU-incubation period was extended to 48 h, instead of the standardized 24 h to tag all activated HBC-like cells. A total of 60 lamellae were analyzed per condition (injured and intact) for quantification purposes.

While OEs that were exposed to diluted Triton X-100 solution largely maintained morphological integrity, the effect of the damage was largely characterized by epithelial thinning and loss of OSNs from the apical surface, as indicated by anti-HuC/D staining (Figure 4.26). There was a considerable increase in HBC-like cell activity and the number of BrdU/Krt5 double-positive cells was elevated uniformly along the OE (arrowheads in Figure 4.26) similar to observations made for the more aggressive 1% Triton X-100 treatment. The numbers of active HBC-like cells along the core sensory region increased 4.7-fold in the injured OE, compared to the internal control (6.6 $\pm$ 0.4 (mean $\pm$ SEM) cells in the injured OE vs. 1.4 $\pm$ 0.2 cells in the internal control($p_{injured/intact}$ = 1.5 x 10^{-19}, unpaired Student's t-test, $t_{injured/intact}$ = -11.5154)(Figure 4.27).

This finding again confirms the stimulatory effects of the diluted detergent exposure on HBC-like cell activation, probably due to molecular alterations in the niche that is caused by the loss of apical cells, without disturbing overall tissue morphology.

4.2.7. HBC-like cell activation occurs after axotomy

Even mild injury conditions using chemical agents affect multiple OE cell types that make contact with the apical surface, such as OSNs and sustentacular cells. Damage to any of these cell types could be the main trigger for HBC activity. Therefore, another question regarding HBC activation may be whether it can be achieved by other methods that selectively affect only a single cell type.

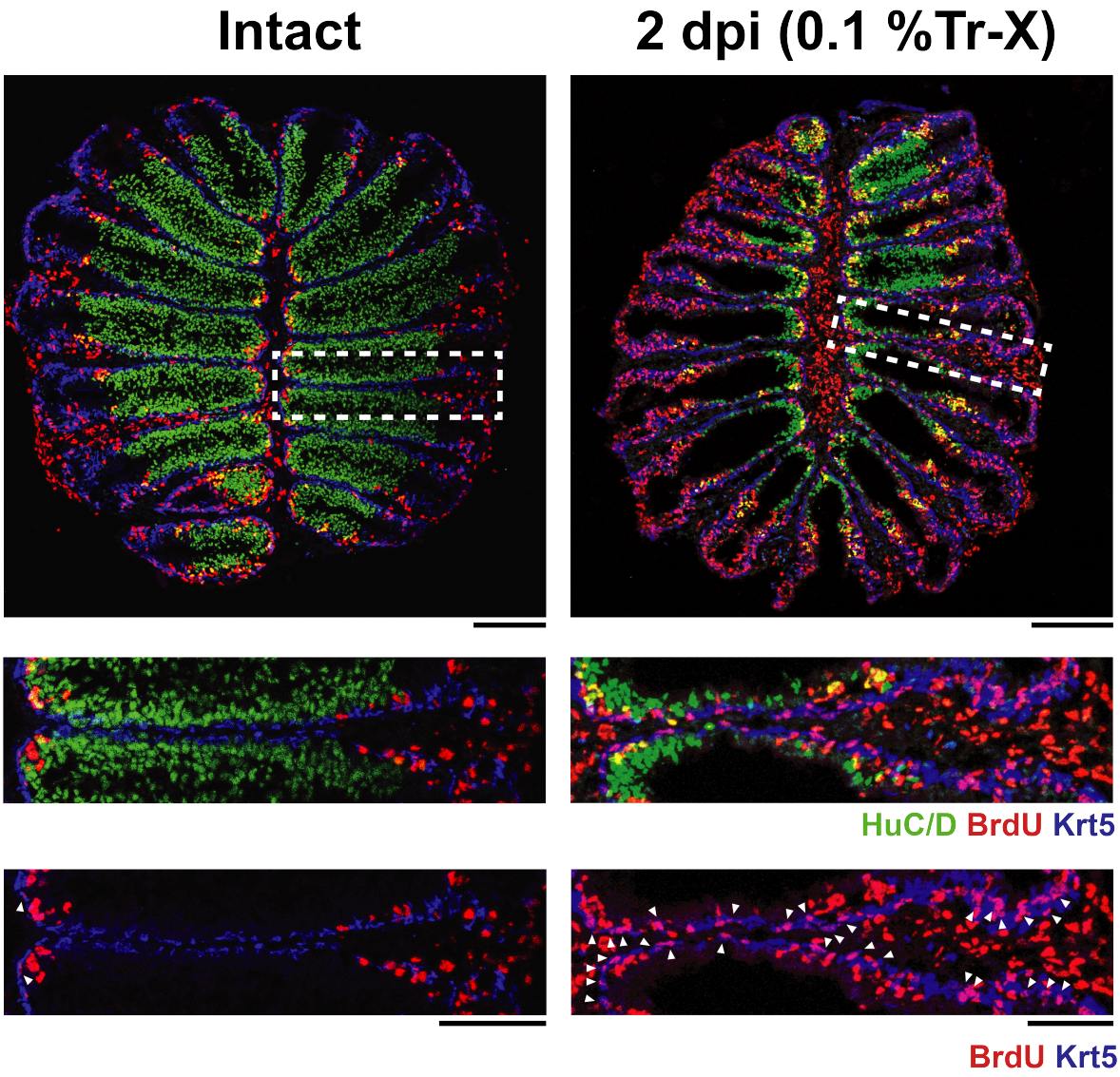

Figure 4.26. HBC-like cells respond to mild chemical injury. A. Representative images of intact and regenerating OE under mild chemical injury at 2dpi. Arrowheads: Krt5/BrdU double-positive cells. Scale bars: 100 µm (section) and 50 µm (lamella).

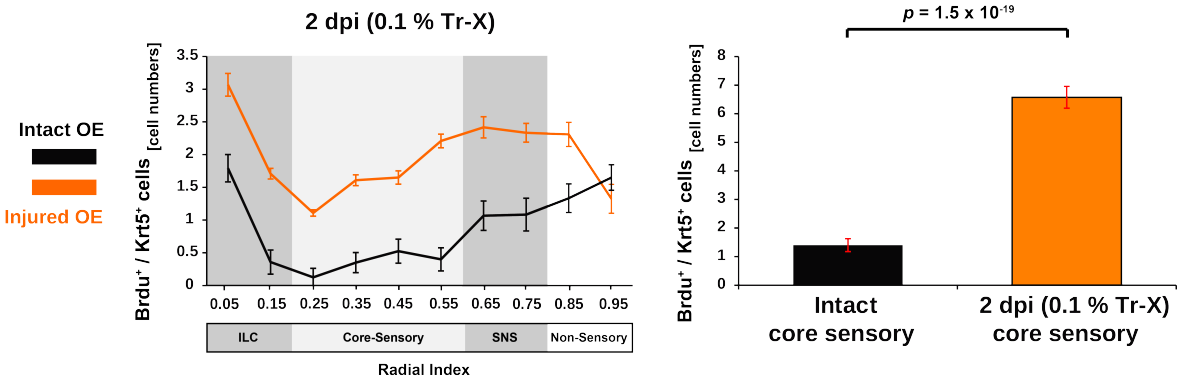

Figure 4.27. Quantitative analysis of mild injury response. Left: Positional profiling of Krt5/BrdU double-positive cells along the intact (black) and regenerating (orange) OEs at 2 dpi. Right: Comparison of the core sensory regions.

In rodent models, it has been shown that surgical removal of the olfactory bulb (bulbectomy) selectively affects OSNs, which extend axons from the OE through the olfactory nerve. Such conditions result in limited HBC activation and suggest that OSN regeneration after axotomy relies predominantly on GBC activation [66, 68]. However, a different study contradicts these findings and reports increased HBC activation and generation of large numbers of HBC-derived OE cells upon bulbectomy-induced OSN depletion [67]. These studies together suggest that HBC contribution to the regeneration after less extensive and more specific injuries than chemical agents can occur under certain conditions, however, its robustness is tightly regulated by the balance between HBCs and other progenitor cells in the basal niche.

In order to investigate the fate of HBC-like cell activation in the selective OSN injury context, the axotomized fish analyzed in Figure 4.14 were further assessed. As expected, axotomy resulted in the ablation of almost all mature neurons at 3 dpi. Notably, there was an induction of cellular proliferation along the sensory region, implying that the regenerative response had been initiated after the axotomy; however only few newborn OSNs could be observed. Quantification of the activated HBC-like cells displayed an increase along the OE in axotomized fish (Figure 4.28A, left).

Within the core sensory region, 1.5 ± 0.2 (mean ± SEM) BrdU/Krt5 positive cells were found in the intact lamella on average, whereas lamellae of axotomized fish contained 5.1 ± 0.5 cells. These numbers correspond to a 3.5-fold increase in the activated HBC cell population upon axotomy ($p_{injured/intact}$ = 1.7 x 10^{-8}, unpaired Student's t-test, $t_{injured/intact}$ = -6.3538).

The uniform spatial pattern and the increased total number of activated HBCs along the sensory region of the axotomized OE appear to be correlated with an increase in the overall number of BrdU-positive cells (Figure 4.14B and 4.28B) but not with the induction of OSN neurogenesis, which was similar to maintenance neurogenesis in terms of quantity and radial position in the OE (Figure 4.14B').

Interestingly, when compared with the immediate activation upon standard 1% Triton X-100 treatment at 3 dpi, the increase in the activation of HBC-like cells within the core sensory upon axotomy was higher (1.6 fold increase upon chemical injury vs. 3.5-fold increase upon axotomy). This result suggests that activation of HBC-like cells is stimulated by axotomy-induced neuron depletion in the zebrafish OE, and not necessarily exclusive for chemical insult. On the other hand, the position and number of newborn OSNs (Figure 4.14B') implies that the activated HBC-like cells do not primarily contribute to OSN neurogenesis at the time of analysis.

As mentioned above, the generation of OSNs was low and ILC-centric at 3 dpi. The newborn OSNs were likely to be generated by constitutively active GBC-like cells at the proliferation zones. The activated HBCs within the sensory region, on the other hand, may differentiate into other non-neuronal cell types in the axotomized OE, such as active GBCs that contribute to OSN neurogenesis at a later time point or sustentacular cells, that are required for OSN neurogenesis as well as restoration of tissue morphology due to the disorganization of the apical surface after severe OSN loss. Therefore, analysis of later time points after bulbectomy should be investigated in more detail.

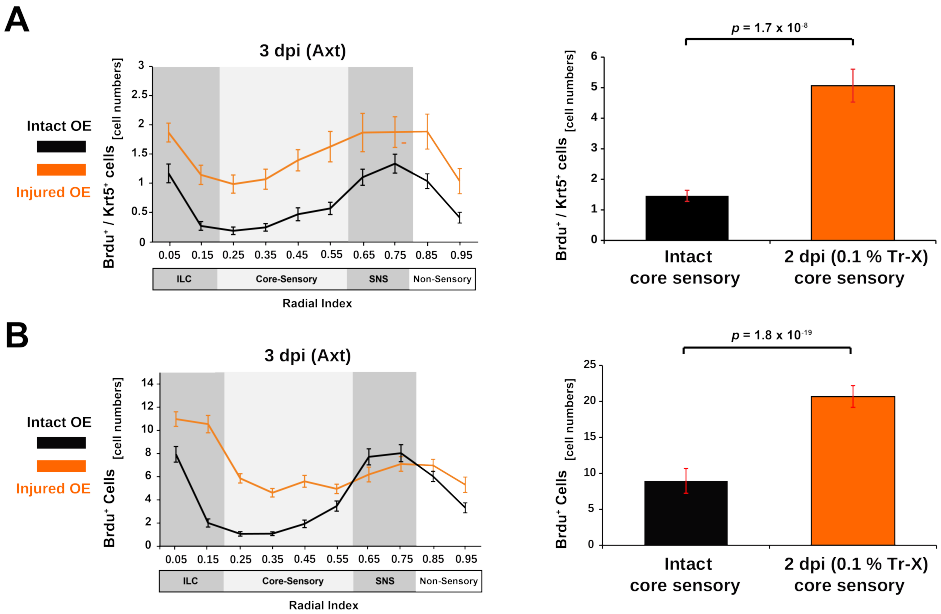

Figure 4.28. Positional profiling and core-sensory-specific comparison of intact (black) and axotomized (orange) OE at 3 dpi. A. Analysis of Krt5/BrdU double-positive cells. B. Analysis of all BrdU-positive cells, left side is reprinted from Figure 4.13.

4.2.8. Generation of *Tg(krt5:EGFP)* reporter line

To simplify further analysis Krt5-expressing HBC-like cells, a *krt5*-specific reporter line was generated. A 2.6 kb-long *krt5* promoter sequence located upstream of the transcription start site (identified by [200]) was cloned in front of the EGFP reporter in pT2AL200R150G, a commonly used vector for reporter line establishment based on Tol2 transposon system [223] and the plasmid was injected into fertilized zebrafish oocytes along with Tol2 transposase mRNA.

The F0 founder fish showed mosaic but strong EGFP expression, mainly in the epidermis and muscle cells (Figure 4.29). F1 progeny, on the other hand showed ubiquitous expression in epithelial cells of ectodermal origin, as described in [200]. Figure 4.29 displays representative images of the embryos of the injected F0 and subsequent F1 progeny. The stable line can be used for future analysis of HBC-like cells in the OE.

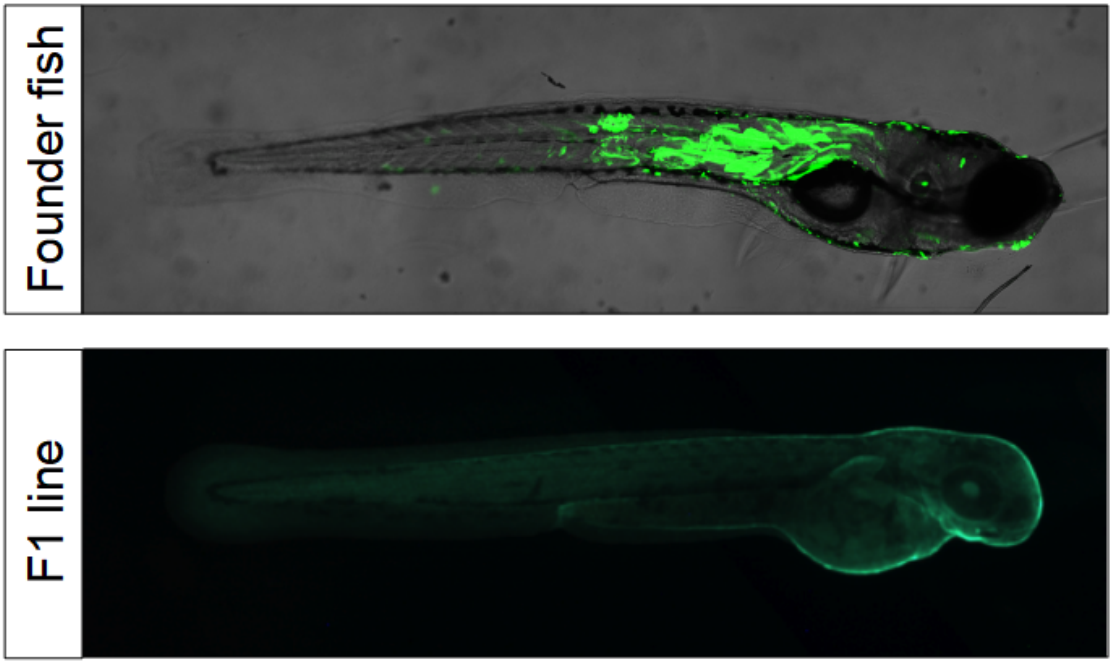

Figure 4.29. Generation of the *Tg(krt5:EGFP)* reporter line. Upper: representative confocal image of an F_0 founder candidate at 2 dpf (days post fertilization). Lower: EGFP expression in an F_1 embryo under a stereomicroscope at 2 dpf.

4.3. Investigation of the role of HB-EGF signaling on cell proliferation and OSN neurogenesis in zebrafish OE

This section focuses on the characterization of HB-EGF activity in injury-induced proliferation and OSN neurogenesis in the zebrafish OE and describe the link between extracellular HB-EGF signaling and the regenerative response. First, the expression profile of zebrafish paralog *hbegfa* will be displayed via transcriptome analysis and in-situ hybridization. Then, the effects of exogenous HB-EGF administration on proliferation and OSN neurogenesis will be discussed. Finally, the loss of HB-EGF activity via pharmacological inhibition of extracellular matrix proteases will be analyzed.

4.3.1. *hbegfa* is upregulated in the regenerating OE

The regenerative response of the zebrafish OE is evident under different tissue conditions; however, molecular components that contribute to stem cell regulation in the regenerative niche are not well-understood. One plausible approach for the identification of progressive molecular changes in the regenerating tissue is the analysis of differential gene expression by transcriptome profiling. This analysis highlights relevant genes in the context of the OE regeneration over a time course. For this purpose, bulk-transcriptome profiling of expressed mRNAs from the regenerating OEs at different time points was conducted. Fish were injured with 1% Triton X-100 solution according to the standard procedure and the regenerating OEs were collected at early (4 hpi, 12 hpi, 24 hpi), mid (3 dpi),and late (5 dpi) time-points. RNA was extracted from the samples by phenol-chloroform extraction. 20 fish were used per time point and total RNA extracts were generated in triplicate (60 OE/time-points). The process generated around 50 million paired-end reads per time point and replicate, which were aligned to the GRCz11 zebrafish genome and an analysis of differentially expressed genes was conducted using standard bioinformatics pipelines (Demirler, unpublished). Among the transcripts that were elevated during the early phases, *hbegfa* and *hbegfb*, the two paralogs of the heparin-binding epidermal growth factor-like growth factor (HB-EGF) gene in zebrafish showed a sharp and transient up-regulation at 4 hpi. The transcript levels declined within 24 hours and stabilized at pre-injury expression by 3 dpi. In contrast, none of the other known EGF receptor ligands (*amphiregulin*, *beta-cellulin* or *tgf-alpha*), except *neuregulin*, showed a significant change in their expression profiles throughout de- and regeneration (Figure 4.30A). Endogenous *egf* expression, on the other hand, could not be detected neither in the intact nor regenerating OE at any time point.

HB-EGF is a member of the EGF family and plays critical roles in wound healing and regeneration in various tissue types [224–226]. HB-EGF is also known for its neuroprotective roles and modulatory effects on neurogenesis in different injury models [113, 185, 227].

One of two identified HB-EGF paralogs in zebrafish, *hbegfa*, was previously shown to play a critical role in the regulatory loop that coordinates dedifferentiation and subsequent cycling of retinal Müller glia cells after retinal lesion [113]. Considering the literature data and the distinct upregulation of *hbegfa* and *hbegfb* revealed by our transcriptome analysis, the pattern of *hbegfa* expression in the regenerating and intact OE was assessed by *in situ* hybridization (initially by myself, later by Kardelen Güler, unpublished). *Hbegfa* is expressed at low levels along the basal layer of the intact OE but strongly upregulated in the regenerating OE at 4 hpi, consistent with the RNA-seq data (Figure 4.30B). At 8 hpi, *hbegfa* transcripts were still upregulated, although the signal intensity was lower than at 4 hpi. This progressive change in tissue expression was, therefore, well-correlated with the expression profiles obtained from the transcriptome analysis.

4.3.2. Recombinant HB-EGF treatment stimulates proliferation in the OE

The detection of cells with *hbegfa* expression during the early time points of regeneration suggests that the growth factor is generated rapidly upon injury and may promote regenerative proliferation in the basal layer of the OE, where non-neuronal progenitors reside. The stimulatory effects of HB-EGF on proliferation can be investigated by exogenous stimulation with recombinant HB-EGF of intact tissue. Reproduction of a regenerative response effect on neurogenesis by HB-EGF infusion has been previously demonstrated in rat model *in vivo* [184].Similar to this rat model, I hypothesized that exogenous administration of recombinant HB-EGF may promote proliferation in the sensory region of the zebrafish OE, resulting in a distribution of proliferating cells similar to the one observed in proliferating basal progenitors after injury.

To investigate if exogenous HB-EGF can provoke proliferative responses in dormant progenitor cells, human recombinant HB-EGF was applied to the nasal cavity. The recombinant protein solution is composed of the active (soluble) form of HBEGF and can activate its target receptor, the zebrafish EGFR as reported in previous studies [113, 228].

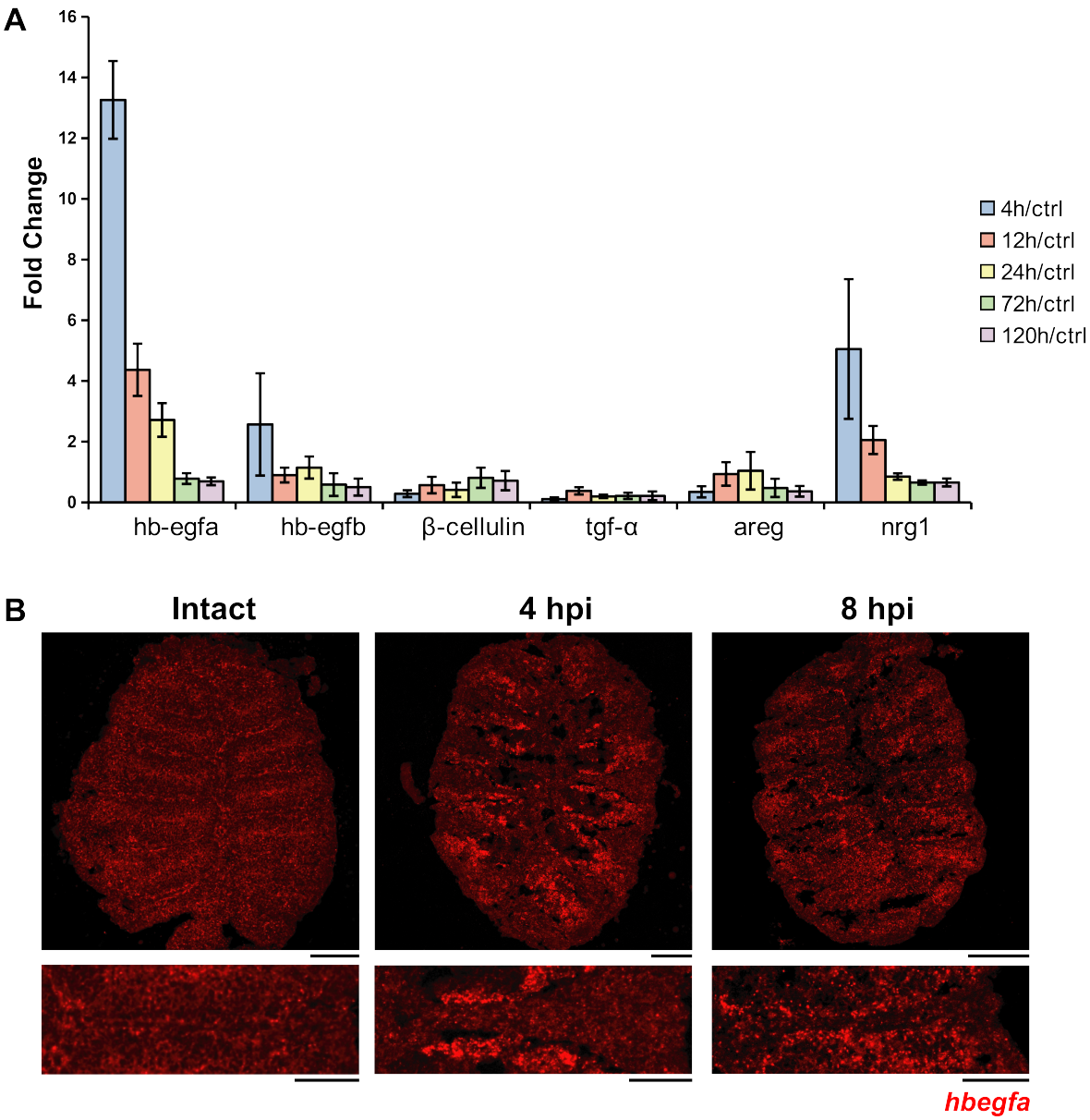

Figure 4.30. *hbegfa* is expressed in the regenerating OE. A. Transcriptome profiles of EGFR ligands during regeneration. B. *In situ* hybridization for *hbegfa* expression (performed by Kardelen Güler). Scale bars: 100 µm (section) and 50 µm (lamella).

In this experiment, human recombinant HB-EGF dissolved in 0.1% BSA/PBS at a concentration of 200 ng/µl was given to the right nasal cavity repeatedly over a 20 minute period. Following the procedure, animals were moved back to freshwater tanks for 24 h before receiving a second HB-EGF injection. Animals were then subjected to BrdU-incorporation for 24 h and analyzed for the BrdU-retaining cells to identify changes in cell proliferation (Figure 4.31A). BrdU-positive cell proliferation was assessed from 60 lamellae of 3 OEs per condition (HB-EGF-treated or untreated). Remarkably, HB-EGF stimulation induced a widespread cellular proliferation across the OE (Figure 4.31B).The radial distribution of BrdU-positive cells in the treated OE had the two-peaked pattern similar to the pattern seen in the intact OE, however, the overall number of dividing cells was significantly higher (2 to 3 fold, depending on radial position), including positions within the sensory OE. This suggests that HB-EGF stimulates progenitor cell activity evenly across the OE, most likely by activating HBCs, which have a similar distribution profile. Individual lamella of the treated OE included 64.3 ± 4.7 for BrdU-positive cells on average (versus 43.4 ± 4.0 in case of the untreated control, ($p_{HB\text{-}EGF/untreated} = 0.0009$, unpaired Student's t-test, $t_{HB\text{-}EGF/untreated} = 3.2382$). When the cells were counted within the core sensory region, in which rare mitotic events are expected in the intact OE, the difference between the treated and untreated OE samples was more significant (22.0 ± 1.9 (mean ± SEM) in treated groups vs. 10.3 ± 1.0 in control, $p_{HB\text{-}EGF/untreated} = 3.8 \text{ x } 10^{-17}$, unpaired Student's t-test, $t_{HB\text{-}EGF/untreated} = 5.1758$) (Figure 4.31C, right). There were increased mitotic activities at the ILC (14.4 ± 1.2 cells/HB-EGF-treated ILC vs. 11.4 ± 1.5 cells/untreated ILC) and SNS (14.6 ± 1.5 cells/HB-EGF-treated SNS vs. 11.4 ± 1.3 cells/untreated SNS), however, the 1.3 fold increase upon HB-EGF treatment in both regions was not statistically significant (ILC: $p_{HB\text{-}EGF/untreated} = 0.1311$, unpaired Student's t-test,$t_{HB\text{-}EGF/untreated} = 1.5201$; SNS: $p_{HB\text{-}EGF/untreated} = 0.1087$, unpaired Student's t-test,$t_{HB\text{-}EGF/untreated} = 1.6162$), The statistical significance between core sensory OE and the lack of significance between other mitotic regions suggest that active HB-EGF, therefore, resembles the effect of injury condition and stimulates proliferation of dormant progenitor cells in the sensory OE, rather than accelerating the division rate of GBC-like cells in the proliferation zones, that are constitutively active.

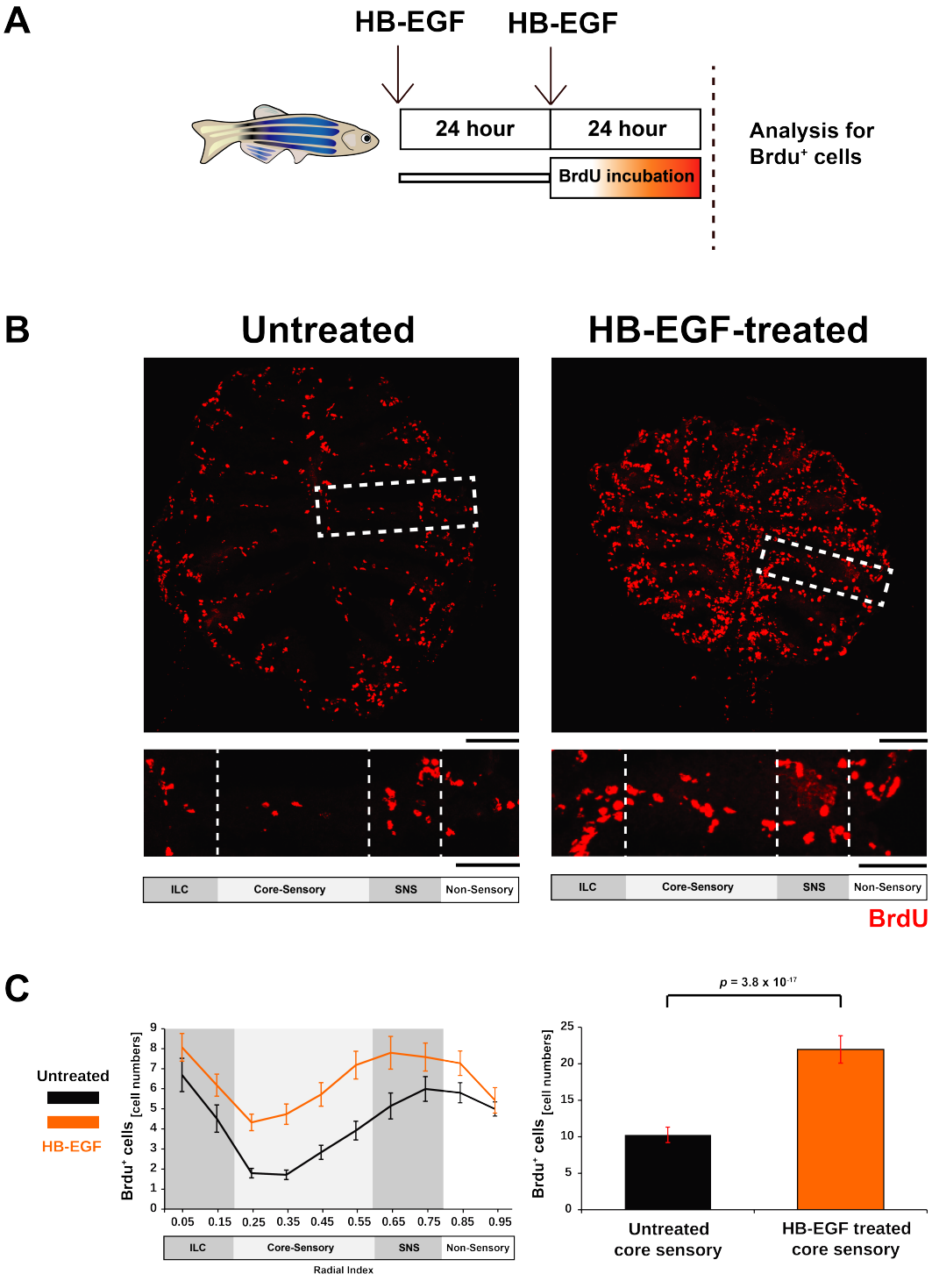

Figure 4.31. HB-EGF enhances cell proliferation in the OE. A. Experimental setup. B. Representative images. C. Analysis of BrdU-positive cells in the untreated (black) and HB-EGF-treated (orange) OE. Scale bars: 100 µm (section) and 50 µm (lamella).

4.3.3. HB-EGF stimulates neurogenesis in the OE

The exogenous administration of HB-EGF resulted in increased mitotic activity in the OE. However, the result does not reveal whether this increased activity is neurogenic. In order to investigate the contribution of the increased mitotic activity to OSN neurogenesis, newborn BrdU/HuC/D double-positive neurons were quantified three days after HB-EGF treatment. Two daily doses of HB-EGF were administered as described in section 4.3.2. After the second application, fish were subjected to BrdU incorporation for 12 h. Fish were then kept in freshwater tanks devoid of BrdU for 60 h to allow some of the labeled cells to mature into OSNs. Dissected tissues were analyzed for BrdU and HuC/D immunoreactivity to detect mature neurons that originated from cell proliferation within the first 12 hours after HB-EGF treatment (Figure 4.32A). BrdU/HuC/D double-positive OSN neurogenesis was assessed from 90 lamella of 3 OEs per condition (HB-EGF-treated or untreated). The numbers of BrdU/HuC/D double-positive neurons after HB-EGF treatment showed an overall increase along the entire sensory region. The distribution of newborn neurons in the treated OE had a two-peaked shape but was significantly elevated, compared to the pattern seen in the control OE (Figure 4.32B and C, left). When the neurons within the core sensory region were quantified, the number obtained from the treated OE was 3.9-fold higher than from the control OE on average (10.1 ± 1.1 (mean ± SEM) cells in the HB-EGF-treated OE vs. 2.6 ± 0.4 cells in control OE, $p_{HB\text{-}EGF/untreated}$ = 5.3 x 10^{-9}, unpaired Student's t-test, $t_{HB\text{-}EGF/untreated}$ = -6.3522) (Figure 4.32C, left). In addition to the increase within the core sensory region, the occurrence of newborn OSNs at the ILC and SNS also was higher in the treated OE than in the untreated OE (11.0 ± 0.9 cells/ILC in the control OE vs 17.6 ± 1.4 cells/ILC in the HB-EGF-treated OE, $p_{HB\text{-}EGF/untreated}$ = 9.5 x 10^{-5}, unpaired Student's t-test, $t_{HB\text{-}EGF/untreated}$ = -4.0144; 7.2 ± 0.7 cells/SNS in the control OE vs 10.4 ± 0.9 cells/SNS in the HB-EGF-treated OE, $p_{HB\text{-}EGF/untreated}$ = 0.0041, unpaired Student's t-test, $t_{HB\text{-}EGF/untreated}$ = -2.9052) suggesting that HB-EGF administration, despite having no significant effect on ILC- and SNS-specific progenitor cell proliferation, may effectively stimulate OSN generation and maturation in these regions through HB-EGF-stimulated HBC activity in these regions as well.

To ensure that the induced increase in neurogenesis is mediated by the administered HB-EGF but not by the experimental design and tissue stress during the procedure, a sham experiment was performed in which one fish received 0.1% BSA solution without HB-EGF. OSN neurogenesis was assessed from 30 lamellae per condition. Both BSA-treated and untreated OE presented identical distribution patterns and quantitative values for BdrU/HuC/D double-positive neurons within the core sensory region on average. (6.0 ± 1.0 cells in untreated control vs. 5.8 ± 0.8 cells in BSA treated OE, $p_{BSA/untreated}$= 0.916, unpaired Student's t-test, $p_{BSA/untreated}$ = 0.1054). This result showed that the generation of newborn neurons in HB-EGF treated samples are mediated by the growth factor.These findings indicate that exogenous HB-EGF administration stimulates neurogenesis in the OE. The neurogenic effect triggered after the administration results in a significant increase in the numbers of newborn OSNs in the sensory region and the uniformity of this increase along the OE shows resemblance to the pattern in the induced proliferation during regenerative neurogenesis. Successive daily administrations of HB-EGF with longer exposure periods may amplify the effect on proliferation.

4.3.4. Pharmacological inhibition of HB-EGF activity during OE regeneration

Gain of function experiments by exogenous HB-EGF administration show an inductive effect on progenitor cell proliferation in the intact OE, suggesting that HB-EGF is sufficient to induce regenerative OSN neurogenesis. Complementary to this, the necessity of the factor to regenerative neurogenesis was examined by loss-of-function experiments. To do so, HB-EGF activity in the regenerating OE was suppressed by the pharmacological administration of specific pathway inhibitors. However, targeting the active form of HB-EGF selectively is challenging and there is only one commercially available drug, CRM197, that has not been tested in non-mammalian vertebrate models so far [229]. Alternatively, HB-EGF activity can be attenuated by preventing cleave of the active extracellular signaling fragment.

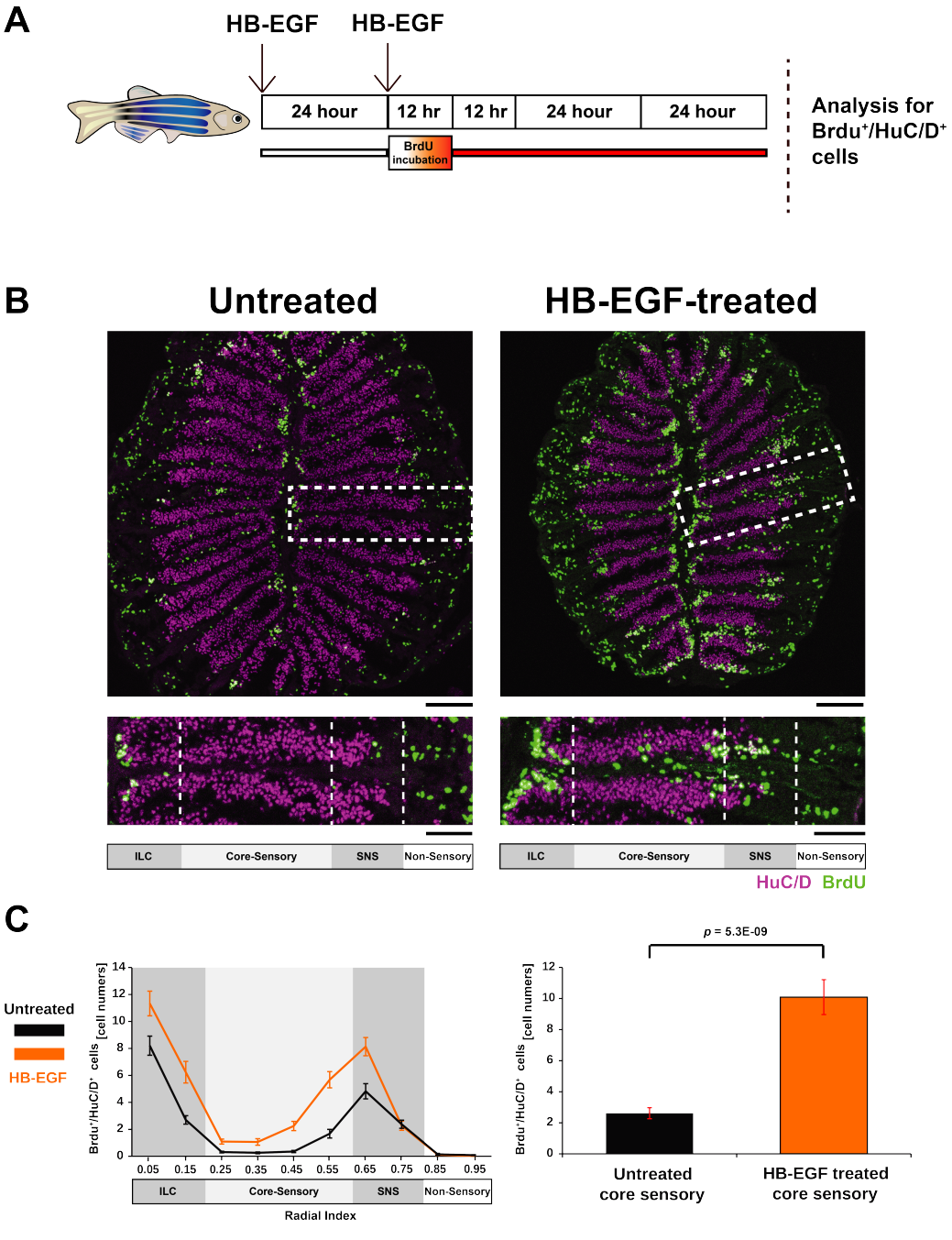

Figure 4.32. HB-EGF enhances neurogenesis. A. Experimental setup. B. Representative images. C. BrdU/HuC/D double-positive cells in untreated (black) and HB-EGF-treated (orange) OE. Scale bars: 100 µm (section) and 50 µm (lamella).

In the uncleaved form, pro-HB-EGF is bound to the cell membrane and has limited mitogenic effect on the adjacent cells, whereas soluble HB-EGF diffuses to distant location, interacts with EGFR on cells and triggers signaling activities in a paracrine and autocrine manner. The proteolytic cleavage is a required step for the conversion of membrane-bound HB-EGF into the soluble form and is achieved by various metalloproteases in the extracellular matrix. Therefore, the inhibition of matrix metalloprotease (MMP) activity in the micro environment can prevent the release of the signaling peptide and inhibit the proliferative effects of soluble HB-EGF on nearby cells that require paracrine stimulation. The pharmacological manipulation of ectodomain shedding by drug administration is a commonly used method in cancer and pathway research, as well as regenerative studies [230–232]. Therefore, two broad-spectrum metalloprotease inhibitors that were previously used in zebrafish [233, 234], GM6001 (also known as Ilomastat) and Marimastat were used to repress HB-EGF shedding during OE regeneration.

4.3.5. Inhibitory effects of GM6001

GM6001 is a synthetic broad-spectrum inhibitor that binds to the zinc-atom located in the active site of MMPs and thereby prevents protease activity [235]. In order to evaluate the effects of GM6001 on OE regeneration, fish (n = 3) were administered with GM6001 (50 μM) by immersion for an hour. Following this priming step, right noses were subjected to 1% Triton X-100 solution. Animals were then transferred to BrdU (30 mg/L) and GM6001-containing (66 µM) water for 24 h. OEs were dissected at the end of BrdU-incorporation and analyzed for BrdU immunoreactivity. Because GM6001 was dissolve in water and received by both injured and intact noses during the treatment, another set of animals (n = 3) was treated with the DMSO solvent and served as control group. HuC/D immunoreactivity was used to visualize mature neurons. The reduced area occupied by HuC/D-positive neurons at 1 dpi indicated that the tissue was damaged properly. The experimental scheme is depicted in Figure 33A.

BrdU-positive cell proliferation was assessed from 60 lamellae of 3 OEs per condition (DMSO- treated and intact, DMSO-treated and Triton X-100-injured, GM6001-treated and intact, GM6001-treated and Triton X-100-injured).

Figure 4.33B displays representative horizontal sections of DMSO and GM6001-treated fish. As expected, BrdU-positive cells were uniformly distributed along the radial axis of the DMSO-treated OE at 1 dpi. On the other hand, GM6001 treatment remarkably reduced the number of BrdU-positive cells in the regenerating OE (Figure 4.34A and A').

The injured OE in the presence of GM6001 still showed the uniform pattern of radial distribution, however, the distribution curve had a lower amplitude than the curve of the injured OEs under DMSO treatment, indicating a decrease in the number of mitotic cells within the sensory OE. Both DMSO- and GM6001-treated intact control groups preserved the bimodal distribution pattern with similar numeric values. Figure 4.34B and B' depict the comparisons of the radial distribution profiles of the control and injured groups within themselves. The quantitative differences were more evident within the core sensory regions between DMSO and GM6001-treated animals; there was a 4.8-fold increase in the average numbers of BrdU-positive cells of the injured OE compared to the average numbers obtained from the intact OE under DMSO treatment (10.4 $\pm$ 0.8 in the injured OE vs. 2.2 $\pm$ 0.2 in the intact OE,$p_{injured/intact}$ = 6.5 x 10^{-14}, unpaired Student's t-test, $t_{injured/intact}$ = -9.3787; Figure 4.34C). The average number of BrdU-positive cells within the core sensory region of the injured OE under GM6001 treatment was higher than its internal control had. However, the increase in the injured OE under drug influence was reduced to only 1.9 fold (6.6 $\pm$ 0.6 cells/lamella in the injured OE vs. 3.4 $\pm$ 0.5 cells in the intact OE , $p_{injured/intact}$ = 3.9 x 10^{-5}, unpaired Student's t-test, $t_{injured/intact}$ = 4.2758), which is less than half of the 4.8-fold increase observed in DMSO control group (Figure 4.34C'). The decrease in fold changes indicates that the administered doses of GM6001 did not shut down the regenerative response but significantly suppressed the response strength.

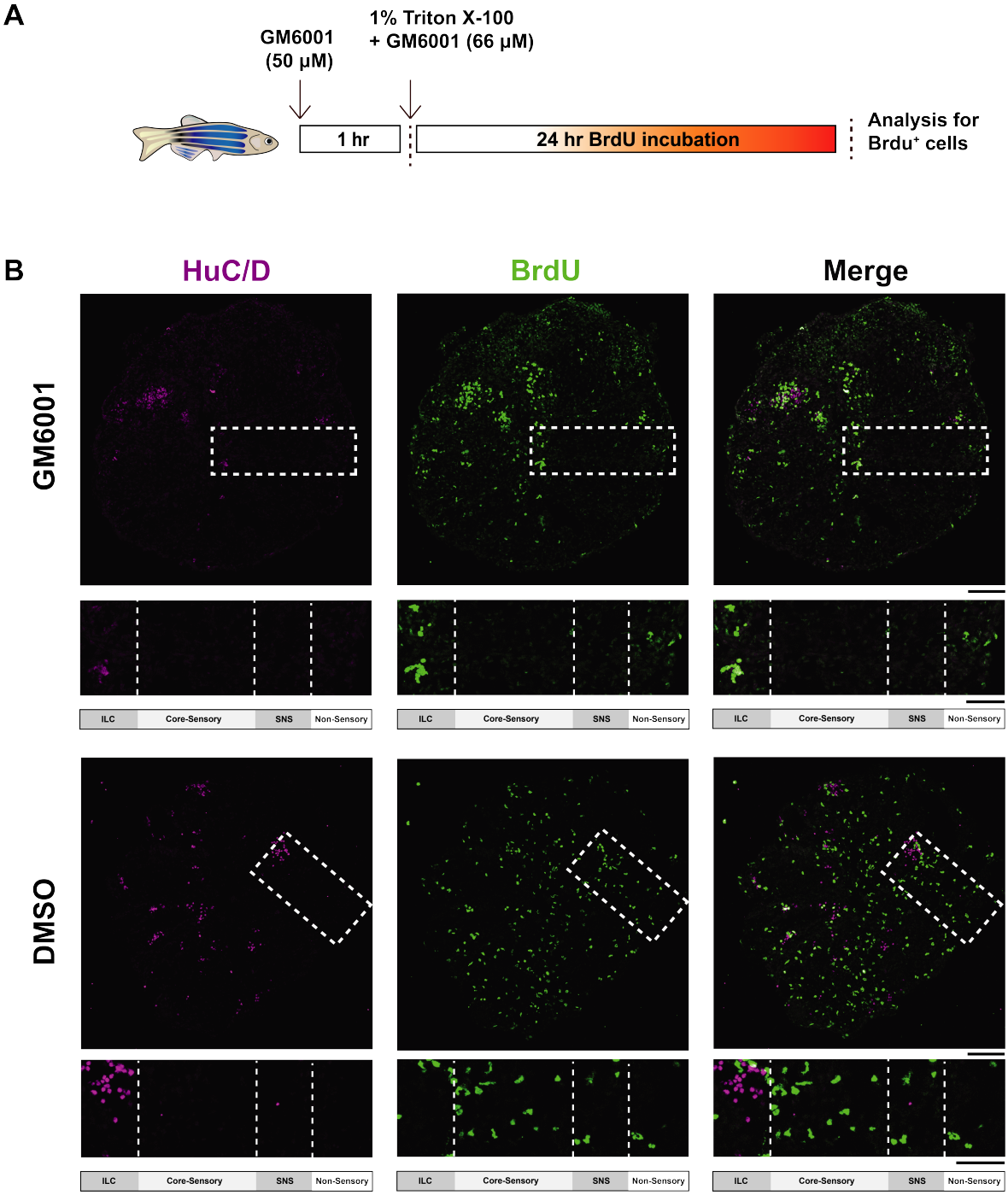

Figure 4.33. GM6001 impairs regenerative proliferation. A. Experimental setup. B. Representative images of regenerating OEs at 1 dpi under GM6001 and DMSO treatment. Scale bars: 100 µm (section) and 50 µm (lamella).

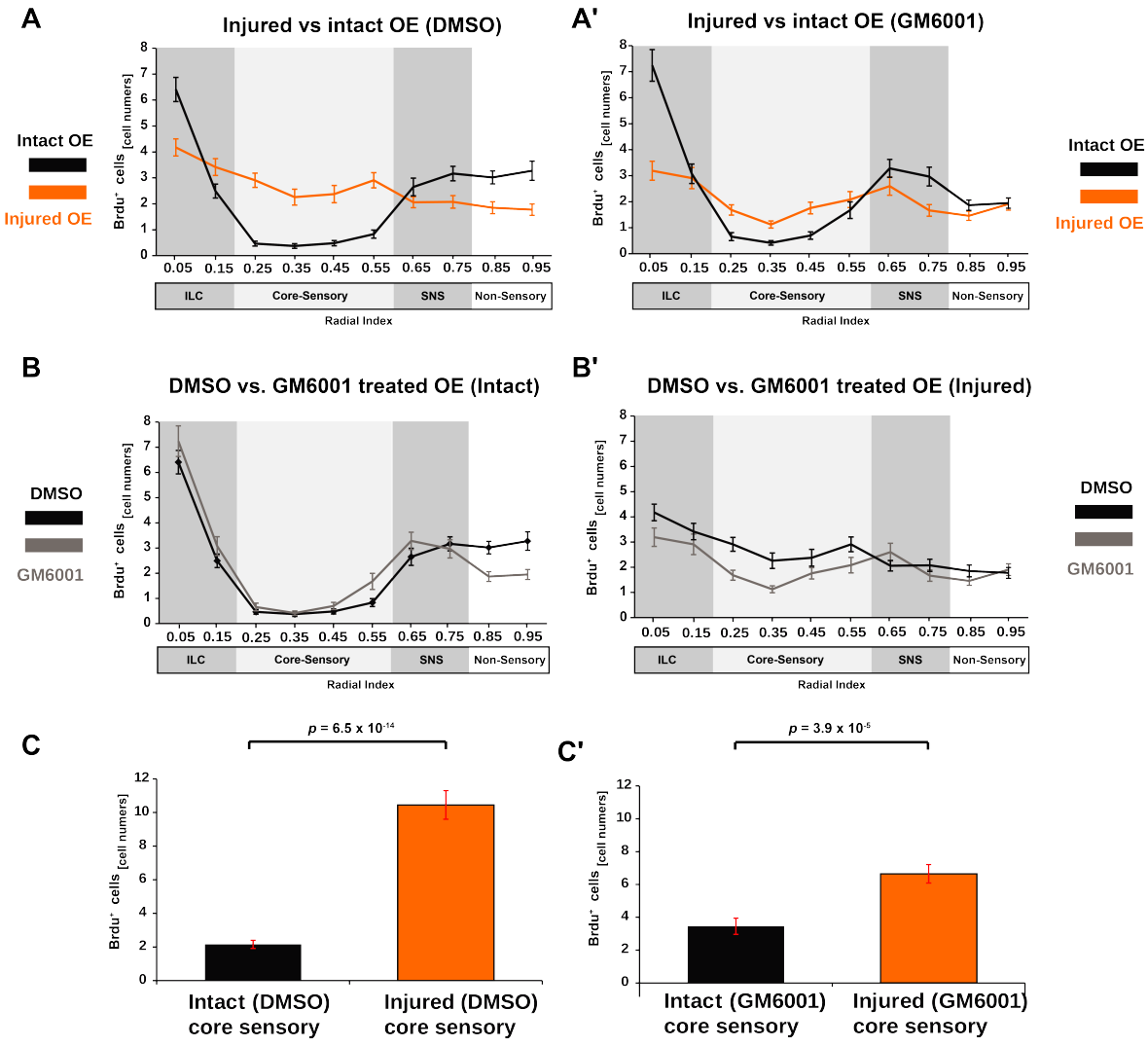

Figure 4.34. Analysis of GM6001-mediated suppression at 1 dpi. A-A' and B-B'. Comparison of positional profiles of BrdU-positive cells. C and C'. Quantitative comparison of core sensory regions.

4.3.6. Inhibitory effects of Marimastat

To demostrate that the reduced proliferative activity in the OE under GM6001 treatment is caused by the inhibition of MMP activity and not by non-specific toxicity, a second broad-spectrum metalloprotease inhibitor, Marimastat, was employed. Marimastat is an antineoplastic compound mostly used in cell culture, although *in vivo* studies with specific phenotypes are also reported in different models [233, 236]. Like GM6001, the agent targets the active site of the metalloproteases and binds to the cataliytic zinc ion covalently, resulting in the inhibition of proteolytic activity.

Studies showed that Marimastat could inhibit multiple EGFR pathways, including the ones triggered by soluble HB-EGF [237]. It was recently shown that Sorafenib-induced shedding of HB-EGF was inhibited when umbilical vein endothelial cells were treated with with Marimastat [238]. Consistently, low proliferative activity due to Marimastat treatment could be rescued by exogenous soluble HB-EGF treatment in cell culture [239].

As in the case of GM6001 experiments, the effects of Marimastat on the OE regeneration were assessed at 1 dpi. Adult fish (n = 3) were intraperitoneally injected with Marimastat (80 µg/g) twice per day. After the third injection (24 hours after the first dose), right OEs were treated with 1% Triton X-100 to provoke the regenerative response. The left OEs remained intact to serve as inernal control. After Triton X-100 application, fish were subjected to BrdU incorporation. A fourth injection was given at 12 hpi, and the OE samples were dissected at 24 hpi for anti-BrdU immunoreactivity analysis (Figure 4.35A) Another set of animals (n = 3) was treated with DMSO to serve as control group. BrdU-positive cell proliferation was assessed from 48 lamellae from 3 DMSO-treated intact OEs, 45 lamellae from 3 DMSO-treated injured OEs, 48 lamellae from Marimastat-treated intact OEs and 53 lamellae from 3 Marimastat-treated injured OEs.

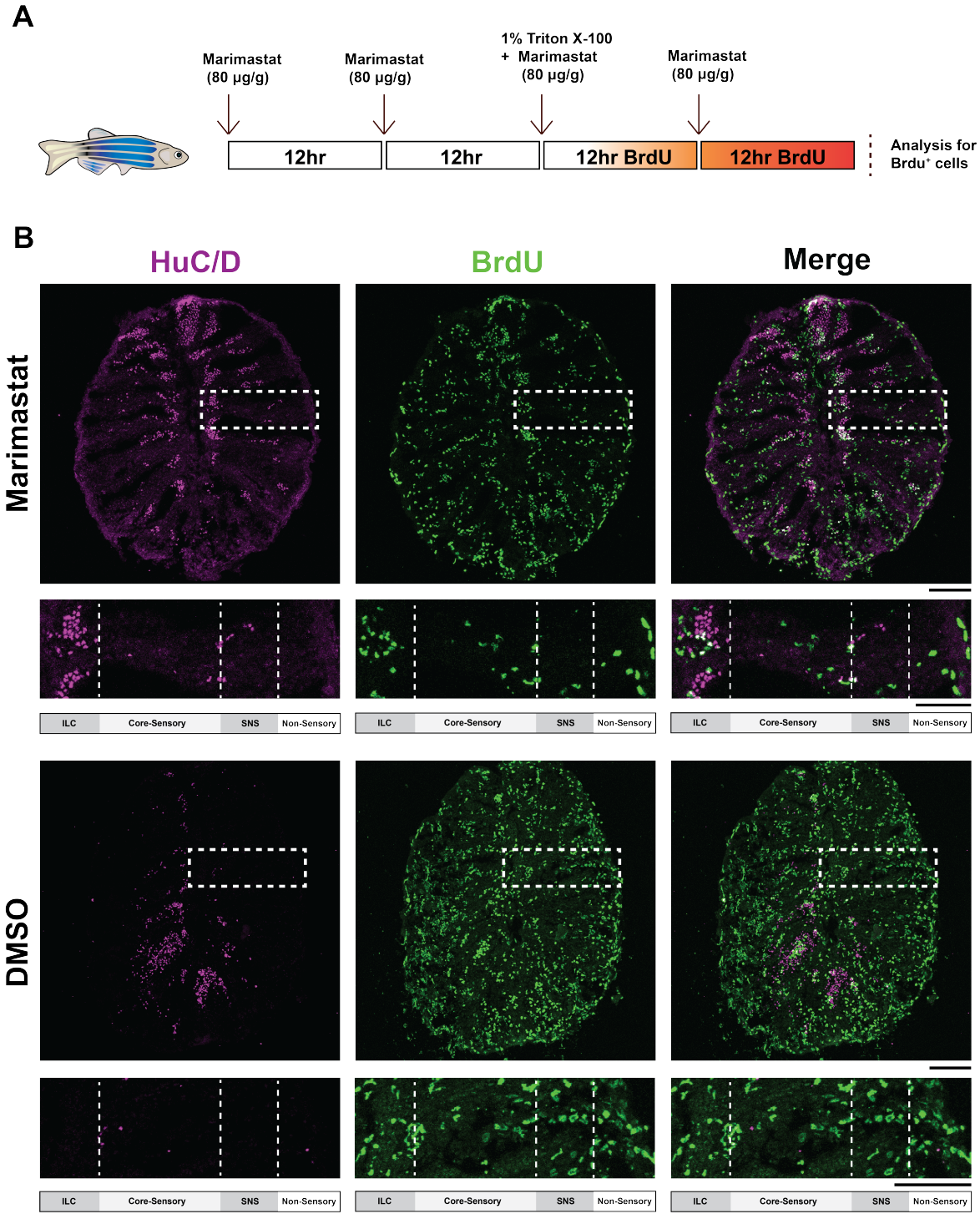

Figure 4.35. Marimastat impairs regenerative proliferation. A. Experimental setup. B. Representative images of regenerating OEs at 1 dpi under Marimastat and DMSO treatment. Scale bars: 100 µm (section) and 50 µm (lamella).

As depicted in Figure 4.35B and 4.36A-A', Marimastat administration greatly suppressed the induced proliferation in the injured OE, making the radial distribution profile of BrdU-positive cells identical with the profile seen in the intact OE. The profile curve of the injured OE under Marimastat-mediated suppression had a lower midline and amplitude, compared to that o the injured OE treated with DMSO vehicle (Figure 4.36 B'). Different from the results of GM6001 treatment, Marimastat also affected the proliferation in the sensory region of the intact tissue, as can be seen when the radial distribution curve of the intact OE is plotted underneath that of the intact OE of the DMSO control group. Still, the suppressive effect on the constitutive proliferation zones appears to be selective, as the number of BrdU-positive cells decreases in the SNS but not at the ILC (Figure 4.36B).

The suppressive effects of Marimastat were even more evident when the total numbers of BrdU-positive cells within the core sensory regions were compared. Upon injury, the proliferative activity increased 3-fold in the injured OE of the DMSO-treated fish set (9.1 $\pm$ 0.7 cells in the intact OE vs. 27.0 $\pm$ 2.0 cells in the injured OE on average, ($p_{injured/intact}$ = 1.8 x 10^{-11}, unpaired Student's t-test, $t_{injured/intact}$ = 8.4763) (Figure 4.36 C).

Under drug treatment, the increase was still visible but considerably lower, reaching only 1.3 fold (5.5 $\pm$ 0.6 cells in the intact OE vs. 7.1 $\pm$ 0.7 cells in the injured OE on average). Importantly, the difference between the means was not statistically different, indicating that the regenerative response in the core sensory OE was almost completely shut down by Marimastat administration ($p_{injured/intact}$ = 0.0815, unpaired Student's t-test, $t_{injured/intact}$ = 1.7600) (Figure 4.36 C').

In conclusion, both metalloprotease inhibitors affect the early phase of regenerative response by slowing down the proliferative activity after injury. Both drugs suppressed the induced proliferation and Marimastat has partial modulatory effects in the constitutive proliferation. These findings together indicate that metalloprotease activity has a crucial role in the proliferation dynamics of the sensory region.

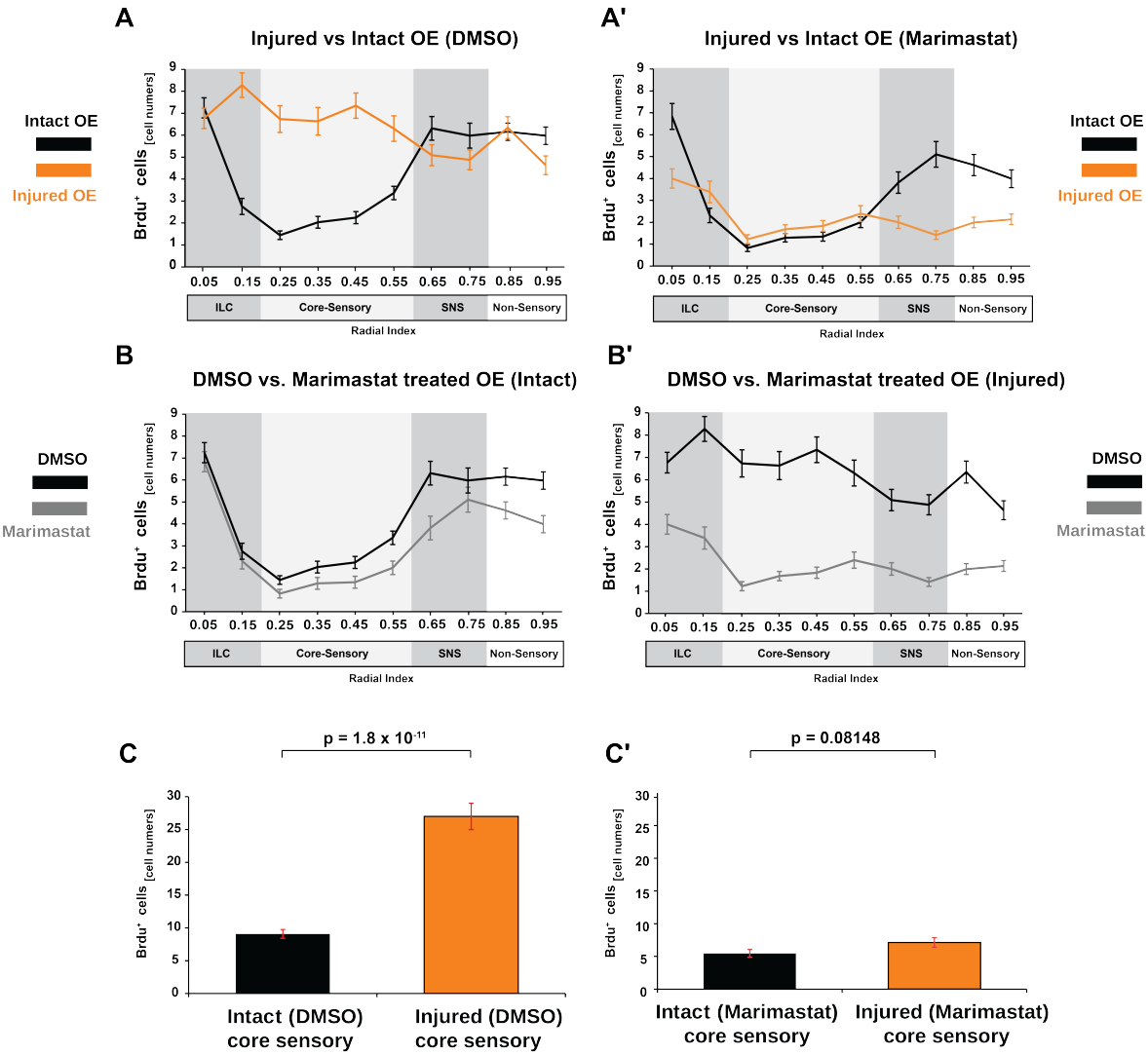

Figure 4.36. Analysis of Marimastat-mediated suppression at 1 dpi. A-A' and B-B'. Comparison of positional profiles of BrdU-positive cells. C and C'. Quantitative comparison of core sensory regions.

5. DISCUSSION

5.1. The unique pattern of proliferation in the zebrafish OE

The persistent OSN regeneration in the zebrafish throughout life makes the OE a unique model for adult neurogenesis. Unlike other OE models, zebrafish OSNs are born in two discontinuous proliferation zones that are located at central and peripheral margins of the sensory OE. Newborn OSNs approach each other from both proliferation zones and meet in the sensory region. OSNs of higher vertebrates follow a zonal organization, in which cells in predefined tissue-domains express a certain set of olfactory-receptor genes, thereby providing fixed distribution patterns for different OSN groups [240, 241].

The distribution of receptor-specific OSNs in zebrafish gives the impression of a similar zone-like organization temporarily; however persistent movement generates dynamic expression patterns of receptor-gene-specific OSN groups at same age, rather than a fixed pattern. This suggests that a unique set of molecular cues regulate tissue dynamics in the zebrafish OE, which is not observed in higher vertebrates [127]. Importantly, these molecular cues promote lateral movement of differentiated neurons but selectively restricts active progenitor cells to discontinuous and predefined positions in the OE, thereby specifying proliferation zones in the intact tissue.

In this study, I presented my findings that describe the characteristics of the injury-response of zebrafish OE and the effects of different injury types on the bicentric OSN neurogenesis and on the activation of potential progenitor cell populations. I showed that the predefined proliferative organization of the intact tissue can be disrupted by different injury methods, particularly by chemical agents, and that this disruption is reversible. Upon Triton X-100 injury, the bimodal distribution of the proliferating cells is replaced with a uniform distribution. The bimodal distribution reappears within a week.

Sequential labeling of the proliferating cells with different thymidine analogues reveals that the injury-induced pattern is not generated by the constitutively proliferating cells at the ILC and SNS but by a unique progenitor group. Activation of HBC-like cells, a quiescent basal population in the OE, is observed upon different type of injuries. The spatiotemporal pattern of active HBC-like cells correlates with OSN regeneration upon chemical injury. Nerve transection, a method to apply physical and cell-specific injury, also triggers a uniform HBC-like cell activation but early-born OSNs don't appear to be generated from active HBC-like cells, as they are positioned not in the core sensory OE but mostly at the ILC. Taken together, the distinct positioning of active and quiescent progenitor cells in the zebrafish OE provides a unique tissue organization that coordinates the mode of regenerative proliferation response under different conditions.

5.2. Two progenitor cell pools in the zebrafish OE

Stem cells in the OE involved in tissue maintenance show certain characteristic that are commonly seen in other tissue-specific stem cells. These characteristics include multipotency, reversible quiescence, and a capacity for (near) limitless self-renewal [242–244]. Proliferation in the OE is maintained primarily by two types of basal cell population that possesses all or some of these three characteristics: GBCs and HBCs. Neuronal commited GBC can be identified by characteristic expression of neurogenic transcription factors such as Ascl1 and Neurod1 [61,63]. In addition, undifferentiated cell marker Sox2 marks multiple basal populations including a broad subset of multipotent GBCs [60]. In zebrafish OE, neuronal committed GBC-like cells are mitotically active and express early neuronal markers *ascl1a*, *dla* and *neurod1/4* [127]. In this study, active GBC-like cells were labeled by BrdU/Ascl1 double-immunoreactivity (Figure 4.17). A separate IHC/FISH assay demonstrated that *ascl1a*-expressing GBC-like cells express Sox2 marker revealing their undifferentiated and multipotent state (Figure 4.16). Importantly, BrdU/Ascl1 double-positive GBC-like cells increase in number and are found along the entire lamella upon chemical injury (Figure 4.17 and 4.18), suggesting the birth of these cells from a dormant, tissue-resident population.

HBCs, which constitute the second progenitor cell group, reside either in quiescence or at a very slow cycling rate in adulthood under physiological conditions (1 division/60 days) [245]. Unlike GBC subsets, quiescent HBCs belong to a homogeneous cell population that shares identical molecular characteristics and can be specifically identified by Krt5-immunoreactivity. The maintenance of the HBC quiescence is largely attributed to Np63 expression, one of two isoforms of p63 whose activity accounts for retention of proliferation activity in adult stem cells [94, 221, 246]. These molecular characteristics appear to be conserved in HBC-like cells of intact zebrafish OE as well (Figure 4. 21).

Because both HBCs and GBCs are potent to give rise to all OE lineages, there has been a discussion on the roles of these multipotent cell pools in the lineage hierarchy [67, 68]. There is lineage-tracing evidence showing that HBCs can differentiate into active GBCs [68]. Overlapping patterns of tissue-resident HBC-like population and newly generated GBC-like cells in the sensory OE also supports a similar HBC-to-GBC transition in zebrafish (Figure 4.21 and 4.17-18) On the other hand, transition of GBCs to HBCs by cellular division has not been shown yet.

So far, HBC population fits into the definition of tissue-specific stem cells that maintain the long-term regenerative capacity [247] and GBCs appear to be progenitor cells that are initially generated by HBC differentiation. In zebrafish OE, I specifically identified a HBC-like population by Sox2-, Krt5- and p63- immunoreactivity. These cells are localized to a single, discontinuous layer in the basal region of the sensory OE (Figure 4.21), resembling the well-defined HBCs in the rodents Similar to their mammalian counterparts, HBC-like cells divide infrequently in the intact tissue when exposed to BrdU for prolonged periods (Figure 4.22). In addition to the HBC-like cells in the sensory region, antibodies against Krt5 and p63 also mark cell populations that are located in multiple layers of the non-sensory region; however, these cells are unlikely to be HBC-related, as they differ from the sensory-specific cell population morphologically and positionally and show no immunoreactivity to Sox2 (Figure 4.21).

HBCs and GBCs occupy non-overlapping tissue layers and are found uniformly along the OE among rodent models. On the other hand, the distribution of basal populations follows a different organization in the zebrafish model. HBC-like cells of the sensory OE appear to conserve the positional arrangement and slow rate of proliferation of higher vertebrate HBCs, whereas GBC-like cell populations are localized to the margins of the sensory OE [127], which is different from the rodent models in which GBCs occupy basal positions without any regional preference [57]. *In situ* hybridization for *ascl1a* shows a positional pattern of transcript-expressing cells, that overlaps with BrdU-retaining proliferation zones in the intact OE (Figure 4.15, [127]). Immunohistochemistry for Ascl1, on the other hand, displays a more restricted yet similar pattern of Ascl1-positive cells that are found mostly at the ILC and rarely at SNS (Figure 4.16 and 4.17). The less broad pattern visualized by anti-Ascl1 staining may be a result of the prolonged tissue fixation (10 min PFA fixation in *in situ* hybridization vs. 24 hour PFA fixation in immunohistochemistry). Nevertheless, the positioning of Ascl1-positive cells at the proliferation zones of the intact OE is consistent with the previous report [127]. The unique positions of GBC-like proliferating cells also suggests the importance of the progressive shift of newborn OSNs towards the central OE region, which is required to compensate for the loss of senescent OSNs under physiological conditions. Direct and extensive epithelial lesion by chemical agents causes the molecular balance sustained by GBC-like cell clusters and uniformly arranged HBC-like cells to be disrupted. This disruption results in the activation and subsequent differentiation of the HBC-like pools. The diversity of proliferation responses among these populations strongly suggest that the zebrafish OE relies on a distinct dual progenitor system for tissue maintenance and OSN neurogenesis, that is tightly regulated under different tissue conditions.

5.3. The functional significance of a dual progenitor system

Progenitor cells in the adult tissue divide without losing their multipotency and differentiate into post-mitotic, specialized cell types when needed. These two tasks are crucial, especially for tissues whose individual cells have a relatively short lifespan.

The average lifespan of OSNs is between 21-29 days [127], this estimation predicts a very short lifetime for a neuron, when compared to the lifespan of the zebrafish, which can be over 5 years in laboratory conditions [248]. Yet, the progenitor cells in the OE appear to compensate for OSN loss effectively without age-related exhaustion, as the sense of olfaction is maintained persistently throughout life.

The maintenance of the balance between cellular self-renewal and differentiation is an intricate management and highly susceptible to molecular changes in the stem cell niche. In a high-turnover tissue, where a steady proliferation rate is necessary, there are always risks for stem cell depletion. These risks increase under extreme conditions, such as tissue damage, in which an accelerated proliferation rate is necessary to reconstitute the tissue in short time.

Theoretically, self-renewal of progenitor cells can be maintained by persistent asymmetric division. However, this mode of proliferation does not allow an independent regulation between tissue maintenance and self-renewal of the stem cell pools and increases the replicative burden on individual stem cells. In other words, constitutive asymmetric division requires more rounds per stem cell for tissue maintenance and results in increasing exhaustion risk. This would lead to a decline in progenitor cell numbers in short time. Therefore, a lifelong and repetitive regenerative capability does not fit into a model of homogeneous population of equipotent progenitors that maintains the OE homeostasis under both physiological and pathological conditions.

Alternatively, the presence of multiple types of progenitors with divergent proliferation properties can create a better division of labor among proliferating cells and minimize the risk for stem cell depletion. In such a model, one group of active progenitors can proliferate to replace the senescent and dying cells while another group of slow-cycling progenitors divide rarely only to renew the active progenitor pool to avoid or decelerate depletion.

There are several representative examples of a dual system in which multiple progenitor cell types reside in separate but close locations in the same tissue (reviewed in detail in [249]). The hair follicle is a commonly used system to study the diversity in progenitor pools under stem cell biology. The follicle is composed of an upper permanent segment with rarely dividing cells and a lower cycling segment, in which transit-amplifying cells are found [250]. Undifferentiated bulge stem cells reside in the permanent segment whereas continuous turnover of the hair is maintained in the lower segment [251, 252]. During the early anagenic growth phase, dermal papilla cells residing in the hair stem secrete signals that recruit bulge stem cells from the upper segment to form the internal follicle [253]. Studies show that not all bulge stem cells respond to the stimulatory cues equally and some retain BrdU-label over months [254, 255]. Stem cells that locate in the lower bulge (thereby closer to the hair stem) proliferate and contribute to the anagenic phase of the hair, whereas quiescent stem cells residing in the upper bulge move to lower positions gradually [256]. In addition to their different positions and label-retaining properties, stem cell groups in the bulge show different molecular characteristics; the proliferating lower bulge cells express LGR5+, a common target for Wnt-driven proliferation, whereas the upper bulge cells express BMP target Nfatc1, which is associated with a state of quiescence [257, 258]. These observations suggest that the hair follicle contain both quiescent and active progenitor populations in separate yet adjacent locations.

Intestinal epithelium is another high-turnover organ which renews every 5 days. In adult intestine, transit-amplifying and quiescent undifferentiated cells reside in the intestinal crypts, while differentiated cells move out to the surface and fulfill their physiological tasks [259]. As progenitor cells differentiate, they migrate out of the crypts. Two distinct cell populations have been identified so far in the small intestine, that display stem cell characteristics in the small intestine. One of these two populations, called “crypt base columnar cells” (CBC), is found among the post-mitotic Paneth cells at the bottom of the crypt, whereas the other population, “+4 cells”, is located at +4 position from the bottom.

Similar to the proliferating bulge cells in the hair follicle model, CBCs in the intestine express LGR5+, proliferate frequently and can give rise to all epithelial lineage in the intestine [260]. +4 cells, on the other hand, retain mitotic label for long periods, which is seen as an indicative of quiescence under physiological conditions [261, 262]. It has been also demonstrated that +4 cells are capable of differentiating into all cell types in the intestine [263]. It is assumed that CBC proliferation contributes to tissue renewal and +4 cells serve as reserve pool to compensate for CBC loss or exhaustion.

Certain observations suggest that the coexistence of progenitor cells with different proliferation properties is crucial also for the maintenance of neural tissue. The brain, in particular, utilizes modes of the symmetric and asymmetric divisions in a tightly regulated manner, as the neurogenic regions can generate young neurons seemingly throughout life. A recent study shows that B1 neural stem cells residing in the ventricular-subventricular zone undergo symmetric differentiation, resulting in eventual B1 depletion at early ages in mice [264]. This depletion is critical, because B1 cells are considered the primary progenitor pool in the ventricular-subventricular zone. Yet, the neurogenesis is maintained in the brain for extended periods in life despite the rapid decline in B1 cells. This raises the question whether a quiescent population exists that compensate for B1 loss in the brain. One possibility that the authors came up with is that non-apical B2 cells that are differentiated from apical-B1 cells are the second progenitor group, because they share a number of astroglial characteristics with B1 and remain in a state of quiescence [264]. Although it is not clear whether B2 cells serve as true progenitors in the tissue, the rapid depletion of B1 pool necessitates the involvement of another progenitor pool to explain the lifelong maintenance of neurogenesis in the brain.

The examples described above comply with an organization in which multiple progenitor populations with divergent proliferation properties maintain tissue homeostasis and progenitor-self-renewal separately. As mentioned above, such an organization may increase the longevity of progenitor pools, delaying the exhaustion and thereby maintaining functional and regenerative capabilities of the tissue for longer periods.

Importantly, multiple progenitor systems appear to position different progenitor types at separate but close locations. The close-distance between the locations may allow rapid replenishment of one population with successive divisions of the other under non-physiological conditions, such as acute injury.

Similar to the examples above, the OE also contain two distinct progenitor types to ensure he maintenance and tissue repair. In rodent models, HBC and GBC populations occupy different epithelial layers which provide a positional separation in the tissue. While basoapical organization of proliferating and quiescent cells persists in fish similarly to rodents, the unique positioning of GBC-like cells at the margins of the sensory region creates a second separation among the progenitors in radial dimension. The progressive shift of newborn cells overcomes the problems that might arise due to the absence of a constitutively active progenitor pool in the central regions and provides a sustainable system for tissue maintenance.

More importantly, the radial separation of distinct progenitor cell groups may keep the stimulatory cues that are secreted in the proliferation zones apart from HBC-like cells in the sensory region and prevent the reserved pools from becoming activated accidentally. The positional organization in the rodent OE, despite its effective and tight regulation, can not provide a limitless capacity for proliferation, as the OSN regeneration is tempered and the OB reinnervation is impaired in aging mice due to rapid depletion of GBCs after injury [265]. On the other hand, the neurogenic activity in the olfactory system do not seem to be affected by age in zebrafish [266]. This near-limitless capacity for proliferation in the fish model may be attributed to the unique positional organization o HBC- and GBC-like cells in the OE, that keeps the reserve pools isolated from stimulatory signals and delays the onset of their possible exhaustion.

5.4. HBC activation in different tissue conditions in relation with OSN neurogenesis

The zebrafish OE reconstitutes itself after injury over a relatively short time by changing the conserved proliferation pattern (Figure 4.4, Figure 4.6). It is critical to clarify whether this progressive yet reversible change in the pattern is caused by injury-induced displacement of continuously proliferating cells or by the activation of a quiescent progenitor population in the sensory region.

The sequential labeling of the OE with different thymidine analogues before and after chemical injury demonstrates that different progenitor pools contribute to different modes of neurogenesis and a dormant cell population starts undergoing multiple rounds of division upon injury (Figure 4.9-12). This labeling assay also shows that the injury-surviving cells at the proliferation zones don't share the same radial distribution with the newly generated cells upon chemical injury in the sensory OE. Upon chemical injury, fewer pre-injury-label-retaining cells are found at the SNS than at the ILC. This may reflect that Triton X-100 affects SNS more severely. Sequential labeling assay also shows that very few cells are co-labeled by IdU and CldU (Figure 4.10). Low numbers of IdU/CldU double-positive cells that are found exclusively at the ILC of the injured tissue also supports that there is a strict separation between pre-injury and post-injury-labeled proliferating cells. A small fraction of pre-injury-labeled proliferating cells at the proliferation zones may persistently divide, but post-injury labeled progenitor group don't show any pre-injury activity. IdU/CldU double-positive cells of the intact tissue preserve the bimodal distribution, which is a characteristic of proliferation patterning under physiological condition; however, their number is also low. This may imply that the GBC-like cells in the proliferation zones don't belong to a homogeneous specialized group that undergoes steady and rapid cell divisions but to separate subtypes with divergent proliferation properties. A recent study on pancreatic beta cell regeneration interprets the abundance of separate analogue-retaining clusters and the low occurrence of double-positive cells after the sequential labeling as an indication of a slow self-renewal activity [267].

In future studies, the heterogeneity and self-renewal properties of zebrafish GBC-like cells can be investigated by the use of different thymidine analogues together with common undifferentiated cell markers, such as Sox2.

This study identifies a discontinuous and single-layered HBC-like population along the sensory OE, that shows high proliferation activity upon injury. The distribution of injury-induced active HBC-like cells follows a pattern similar to the post-injury-label-retaining cells described above. Quiescent HBC-like cells express stemness regulator p63 characteristically (Figure 4.21). The p63 protein, belonging to p53 transcription factor family, is crucial for the regulation of progenitor pools in ectoderm-derived tissues and its deficiency leads to progenitor depletion [268]. The p63 protein is exclusively found in quiescent HBCs in the rodent OE and the expression is down-regulated in active HBCs after chemical injury [94]. High levels and specific expression pattern of p63 are also conserved in the intact zebrafish OE. The level of p63 in Krt5-expressing HBC-like cells after injury could not be determined by immunohistochemistry techniques in this study, possibly due to reduced expression of p63 and low sensitivity of primary antibody mixes (Krt5 and p63) that are raised in the same host species. Immunohistochemistry analysis on regenerating *Tg(krt5:EGFP)* zebrafish line that was generated during this study (Figure 4.29) may overcome this problem and reveal a better profile of p63 levels in active HBC-like cells in the future. Similar to HBCs in the rodent OE, HBC-like cells of the zebrafish OE show a slow proliferation rate in the intact tissue. BrdU-incubation for 24 hours can capture only a few Krt5-expressing HBC-like cells along the sensory OE (Figure 4.22). The numbers of BrdU/Krt5 double-positive cells are elevated after chemical injury, and the cells grow protrusions to invade supra-basal layers of the tissue.The stem cell niche in epithelial tissues is maintained by persistent adhesion to basal lamina and high expression of adhesion-molecules mediate cell-to-cell interaction, regulate proliferation and inhibit stem cell differentiation [269]. Disruption of the basal integrity upon injury may cause detachment from the lamina and result in the morphological changes in the HBC-like cells. These morphological changes include formation of protrusions that HBC-like cells use to invade more apical layers.

Both robust HBC-like cell activation and positioning in supra-basal layers are observed in mouse model upon chemical injury [96]. However, morphological changes doesn't seem to be a necessity for HBC-like cell activation in the OE, as a milder chemical injury condition with less concentrated Triton X-100 irrigation can also stimulate this population without causing any apparent change in cell morphology (Figure 4.25-27). This observation indicates that disruption in tissue integrity may not be an essential factor that determines HBC-like cell activation. Yet, it is possible that irrigation with 0.1% Triton X-100 may create a fast-healed disruption that can still affect the levels of adhesion molecules but is not noticeable at morphological level at 2 dpi. Another possibility is that HBC-like cell activation is independent of tissue integrity and is stimulated by proliferation signals that are released from the dying cells. The HBC-like cell activation upon axotomy favors the latter possibility.

A robust 15-fold-increase in the number of active HBC-like cells in the OE by 1 dpi was observed previously [73]. HBC-like cell activation in this study was not as high as reported, but still statistically highly significant. Time course analysis of BrdU/Krt5 double-positive cells shows that the number of active HBC-like cells along the sensory region increases within the first three days after injury, followed by a decline by 5 dpi (Figure 4.23). Importantly, this temporal pattern coincides with the robust and uniform increase of new OSNs in the sensory region at 3 dpi, which is followed by the recurrence of a two peaked distribution at 5 dpi (Figure 4.19 and 4.20). Therefore, the data strongly suggest that OSN regeneration upon chemical injury is associated with spatiotemporal pattern of HBC-like cell activity. Axotomy, which is the physical injury method used in this study, leads to massive OSN elimination as evidenced by the shrinkage in the size of HuC/D-positive area. At 3 dpi, the remaining HuC/D-positive area is much smaller in the axotomized OE than in the Triton X-100-treated OE (Figure 4.2 and 4.14). Interestingly, most of both BrdU-positive and -negative OSNs are localized to the ILC by 3 dpi. It is not clear whether BrdU-negative OSNs are newborn neurons generated before BrdU-exposure or old neurons whose axons survived the transection. Yet, the majority and a small group of the newborn BrdU-positive OSNs are found at the ILC and at the SNS, respectively.

This observation suggests that the regenerative neurogenesis is maintained primarily by GBC-like cells by 3 dpi. In addition to the OSN neurogenesis, there is also a significant HBC-like activation in the axotomized OE at the time of analysis (Figure 4.28). Later time points of axotomy-induced regeneration requires further analysis in order to understand whether axotomy-induced HBC-like cell activation contributes to OSN neurogenesis at later time points. Upon chemical injury, Ascl1-positive cells increase in number and their distribution overlaps with the pattern of uniform HBC-like cell activation hese provide evidence for the neuronal commitment of active HBC-like cells. Similarly, measuring the number and distribution profile of Ascl1-positive cells may provide data on the contribution of HBC-like cell activation to axotomy-induced OSN neurogenesis.

In higher vertebrates, bulbectomy experiments, which follows a similar logical basis with axotomy in terms of specific OSN elimination, results in rapid OSN degeneration and a subsequent regenerative response launched by GBCs [270]. A cell-lineage analysis on inducible Krt5-Cre mice previously concluded that HBC recruitment by the OE does not occur after bulbectomy but is only achieved under injury conditions where the integrity is severely disrupted by chemical lesions, commonly made with methyl bromide [68]. In direct conflict, another study demonstrates HBC recruitment upon bulbectomy [67]. In my study, the integrity of zebrafish OE was disrupted and slightly shrunk as a consequence of axotomy-induced OSN elimination. However, active Krt5/BrdU double positive HBC-like cells were flat in shape, as opposed to the branching cellular morphology seen in Triton X-100-treated tissue in which the integrity is severely damaged. This, as mentioned above, suggests that not an immediate change in tissue integrity but massive OSN elimination stimulates HBC-like cell activation, possibly by the release of stimulatory content from dying neurons. These observations above suggest that HBC activation is stimulated by both physical and chemical tissue perturbation but with a selective contribution to OSN regeneration at early regenerative phases. While OSN regeneration is maintained by chemically-induced HBCs almost immediately, newborn OSNs appear to be generated not by HBC-like cells but by GBC-like cells at the onset of the axotomy response.

Investigation of HBC-like cell activation together with the use of pro-neuronal and non-neuronal markers will reveal more on the functional significance of HBC-like cell activation upon axotomy.

5.5. Characterization of the OE degeneration and regeneration upon injury

The most striking proliferation property of the zebrafish OE is the rapid recovery of the conserved proliferation zones at the ILC and SNS. The recovery appears to be achieved within a week after extensive chemical injury. The reversible effects of chemical injury on the OE were previously characterized in various teleost species.

Triton X-100 is previously shown to cause OE degradation in catfish [85]). At high concentrations, Triton X-100 harms both the sensory and the non-sensory OE. The whole tissue reconstitutes itself within 2 months [85]. Studies on the zebrafish OE proposes that the degenerative effect of Triton X-100 is selective and that the chemical agent kills mostly ciliated OSNs but spare most of OSNs microvillous [271, 272]. The numbers and pattern organization of microvillous and ciliated OSNs are very similar in the zebrafish OE. A major positional difference is that the microvillous OSNs are closer to the surface and located in more apical layers that ciliated OSNs are [129]. Anti-HuC/D staining within the first 24 hours of degeneration that was performed in this study can not distinguish different OSN subtypes; however, Triton X-100 application affects 88% of the overall neuronal area and disrupts the neuron patterning (Figure 4.1 and 4.2). Some lamellae are completely devoid of OSNs due to Triton X-100 exposure. The scale of the loss in the HuC/D-positive area suggests that both major OSN subtypes degenerate non-selectively upon Triton X-100 contact. Morphological abnormalities after extensive injury, such as lamella fusion, were also reported previously [86], however, no fusion was observed in this study. Primary morphological changes were epithelial thinning, detachment and denudation.

The radial distribution of the proliferating cells becomes uniform upon injury, instead of bimodal. However, the change is transient and the pattern revert to a two-peaked radial distribution at 5 dpi (Figure 4.6). The regenerated OSNs continue to shift progressively after the tissue reconstitution is complete and their long-term positional distribution looks identical to the profile in the intact OE (Figure 4.8). The recovery of bicentric proliferation pattern and radial cell movement points out that the regenerated OE reconstructs the topographic map of the intact OE without any major change.

My analysis on the HuC/D-positive area in the OE investigates the time course of the degeneration and reveals that the chemical injury is extensive and timed, instead of being instantaneous. The corrosive effects of Triton X-100 on the OE is well-known across species; however, the early outcomes of these effects within 24 hours after injury were not observed in detail previously. In my analysis, the epithelial contact with 1% Triton X-100 solution degrades OSNs gradually by stimulating an extensive death signal. Death of OSNs by injury and by senescence are often attributed to apoptotic activities [213, 273]. TUNEL assay on the zebrafish OE shows that cell death is a frequent and position-free event among OSNs in the intact tissue [127]. However, high levels of fragmented DNA particles that are detected by TUNEL may be generated by alternative death mechanisms, because only a few apoptotic cells could be detected by caspase-3 assay in the OEs under injury and physiological conditions (Figure 4.13). This finding strongly suggests that OSN death is mediated largely by caspase independent death mechanism, such as necrosis and necroptosis [274]. The morphological and cellular reconstitution of the OE after injury is apparent; however, the extent and accuracy of reinnervation of the olfactory bulb are not known in detail in the zebrafish model. The degree of extensive chemical injury and nerve transection may affect the success of reinnervation, as newborn neurons need pre-existing axonal projections for guidance [275]. In zebrafish, functional recovery in the olfactory-mediated behavior is observed in 10 days [276], however the organization of the reinnervation requires an in-depth analysis, because not only OSN projections but also ongoing neurogenic events in the bulb is affected by diverse injury conditions. It would be interesting to investigate how the glomerular remapping during OE regeneration works and whether

the odorant-evoked patterns of sensory input is conserved spatially in the regenerated OE-bulb circuit in zebrafish.

An important question for future studies concerns whether the regenerative capacity of the OE is disrupted by age or not. Studies demonstrated increased susceptibility to damage and a decline in the lesion-induced proliferation in the OE of aged rodents [277, 278]; however, the effects of aging on the zebrafish OE regeneration remains largely elusive. All fish analyzed in this study were young adults (<2 years) and therefore were not eligible to be used for the examination of possible age-related changes in the OE regeneration. Future work on aged animals may elucidate whether the robust and rapid regenerative response of the zebrafish OE is regulated by aging or remains unaffected.

5.6. Sustentacular cells as a third non-neuronal basal population

The regenerative process in the OE complies with a dual progenitor cell system proposed above. however, the contribution of other cell types to the cellular proliferation should not be overlooked. Among the other non-neuronal populations residing in the OE, glia-like sustentacular cells are particularly important, particularly when their abundance and unique positions in the tissue are considered. Fully differentiated sustantecular cells are highly keratin-rich and have an elongated shape in contact with multiple OE layers. Although their functional significance is not completely understood, sustentacular cells are believed to provide metabolic and structural support and isolation for OSNs in the OE [70, 143, 279]. They may have regulatory influence on cellular proliferation, as a recent study also proposes that sustentacular cells have a critical role in HBC activation upon injury [211]. it is unclear whether sustentacular cells give rise to other cell types in rodent models, however bulbectomy experiments demonstrate distinct morphological changes in the supporting cell population, suggesting that sustentacular cells may be responsive to injury conditions [280] either by releasing HBC-stimulatory signals or by dividing.

Sustentacular cells have an inverted morphology in zebrafish OE and cell bodies are located in basal layers together with other non-neuronal cell types [73]. Selective identification of sustentacular cells in zebrafish OE is challenging due to limited marker options. BrdU assays with immunohistostaining against Cytokeratin type II family and Sox2 reveal rapid sustentacular cell production upon injury (Demirler, unpublished). However, it is not clear whether these cells are post-mitotic or can give rise to other lineages.

Successive divisions of differentiated glia-like cell types has been demonstrated in other sensory organs. Particularly the Müller glia cells in zebrafish retina show a resemblence to sustentacular cells with their elongated body shapes and their participation in glia-neuron interaction. In addition to their role in cellular communication, Müller glia cells also function as quiescent progenitor cells and either dedifferentiate and proliferate or transdifferentiate to retinal sensory neurons [113, 281, 282]. Neither of these cellular processes is observed in rodent OE models; however, the aforementioned basal positioning in the zebrafish raises the question whether sustentacular cells acquire stem cell traits in addition to their regulatory roles in HBC activation. Therefore, identification of a true sustentacular cell marker is essential for further research. Transcription factor six1 and transmembrane protein notch2 are shown to be necessary for sustentacular cell maintenance [283, 284]. Investigation of the expression profiles of these two genes in the zebrafish OE may allow to identify a sustentacular cell marker that can be used to characterize this population better. Finally, their unique basal positioning provide the zebrafish sustentacular cells with close-proximity to the two primary progenitor types. This close-proximity may have additional regulatory effects on the neighboring cells, that can explain the certain properties of OE regeneration under different tissue conditions. As mentioned above, axotomy induces robust HBC activation in zebrafish model at 3 dpi, which is not seen in rodent models (Figure 4.28). Sustentacular cells' positional features may have a direct influence on this activation. Analysis of morphological and functional changes in the sustentacular cells upon axotomy may shed light upon the characterization of HBC activation and OE regeneration under different tissue conditions.

5.7. Molecular cues that play stimulatory role in HBC activation

The robust proliferation activity of progenitor cell types under chemical and physical injury conditions demonstrates that self-renewal of the OE can occur under two very different settings, one where all cell types are exposed to damage and need to be replaced, and the other where only neurons are depleted. Distinct distribution profiles of newborn OSNs among the intact and injured OEs suggest that the dual progenitor system requires a tight regulation of molecular cues to initiate the appropriate neurogenic response. The molecular profile of the niches in the intact OE is expected to be substantially different from those in the axotomized and chemically-inujred OE. As an example, bulk-transcriptome analysis from bulbectomized rat OE at 5 dpi reveals that 24% of total mRNA that are abundantly expressed under physiological condition is affected by the procedure. While most of these affected mRNAs are downregulated due to massive OSN loss, the upregulated rest mostly encodes proteins involved in cell proliferation, transcriptional regulation and immune response; which are associated with tissue renewal [285]. A similar analysis of chemically-injured zebrafish OE over a 5-day-long time course also indicates that distinct transcriptional changes occur in the tissue, most of which are related to pathways involved in cell proliferation and immune response (Demirler, unpublished). One of the most critical requirements for HBC activation is the loss of p63 expression. *p63* gene encodes two isoforms, TAp63 and Np63, that work in competition. The maintenance of quiescent state and long-term replicative capacity is largely attributed to Np63 activities in progenitor cells from different tissue models, including HBCs [96, 246]. Cellular levels of both p63 isoforms are regulated by protein degradation via proteosome activity. Various regulatory proteins, including ubiquitin E3 ligases and damage-induced kinases, have been reported to modulate protein stability of p63 [222, 286]. Activities of these regulatory proteins are affected by the changes in progenitor cell niche, such as alteration in the levels of growth factors, chemokines, cytokines and other secreted molecules that are involved in cell-extrinsic networks. Studies demonstrate that NF-KB signaling pathway, that responds to diverse stress stimuli, also promotes ubiquitin-mediated proteosomal degradation of Np63 [287, 288].

Interestingly, HBCs include NF-KB signaling components abundantly [289] and genetic perturbation of the NF-KB signaling impairs HBC proliferation upon injury [290]. These findings emphasize on the importance of inflammatory signals in the OE regeneration.

The increased release of endogenous biomolecules as a consequence of cellular stress has a key role in the inflammatory response. The damage-associated molecular patterns (DAMP) stimulate and coordinate numerous cellular functions, including migration, chemotaxis, activation, maturation, and proliferation [291, 292]. The content released from a dying cell comprises molecules with divergent properties; some factors may initiate progenitor activation while others accelerate the proliferation activity of persistently dividing cells. For instance, it has been demonstrated that ATP and other purine compounds, which are abundant molecules released from dying neurons, modulates active GBC-like populations by purinergic signal transduction but does not stimulate HBC-like cell activation in zebrafish OE [73]. Other DAMPs may operate to induce HBC-like activation either by directly or coordinating cytokine production by tissue-resident macrophages. Therefore the biodiversity of DAMPs in the injured OE should be analyzed in detail. Particularly, cytokines and other immune system components constitute a crucial molecular group due to their heterogeneity and inductive capabilities on regenerative response in other neural tissue models. The manipulation of certain cytokines, such as IL-6 and TNF-alpha, that are associated with neurogenic activity, [293, 294], may have utility in reproducing conditions suitable to enhanced OSN neurogenesis and HBC activation without causing tissue degeneration. In addition to released factors, direct cell-to-cell and cell-to-lamina interactions play vital roles in progenitor cell activation. Extensive disruption in epithelial integrity under severe injury conditions stimulates HBC proliferation [68]. It has been also previously demonstrated that expression of integrins, which are known to be directly involved in cell adhesion signaling, is downregulated in mitotically active HBCs [66]. In zebrafish OE, the observation that mitotically active flat-shaped HBC-like cells are attached to basal lamina indicates that detachment and visible morphological changes may not be necessary for activation.

My observation in the zebrafish OE complies with a conflicting observation from the rodent model that HBCs become activated in the intact and bulbectomized mouse OE, in which the tissue integrity is preserved [67]. Yet, the change in the expression profile of adhesion-related genes need to be investigated in our zebrafish model.

On the other hand, cell-to-cell interaction between sustentacular cells and HBCs after injury is not known in detail. It is suggested that the interaction these two cell types is mediated by Notch-mediated signaling and the former provides Notch ligand jagged1 to maintain the latter's quiescent state in the intact tissue [211]. Persistent Notch signaling is crucial for HBC quiescence, because it directly represses proneural Ascl1 expression, which is essential for neuronal differentiation [295]. The downregulation of jagged1 due to the direct effects of chemical injury and indirect effects of axotomy on sustentacular cells may modulate the cellular communication and contribute to HBC activation. On the other hand, the interaction between Notch and p63 is counteractive, as notch directly represses p63 expression in different epithelial models [296, 297]. The inhibitory effects of notch signaling on both ascl1 and p63 suggests that neuronal differentiation and quiescence may be regulated by different molecular components. Therefore the investigation of notch signaling and its relevance to HBC activation may shed light upon the OE regeneration in the future studies.

Finally, it should be also emphasized that different tissue needs (i.e. robust replacement of dying neurons after axotomy or of all cell types after extensive chemical injury) may lead to different lineage trajectories of HBC-like cells following the activation. In fact, a recent study shows that active HBCs don't comprise a homogeneous but a heterogeneous population with divergent transcriptome profiles and lineage capacities in rodents [289]. Interestingly, mutant active HBCs with Sox2 deficiency, which is a characteristic marker for undifferentiated state, can retain their capability to self-renew or to differentiate into sustentacular cells, although they can not give rise to neuronal lineage [289]; suggesting that heterogeneity of active HBCs may emerge very early after the activation.

A similar heterogeneity may also be conserved in the zebrafish OE, particularly between HBC-like cells that are closer to the constitutive proliferation zones where GBC-like cells need to be replaced often and that are in the more central regions where the demand for proliferation is low. Generation of the *Tg(krt5:EGFP)* line in this study (Figure 4.29) is therefore a valuable tool to analyze the molecular changes in the HBC-like pools under different tissue conditions a. Future studies employing such as transcriptome analysis of *Tg(krt5:EGFP)* HBC-like cells over the course of regeneration would clarify whether multiple HBC-like clusters exist in the zebrafish OE.

5.8. HB-EGF: a key component in regenerative response?

Among various modulatory molecules that are released to the extracellular matrix upon injury, the growth factors are particularly important in the regulation of stress-induced inflammation and proliferation. The bulk-transcriptome analysis performed at the beginning of this study reveals a transient and robust increase in the expression levels of *hb-egfa*, one of two paralogues of HB-EGF in zebrafish, at the onset of regeneration (Figure 4.30). Consistently, *in situ* hybridization for *hb-egfa* assay similarly shows numerous gene-expressing cells along the injured OE at 4 hpi and thereby validates the estimation of transcript abundance (Figure 4.30). Activation of EGF receptor by HB-EGF often promotes further transcription of HB-EGF and constitute an autocrine positive-feedback loop [298]. Activity of a positive-feedback loop during the regenerative response may explain the rapid increase in transcript levels that is observed in the OE within 1 dpi.

Elevated HB-EGF levels upon injury has been demonstrated numerously by different neural tissue models [113, 184, 188]. In rats, kainate-induced excitotoxicity leads to an increase in HB-EGF abundance in the hippocampus, starting from 3 hpi [299]. Similarly, HB-EGF transcript level shows an increase upon cerebral ischemia, while the levels of other EGF ligands remain unchanged. In this model, the transient HB-EGF expression peaks at 2 hpi and reverts to basal levels between 6-24 hpi [300].

The selective and transient increase in HB-EGF expression in the injured rodent brain shows constitutes a temporal profile similar to that observed in the zebrafish OE, suggesting that the rapid upgregulation of the growth factor in the early phase of injury response is conserved among multiple species and tissues. As mentioned above, *in situ* hybridization for *hb-egfa* suggests that the injury-induced expression is abundant among basal cells in the OE at 4 hpi; however, this observation may be perceptual because the severe disruption in the tissue integrity complicates the positional identification of gene-expressing cells at the time of analysis.

Examination of gene expression under a different tissue condition may overcome the problem mentioned above. As it is shown in the titration assay in Figure 4.25, exposure to dilute Triton X-100 solution can also induce robust proliferation response without severe loss in tissue integrity. Thus, in situ detection of *hb-egfa* transcription after milder degrees of chemical injury may provide a better tissue structure and allow accurate identification of hb-egfa-positive cells upon exposure.

Numerous studies demonstrate the stimulatory role of HB-EGF in neurogenesis *in vivo* and *in vitro* by HB-EGF administration [185, 187, 301], however effects of exogenous HB-EGF on the OE has not been analyzed before. BrdU assays following active recombinant HB-EGF administration display an increase in general proliferation activity as well as the number of BrdU-positive OSNs, and reveals the stimulatory role of HB-EGF in the zebrafish OE (Figure 4.31 and 4.32).

HB-EGF's production and extracellular release as signaling molecule are directly affected by the molecular changes in extracellular matrix, particularly by the levels of functional metalloproteases under non-physiological conditions. Consistently, modulation of metalloprotease activity by broad-spectrum inhibitors suppresses the regenerative proliferation significantly (Figure 4.33-36). These results reveal that HB-EGF is potent to initiate proliferation and its metalloprotease-mediated activity is involved in the OE regeneration upon extensive injury.

Several articles from 1990s report that EGF receptor in the OE is responsive to EGF ligands [302, 303]; however these studies are limited to *in vitro* assays and don't include HB-EGF as potential ligand. In my study, intranasal administration assays that are mentioned above demonstrate a 2.1 fold and a 3.9 fold increase in cellular proliferation and OSN neurogenesis in the core sensory OE, respectively (Figure 4.31 and 4.32).

The region-specific effect suggests that HB-EGF administration activates dormant progenitor cell populations, as the sensory OE is mostly devoid of active proliferating cells under untreated condition. Still, detailed identification of HB-EGF-responsive cells is essential to understand the stimulatory effect on the tissue.

The paracrine stimulation of cellular proliferation by HB-EGF depends on EGFR signaling. In rodent models, EGFR expression has been observed characteristically in HBCs [190]; however, its functional significance has not been investigated in detail. Based on that, it is necessary to show whether EGFR is also specifically localized to HBC-like cells in the zebrafish OE. In parallel to the identification of receptor-expressing cells, assessing the activation of HBC-like cells upon HB-EGF administration by the use of anti-Krt5 and anti-BrdU immunostaining assays would allow to characterize the specific stimulatory effect of HB-EGF on this particular quiescent population.

The reduction upon the use of metalloprotease inhibitors in the injured OE suggests the necessity of proHB-EGF cleavage and its subsequent paracrine activity for the regenerative response. However, it can not be excluded that the inhibitors used in this study are designed to affect the activity of a number of different proteases with multiple targets. Therefore, it is necessary to use agents that target either specific metalloproteases or HB-EGF directly. Because proteases that involve in HB-EGF shedding are not identified in zebrafish at the moment, a more plausible approach would be the use of a specific HB-EGF inhibitor that binds to the growth factor and blocks its signaling activity.

One candidate molecule, the non-toxic mutant of diphteria toxin CRM197 is known for binding to uncleaved as well as soluable forms of HB-EGF and inhibiting its proliferative signaling actions [304]. Intranasal administration of CRM197,as a HB-EGF-targeted agent, can provide direct evidence on the involvement of HB-EGF activity in the regenerative response in the future.

Another critical issue is the identification of downstream pathways that are activated. Investigating HB-EGF-mediated downstream pathways in the OE is a challenging task, because EGFR activates a large number of unique signaling pathways, including ERK-MAPK, PIK3-AKT,JNK and JAK-STAT pathways [164]. As these pathways are highly interconnected, activation of EGFR affects entire molecular networks that control various physiological tasks, such as cell growth, proliferation and differentiation. Because components within EGFR-mediated signaling pathways have been important target molecules of pharmacological cancer research, the effects of different downstream pathways on the OE regeneration can be easily examined by the use of various specific inhibitors.Preliminary studies from our group suggest that pharmacological inhibition of either of two downstream pathways, JAK-STAT and ERK-MAPK pathways, impairs OE regeneration and causes tissue phenotypes that are similar to those observed after metalloprotease inhibition (Alkiraz and Dokuzluoğlu, unpublished observations). In-depth examination of these pharmacological manipulations and their long-term effects on the tissue will elucidate HB-EGF-mediated pathways that play essential role in the OE regeneration.

Finally, HB-EGF's neuroprotective roles in the healing tissues shouldn't be overlooked in the context of OE regeneration. Neuroprotection, which refers to the relative preservation of the neuronal intactness, is often associated with rapid HB-EGF regeneration upon injury [305, 306]. The observation that the upregulation in *hb-egfa* expression in the OE occurs much earlier than the robust proliferation response (Figure 4.30 and 4.7) suggests that HB-EGF may also play a neuroprotective role at the onset of OE regeneration in addition to progenitor cell activation, such as slowing down neuronal loss and modulating inflammatory changes.

It is possible that a subset, if not all, of *hb-egfa*-expressing cells serve primarily for the maintenance of high neuroprotection at early regenerative time points in order to preserve the surviving cells and minimize the degenerative effects. Future studies employing loss-of-function strategies, such as disruption of signaling activity by cell-specific HB-EGF or EGFR knockout lines may allow to clarify the functional significance of the early robust gene expression and distinguish cellular subsets that may serve for early neuroprotective effects from subsets that primarily contribute to the late proliferation response.

REFERENCES

1. Bonfanti, L., "Adult Neurogenesis 50 years Later: Limits and Opportunities in Mammals", *Frontiers in Neuroscience*, Vol. 10, No. FEB, pp. 1–7, 2016.

2. Gage, F. H., "Mammalian Neural Stem Cells", *Science*, Vol. 287, No. 5457, pp. 1433–1438, 2000.

3. Altman, J., "Are New Neurons Formed in the Brains of Adult Mammals?", *Science*, Vol. 135, No. 3509, pp. 1127–1128, 1962.

4. Kaplan, M. S. and J. W. Hinds, "Neurogenesis in the Adult Rat: Electron Microscopic Analysis of Light Radioautographs", *Science*, Vol. 197, No. 4308, pp. 1092–1094, 1977.

5. Bayer, S. A., J. W. Yackel and P. S. Puri, "Neurons in the Rat Dentate Gyrus Granular Layer Substantially Increase During Juvenile and Adult Life", *Science*, Vol. 216, No. 4548, pp. 890–892, 1982.

6. Anderson, M. J. and S. G. Waxman, "Caudal spinal cord of the teleost Sternarchus albifrons resembles regenerating cord", *The Anatomical Record*, Vol. 205, No. 1, pp. 85–92, 1983.

7. Goldman, S. A. and F. Nottebohm, "Neuronal Production, Migration, and Differentiation in a Vocal Control Nucleus of the Adult Female Canary Brain", *Proceedings of the National Academy of Sciences of the United States of America*, Vol. 80, No. 8 I, pp. 2390–2394, 1983.

8. Eriksson, P. S., E. Perfilieva, T. Björk-Eriksson, A. M. Alborn, C. Nordborg, D. A. Peterson and F. H. Gage, "Neurogenesis in the Adult Human Hippocampus", *Nature Medicine*, Vol. 4, No. 11, pp. 1313–1317, 1998.

9. Kaslin, J., J. Ganz and M. Brand, "Proliferation, Neurogenesis and Regeneration in the Non-mammalian Vertebrate Brain", *Philosophical Transactions of the Royal Society B: Biological Sciences*, Vol. 363, No. 1489, pp. 101–122, 2008.

10. Kempermann, G., H. G. Kuhn and F. H. Gage, "More Hippocampal Neurons in Adult Mice Living in an Enriched Environment", *Nature*, Vol. 386, No. 6624, pp. 493–495, 1997.

11. Tsien, J. Z., "Cre-Lox Neurogenetics: 20 Years of Versatile Applications in Brain Research and Counting...", *Frontiers in Genetics*, Vol. 7, 19, pp. 1–7, 2016.

12. Kaplan, M. S. and D. H. Bell, "Neuronal Proliferation in the 9-Month-Old Rodent - Radioautographic Study of Granule Cells in the Hippocampus", *Experimental Brain Research*, Vol. 52, No. 1, pp. 1–5, 1983.

13. Kaplan, M. S., "Neurogenesis in the 3-Month-Old Rat Visual Cortex", *Journal of Comparative Neurology*, Vol. 195, No. 2, pp. 323–338, 1981.

14. Fiorelli, R., K. Azim, B. Fischer and O. Raineteau, "Adding a Spatial Dimension to Postnatal Ventricular-Subventricular Zone Neurogenesis", *Development (Cambridge)*, Vol. 142, No. 12, pp. 2109–2120, 2015.

15. Ming, G.-L. and H. Song, "Adult Neurogenesis in the Mammalian Brain: Significant Answers and Significant Questions", *Neuron*, Vol. 70, No. 4, pp. 687–702, 2011.

16. Hayashi, K., K. I. Kubo, A. Kitazawa and K. Nakajima, "Cellular Dynamics of Neuronal Migration in The Hippocampus", *Frontiers in Neuroscience*, Vol. 9, No. 135, pp. 1–11, 2015.

17. Kyritsis, N., C. Kizil, S. Zocher, V. Kroehne, J. Kaslin, D. Freudenreich, A. Iltzsche and M. Brand, "Acute Inflammation Initiates the Regenerative Response in the Adult Zebrafish Brain", *Science*, Vol. 338, No. 6112, pp. 1353–1356,

2012.

18. Cayre, M., J. Malaterre, S. Scotto-Lomassese, C. Strambi and A. Strambi, "The Common Properties of Neurogenesis in the Adult Brain: From Invertebrates to Vertebrates", *Comparative Biochemistry and Physiology - B Biochemistry and Molecular Biology*, Vol. 132, No. 1, pp. 1–15, 2002.

19. Rusznák, Z., W. Henskens, E. Schofield, W. S. Kim and Y. H. Fu, "Adult Neurogenesis and Gliogenesis: Possible Mechanisms for Neurorestoration", *Experimental Neurobiology*, Vol. 25, No. 3, pp. 103–112, 2016.

20. Sanai, N., T. Nguyen, R. A. Ihrie, Z. Mirzadeh, H. H. Tsai, M. Wong, N. Gupta, M. S. Berger, E. Huang, J. M. Garcia-Verdugo, D. H. Rowitch and A. Alvarez-Buylla, "Corridors of Migrating Neurons in the Human Brain and Their Decline during Infancy", *Nature*, Vol. 478, No. 7369, pp. 382–386, 2011.

21. Bergmann, O., J. Liebl, S. Bernard, K. Alkass, M. S. Yeung, P. Steier, W. Kutschera, L. Johnson, M. Landén, H. Druid, K. L. Spalding and J. Frisén, "The Age of Olfactory Bulb Neurons in Humans", *Neuron*, Vol. 74, No. 4, pp. 634–639, 2012.

22. Lledo, P. M. and M. Valley, "Adult Olfactory Bulb Neurogenesis", *Cold Spring Harbor Perspectives in Biology*, Vol. 8, No. 8, 2016.

23. Boldrini, M., C. A. Fulmore, A. N. Tartt, L. R. Simeon, I. Pavlova, V. Poposka, G. B. Rosoklija, A. Stankov, V. Arango, A. J. Dwork, R. Hen and J. J. Mann, "Human Hippocampal Neurogenesis Persists throughout Aging", *Cell Stem Cell*, Vol. 22, No. 4, pp. 589–599.e5, 2018.

24. Sorrells, S. F., M. F. Paredes, A. Cebrian-silla, D. Qi, K. W. Kelley, D. James, S. Mayer, J. Chang, K. I. Auguste, E. Chang, A. J. G. Martin, A. R. Kriegstein, G. W. Mathern, M. C. Oldham, E. J. Huang, J. M. Garcia-verdugo, Z. Yang and A. Alvarez-buylla, "Human Hippocampal Neurogenesis Drops Sharply", *Nature*,

Vol. 555, No. 7696, pp. 377–381, 2018.

25. Alvarez-Buylla, A., M. Theelen and F. Nottebohm, "Proliferation "Hot Spots" in Adult Avian Ventricular Zone Reveal Radial Cell Division", *Neuron*, Vol. 5, No. 1, pp. 101–109, 1990.

26. Vellema, M., A. Van Der Linden and M. Gahr, "Area-Specific Migration and Recruitment of New Neurons in the Adult Songbird Brain", *Journal of Comparative Neurology*, Vol. 518, No. 9, pp. 1442–1459, 2010.

27. Alvarez-Buylla, A. and F. Nottebohm, "Migration of Young Neurons in Adult Avian Brain", *Nature*, Vol. 335, No. 6188, pp. 353–354, 1988.

28. Alvarez-Buylla, A., M. Theelen and F. Nottebohm, "Mapping of Radial Glia and of a New Cell Type in Adult Canary Brain", *Journal of Neuroscience*, Vol. 8, No. 8, pp. 2707–2712, 1988.

29. Font, E., E. Desfilis, Garcia-Verdugo and J. Manuel, "Neurogenesis and Neuronal Regeneration in the Adult Reptilian Brain", *Brain, Behavior and Evolution*, Vol. 58, pp. 276–295, 2001.

30. D'Amico, L. A., D. Boujard and P. Coumailleau, "Proliferation, Migration and Differentiation in Juvenile and Adult Xenopus laevis Brains", *Brain Research*, Vol. 1405, pp. 31–48, 2011.

31. Raucci, F., M. M. Di Fiore, C. Pinelli, B. D'Aniello, L. Luongo, G. Polese and R. K. Rastogi, "Proliferative Activity in the Frog Brain: A PCNA-Immunohistochemistry Analysis", *Journal of Chemical Neuroanatomy*, Vol. 32, No. 2-4, pp. 127–142, 2006.

32. Zupanc, G. K., "Adult Neurogenesis and Neuronal Regeneration in the Brain of Teleost fish", *Journal of Physiology Paris*, Vol. 102, No. 4-6, pp. 357–373, 2008.

33. Zupanc, G. K. H. and I. Horschke, "Proliferation Zones in the Brain of Adult Gymnotiform Fish: A Quantitative Mapping Study", *The Journal of Comparative Neurology*, Vol. 233, pp. 213–233, 1995.

34. Winner, B. and J. Winkler, "Adult Neurogenesis in Neurodegenerative Diseases", *Cold Spring Harbor Perspectives in Biology*, Vol. 7, No. 4, 2015.

35. Brann, J. H. and S. J. Firestein, "A Lifetime of Neurogenesis in the Olfactory System", *Frontiers in Neuroscience*, Vol. 8, No. 8 JUN, pp. 1–11, 2014.

36. Labarca, P. and J. Bacigalupo, "Ion Channels from Chemosensory Olfactory Neurons", *Journal of Bioenergetics and Biomembranes*, Vol. 20, No. 5, pp. 551–569, 1988.

37. Schild, D. and D. Restrepo, "Transduction Mechanisms in Vertebrate Olfactory Receptor Cells", *Physiological Reviews*, Vol. 78, No. 2, pp. 429–466, 1998.

38. Witt, M. and W. Wozniak, "Structure and Function of the Vomeronasal Organ", *Advances in Oto-Rhino-Laryngology*, Vol. 63, pp. 70–83, 2006.

39. Mucignat-Caretta, C., M. Redaelli and A. Caretta, "One Nose, One Brain: Contribution of The Main and Accessory Olfactory System to Chemosensation", *Frontiers in Neuroanatomy*, Vol. 6, pp. 1–9, 2012.

40. Vassar, R., S. K. Chao, R. Sitcheran, M. Nuiiez, L. B. Vosshall and R. Axel, "Topographic Organization of Sensory Projection to the Olfactory Bulb", Vol. 79, 1994.

41. Chen, W. R. and G. M. Shepherd, "The Olfactory Glomerulus: A Cortical Module with Specific Functions", *Journal of Neurocytology*, Vol. 34, No. 3-5, pp. 353–360, 2005.

42. Mombaerts, P., "How Smell Develops", *Nature Neuroscience*, Vol. 4, No. 11s, pp.

1192–1198, 2001.

43. Mombaerts, P., "Axonal Wiring in the Mouse Olfactory System.", *Annual review of cell and developmental biology*, Vol. 22, pp. 713–737, 2006.

44. Baier, H. and S. Korsching, "Olfactory Glomeruli in the Zebrafish Are Identifiable across Animals", *The Journal of Neuroscience*, Vol. 14, No. January, pp. 219–230, 1994.

45. Braubach, O. R., A. Fine and R. P. Croll, "Distribution and Functional Organization of Glomeruli in the Olfactory Bulbs of Zebrafish (Danio Rerio)", *Journal of Comparative Neurology*, Vol. 520, No. 11, pp. 2317–2339, 2012.

46. Shi, P. and J. Zhang, "Extraordinary Diversity of Chemosensory Receptor Gene Repertoires among Vertebrates", *Results and Problems in Cell Differentiation.*, Vol. 47, pp. 1–23, 2009.

47. D'Aniello, B., G. R. Semin, A. Scandurra and C. Pinelli, "The Vomeronasal Organ: A Neglected Organ", *Frontiers in Neuroanatomy*, Vol. 11, No. 70, pp. 1–2, 2017.

48. McGann, J. P., "Poor Human Olfaction is a 19th-Century Myth", *Science*, Vol. 356, No. 6338, 2017.

49. Wang, Y., H. Jiang and L. Yang, "Transcriptome Analysis of Zebrafish Olfactory Epithelium Reveal Sexual Differences in Odorant Detection", *Genes*, Vol. 11, No. 6, 2020.

50. Ma, M., X. Grosmaitre, C. L. Iwema, H. Baker, C. A. Greer and G. M. Shepherd, "Olfactory Signal Transduction in the Mouse Septal Organ", *Journal of Neuroscience*, Vol. 23, No. 1, pp. 317–324, 2003.

51. Brechbühl, J., M. Klaey and M. C. Broillet, "Grueneberg Ganglion Cells Mediate

Alarm Pheromone Detection in Mice", *Science*, Vol. 321, No. 5892, pp. 1092–1095, 2008.

52. Buck, L. B. and R. Axel, "A Novel Multigene Family May Encode Odorant Receptors: A Molecular Basis for Odor Recognition", *Cell*, Vol. 65, pp. 175–187, 1991.

53. Liberles, S. D., "Trace Amine-Associated Receptors Are Olfactory Receptors in Vertebrates", *Annals of the New York Academy of Sciences*, Vol. 1170, pp. 168–172, 2009.

54. Matsunami, H. and L. B. Buck, "A Multigene Family Encoding A Diverse Array of Putative Pheromone Receptors in Mammals", *Cell*, Vol. 90, No. 4, pp. 775–784, 1997.

55. Genovese, F. and M. Tizzano, "Microvillous cells in the olfactory epithelium express elements of the solitary chemosensory cell transduction signaling cascade", *PLoS ONE*, Vol. 13, No. 9, pp. 1–15, 2018.

56. Schwob, J. E., W. Jang, E. H. Holbrook, B. Lin, D. B. Herrick, J. Peterson and J. H. Coleman, "Stem and Progenitor Cells of the Mammalian Olfactory Epithelium: Taking Poietic License", *Journal of Comparative Neurology*, Vol. 525, No. 4, pp. 1034–1054, 2016.

57. Huard, J. M., S. L. Youngentob, B. J. Goldstein, M. B. Luskin and J. E. Schwob, "Adult Olfactory Epithelium Contains Multipotent Progenitors That Give Rise to Neurons and Non-Neural Cells", *Journal of Comparative Neurology*, Vol. 400, No. 4, pp. 469–486, 1998.

58. Jang, W., S. L. Youngentob and J. E. Schwob, "Globose Basal Cells are Required for Reconstitution of Olfactory Epithelium after Methyl Bromide Lesion", *Journal of Comparative Neurology*, Vol. 460, No. 1, pp. 123–140, 2003.

59. Schwob, J. E. and W. Jang, "Stem Cells of the Adult Olfactory Epithelium", M. S. Rao (Editor), *Neural Development and Stem Cells*, pp. 219–233, Humana Press, Totowa, NJ, 2006.

60. Guo, Z., A. Packard, R. C. Krolewski, M. T. Harris, G. L. Manglapus and J. E. Schwob, "Expression of Pax6 and Sox2 in Adult Olfactory Epithelium.", *The Journal of Comparative Neurology*, Vol. 518, No. 21, pp. 4395–4418, 2010.

61. Beites, C. L., S. Kawauchi, C. E. Crocker and A. L. Calof, "Identification and Molecular Regulation of Neural Stem Cells in the Olfactory Epithelium", *Experimental Cell Research*, Vol. 306, No. 2, pp. 309–316, 2005.

62. Krolewski, R. C., A. Packard, W. Jang, H. Wildner and J. E. Schwob, "Ascl1 (Mash1) Knockout Perturbs Differentiation of Nonneuronal Cells in Olfactory Epithelium", *PLOS ONE*, Vol. 7, No. 12, pp. 1–16, 2012.

63. Packard, A., M. Giel-Moloney, A. Leiter and J. E. Schwob, "Progenitor Cell Capacity of NeuroD1-Expressing Globose Basal Cells in the Mouse Olfactory Epithelium.", *The Journal of Comparative Neurology*, Vol. 519, No. 17, pp. 3580–3596, 2011.

64. Huard, J. M. and J. E. Schwob, "Cell Cycle of Globose Basal Cells in Rat Olfactory Epithelium", *Developmental Dynamics*, Vol. 203, No. 1, pp. 17–26, 1995.

65. Jang, W., X. Chen, D. Flis, M. Harris and J. E. Schwob, "Label-Retaining, Quiescent Globose Basal Cells Are Found in the Olfactory Epithelium", *Journal of Comparative Neurology*, Vol. 522, No. 4, pp. 731–749, 2014.

66. Carter, L. A., J. L. MacDonald and A. J. Roskams, "Olfactory Horizontal Basal Cells Demonstrate a Conserved Multipotent Progenitor Phenotype.", *The Journal of Neuroscience: The Official Journal of the Society for Neuroscience*, Vol. 24, No. 25, pp. 5670–5683, 2004.

67. Iwai, N., Z. Zhou, D. R. Roop and R. R. Behringer, "Horizontal Basal Cells Are Multipotent Progenitors in Normal and Injured Adult Olfactory Epithelium", *Stem Cells*, Vol. 26, No. 5, pp. 1298–1306, 2008.

68. Leung, C. T., P. A. Coulombe and R. R. Reed, "Contribution of Olfactory Neural Stem Cells to Tissue Maintenance and Regeneration.", *Nature Neuroscience*, Vol. 10, No. 6, pp. 720–726, jun 2007.

69. Schubert, D., W. Stallcup, M. LaCorbiere, Y. Kidokoro and L. Orgel, "Ontogeny of Electrically Excitable Cells in Cultured Olfactory Epithelium", *Proceedings of the National Academy of Sciences of the United States of America*, Vol. 82, No. 22, pp. 7782–7786, 1985.

70. Liang, F., "Sustentacular Cell Enwrapment of Olfactory Receptor Neuronal Dendrites: An Update", *Genes*, Vol. 11, No. 5, pp. 14–17, 2020.

71. Vogalis, F., C. C. Hegg and M. T. Lucero, "Electrical Coupling in Sustentacular Cells of the Mouse Olfactory Epithelium", *Journal of Neurophysiology*, Vol. 94, No. 2, pp. 1001–1012, 2005.

72. Czesnik, D., J. Kuduz, D. Schild and I. Manzini, "ATP Activates Both Receptor and Sustentacular Supporting Cells in the Olfactory Epithelium of Xenopus laevis Tadpoles", *European Journal of Neuroscience*, Vol. 23, No. 1, pp. 119–128, 2006.

73. Demirler, M. C., U. Sakizli, B. Bali, Y. Kocagöz, S. E. Eski, A. Ergönen, A. S. Alkiraz, X. Bayramli, T. Hassenklöver, I. Manzini and S. H. Fuss, "Purinergic Signalling Selectively Modulates Maintenance but Not Repair Neurogenesis in the Zebrafish Olfactory Epithelium", *FEBS Journal*, Vol. 287, No. 13, pp. 2699–2722, 2020.

74. Takagi, S. F., "Degeneration and Regeneration of the Olfactory Epithelium", B. L.M. (Editor), *Olfaction. Handbook of Sensory Physiology*, Vol. 4, pp. 75–94, Springer Berlin Heidelberg, 1971.

75. Nagahara, Y., "Experimentelle Studien über die histologischen Veränderungen des Geruchsorgans nach der Olfactoriusdurchschneideidung", *Japanse Journal of Medical Sciences V. Pathology.*, Vol. V, pp. 165–199, 1940.

76. Graziadei, P. P. C. and G. A. Monti Graziadei, "Continuous Nerve Cell Renewal in The Olfactory System", Jacobson M. (Editor), *Development of Sensory Systems. Handbook of Sensory Physiology vol9*, chap. 2, pp. 55–83, Springer Berlin Heidelberg, 1978.

77. Graziadei, P. P. and G. A. Monti Graziadei, "Neurogenesis and Neuron Regeneration in the Olfactory System of Mammals. III. Deafferentation and Reinnervation of the Olfactory Bulb Following Section of the Fila Olfactoria in Rat", *Journal of Neurocytology*, Vol. 9, No. 2, pp. 145–162, 1980.

78. Costanzo, R. M., "Neural Regeneration and Functional Reconnection Following Olfactory Nerve Transection in Hamster", *Brain Research*, Vol. 361, No. 1-2, pp. 258–266, 1985.

79. Christensen, M. D., E. H. Holbrook, R. M. Costanzo and J. E. Schwob, "Rhinotopy Is Disrupted during the Re-Innervation of the Olfactory Bulb That Follows Transection of the Olfactory Nerve", *Chemical Senses*, Vol. 26, No. 4, pp. 359–369, 2001.

80. Yee, K. K. and R. M. Costanzo, "Changes in Odor Quality Discrimination Following Recovery from Olfactory Nerve Transection", *Chemical Senses*, Vol. 23, No. 5, pp. 513–519, 1998.

81. Mulvaney, B. D. and H. E. Heist, "Regeneration of Rabbit Olfactory Epithelium.", *The American Journal of Anatomy*, Vol. 131, No. 2, pp. 241–251, 1971.

82. Schultz, E. W., "Regeneration of Olfactory Cells", *Experimental Biology and Medicine*, Vol. 46, No. 1, pp. 41–43, 1941.

83. Smith, C. G., "Regeneration of Sensory Olfactory Epithelium and Nerves in Adult Frogs.", *The Anatomical Record*, Vol. 109, No. 4, pp. 661–671, 1951.

84. Baker, H., T. Kawano, F. L. Margolis and T. H. Joh, "Transneuronal Regulation of Tyrosine Hydroxylase Expression in Olfactory Bulb of Mouse and Rat", *Journal of Neuroscience*, Vol. 3, No. 1, pp. 69–78, 1983.

85. Cancalon, P., "Influence of A Detergent on the Catfish Olfactory Mucosa", *Tissue and Cell*, Vol. 15, No. 2, pp. 245–258, 1983.

86. Iqbal, T. and C. Byrd-Jacobs, "Rapid Degeneration and Regeneration of the Zebrafish Olfactory Epithelium after Triton X-100 Application.", *Chemical Senses*, Vol. 35, No. 5, pp. 351–361, 2010.

87. Schwob, J. E., S. L. Youngentob and R. C. Mezza, "Reconstitution of the Rat Olfactory Epithelium after Methyl Bromide-Induced Lesion.", *The Journal of Comparative Neurology*, Vol. 359, No. 1, pp. 15–37, 1995.

88. Sansom, S. N., D. S. Griffiths, A. Faedo, D. J. Kleinjan, Y. Ruan, J. Smith, V. Van Heyningen, J. L. Rubenstein and F. J. Livesey, "The level of the Transcription Factor Pax6 is Essential for Controlling the Balance between Neural Stem Cell Self-Renewal and Neurogenesis", *PLoS Genetics*, Vol. 5, No. 6, pp. 20–23, 2009.

89. Packard, A. I., B. Lin and J. E. Schwob, "Sox2 and Pax6 Play Counteracting Roles in Regulating Neurogenesis within the Murine Olfactory Epithelium", *PLoS ONE*, Vol. 11, No. 5, pp. 1–28, 2016.

90. Cau, E., G. Gradwohl, C. Fode and F. Guillemot, "Mash1 Activates a Cascade of BHLH Regulators in Olfactory Neuron Progenitors", *Development*, Vol. 124, No. 8, pp. 1611–1621, 1997.

91. Cau, E., S. Casarosa and F. Guillemot, "Mash1 and Ngn1 Control Distinct Steps of Determination and Differentiation in the Olfactory Sensory Neuron Lineage",

Development, Vol. 129, No. 8, pp. 1871–1880, 2002.

92. Holtmaat, J. G. D., V. D. Lugt, A. Bert-q, P. A. Dijkhuizen, F. L. Margolis, W. H. Gispen and J. Verhaagenl, "Directed Expression of the Growth-Associated Protein B-50/GAP-43 to Olfactory Neurons in Transgenic Mice Results in Changes in Axon Morphology and Extraglomerular Fiber Growth", *The Journal of Neuroscience*, Vol. 25, No. 12, pp. 7953–7965, 1995.

93. Lee, A. C., J. He and M. Ma, "Olfactory Marker Protein is Critical for Functional Maturation of Olfactory Sensory Neurons and Development of Mother Preference", *Journal of Neuroscience*, Vol. 31, No. 8, pp. 2974–2982, 2011.

94. Schnittke, N., D. B. Herrick, B. Lin, J. Peterson, J. H. Coleman, A. I. Packard, W. Jang and J. E. Schwob, "Transcription Factor P63 Controls the Reserve Status but Not the Stemness of Horizontal Basal Cells in the Olfactory Epithelium", *Proceedings of the National Academy of Sciences of the United States of America*, Vol. 112, No. 36, pp. E5068–E5077, 2015.

95. Caggiano, M., J. S. Kauer and D. D. Hunter, "Globose Basal Cells Are Neuronal Progenitors in the Olfactory Epithelium: A Lineage Analysis Using a Replication-Incompetent Retrovirus", *Neuron*, Vol. 13, No. 2, pp. 339–352, 1994.

96. Packard, A., N. Schnittke, R. A. Romano, S. Sinha and J. E. Schwob, "ΔNp63 Regulates Stem Cell Dynamics in the Mammalian Olfactory Epithelium", *Journal of Neuroscience*, Vol. 31, No. 24, pp. 8748–8759, 2011.

97. Seifert, A. W. and M. Maden, *New Insights into Vertebrate Skin Regeneration*, Vol. 310, Elsevier Inc., 1 edn., 2014.

98. Porrello, E. R., A. I. Mahmoud, E. Simpson, J. A. Hill, J. A. Richardson, E. N. Olson and H. A. Sadek, "Transient Regenerative Potential of the Neonatal Mouse Heart", *Science*, Vol. 331, No. 12, pp. 2–4, 2011.

99. Streisinger, G., C. Walker, N. Dower, D. Knauber and F. Singer, "Production of Homozygous Diploid Zebra Fish (Brachydanio Rerio)", *Nature*, Vol. 291, pp. 293–296, 1981.

100. Walker, C. and G. Streisinger, "Induction of Mutations by γ-Rays in Pregonial Germ Cells of Zebrafish Embryos", *Genetics*, Vol. 103, No. 1, pp. 125–136, 1983.

101. Gao, X. and J. Chen, "Moderate Traumatic Brain Injury Promotes Neural Precursor Proliferation without Increasing Neurogenesis in the Adult Hippocampus", *Experimental Neurology*, Vol. 239, No. 1, pp. 38–48, 2013.

102. Cigliola, V., C. J. Becker and K. D. Poss, "Building Bridges, Not Walls: Spinal Cord Regeneration in Zebrafish", *DMM Disease Models and Mechanisms*, Vol. 13, No. 5, 2020.

103. Kizil, C., J. Kaslin, V. Kroehne and M. Brand, "Adult Neurogenesis and Brain Regeneration in Zebrafish", *Developmental Neurobiology*, Vol. 72, No. 3, pp. 429–461, 2012.

104. Wan, J. and D. Goldman, "Retina Regeneration in Zebrafish", *Current Opinion in Genetics and Development*, Vol. 40, No. Figure 1, pp. 41–47, 2016.

105. Kroehne, V., D. Freudenreich, S. Hans, J. Kaslin and M. Brand, "Regeneration of the Adult Zebrafish Brain from Neurogenic Radial Glia-Type Progenitors", *Development*, Vol. 138, No. 22, pp. 4831–4841, 2011.

106. Reimer, M. M., I. Sörensen, V. Kuscha, R. E. Frank, C. Liu, C. G. Becker and T. Becker, "Motor Neuron Regeneration in Adult Zebrafish", *Journal of Neuroscience*, Vol. 28, No. 34, pp. 8510–8516, 2008.

107. Bähr, M. and F. Bonhoeffer, "Perspectives on Axonal Regeneration in the Mammalian CNS", *Trends in Neuroscience*, Vol. 17, No. 11, pp. 473–479, 1994.

108. Huebner, E. A. and S. M. Strittmatter, "Axon Regeneration in the Peripheral and Central Nervous Systems", *Results and Problems in Cell Differentiation*, Vol. 48, pp. 339–351, 2009.

109. Becker, T. and C. G. Becker, "Axonal Regeneration in Zebrafish", *Current Opinion in Neurobiology*, Vol. 27, pp. 186–191, 2014.

110. Vajn, K., D. Suler, J. A. Plunkett and M. Oudega, "Temporal Profile of Endogenous Anatomical Repair and Functional Recovery Following Spinal Cord Injury in Adult Zebrafish", *PLoS ONE*, Vol. 9, No. 8, pp. 1–9, 2014.

111. Thomas, E. D. and D. W. Raible, "Distinct Progenitor Populations Mediate Regeneration in the Zebrafish Lateral Line", *eLife*, Vol. 8, pp. 1–27, 2019.

112. Thummel, R., S. C. Kassen, J. M. Enright, C. M. Nelson, J. E. Montgomery and D. R. Hyde, "Characterization of Müller Glia and Neuronal Progenitors during Adult Zebrafish Retinal Regeneration", *Experimental Eye Research*, Vol. 87, No. 5, pp. 433–444, 2008.

113. Wan, J., R. Ramachandran and D. Goldman, "HB-EGF Is Necessary and Sufficient for Müller Glia Dedifferentiation and Retina Regeneration", *Developmental Cell*, Vol. 22, No. 2, pp. 334–347, 2012.

114. Gemberling, M., T. J. Bailey, D. R. Hyde and K. D. Poss, "The Zebrafish as a Model for Complex Tissue Regeneration", *Trends in Genetics : TIG*, Vol. 29, No. 11, pp. 611–620, 2013.

115. Bally-Cuif, L. and W. Norton, "Adult Zebrafish as a Model Organism for Behavioural Genetics", *BMC Neuroscience*, Vol. 11, No. 1, pp. 11–90, 2010,

116. MacRae, C. A. and R. T. Peterson, "Zebrafish as Tools for Drug Discovery", *Nature Reviews Drug Discovery*, Vol. 14, No. 10, pp. 721–731, 2015.

117. Pugach, E. K., K. R. Finley and L. I. Zon, *Zebrafish and Stem Cell Research*, Elsevier Inc., 2nd edn., 2009.

118. Felker, A. and C. Mosimann, *Contemporary Zebrafish Transgenesis with Tol2 and Application for Cre/lox Recombination Experiments*, Vol. 135, Elsevier Ltd, 2016.

119. Hans, S., D. Zöller, J. Hammer, J. Stucke, S. Spieß, G. Kesavan, V. Kroehne, J. S. Eguiguren, D. Ezhkova, A. Petzold, A. Dahl and M. Brand, "Cre-Controlled CRISPR Mutagenesis Provides Fast and Easy Conditional Gene Inactivation in Zebrafish", *Nature Communications*, Vol. 12, No. 1, pp. 1–12, 2021.

120. Li, W., Y. Zhang, B. Han, L. Li, M. Li, X. Lu, C. Chen, M. Lu, Y. Zhang, X. Jia, Z. Zhu, X. Tong and B. Zhang, "One-Step Efficient Generation of Dual-Function Conditional Knockout and Geno-Tagging Alleles in Zebrafish", *eLife*, Vol. 8, pp. 1–21, 2019.

121. Hara, T. J., *Role of Olfaction in Fish Behaviour*, Springer, 1st edn., 1986.

122. Hara, T. J., "The diversity of Chemical Stimulation in Fish Olfaction and Gustation", *Reviews in Fish Biology and Fisheries*, Vol. 4, No. 1, pp. 1–35, 1994.

123. Kermen, F., L. M. Franco, C. Wyatt and E. Yaksi, "Neural Circuits Mediating Olfactory-Driven Behavior in Fish", *Frontiers in Neural Circuits*, Vol. 7, No. MAR, pp. 1–9, 2013.

124. Laberge, F. and T. J. Hara, "Neurobiology of Fish Olfaction: A Review", *Brain Research Reviews*, Vol. 36, No. 1, pp. 46–59, 2001.

125. Hansen, A. and E. Zeiske, "The Peripheral Olfactory Organ of the Zebrafish, Danio Rerio: An Ultrastructural Study", *Chemical Senses*, Vol. 23, No. 1, pp. 39–48, 1998.

126. Calvo-Ochoa, E., C. A. Byrd-Jacobs and S. H. Fuss, "Diving into the Streams

and Waves of Constitutive and Regenerative Olfactory Neurogenesis: Insights from Zebrafish", *Cell and Tissue Research*, Vol. 383, pp. 227–253, 2021.

127. Bayramli, X., Y. Kocagöz, U. Sakizli and S. H. Fuss, "Patterned Arrangements of Olfactory Receptor Gene Expression in Zebrafish are Established by Radial Movement of Specified Olfactory Sensory Neurons", *Scientific Reports*, Vol. 7, No. 1, pp. 1–16, 2017.

128. Çelik, A., S. H. Fuss and S. I. Korsching, "Selective Targeting of Zebrafish Olfactory Receptor Neurons by the Endogenous OMP Promoter", *European Journal of Neuroscience*, Vol. 15, No. 5, pp. 798–806, 2002.

129. Sato, Y., N. Miyasaka and Y. Yoshihara, "Mutually Exclusive Glomerular Innervation by Two Distinct Types of Olfactory Sensory Neurons Revealed in Transgenic Zebrafish", *Journal of Neuroscience*, Vol. 25, No. 20, pp. 4889–4897, 2005.

130. Pelosi, P., "The role of Perireceptor Events in Vertebrate Olfaction", *Cellular and Molecular Life Sciences*, Vol. 58, No. 4, pp. 503–509, 2001.

131. Ahuja, G., I. Ivandic, M. Saltürk, Y. Oka, W. Nadler and S. I. Korsching, "Zebrafish Crypt Neurons Project to a Single, Identified Mediodorsal Glomerulus", *Scientific Reports*, Vol. 3, 2013.

132. Ahuja, G., S. B. Nia, V. Zapilko, V. Shiriagin, D. Kowatschew, Y. Oka and S. I. Korsching, "Kappe Neurons, a Novel Population of Olfactory Sensory Neurons", *Scientific Reports*, Vol. 4, pp. 1–8, 2015.

133. Calvo-Ochoa, E. and C. A. Byrd-Jacobs, "The Olfactory System of Zebrafish as a Model for the Study of Neurotoxicity and Injury: Implications for Neuroplasticity and Disease", *International Journal of Molecular Sciences*, Vol. 20, No. 7, 2019.

134. Wakisaka, N., N. Miyasaka, T. Koide, M. Masuda, T. Hiraki-Kajiyama and Y. Yoshihara, "An Adenosine Receptor for Olfaction in Fish", *Current Biology*,

Vol. 27, No. 10, pp. 1437–1447.e4, 2017.

135. Johnson, M. A., L. Tsai, D. S. Roy, D. H. Valenzuela, C. Mosley, A. Magklara, S. Lomvardas, S. D. Liberles and G. Barnea, "Neurons Expressing Trace Amine-Associated Receptors Project to Discrete Glomeruli and Constitute an Olfactory Subsystem", *Proceedings of the National Academy of Sciences of the United States of America*, Vol. 109, No. 33, pp. 13410–13415, 2012.

136. Mombaerts, P., F. Wang, C. Dulac, S. K. Chao, A. Nemes, M. Mendelsohn, J. Edmondson and R. Axel, "Visualizing an Olfactory Sensory Map", *Cell*, Vol. 87, No. 4, pp. 675–686, 1996.

137. Wagner, S., A. L. Gresser, A. T. Torello and C. Dulac, "A Multireceptor Genetic Approach Uncovers an Ordered Integration of VNO Sensory Inputs in the Accessory Olfactory Bulb", *Neuron*, Vol. 50, No. 5, pp. 697–709, 2006.

138. Catania, S., A. Germanà, R. Laurà, T. Gonzalez-Martinez, E. Ciriaco and J. A. Vega, "The Crypt Neurons in the Olfactory Epithelium of the Adult Zebrafish Express TrkA-Like Immunoreactivity", *Neuroscience Letters*, Vol. 350, No. 1, pp. 5–8, 2003.

139. Germanà, A., G. Montalbano, R. Laurà, E. Ciriaco, M. E. Del Valle and J. A. Vega, "S100 Protein-Like Immunoreactivity in the Crypt Olfactory Neurons of the Adult Zebrafish", *Neuroscience Letters*, Vol. 371, No. 2-3, pp. 196–198, 2004.

140. Parisi, V., M. C. Guerrera, F. Abbate, O. Garcia-Suarez, E. Viña, J. A. Vega and A. Germanà, "Immunohistochemical Characterization of the Crypt Neurons in the Olfactory Epithelium of Adult Zebrafish", *Annals of Anatomy*, Vol. 196, No. 4, pp. 178–182, 2014.

141. Oka, Y., L. R. Saraiva and S. I. Korsching, "Crypt Neurons Express a Single V1r-Related Ora Gene", *Chemical Senses*, Vol. 37, No. 3, pp. 219–227, 2012.

142. Hassenklöver, T., P. Schwartz, D. Schild and I. Manzini, "Purinergic Signaling Regulates Cell Proliferation of Olfactory Epithelium Progenitors", *Stem Cells*, Vol. 27, No. 8, pp. 2022–2031, 2009.

143. Hassenklöver, T., S. Kurtanska, I. Bartoszek, S. Junek, D. Schild and I. Manzini, "Nucleotide-Induced Ca2+ Signaling in Sustentacular Supporting Cells of the Olfactory Epithelium", *Glia*, Vol. 56, No. 15, pp. 1614–1624, 2008.

144. Weth, F., W. Nadler and S. Korsching, "Nested Expression Domains for Odorant Receptors in Zebrafish Olfactory Epithelium", *Proceedings of the National Academy of Sciences of the United States of America*, Vol. 93, No. 23, pp. 13321–13326, 1996.

145. Chen, M., S. Tian, X. Yang, A. P. Lane, R. R. Reed and H. Liu, "Wnt-Responsive Lgr5(+) Globose Basal Cells Function as Multipotent Olfactory Epithelium Progenitor Cells.", *The Journal of Neuroscience: The Official Journal of the Society for Neuroscience*, Vol. 34, No. 24, pp. 8268–8276, 2014.

146. Abreu, M. S., A. C. Giacomini, R. Rodriguez, A. V. Kalueff and L. J. Barcellos, "Effects of ZnSO4-Induced Peripheral Anosmia on Zebrafish Behavior and Physiology", *Behavioural Brain Research*, Vol. 320, pp. 275–281, 2017.

147. Scheib, J. J., J. M. Pozzuto and C. A. Byrd-Jacobs, "Reversible Deafferentation of the Zebrafish Olfactory Bulb with Wax Plug Insertion", *Journal of Neuroscience Methods*, Vol. 311, pp. 47–56, 2019.

148. Hentig, J. T. and C. A. Byrd-Jacobs, "Exposure to Zinc Sulfate Results in Differential Effects on Olfactory Sensory Neuron Subtypes in Adult Zebrafish", *International Journal of Molecular Sciences*, Vol. 17, No. 9, 2016.

149. Rekatsina, M., A. Paladini, A. Piroli, P. Zis, J. V. Pergolizzi and G. Varrassi, "Pathophysiology and Therapeutic Perspectives of Oxidative Stress and Neurodegenerative Diseases: A Narrative Review", *Advances in Therapy*, Vol. 37, No. 1,

pp. 113–139, 2020.

150. Sayre, L., M. Smith and G. Perry, "Chemistry and Biochemistry of Oxidative Stress in Neurodegenerative Disease", *Current Medicinal Chemistry*, Vol. 8, No. 7, pp. 721–738, 2001.

151. Serras, F., "The Benefits of Oxidative Stress for Tissue Repair and Regeneration", *Fly*, Vol. 10, No. 3, pp. 128–133, 2016.

152. Romero, M. M. G., G. McCathie, P. Jankun and H. H. Roehl, "Damage-Induced Reactive Oxygen Species Enable Zebrafish Tail Regeneration by Repositioning of Hedgehog Expressing Cells", *Nature Communications*, Vol. 9, No. 1, 2018.

153. Ongusaha, P. P., J. C. Kwak, A. J. Zwible, S. Macip, S. Higashiyama, N. Taniguchi, L. Fang and S. W. Lee, "HB-EGF is a Potent Inducer of Tumor Growth and Angiogenesis", *Cancer Research*, Vol. 64, No. 15, pp. 5283–5290, 2004.

154. Yotsumoto, F., E. Tokunaga, E. Oki, Y. Maehara, H. Yamada, K. Nakajima, S. O. Nam, K. Miyata, M. Koyanagi, K. Doi, S. Shirasawa, M. Kuroki and S. Miyamoto, "Molecular Hierarchy of Heparin-Binding EGF-Like Growth Factor-Regulated Angiogenesis in Triple-Negative Breast Cancer", *Molecular Cancer Research*, Vol. 11, No. 5, pp. 506–517, 2013.

155. Cribbs, R. K., P. A. Harding, M. H. Luquette and G. E. Besner, "Endogenous Production of Heparin-Binding EGF-Like Growth Factor during Murine Partial-Thickness Burn Wound Healing", *Journal of Burn Care and Rehabilitation*, Vol. 23, No. 2, pp. 116–125, 2002.

156. El-Assal, O. N. and G. E. Besner, "HB-EGF Enhances Restitution After Intestinal Ischemia/Reperfusion via PI3K/Akt and MEK/ERK1/2 Activation", *Gastroenterology*, Vol. 129, No. 2, pp. 609–625, 2005.

157. Xu, K. P., Y. Ding, J. Ling, Z. Dong and F. S. X. Yu, "Wound-Induced HB-EGF Ectodomain Shedding and EGFR Activation in Corneal Epithelial Cells", *Investigative Ophthalmology and Visual Science*, Vol. 45, No. 3, pp. 813–820, 2004.

158. Iwamoto, R., N. Mine, T. Kawaguchi, S. Minami, K. Saeki and E. Mekada, "HB-EGF Function in Cardiac Valve Development Requires Interaction with Heparan Sulfate Proteoglycans", *Development*, Vol. 137, No. 13, pp. 2205–2214, 2010.

159. Iwamoto, R., N. Mine, H. Mizushima and E. Mekada, "ErbB1 and ErbB4 Generate Opposing Signals Regulating Mesenchymal Cell Proliferation during Valvulogenesis", *Journal of Cell Science*, Vol. 130, No. 7, pp. 1321–1332, 2017.

160. Paria, B. C., K. Elenius, M. Klagsbrun and S. K. Dey, "Heparin-Binding EGF-Like Growth Factor Interacts with Mouse Blastocysts Independently of ErbB1: A Possible Role for Heparan Sulfate Proteoglycans and ErbB4 in Blastocyst Implantation", *Development*, Vol. 126, No. 9, pp. 1997–2005, 1999.

161. Nolan, T. M., N. Di Girolamo, M. T. Coroneo and D. Wakefield, "Proliferative Effects of Heparin-Binding Epidermal Growth Factor-like Growth Factor on Pterygium Epithelial Cells and Fibroblasts", *Investigative Ophthalmology and Visual Science*, Vol. 45, No. 1, pp. 110–113, 2004.

162. Su, Y. and G. E. Besner, "Heparin-Binding EGF-Like Growth Factor (HB-EGF) Promotes Cell Migration and Adhesion via Focal Adhesion Kinase", *Journal of Surgical Research*, Vol. 189, No. 2, pp. 222–231, 2014.

163. Andl, C. D., T. Mizushima, K. Oyama, M. Bowser, H. Nakagawa and A. K. Rustgi, "EGFR-Induced Cell Migration is Mediated Predominantly by the JAK-STAT Pathway in Primary Esophageal Keratinocytes", *American Journal of Physiology - Gastrointestinal and Liver Physiology*, Vol. 287, No. 6 50-6, pp. 1227–1237, 2004.

164. Wee, P. and Z. Wang, "Epidermal Growth Factor Receptor Cell Proliferation

Signaling Pathways", *Cancers*, Vol. 9, No. 5, pp. 1–45, 2017.

165. Naglich, J. G., J. E. Metherall, D. W. Russell and L. Eidels, "Expression Cloning of a Diphtheria Toxin Receptor: Identity with a Heparin-Binding EGF-Like Growth Factor Precursor", *Cell*, Vol. 69, No. 6, pp. 1051–1061, 1992.

166. Iwamoto, R. and E. Mekada, "Heparin-Binding EGF-Like Growth Factor: A Juxtacrine Growth Factor", *Cytokine and Growth Factor Reviews*, Vol. 11, No. 4, pp. 335–344, 2000.

167. Singh, A. B., K. Sugimoto and R. C. Harris, "Juxtacrine Activation of Epidermal Growth Factor (EGF) Receptor by Membrane-Anchored Heparin-Binding EGF-Like Growth Factor Protects Epithelial Cells from Anoikis while Maintaining an Epithelial Phenotype", *Journal of Biological Chemistry*, Vol. 282, No. 45, pp. 32890–32901, 2007.

168. Miyazono, K., "Ectodomain Shedding of HB-EGF: A Potential Target for Cancer Therapy", *Journal of Biochemistry*, Vol. 151, No. 1, pp. 1–3, 2012.

169. Higashiyama, S. and D. Nanba, "ADAM-Mediated Ectodomain Shedding of HB-EGF in Receptor Cross-Talk", *Biochimica et Biophysica Acta - Proteins and Proteomics*, Vol. 1751, No. 1, pp. 110–117, 2005.

170. Ebi, M., H. Kataoka, T. Shimura, E. Kubota, Y. Hirata, T. Mizushima, T. Mizoshita, M. Tanaka, M. Mabuchi, H. Tsukamoto, S. Tanida, T. Kamiya, S. Higashiyama and T. Joh, "TGFβ Induces ProHB-EGF Shedding and EGFR Transactivation through ADAM Activation in Gastric Cancer Cells", *Biochemical and Biophysical Research Communications*, Vol. 402, No. 3, pp. 449–454, 2010.

171. Fridman, J. S., E. Caulder, M. Hansbury, X. Liu, G. Yang, Q. Wang, Y. Lo, B. B. Zhou, M. Pan, S. M. Thomas, J. R. Grandis, J. Zhuo, W. Yao, R. C. Newton, S. M. Friedman, P. A. Scherle and K. Vaddi, "Selective Inhibition of ADAM Metalloproteases as a Novel Approach for Modulating ErbB Pathways in

Cancer", *Clinical Cancer Research*, Vol. 13, No. 6, pp. 1892–1902, 2007.

172. Iwamoto, R., S. Yamazaki, M. Asakura, S. Takashima, H. Hasuwa, K. Miyado, S. Adachi, M. Kitakaze, K. Hashimoto, G. Raab, D. Nanba, S. Higashiyama, M. Hori, M. Klagsbrun and E. Mekada, "Heparin-Binding EGF-like Growth Factor and ErbB Signaling Is Essential for Heart Function", *Proceedings of the National Academy of Sciences of the United States of America*, Vol. 100, No. 6, pp. 3221–3226, 2003.

173. Nanba, D., Y. Kinugasa, C. Morimoto, M. Koizumi, H. Yamamura, K. Takahashi, N. Takakura, E. Mekada, K. Hashimoto and S. Higashiyama, "Loss of HB-EGF in Smooth Muscle or Endothelial Cell Lineages Causes Heart Malformation", *Biochemical and Biophysical Research Communications*, Vol. 350, No. 2, pp. 315–321, 2006.

174. Means, A. L., K. C. Ray, A. B. Singh, M. K. Washington, R. H. Whitehead, R. C. Harris, C. V. Wright, R. J. Coffey and S. D. Leach, "Overexpression of Heparin-Binding EGF-Like Growth Factor in Mouse Pancreas Results in Fibrosis and Epithelial Metaplasia", *Gastroenterology*, Vol. 124, No. 4, pp. 1020–1036, 2003.

175. Radulescu, A., X. Yu, N. D. Orvets, Y. Chen, H. Y. Zhang and G. E. Besner, "Deletion of the Heparin-Binding Epidermal Growth Factor-Like Growth Factor Gene Increases Susceptibility to Necrotizing Enterocolitis", *Journal of Pediatric Surgery*, Vol. 45, No. 4, pp. 729–734, 2010.

176. McCarthy, D. W., M. T. Downing, D. R. Brigstock, M. H. Luquette, K. D. Brown, M. S. Abad and G. E. Besner, "Production of Heparin-Binding Epidermal Growth Factor-Like Growth Factor (HB-EGF) at Sites of Thermal Injury in Pediatric Patients", *Journal of Investigative Dermatology*, Vol. 106, No. 1, pp. 49–56, 1996.

177. Marikovsky, M., K. Breuing, P. Y. Liu, E. Eriksson, S. Higashiyama, P. Farber, J. Abraham and M. Klagsbrun, "Appearance of Heparin-Binding EGF-Like

Growth Factor in Wound Fluid as a Response to Injury", *Proceedings of the National Academy of Sciences of the United States of America*, Vol. 90, No. 9, pp. 3889–3893, 1993.

178. Mathay, C., S. Giltaire, F. Minner, E. Bera, M. Hérin and Y. Poumay, "Heparin-Binding EGF-Like Growth Factor Is Induced by Disruption of Lipid Rafts and Oxidative Stress in Keratinocytes and Participates in the Epidermal Response to Cutaneous Wounds", *Journal of Investigative Dermatology*, Vol. 128, No. 3, pp. 717–727, 2008.

179. Shirakata, Y., R. Kimura, D. Nanba, R. Iwamoto, S. Tokumaru, C. Morimoto, K. Yokota, M. Nakamura, K. Sayama, E. Mekada, S. Higashiyama and K. Hashimoto, "Heparin-Binding EGF-Like Growth Factor Accelerates Keratinocyte Migration and Skin Wound Healing.", *Journal of Cell Science*, Vol. 118, No. 11, pp. 2363–2370, 2005.

180. Mitchell, C., M. Nivison, L. F. Jackson, R. Fox, D. C. Lee, J. S. Campbell and N. Fausto, "Heparin-Binding Epidermal Growth Factor-Like Growth Factor Links Hepatocyte Priming with Cell Cycle Progression during Liver Regeneration", *Journal of Biological Chemistry*, Vol. 280, No. 4, pp. 2562–2568, 2005.

181. Huang, G., G. E. Besner and D. R. Brigstock, "Heparin-Binding Epidermal Growth Factor-Like Growth Factor Suppresses Experimental Liver Fibrosis in Mice", *Laboratory Investigation*, Vol. 92, No. 5, pp. 703–712, 2012.

182. Oyagi, A. and H. Hara, "Essential Roles of Heparin-Binding Epidermal Growth Factor-Like Growth Factor in the Brain", *CNS Neuroscience and Therapeutics*, Vol. 18, No. 10, pp. 803–810, 2012.

183. Jin, K., Y. Sun, L. Xie, S. Batteur, X. O. Mao, C. Smelick, A. Logvinova and D. A. Greenberg, "Neurogenesis and Aging: FGF-2 and HB-EGF Restore Neurogenesis in Hippocampus and Subventricular Zone of Aged Mice.", *Aging Cell*, Vol. 2, No. 3, pp. 175–183, 2003.

184. Jin, K., X. O. Mao, Y. Sun, L. Xie, L. Jin, E. Nishi, M. Klagsbrun and D. A. Greenberg, "Heparin-Binding Epidermal Growth Factor-Like Growth Factor: Hypoxia-Inducible Expression in Vitro and Stimulation of Neurogenesis in Vitro and in Vivo.", *The Journal of neuroscience: The Official Journal of the Society for Neuroscience*, Vol. 22, No. 13, pp. 5365–5373, jul 2002.

185. Jin, K., Y. Sun, L. Xie, J. Childs, X. O. Mao and D. A. Greenberg, "Post-Ischemic Administration of Heparin-Binding Epidermal Growth Factor-Like Growth Factor (HB-EGF) Reduces Infarct Size and Modifies Neurogenesis after Focal Cerebral Ischemia in the Rat", *Journal of Cerebral Blood Flow and Metabolism*, Vol. 24, No. 4, pp. 399–408, 2004.

186. Sugiura, S., K. Kitagawa, S. Tanaka, K. Todo, E. Omura-Matsuoka, T. Sasaki, T. Mabuchi, K. Matsushita, Y. Yagita and M. Hori, "Adenovirus-Mediated Gene Transfer of Heparin-Binding Epidermal Growth Factor-Like Growth Factor Enhances Neurogenesis and Angiogenesis after Focal Cerebral Ischemia in Rats", *Stroke*, Vol. 36, No. 4, pp. 859–864, 2005.

187. Cantarella, C., M. Cayre, K. Magalon and D. Pascale, "Intranasal HB-EGF Administration Favors Adult SVZ Cell Mobilization to Demyelinated Lesions in Mouse Corpus Callosum", *Developmental Neurobiology*, Vol. 68, No. 2, pp. 223–236, 2008.

188. Weuste, M., A. Wurm, I. Iandiev, P. Wiedemann, A. Reichenbach and A. Bringmann, "HB-EGF: Increase in the Ischemic Rat Retina and Inhibition of Osmotic Glial Cell Swelling", *Biochemical and Biophysical Research Communications*, Vol. 347, No. 1, pp. 310–318, 2006.

189. Reichenbach, A., A. Wurm, T. Pannicke, I. Iandiev, P. Wiedemann and A. Bringmann, "Müller Cells as Players in Retinal Degeneration and Edema", *Graefe's Archive for Clinical and Experimental Ophthalmology*, Vol. 245, No. 5, pp. 627–636, 2007.

190. Holbrook, E. H., K. E. Szumowski and J. E. Schwob, "An Immunochemical, Ultrastructural, and Developmental Characterization of the Horizontal Basal Cells of Rat Olfactory Epithelium.", *The Journal of Comparative Neurology*, Vol. 363, No. 1, pp. 129–146, dec 1995.

191. Westerfield, M., *The Zebrafish Book: A Guide for the Laboratory Use of Zebrafish Danio Rerio*, University of Oregon Press, Euegene,Oregon, 2007.

192. Maaswinkel, H. and L. Li, "Olfactory Input Increases Visual Sensitivity in Zebrafish: A Possible Function for the Terminal Nerve and Dopaminergic Interplexiform Cells", *Journal of Experimental Biology*, Vol. 206, No. 13, pp. 2201–2209, 2003.

193. Wilson, J. M., R. M. Bunte and A. J. Carty, "Evaluation of Rapid Cooling and Tricaine Methanesulfonate (MS222) as Methods of Euthanasia in Zebrafish (Danio Rerio)", *Journal of the American Association for Laboratory Animal Science*, Vol. 48, No. 6, pp. 785–789, 2009.

194. Inoue, D. and J. Wittbrodt, "One for All-a Highly Efficient and Versatile Method for Fluorescent Immunostaining in Fish Embryos", *PLoS ONE*, Vol. 6, No. 5, pp. 1–7, 2011.

195. Tang, X., D. L. Falls, X. Li, T. Lane and M. B. Luskin, "Antigen-Retrieval Procedure for Bromodeoxyuridine Immunolabeling with Concurrent Labeling of Nuclear DNA and Antigens Damaged by HCl Pretreatment", *Journal of Neuroscience*, Vol. 27, No. 22, pp. 5837–5844, 2007.

196. Nelson, C. M., R. A. Gorsuch, T. J. Bailey, K. M. Ackerman, S. C. Kassen and D. R. Hyde, "Stat3 Defines Three Populations of Müller Glia and Is Required for Initiating Maximal Müller Glia Proliferation in the Regenerating Zebrafish Retina", *Journal of Comparative Neurology*, Vol. 520, No. 18, pp. 4294–4311, 2012.

197. Tuttle, A. H., M. M. Rankin, M. Teta, D. J. Sartori, G. M. Stein, G. J. Kim, C. Virgilio, A. Granger, D. Zhou, S. H. Long, A. B. Schiffman and J. A. Kushner, "Immunofluorescent Detection of Two Thymidine Analogues (CldU and IdU) in Primary Tissue", *Journal of Visualized Experiments*, , No. 46, pp. 1–5, 2010.

198. Santos-Pereira, J. M., L. Gallardo-Fuentes, A. Neto, R. D. Acemel and J. J. Tena, "Pioneer and Repressive Functions of P63 during Zebrafish Embryonic Ectoderm Specification", *Nature Communications*, Vol. 10, No. 1, pp. 1–13, 2019.

199. Ansorg, A., K. Bornkessel, O. W. Witte and A. Urbach, "Immunohistochemistry and Multiple Labeling with Antibodies from the Same Host Species to Study Adult Hippocampal Neurogenesis", *Journal of Visualized Experiments*, Vol. 2015, No. 98, pp. 1–13, 2015.

200. Hu, B., C. Zhang, K. Baawo, R. Qin, G. J. Cole, J. A. Lee and X. Chen, "Zebrafish K5 Promoter Driven GFP Expression as a Transgenic System for Oral Research", *Oral Oncology*, Vol. 46, No. 1, pp. 31–37, 2010.

201. Cervino, A. S., D. A. Paz and J. L. Frontera, "Neuronal Degeneration and Regeneration Induced by Axotomy in the Olfactory Epithelium of Xenopus Laevis", *Developmental Neurobiology*, Vol. 77, No. 11, pp. 1308–1320, 2017.

202. Moulton, D. G., "Dynamics of Cell Populations in the Olfactory Epithelium", *Annals of the New York Academy of Sciences*, Vol. 237, No. 1, pp. 52–61, 1974.

203. Burd, G. D., "Morphological Study of the Effects of Intranasal Zinc Sulfate Irrigation on the Mouse Olfactory Epithelium and Olfactory Bulb", *Microscopy Research and Technique*, Vol. 24, No. 3, pp. 195–213, 1993.

204. Nadi, N. S., R. Head, M. Grillo, J. Hempstead, N. Grannot-Reisfeld and F. L. Margolis, "Chemical Deafferentation of the Olfactory Bulb: Plasticity of the Levels of Tyrosine Hydroxylase, Dopamine and Norepinephrine", *Brain Research*, Vol. 213, No. 2, pp. 365–377, 1981.

205. Yao, M., K., L. Samson, M., R. Reeves and K. White, "Gene Elav of Drosophila Melanogaster: A Prototype for Neuronal-Specific RNA Binding Protein Gene Family that Is Conserved in Flies and Humans", *Journal of Neurobiology*, Vol. 24, No. 6, pp. 723–739, 1993.

206. Hinman, M. N. and H. Lou, "Diverse Molecular Functions of Hu Proteins", *Cellular and Molecular Life Sciences*, Vol. 65, No. 20, pp. 3168–3181, 2008.

207. Gratzner, H. G., "Monoclonal Antibody to 5-Bromo- and 5-Iododeoxyuridine : A New Reagent for Detection of DNA Replication Placental Mononuclear Phagocytes as a Source of Interleukin-1", *Science*, Vol. 218, No. October, pp. 474–475, 1982.

208. Byrd, C. A. and P. C. Brunjes, "Neurogenesis in the Olfactory Bulb of Adult Zebrafish", *Neuroscience*, Vol. 105, No. 4, pp. 793–801, 2001.

209. Oehlmann, V. D., S. Berger, C. Sterner and S. I. Korsching, "Zebrafish Beta Tubulin 1 Expression Is Limited to the Nervous System throughout Development, and in the Adult Brain Is Restricted to a Subset of Proliferative Regions.", *Gene expression patterns : GEP*, Vol. 4, No. 2, pp. 191–198, mar 2004.

210. Hendzel, M. J., Y. Wei, M. A. Mancini, A. Van Hooser, T. Ranalli, B. R. Brinkley, D. P. Bazett-Jones and C. D. Allis, "Mitosis-Specific Phosphorylation of Histone H3 Initiates Primarily within Pericentromeric Heterochromatin during G2 and Spreads in an Ordered Fashion Coincident with Mitotic Chromosome Condensation", *Chromosoma*, Vol. 106, No. 6, pp. 348–360, 1997.

211. Herrick, D. B., B. Lin, J. Peterson, N. Schnittke and J. E. Schwob, "Notch1 Maintains Dormancy of Olfactory Horizontal Basal Cells, a Reserve Neural Stem Cell", *Proceedings of the National Academy of Sciences of the United States of America*, Vol. 114, No. 28, pp. E5589–E5598, 2017.

212. Graziadei, P. P. and M. Okano, "Neuronal Degeneration and Regeneration in the

Olfactory Epithelium of Pigeon Following Transection of the First Cranial Nerve", *Cells Tissues Organs*, Vol. 104, No. 2, pp. 220–236, 1979.

213. Cowan, C. M. and A. J. Roskams, "Apoptosis in the Mature and Developing Olfactory Neuroepithelium", *Microscopy Research and Technique*, Vol. 58, No. 3, pp. 204–215, 2002.

214. Magrassi, L. and P. P. Graziadei, "Cell Death in the Olfactory Epithelium", *Anatomy and Embryology*, Vol. 192, No. 1, pp. 77–87, 1995.

215. Voyron, S., P. Giacobini, G. Tarozzo, P. Cappello, I. Perroteau and A. Fasolo, "Apoptosis in the Development of the Mouse Olfactory Epithelium", *Developmental Brain Research*, Vol. 115, No. 1, pp. 49–55, 1999.

216. Holcomb, J. D., J. S. Mumm and A. L. Calof, "Apoptosis in the Neuronal Lineage of the Mouse Olfactory Epithelium: Regulation in Vivo and in Vitro", *Developmental Biology*, Vol. 172, No. 1, pp. 307–323, 1995.

217. Tait, S. W. and D. R. Green, "Caspase-Independent Cell Death: Leaving the Set without the Final Cut", *Oncogene*, Vol. 27, No. 50, pp. 6452–6461, 2008.

218. Akamatsu, W., H. Fujihara, T. Mitsuhashi, M. Yano, S. Shibata, Y. Hayakawa, H. J. Okano, S. I. Sakakibara, H. Takano, T. Takano, T. Takahashi, T. Noda and H. Okano, "The RNA-binding protein HuD regulates neuronal cell identity and maturation", *Proceedings of the National Academy of Sciences of the United States of America*, Vol. 102, No. 12, pp. 4625–4630, 2005.

219. Allende, M. L. and E. S. Weinberg, "The Expression Pattern of Two Zebrafish Achaete-Scute Homolog (ash) Genes is Altered in the Embryonic Brain of the cyclops Mutant", *Development*, , No. 166, pp. 509–530, 1994.

220. Soares, E. and H. Zhou, "Master Regulatory Role of P63 in Epidermal Development and Disease", *Cellular and Molecular Life Sciences*, Vol. 75, No. 7, pp.

1179–1190, 2018.

221. Fletcher, R. B., M. S. Prasol, J. Estrada, A. Baudhuin, K. Vranizan, Y. G. Choi and J. Ngai, "P63 Regulates Olfactory Stem Cell Self-Renewal and Differentiation", *Neuron*, Vol. 72, No. 5, pp. 748–759, 2011.

222. Li, C. and Z. X. Xiao, "Regulation of P63 Protein Stability via Ubiquitin-Proteasome Pathway", *BioMed Research International*, Vol. 2014, 2014.

223. Kawakami, K., "Tol2: A Versatile Gene Transfer Vector in Vertebrates", *Genome Biology*, Vol. 8, No. SUPPL. 1, pp. 1–10, 2007.

224. Choi, N., W. S. Kim, S. H. Oh and J. H. Sung, "HB-EGF Improves the Hair Regenerative Potential of Adipose-Derived Stem Cells via ROS Generation and Hck Phosphorylation", *International Journal of Molecular Sciences*, Vol. 21, No. 1, 2020.

225. Dao, D. T., L. Anez-Bustillos, R. M. Adam, M. Puder and D. R. Bielenberg, "Heparin-Binding Epidermal Growth Factor–Like Growth Factor as a Critical Mediator of Tissue Repair and Regeneration", *American Journal of Pathology*, Vol. 188, No. 11, pp. 2446–2456, 2018.

226. Kiso, S., S. Kawata, S. Tamura, Y. Inui, Y. Yoshida, Y. Sawai, S. Umeki, N. Ito, A. Yamada, J. I. Miyagawa, S. Higashiyama, T. Iwawaki, M. Saito, N. Taniguchi, Y. Matsuzawa and K. Kohno, "Liver Regeneration in Heparin-Binding EGF-Like Growth Factor Transgenic Mice after Partial Hepatectomy", *Gastroenterology*, Vol. 124, No. 3, pp. 701–707, 2003.

227. Oyagi, A., N. Morimoto, J. Hamanaka, M. Ishiguro, K. Tsuruma, M. Shimazawa and H. Hara, "Forebrain Specific Heparin-Binding Epidermal Growth Factor-Like Growth Factor Knockout Mice Show Exacerbated Ischemia and Reperfusion Injury", *Neuroscience*, Vol. 185, pp. 116–124, 2011.

228. Goishi, K., P. Lee, A. J. Davidson, E. Nishi, L. I. Zon and M. Klagsbrun, "Inhibition of Zebrafish Epidermal Growth Factor Receptor Activity Results in Cardiovascular Defects", *Mechanisms of Development*, Vol. 120, No. 7, pp. 811–822, 2003.

229. Dateoka, S., Y. Ohnishi and K. Kakudo, "Effects of CRM197, a Specific Inhibitor of HB-EGF, in Oral Cancer", *Medical Molecular Morphology*, Vol. 45, No. 2, pp. 91–97, 2012.

230. Ågren, M. S., U. Mirastschijski, T. Karlsmark and U. K. Saarialho-Kere, "Topical Synthetic Inhibitor of Matrix Metalloproteinases Delays Epidermal Regeneration of Human Wounds", *Experimental Dermatology*, Vol. 10, No. 5, pp. 337–348, 2001.

231. Benjamin, M. M. and R. A. Khalil, "Matrix Metalloproteinase Inhibitors as Investigative Tools in the Pathogenesis and Management of Vascular Disease.", *Experientia Supplementum*, Vol. 103, pp. 209–279, 2012.

232. Winer, A., S. Adams and P. Mignatti, "Matrix Metalloproteinase Inhibitors in Cancer Therapy: Turning Past Failures into Future Successes", *Mol Cancer Ther*, Vol. 17, No. 6, pp. 1147–1155, 2018.

233. Leigh, N. R., M. O. Schupp, K. Li, V. Padmanabhan, A. Gastonguay, L. Wang, C. Z. Chun, G. A. Wilkinson and R. Ramchandran, "Mmp17b Is Essential for Proper Neural Crest Cell Migration In Vivo", *PLoS ONE*, Vol. 8, No. 10, pp. 1–12, 2013.

234. Xu, S., S. E. Webb, T. C. K. Lau and S. H. Cheng, "Matrix Metalloproteinases (MMPs) Mediate Leukocyte Recruitment during the Inflammatory Phase of Zebrafish Heart Regeneration", *Scientific Reports*, Vol. 8, No. 1, pp. 1–14, 2018.

235. Kocer, S. S., S. G. Walker, B. Zerler, L. M. Golub and S. R. Simon, "Metalloproteinase Inhibitors, Nonantimicrobial Chemically Modified Tetracyclines, and

Ilomastat Block Bacillus Anthracis Lethal Factor Activity in Viable Cells", *Infection and Immunity*, Vol. 73, No. 11, pp. 7548–7557, 2005.

236. Novak, K. B., H. D. Le, E. R. Christison-Lagay, V. Nose, R. J. Doiron, M. A. Moses and M. Puder, "Effects of Metalloproteinase Inhibition in a Murine Model of Renal Ischemia-Reperfusion Injury", *Pediatric Research*, Vol. 67, No. 3, pp. 257–262, 2010.

237. Zhou, B. B. S., M. Peyton, B. He, C. Liu, L. Girard, E. Caudler, Y. Lo, F. Baribaud, I. Mikami, N. Reguart, G. Yang, Y. Li, W. Yao, K. Vaddi, A. F. Gazdar, S. M. Friedman, D. M. Jablons, R. C. Newton, J. S. Fridman, J. D. Minna and P. A. Scherle, "Targeting ADAM-Mediated Ligand Cleavage to Inhibit HER3 and EGFR Pathways in Non-Small Cell Lung Cancer", *Cancer Cell*, Vol. 10, No. 1, pp. 39–50, 2006.

238. Luo, P., H. Yan, X. Chen, Y. Zhang, Z. Zhao, J. Cao, Y. Zhu, J. Du, Z. Xu, X. Zhang, S. Zeng, B. Yang, S. Ma and Q. He, "s-HBEGF/SIRT1 Circuit-Dictated Crosstalk between Vascular Endothelial Cells and Keratinocytes Mediates Sorafenib-Induced Hand–Foot Skin Reaction that Can Be Reversed by Nicotinamide", *Cell Research*, Vol. 30, No. 9, pp. 779–793, 2020.

239. O-Charoenrat, P., P. Rhys-Evans and S. Eccles, "A Synthetic Matrix Metalloproteinase Inhibitor Prevents Squamous Carcinoma Cell Proliferation by Interfering with Epidermal Growth Factor Receptor Autocrine Loops", *International Journal of Cancer*, Vol. 100, No. 5, pp. 527–533, 2002.

240. Malnic, B., J. Hirono, T. Sato, L. B. Buck and H. Hughes, "Combinatorial Receptor Code for Odors", *Cell*, Vol. 96, pp. 713–723, 2000.

241. Zapiec, B. and P. Mombaerts, "The Zonal Organization of Odorant Receptor Gene Choice in the Main Olfactory Epithelium of the Mouse", *Cell Reports*, Vol. 30, No. 12, pp. 4220–4234.e5, 2020.

242. Biehl, J. K. and B. Russell, "Introduction to Stem Cell Therapy", *Journal of Cardiovascular Nursing*, Vol. 24, No. 2, pp. 98–103, 2009.

243. Cheung, T. H. and T. A. Rando, "Molecular Regulation of Stem Cell Quiescence", *Nature Reviews Molecular Cell Biology*, Vol. 14, No. 6, pp. 329–340, 2013.

244. Gonzalez, M. A. and A. Bernad, "Characteristics of Adult Stem Cells", *Advances in Experimental Medicine and Biology*, Vol. 741, pp. 103–120, 2012.

245. Mackay-Sim, A. and P. Kittel, "Cell Dynamics in the Adult Mouse Olfactory Epithelium: A Quantitative Autoradiographic Study", *Journal of Neuroscience*, Vol. 11, No. 4, pp. 979–984, 1991.

246. Kent, S., J. Hutchinson, A. Balboni, A. DeCastro, P. Cherukuri and J. DiRenzo, "ΔNp63α Promotes Cellular Quiescence via Induction and Activation of Notch3", *Cell Cycle*, Vol. 10, No. 18, pp. 3111–3118, 2011.

247. MacKay-Sim, A., "Stem Cells and Their Niche in the Adult Olfactory Mucosa", *Archives Italiennes de Biologie*, Vol. 148, No. 2, pp. 47–58, 2010.

248. Gerhard, G. S., E. J. Kauffman, X. Wang, R. Stewart, J. L. Moore, C. J. Kasales, E. Demidenko and K. C. Cheng, "Life Spans and Senescent Phenotypes in Two Strains of Zebrafish (Danio Rerio)", *Experimental Gerontology*, Vol. 37, No. 8-9, pp. 1055–1068, 2002.

249. Li, N. and H. Clevers, "Coexistence of Quiescent and Active Adult Stem Cells in Mammals", *Science*, Vol. 327, No. 5965, pp. 542–545, 2010.

250. Hsu, Y. C., H. A. Pasolli and E. Fuchs, "Dynamics between Stem Cells, Niche, and Progeny in the Hair Follicle", *Cell*, Vol. 144, No. 1, pp. 92–105, 2011.

251. Cotsarelis, G., T. T. Sun and R. M. Lavker, "Label-Retaining Cells Reside in the Bulge Area of Pilosebaceous Unit: Implications for Follicular Stem Cells, Hair

Cycle, and Skin Carcinogenesis", *Cell*, Vol. 61, No. 7, pp. 1329–1337, 1990.

252. Oshima, H., A. Rochat, C. Kedzia, K. Kobayashi and Y. Barrandon, "Morphogenesis and Renewal of Hair Follicles from Adult Multipotent Stem Cells", *Cell*, Vol. 104, No. 2, pp. 233–245, 2001.

253. Tung-Tien, S., G. Cotsarelis and R. M. Lavker, "Hair Follicular Stem Cells: The Bulge-Activation Hypothesis", *Journal of Investigative Dermatology*, Vol. 96, No. 5, pp. 775–785, 1991.

254. Waghmare, S. K., R. Bansal, J. Lee, Y. V. Zhang, D. J. McDermitt and T. Tumbar, "Quantitative Proliferation Dynamics and Random Chromosome Segregation of Hair Follicle Stem Cells", *EMBO Journal*, Vol. 27, No. 9, pp. 1309–1320, 2008.

255. Janich, P., G. Pascual, A. Merlos-Suárez, E. Batlle, J. Ripperger, U. Albrecht, H. Y. M. Cheng, K. Obrietan, L. Di Croce and S. A. Benitah, "The Circadian Molecular Clock Creates Epidermal Stem Cell Heterogeneity", *Nature*, Vol. 480, No. 7376, pp. 209–214, 2011.

256. Rompolas, P., K. R. Mesa and V. Greco, "Spatial Organization within a Niche as a Determinant of Stem-Cell Fate", *Nature*, Vol. 502, No. 7472, pp. 513–518, 2013.

257. Jaks, V., N. Barker, M. Kasper, J. H. Van Es, H. J. Snippert, H. Clevers and R. Toftgård, "Lgr5 Marks Cycling, yet Long-Lived, Hair Follicle Stem Cells", *Nature Genetics*, Vol. 40, No. 11, pp. 1291–1299, 2008.

258. Hoeck, J. D., B. Biehs, A. V. Kurtova, N. M. Kljavin, F. De Sousa E Melo, B. Alicke, H. Koeppen, Z. Modrusan, R. Piskol and F. J. De Sauvage, "Stem Cell Plasticity Enables Hair Regeneration following Lgr5 + Cell loss", *Nature Cell Biology*, Vol. 19, No. 6, pp. 666–676, 2017.

259. Qi, D., W. Shi, A. R. Black, M. A. Kuss, X. Pang, Y. He, B. Liu and B. Duan,

"Repair and Regeneration of Small Intestine: A Review of Current Engineering Approaches", *Biomaterials*, Vol. 240, p. 119832, 2020.

260. Barker, N., J. H. Van Es, J. Kuipers, P. Kujala, M. Van Den Born, M. Cozijnsen, A. Haegebarth, J. Korving, H. Begthel, P. J. Peters and H. Clevers, "Identification of Stem Cells in Small Intestine and Colon by Marker Gene Lgr5", *Nature*, Vol. 449, No. 7165, pp. 1003–1007, 2007.

261. Barker, N., A. Van Oudenaarden and H. Clevers, "Identifying the Stem Cell of the Intestinal Crypt: Strategies and Pitfalls", *Cell Stem Cell*, Vol. 11, No. 4, pp. 452–460, 2012.

262. Potten, C. S., "Extreme Sensitivity of Some Intestinal Crypt Cells to X and γ Irradiation", *Nature*, , No. 269, pp. 518–521, 1977.

263. Sangiorgi, E. and M. R. Capecchi, "Bmi1 Is Expressed in Vivo in Intestinal Stem Cells", *Nature Genetics*, Vol. 40, No. 7, pp. 915–920, 2008.

264. Obernier, K., A. Cebrian-Silla, M. Thomson, J. I. Parraguez, R. Anderson, C. Guinto, J. Rodas Rodriguez, J. M. Garcia-Verdugo and A. Alvarez-Buylla, "Adult Neurogenesis Is Sustained by Symmetric Self-Renewal and Differentiation", *Cell Stem Cell*, Vol. 22, No. 2, pp. 221–234.e8, 2018.

265. Child, K. M., D. B. Herrick, J. E. Schwob, E. H. Holbrook and W. Jang, "The Neuroregenerative Capacity of Olfactory Stem Cells Is Not Limitless: Implications for Aging", *Journal of Neuroscience*, Vol. 38, No. 31, pp. 6806–6824, 2018.

266. Trimpe, D. M. and C. A. Byrd-Jacobs, "Patterns of Olfactory Bulb Neurogenesis in the Adult Zebrafish Are Altered Following Reversible Deafferentation", *Neuroscience*, Vol. 331, pp. 134–147, 2016.

267. Teta, M., M. M. Rankin, S. Y. Long, G. M. Stein and J. A. Kushner, "Growth and Regeneration of Adult β Cells Does Not Involve Specialized Progenitors",

Developmental Cell, Vol. 12, No. 5, pp. 817–826, 2007.

268. Keyes, W. M., Y. Wu, H. Vogel, X. Guo, S. W. Lowe and A. A. Mills, "P63 Deficiency Activates a Program of Cellular Senescence and Leads To Accelerated Aging", *Genes and Development*, Vol. 19, No. 17, pp. 1986–1999, 2005.

269. Chen, S., M. Lewallen and T. Xie, "Adhesion in the Stem Cell Niche: Biological Roles and Regulation", *Development (Cambridge)*, Vol. 140, No. 2, pp. 255–265, 2013.

270. Schwob, J. E., W. Jang, E. H. Holbrook, B. Lin, D. B. Herrick, J. Peterson and J. H. Coleman, "Stem and Progenitor Cells of the Mammalian Olfactory Epithelium: Taking Poietic License James", *Journal of Comparative Neurology*, Vol. 525, No. 4, pp. 1034–1054, 2017.

271. Paskin, T. R., T. R. Iqbal and C. A. Byrd-Jacobs, "Olfactory Bulb Recovery Following Reversible Deafferentation with Repeated Detergent Application in the Adult Zebrafish.", *Neuroscience*, Vol. 196, pp. 276–284, 2011.

272. Paskin, T. R. and C. A. Byrd-Jacobs, "Reversible Deafferentation of the Adult Zebrafish Olfactory Bulb Affects Glomerular Distribution and Olfactory-Mediated Behavior", *Behavioural Brain Research*, Vol. 235, No. 2, pp. 293–301, 2012.

273. Carson, C., M. Saleh, F. W. Fung, D. W. Nicholson and A. J. Roskams, "Axonal Dynactin P150Glued Transports Caspase-8 to Drive Retrograde Olfactory Receptor Neuron Apoptosis", *Journal of Neuroscience*, Vol. 25, No. 26, pp. 6092–6104, 2005.

274. Vandenabeele, P., L. Galluzzi, T. Vanden Berghe and G. Kroemer, "Molecular Mechanisms of Necroptosis: An Ordered Cellular Explosion", *Nature Reviews Molecular Cell Biology*, Vol. 11, No. 10, pp. 700–714, 2010.

275. Schwob, J. E., S. L. Youngentob, G. Ring, C. L. Iwema and R. C. Mezza, "Reinner-

vation of the Rat Olfactory Bulb after Methyl Bromide-Induced Lesion: Timing and Extent of Reinnervation.", *The Journal of Comparative Neurology*, Vol. 412, No. 3, pp. 439–457, sep 1999.

276. White, E. J., S. K. Kounelis and C. A. Byrd-Jacobs, "Plasticity of Glomeruli and Olfactory-Mediated Behavior in Zebrafish Following Detergent Lesioning of the Olfactory Epithelium", *Neuroscience*, Vol. 284, pp. 622–631, 2015.

277. Genter, M. B. and S. Ali, "Age-Related Susceptibility to 3,3'-Iminodipropionitrile-Induced Olfactory Mucosal Damage", *Neurobiology of Aging*, Vol. 19, No. 6, pp. 569–574, 1998.

278. Suzukawa, K., K. Kondo, K. Kanaya, T. Sakamoto, K. Watanabe, M. Ushio, K. Kaga and T. Yamasoba, "Age-Related Changes of the Regeneration Mode in the Mouse Peripheral Olfactory System Following Olfactotoxic Drug Methimazole-Induced Damage", *Journal of Comparative Neurology*, Vol. 519, No. 11, pp. 2154–2174, 2011.

279. Breipohl, W., H. J. Laugwitz and N. Bornfeld, "Topological Relations between the Dendrites of Olfactory Sensory Cells and Sustentacular Cells in Different Vertebrates. An Ultrastructural Study.", *Journal of Anatomy*, Vol. 117, No. Pt 1, pp. 89–94, 1974,

280. Makino, N., S. Ookawara, K. Katoh, Y. Ohta, M. Ichikawa and K. Ichimura, "The Morphological Change of Supporting Cells in the Olfactory Epithelium after Bulbectomy", *Chemical Senses*, Vol. 34, No. 2, pp. 171–179, 2009.

281. Hitchcock, P., M. Ochocinska, A. Sieh and D. Otteson, "Persistent and Injury-Induced Neurogenesis in the Vertebrate Retina", *Progress in Retinal and Eye Research*, Vol. 23, No. 2, pp. 183–194, 2004.

282. Wan, J., H. Zheng, Z. L. Chen, H. L. Xiao, Z. J. Shen and G. M. Zhou, "Preferential Regeneration of Photoreceptor from Müller Glia after Retinal Degeneration

in Adult Rat", *Vision Research*, Vol. 48, No. 2, pp. 223–234, 2008.

283. Ikeda, K., R. Kageyama, Y. Suzuki and K. Kawakami, "Six1 Is Indispensable for Production of Functional Progenitor Cells during Olfactory Epithelial Development", *International Journal of Developmental Biology*, Vol. 54, No. 10, pp. 1453–1464, 2010.

284. Rodriguez, S., H. M. Sickles, C. DeLeonardis, A. Alcaraz, T. Gridley and D. M. Lin, "Notch2 Is Required for Maintaining Sustentacular Cell Function in the Adult Mouse Main Olfactory Epithelium", *Developmental Biology*, Vol. 314, No. 1, pp. 40–58, 2008.

285. Heron, P. M., A. J. Stromberg, P. Breheny and T. S. McClintock, "Molecular Events in the Cell Types of the Olfactory Epithelium during Adult Neurogenesis", *Molecular Brain*, Vol. 6, No. 1, pp. 1–14, 2013.

286. Yoh, K. and R. Prywes, "Pathway Regulation of P63, a Director of Epithelial Cell Fate", *Frontiers in Endocrinology*, Vol. 6, No. APR, pp. 1–9, 2015.

287. Chatterjee, A., X. Chang, T. Sen, R. Ravi, A. Bedi and D. Sidransky, "Regulation of P53 Family Member Isoform ΔNp63α by the Nuclear Factor-κB Targeting Kinase IκB Kinase β", *Cancer Research*, Vol. 70, No. 4, pp. 1419–1429, 2010.

288. Sen, T., X. Chang, D. Sidransky and A. Chatterjee, "Regulation of ΔNp63α by NFκB", *Cell Cycle*, Vol. 9, No. 24, pp. 4841–4847, 2010.

289. Fletcher, R. B., D. Das, L. Gadye, K. N. Street, A. Baudhuin, A. Wagner, M. B. Cole, Q. Flores, Y. G. Choi, N. Yosef, E. Purdom, S. Dudoit, D. Risso and J. Ngai, "Deconstructing Olfactory Stem Cell Trajectories at Single-Cell Resolution", *Cell Stem Cell*, Vol. 20, No. 6, pp. 817–830.e8, 2017.

290. Chen, M., R. R. Reed and A. P. Lane, "Acute Inflammation Regulates Neuroregeneration through the NF-κB Pathway in Olfactory Epithelium", *Proceedings*

of the National Academy of Sciences of the United States of America, Vol. 114, No. 30, pp. 8089–8094, 2017.

291. Anders, H. J. and L. Schaefer, "Beyond Tissue Injury - Damage-Associated Molecular Patterns, Toll-Like Receptors, and Inflammasomes Also Drive Regeneration and Fibrosis", *Journal of the American Society of Nephrology*, Vol. 25, No. 7, pp. 1387–1400, 2014.

292. Roh, J. S. and D. H. Sohn, "Damage-Associated Molecular Patterns in Inflammatory Diseases", *Immune Network*, Vol. 18, No. 4, pp. 1–14, 2018.

293. Erta, M., A. Quintana and J. Hidalgo, "Interleukin-6, a Major Cytokine in the Central Nervous System", *International Journal of Biological Sciences*, Vol. 8, No. 9, pp. 1254–1266, 2012.

294. Bernardino, L., F. Agasse, B. Silva, R. Ferreira, S. Grade and J. O. Malva, "Tumor Necrosis Factor-α Modulates Survival, Proliferation, and Neuronal Differentiation in Neonatal Subventricular Zone Cell Cultures", *Stem Cells*, Vol. 26, No. 9, pp. 2361–2371, 2008.

295. Kageyama, R., T. Ohtsuka, J. Hatakeyama and R. Ohsawa, "Roles of BHLH genes in Neural Stem Cell Differentiation", *Experimental Cell Research*, Vol. 306, No. 2, pp. 343–348, 2005.

296. Nguyen, B. C., K. Lefort, A. Mandinova, D. Antonini, V. Devgan, G. D. Gatta, M. I. Koster, Z. Zhang, J. Wang, A. T. Di Vignano, J. Kitajewski, G. Chiorino, D. R. Roop, C. Missero and G. P. Dotto, "Cross-Regulation between Notch and P63 in Keratinocyte Commitment to Differentiation", *Genes and Development*, Vol. 20, No. 8, pp. 1028–1042, 2006.

297. Tadeu, A. M. B. and V. Horsley, "Notch Signaling Represses P63 Expression in the Developing Surface Ectoderm", *Development (Cambridge)*, Vol. 140, No. 18, pp. 3777–3786, 2013.

298. Iwamoto, R. and E. Mekada, *HB-EGF (Heparin-Binding EGF-like Growth Factor)*, Springer, New York, NY, New York, NY., 2016.

299. Opanashuk, L. A., R. J. Mark, J. Porter, D. Damm, M. P. Mattson and K. B. Seroogy, "Heparin-Binding Epidermal Growth Factor-Like Growth Factor in Hippocampus: Modulation of Expression by Seizures and Anti-Excitotoxic Action", *Journal of Neuroscience*, Vol. 19, No. 1, pp. 133–146, 1999.

300. Kawahara, N., K. Mishima, S. Higashiyama, N. Taniguchi, A. Tamura and T. Kirino, "The Gene for Heparin-Binding Epidermal Growth Factor-Like Growth Factor Is Stress-Inducible: Its Role in Cerebral Ischemia", *Journal of Cerebral Blood Flow and Metabolism*, Vol. 19, No. 3, pp. 307–320, 1999.

301. Jin, K., L. Xie, J. Childs, Y. Sun, X. O. Mao, A. Logvinova and D. A. Greenberg, "Cerebral Neurogenesis Is Induced by Intranasal Administration of Growth Factors", *Annals of Neurology*, Vol. 53, No. 3, pp. 405–409, 2003.

302. Farbman, A. I. and J. A. Buchholz, "Transforming Growth Factor-α and Other Growth Factors Stimulate Cell Division in Olfactory Epithelium in Vitro", *Journal of Neurobiology*, Vol. 30, No. 2, pp. 267–280, 1996.

303. Mahanthappa, N. K. and G. A. Schwarting, "Peptide Growth Factor Control of Olfactory Neurogenesis and Neuron Survival in Vitro: Roles of EGF and TGF-βs", *Neuron*, Vol. 10, No. 2, pp. 293–305, 1993.

304. Mitamura, T., S. Higashiyama, N. Taniguchi, M. Klagsbrun and E. Mekada, "Diphtheria Toxin Binds to the Epidermal Growth Factor (EGF)-Like Domain of Human Heparin-Binding EGF-Like Growth Factor/Diphtheria Toxin Receptor and Inhibits Specifically Its Mitogenic Activity", *Journal of Biological Chemistry*, Vol. 270, No. 3, pp. 1015–1019, 1995.

305. Peng, H., T.-C. Wen, J. Tanaka, N. Maeda, S. Matsuda, J. Desaki, S. Sudo, B. Zhang and M. Sakanaka, " Epidermal Growth Factor Protects Neuronal Cells

In Vivo and In Vitro against Transient Forebrain Ischemia- and Free Radical-Induced Injuries ", *Journal of Cerebral Blood Flow Metabolism*, Vol. 18, No. 4, pp. 349–360, 1998.

306. Zhou, Y. and G. E. Besner, "Heparin-Binding Epidermal Growth Factor-Like Growth Factor Is a Potent Neurotrophic Factor for PC12 Cells", *NeuroSignals*, Vol. 18, No. 3, pp. 141–151, 2011.

APPENDIX A: Chemicals and reagents

Table A.1. List of chemicals and reagents (Antibodies excluded)

Name	**Manufacturer**
1 kb DNA ladder	New England Biolabs, USA
6X Loading Dye	New England Biolabs, USA
Absolute Ethanol	Sigma-Aldrich, USA
Agarose	Cambrex, USA
Bovine Serum Albumin (BSA)	New England Biolabs, USA
BrdU	Alfa Aesar, Germany
Calcium Sulfate	Alfa Aesar, Germany
Chloroform	Sigma-Aldrich, USA
Diethyl pyrocarbonate (DEPC)	Sigma-Aldrich, USA
Dimethyl Sulphoxide (DMSO)	Sigma-Aldrich, USA
DIG RNA Labelling Kit	Roche, Germany
dNTP	New England Biolabs, USA
Ethidium Bromide	Sigma-Aldrich, USA
Fab Fragments Anti-Rabbit	Jackson ImmunoResearch, UK
Formamide	Sigma-Aldrich, USA
GM6001	Tocris,UK
High Pure PCR Product Purification Kit	Roche, Germany
High Pure Plasmid Isolation Kit	Roche, Germany
Isopropanol	Sigma-Aldrich, USA
Hydrochloric Acid	Sigma-Aldrich, USA

Detailed lists of primary and secondary antibodies can be found in Materials and Methods section.

Table A.1. List of chemicals and reagents (cont.)

Name	**Manufacturer**
LB Agar	Sigma-Aldrich, USA
LB Broth	Sigma-Aldrich, USA
Marimastat	Sigma-Aldrich, USA
mMESSAGE mMACHINE™ SP6 Trans. Kit	Ambion, USA
NcoI Restriction Enzyme	New England Biolabs, USA
Onetaq DNA polymerase	New England Biolabs, USA
Optimal Cutting Temperature medium	Sakura Finetek, USA
Paraformaldehyde	Sigma-Aldrich, USA
pGEM-T Easy Vector System	Promega, USA
Phenol Red	AppliChem, USA
pJET 1.2 Blunt Vector System	Thermo Fisher, USA
Potassium Phosphate Monobasic	Sigma-Aldrich, USA
Potassium Chloride	Sigma-Aldrich, USA
Q5 DNA Polymerase	New England Biolabs, USA
pCS-TP vector	Kawakami Lab, Japan
Proteinase K	Roche, Germany
pTAL vector (pT2AL200R150G)	Kawakami Lab, Japan
Rabbit Serum	Boğaziçi Üniversity, Turkey
Sodium Bicarbonate	Acquatic Habitats, USA
Sodium Chloride	Sigma-Aldrich, USA
Sodium Citrate Tribasic Dihydrate	Sigma-Aldrich, USA
Sodium Deoxycholate	Sigma-Aldrich, USA
Sodium Hydroxide	Sigma-Aldrich, USA
Sodium Phosphate Dibasic	Sigma-Aldrich, USA
T4 DNA Ligase	New England Biolabs, USA

Table A.1. List of chemicals and reagents (cont.)

Name	**Manufacturer**
Transcriptor First Strand cDNA Synthesis kit	Roche, Germany
Triton X-100	AppliChem, Germany
Tricaine (MS-222)	Sigma-Aldrich, USA
TRIzol™ Reagent	Life Technologies, USA
Trizma Base	Sigma-Aldrich, USA
Tween20	Roche, Germany
XhoI Restriction Enzyme	New England Biolabs, USA

APPENDIX B: Disposable and non-disposable Equipments

Table B.1. List of disposable and non-disposable equipments

Name	**Manufacturer**
Confocal Microscope SP5	Leica, Germany
Confocal Microscope SP8	Leica, Germany
Cryostat CM3050S	Leica, Germany
Coplin Jars	Wheathon-VWR, The Netherlands
Dissection forceps	Dumont, Switzerland
Drying oven	Nüve, Turkey
Microwave oven	Vestel, Turkey
Electrophoresis chambers	Bio-Rad Labs, USA
Electrophoresis supply	Bio-Rad Labs, USA
Filter tips (10-1000μl)	Greiner Bio-One, Germany
Freezer -20°C	Uğur, Turkey
Freezer -86°C	ThermoForma, USA
Fluorescence stereomicroscope	Leica, Germany
GelDoc XR	Bio-Rad Labs, USA
Glassware	Isolab, Germany
Insulin needle 0.5 ml (30G)	Beckon Dickinson, USA
Microblade	Lalvolin,Turkey
Microinjector, FemtoJet	Eppendorf, Germany
Microinjection needles	Warner Instruments, USA
Micropipettes (10-1000μl)	Eppendorf, Germany

Table B.1. List of disposable and non-disposable equipments (cont.)

Name	**Manufacturer**
NanoDrop 2000 Spectrophotometer	Thermo Fisher, USA
pHmeter	WTW, Germany
Pipette Tips	VWR,USA
PCR tubes 0.2 ml	Axygen,USA
Superfrost Plus Micro Slides	VWR, USA
Super PAP Pen	Liquid Blocker, Japan
Surgical blade	Swann-Morton, UK
Syringe filter 0.22 μm	TPP, Switzerland
Tabletop centrifuges 5424,5417R	Eppendorf, Germany
Test tubes (0.5-2 ml)	Citotest, China
Test tubes (15-50 ml)	Citotest, China
Thermal cycler	Bio-Rad,USA
Vortex mixer	Scientific Industries,USA